



**Molecular mechanisms of growth responses to elevated atmospheric carbon dioxide in  
wheat (*Triticum aestivum* L.)**

A Thesis submitted by

Dananjali Mekhala Gamage

BSc (Agriculture) (Hons)

For the award of

Doctor of Philosophy

2018

## Abstract

The carbon dioxide concentration [CO<sub>2</sub>] in the current atmosphere is increasing at a significant rate and is predicted to reach up to 700 μmol mol<sup>-1</sup> by the end of this century. Elevated ([CO<sub>2</sub>]) has the potential to increase the growth and yield of crops. Being the primary substrate for photosynthesis, increased CO<sub>2</sub> levels significantly promote the growth of most C<sub>3</sub> crops through increased photosynthesis capacity and reduced stomatal conductance. This stimulation of photosynthesis is central to other post-photosynthetic key metabolic processes such as carbon and nitrogen metabolism, cell cycle functions and hormonal regulation, which may lead to changes in whole plant growth. The magnitude of these responses to elevated [CO<sub>2</sub>] varies even within same species, indicating a significant genetic variation for CO<sub>2</sub> responsiveness within plant communities. In addition, the CO<sub>2</sub> responsiveness of plants depends on their ontogeny and is found to be more pronounced in the early development stages of the crops. However, there is a limited understanding of underlying molecular mechanisms of plant growth responses to elevated [CO<sub>2</sub>] which is crucial for developing crop breeding strategies to improve crop productivity in a changing climate. Therefore, this project broadly aimed to dissect the molecular mechanisms of plant growth responses to elevated [CO<sub>2</sub>] in wheat (*Triticum aestivum* L.), focusing on three unexplored aspects of this underlying mechanism. This project focused primarily on the early vegetative stage of wheat to study the increased CO<sub>2</sub> responsiveness of crops in their early ontogeny.

First, putative quantitative trait loci (QTL) for major early growth traits at elevated [CO<sub>2</sub>] were identified using a doubled haploid population of a cross between RAC875 and Kukri, to identify the genetic regions potentially associated with CO<sub>2</sub> responsiveness. In total 24 putative QTL for CO<sub>2</sub> responsiveness were identified for different growth traits. Three QTL, worthy for future research, were identified on chromosome 2A, 1B and 4B that showed an increased response for biomass accumulation at elevated [CO<sub>2</sub>]. Secondly, the role of photosynthesis and post-photosynthetic metabolic processes in moderating growth responses to elevated [CO<sub>2</sub>] was investigated through developing an understanding of the source and sink interaction of wheat. Transcript abundance of key genes involved in carbon and nitrogen metabolism, and cell cycle functions varied greatly among CO<sub>2</sub> levels (400 and 700 μmol mol<sup>-1</sup>), organ types (last fully expanded leaves, expanding leaves, leaf cell elongation zone and shoot apex region) and genotypes. Finally, the interplay of different regulatory mechanisms involved in plant growth at elevated [CO<sub>2</sub>] was investigated through a comparative proteomics analysis. Most of the differentially expressed proteins at elevated [CO<sub>2</sub>] were involved in carbon metabolism, energy pathways, protein synthesis and cell cycle functions. However, the leaf proteome responses to elevated [CO<sub>2</sub>] were highly genotype dependent. Overall, the results indicated that post-photosynthetic metabolic processes play a significant role in moderating plant growth responses at elevated [CO<sub>2</sub>]. Molecular level responses of these processes are subject to developmental regulation and thus, are involved in determining the source and sink integration of plants. This study has demonstrated the intraspecific variability of growth responses to elevated [CO<sub>2</sub>] at the genetic, transcriptomic and proteomic level. These variable responses provide valuable targets for the selection of genotypes that can thrive well in the future CO<sub>2</sub> enriched atmosphere.

## **Certification of Thesis**

This Thesis is the work of Dananjali Gamage except where otherwise acknowledged, with the majority of the authorship of the papers presented as a Thesis by Publication undertaken by the Student. The work is original and has not previously been submitted for any other award, except where acknowledged.

Principal Supervisor: Professor Saman Seneweera

Associate Supervisor: Associate Professor Naoki Hirotsu

Associate Supervisor: Professor Mark W. Sutherland

Student and supervisors signatures of endorsement are held at the University.

## Statement of Authorship

**Chapter 2:** New insights into the cellular mechanisms of plant growth at elevated atmospheric carbon dioxide. **Gamage D**, Thompson M, Sutherland M, Hirotsu N, Makino A, Seneweera S 2018, *Plant, Cell & Environment*, 41(6), 1233-1246.

Dananjali Gamage (DG) contributed to 60% of the paper, consisting of the paper's design, literature collection and interpretation, and writing of the manuscript. Saman Seneweera (SS) contributed to 20% of the paper, consisting of the paper's design, revision of the paper and editorial input. Michael Thompson (MT), Amane Makino (AM), Mark W. Sutherland (MWS) and Naoki Hirotsu (NH) contributed to 20% of the paper, consisting of revision and editorial input.

**Chapter 3:** Early growth mechanism of wheat (*Triticum aestivum* L.) at elevated atmospheric carbon dioxide: New physiological evidence with quantitative trait loci data. **Gamage D**, Thompson M, Okamoto M, Moriyama N, Sutherland M.W., Hirotsu N, Seneweera S. (Prepared for publication)

DG contributed to 60% of the paper, consisting of experimental design; acquisition, analysis and interpretation of data; drafting and revising the manuscript. SS and NH contributed 20% and 10%, respectively consisting of the study conception and design, analysis and interpretation of data, critical revision of the manuscript. Mamoru Okamoto (MO), Nao Moriyama (NM), MWS, MT contributed 10%, consisting of data collection, revision of the manuscript and editorial input.

**Chapter 4:** Elevated carbon dioxide mediated early growth responses of wheat (*Triticum aestivum* L.): an analysis of source and sink interactions. **Gamage D**, Thompson M, Dehigaspitiya P, Fukushima A, Sutherland M.W., Hirotsu N, Seneweera S. (Prepared for publication)

DG contributed to 60% of the paper, consisting of experimental design; acquisition, analysis and interpretation of data; drafting and revising the manuscript. SS and NH contributed 20% and 10%, respectively consisting of the study conception and design, analysis and interpretation of data, critical revision of the manuscript. Prabuddha Dehigaspitiya (PD), Ayaka

Fukushima (AF), MT and MWS contributed 10%, consisting of data collection, revision of the manuscript and editorial input.

**Chapter 5:** Leaf proteome responses of wheat (*Triticum aestivum* L.) to elevated atmospheric carbon dioxide during early vegetative growth. **Gamage D**, Thompson M, Dehigaspitiya P, Faou P, Rajapaksha KH, Downs R, Sutherland M.W., Hirotsu N, Seneweera S. (Prepared for publication)

DG contributed to 60% of the paper, consisting of experimental design; acquisition, analysis and interpretation of data; drafting and revising the manuscript. SS contributed 20% a conception and design, analysis and interpretation of data, critical revision of the manuscript. NH and Harinda Rajapaksha (HR) contributed 10% consisting of data analysis, interpretation and revision of the manuscript. Pierre Faou (PF), Rachael Downs (RD), MWS, MT and PD contributed 10%, consisting of data collection, analysis, revision of the manuscript and editorial input.

## Acknowledgment

This PhD has been one of the most amazing experiences of my life and I am truly grateful for all those who have supported me throughout this journey. First and foremost, I would like to acknowledge the University of Southern Queensland for providing me this great opportunity to pursue my doctoral degree along with a USQ Postgraduate Research Scholarship. I would like to express my special appreciation and sincere gratitude to my principal supervisor, Professor Saman Seneweera, for his tremendous academic support, valuable guidance and constant encouragement throughout this journey. I am also indebted to Associate Professor Naoki Hirotsu, associate supervisor of my PhD project for his great scholarly input into my research experiments and constructive discussions on data analysis and interpretation. Whenever I had doubts and questions, Prof. Hirotsu was always made himself available to clarify them despite his busy schedule. Similar profound gratitude goes to Professor Mark Sutherland, my associate supervisor, for his academic support and critical revision of all the scholarly outputs generated from this PhD study. I consider it a great opportunity to pursue my doctoral degree under the great supervision of these three exemplary academics.

I am also hugely appreciative to Dr. Anke Martin from the University of Southern Queensland who has been a dedicated mentor of molecular biology laboratory work and for her kind support during tough times in the PhD pursuit. Further, I would like to express my gratitude for Prof. Peter Terry, Director/Training and Research, USQ for his kind support during my studies at USQ. I also extend my sincere thanks to Professor Achini De Silva, Professor Seiji Nagasaka and Dr. Hao for their support in different stages of my PhD. In addition, I would like to thank Dr. Mamoru Okamoto for supplying the wheat population used in my experiments and Dr. Kolin Harinda Rajapaksha for his great support with the proteomics analysis. I'm truly grateful for Professor Amane Makino and Professor Paul Milham for their support extended during scholarly article preparation. Further, I would like to appreciate the support of Nao Moriyama and Ayaka Fukushima from Toyo University, Japan for their kind support with some of my data analyses. I'm also grateful for Dr. Barbara Harmes, Dr. Marcus Harmes and Dr. Ananda Abeysekara for their great support in improving my academic writing. Additionally, I would like to thank all the staff members in the CCH who have given support over the years.

My deepest thanks go to my research buddy, Michael Thompson who has started his PhD along with me and worked together throughout this entire PhD journey. His great support with my

experiments and as a co-author of my research outputs was remarkable. I would like to extend my love and thanks to all my friends at CCH: Sriram, Barsha, Kiruba, Mela, Joe, Ahmed, Rio and Motiur who were there to share my happy and bitter moments throughout this long journey. Also, I want to give a big shout-out to my junior colleague, Prabuddha who helped and encouraged me in every possible way during this challenging period and pushed me to finish my research and thesis writing work on time. Additionally, I thank Indika, Madhubhashitha and Prasanna for their support.

I am indebted to all my friends in Brisbane and Toowoomba, Australia who were always so helpful in numerous ways. A huge appreciation goes to Dr. Jay Bandara, Gayani Bandara, Dumila Perera, Chaturika Gunatunga, Piyum Herath, Mythree Seneweera and Pramesha Madurangi for their kind support.

I would also like to extend my sincere thanks to my home university; the University of Ruhuna, Sri Lanka for granting me permission to study abroad and strengthen my knowledge and skills in plant science. I must acknowledge all the staff members of the Department of Agricultural Biology, Faculty of Agriculture for taking care of my academic duties while I was on study leave to complete this PhD. My sincere thanks go to all my cousins back home: Thiwanka, Niluka, Tharaka, Nandika and Sampath for taking good care of my family while I was away from Sri Lanka.

Last but not least, my heartfelt love and appreciation go to my dad and sister, Danu who have been by my side throughout this long academic journey from primary school to grad school. Also, today I deeply miss my darling mum who gave me all the courage and inspiration to start this challenging journey. Without their love and encouragement, I would not have finished my thesis successfully.

For me, this PhD journey was a life-changing experience. I deeply treasure every single minute of it and I am truly grateful for all the people who supported me to turn this big dream into a reality.

### **List of publications and submitted articles**

**Gamage, D.**, M. Thompson, M. Sutherland, N. Hirotsu, A. Makino and S. Seneweera (2018). "New insights into the cellular mechanisms of plant growth at elevated atmospheric carbon dioxide." *Plant, cell & environment* 41(6): 1233-1246.

**Gamage D**, Thompson M, Okamoto M, Moriyama N, Sutherland M.W., Hirotsu N, Seneweera S. Early growth mechanism of wheat (*Triticum aestivum* L.) at elevated atmospheric carbon dioxide: New physiological evidence with quantitative trait loci data (Currently under review in *Plant, Cell and Environment*)

### **List of conferences attended and other co-authored scholarly articles during PhD candidature**

**Gamage D**, Thompson M, Okamoto M, Moriyama N, Sutherland M, Hirotsu N, Seneweera S 'Early growth response of wheat (*Triticum aestivum* L.) to elevated atmospheric carbon dioxide: Quantitative trait loci for major growth traits'. Participated in the poster presentations at the *American Society of Plant Biologists' Plant Biology 2017* conference in Honolulu, Hawaii, USA.

Nagai Y, Matsumoto K, Kakinuma Y, Ujiie K, Ishimaru K, **Gamage D**, Thompson D, Milham PJ, Seneweera S and Hirotsu N (2016). "The chromosome regions for increasing early growth in rice: role of sucrose biosynthesis and NH<sub>4</sub><sup>+</sup> uptake." *Euphytica* 211(3): 343-352.

Thompson M, **Gamage D**, Hirotsu N, Martin A & Seneweera S 2017, 'Effects of Elevated Carbon Dioxide on Photosynthesis and Carbon Partitioning: A Perspective on Root Sugar Sensing and Hormonal Crosstalk', *Frontiers in Physiology*, 8:578, 10.3389/fphys.2017.00578.

## Table of Contents

<b>Abstract</b> .....	ii
<b>Certification of Thesis</b> .....	iii
<b>Statement of authorship</b> .....	iv
<b>Acknowledgement</b> .....	vi
<b>List of publications and submitted articles</b> .....	viii
<b>Chapter 1: Introduction and Literature Review</b> .....	1
1.1 Climate change and future projections.....	1
1.2 Wheat production under future climate .....	1
1.3 Plant responses to rising atmospheric [CO <sub>2</sub> ].....	3
1.3.1 Plant photosynthetic responses to elevated [CO <sub>2</sub> ].....	3
1.3.2 Photosynthetic acclimation of C <sub>3</sub> plants to long-term elevated [CO <sub>2</sub> ] exposure .....	3
1.3.3 Post-photosynthetic responses of plants to elevated [CO <sub>2</sub> ].....	4
1.4 CO <sub>2</sub> responsiveness and plant growth stages .....	6
1.5 Knowledge gaps in the understanding of plant growth responses to elevated [CO <sub>2</sub> ] .....	6
1.6 Contribution of the present study to the scientific theory and knowledge .....	8
1.7 Objectives of the study .....	9
1.8 References .....	11
<b>Chapter 2: Literature Review</b> .....	16
<b>Chapter 3: Early growth mechanism of wheat (<i>Triticum aestivum</i> L.) at elevated atmospheric carbon dioxide: New physiological evidence with quantitative trait loci data....</b>	31
<b>Chapter 4: Elevated carbon dioxide mediated early growth responses of wheat (<i>Triticum aestivum</i> L.): an analysis of source and sink interactions .....</b>	82
<b>Chapter 5: Leaf proteome responses of wheat (<i>Triticum aestivum</i> L.) to elevated atmospheric carbon dioxide during early vegetative growth .....</b>	145

<b>Chapter 6: Discussion, Conclusions and Future Directions</b> .....	191
6.1 Significant findings of the study .....	192
6.2 Proposed mechanism for early growth stimulation of wheat at elevated [CO <sub>2</sub> ] .....	194
6.3 Future directions .....	199
6.4 Conclusion.....	201
6.5 References .....	202

## Chapter 1

### Introduction and Literature Review

#### 1.1 Climate change and future projections

Climate change is currently exerting additional pressure on global agricultural productivity and thereby threatens future global food security ([Ainsworth \*et al.\*, 2008](#)). The causes behind climate change are diverse. Increased emission of greenhouse gases such as carbon dioxide (CO<sub>2</sub>), methane (CH<sub>4</sub>), nitrous oxide (N<sub>2</sub>O) and halocarbons into the atmosphere is considered to be one of the main causes behind global climate change ([IPCC, 2007](#)). Among all greenhouse gases, CO<sub>2</sub> contributes more than 70% to global climate change ([IPCC, 2007](#)). The carbon dioxide concentration ([CO<sub>2</sub>]) of the earth's atmosphere has increased since the industrial revolution, with human activities consequently contributing strongly to climate change ([IPCC, 2007](#), [Qaderi & Reid, 2009](#)).

Since the industrial revolution, the atmospheric [CO<sub>2</sub>] has increased by more than 40%, and it is predicted to further increase by the middle of the century ([IPCC, 2013](#)). The current ambient [CO<sub>2</sub>] has already exceeded 400 μmol CO<sub>2</sub> mol<sup>-1</sup> ([Tans & Keeling, 2018](#)) and is expected to reach between 730 to 1020 μmol mol<sup>-1</sup> by 2100 ([Solomon \*et al.\*, 2007](#)). At present, the CO<sub>2</sub> concentration in the atmosphere is linearly increasing. For example, in the past ten years, increase in atmospheric [CO<sub>2</sub>] was recorded at a rate of 2.1 μmol mol<sup>-1</sup> per year, double what was observed in the 1960's ([IPCC, 2007](#)). The increasing atmospheric [CO<sub>2</sub>] has a significant impact on global temperature and thus precipitation patterns; projections predict global temperature will increase by 1.5-4.5°C while the distribution of rainfall decreases ([IPCC, 2007](#)). Changes in [CO<sub>2</sub>], temperature and water balance will influence climate and consequently the balance of ecosystem processes.

#### 1.2 Wheat production under future climate

Wheat is the most widely cultivated cereal crop, an important carbohydrate source, and the most important grain protein source for a majority of the human population. Wheat contains

essential amino acids, minerals, vitamins, beneficial phytochemicals and dietary fiber components required for human nutrition ([Shewry, 2009](#)). It is predicted that the human population will increase to 9.1 billion by 2050, which will require an increase in cereal production of 3 billion tonnes to feed the growing world population ([FAO, 2009](#)). In order to satisfy the global demand for wheat, the production of more than 850 million tonnes by 2030 ([FAO, 2003](#)) is required. However, achieving these targets while conserving the quality will become a challenge under a changing climate. Australia is one of the largest wheat exporters in the world and a majority of arable lands are employed for wheat production. Climate change, including an increase in [CO<sub>2</sub>] in the atmosphere together with high temperatures and reduced average annual rainfall, will affect the Australian wheat industry. It has been demonstrated that increasing temperature together with low precipitation is predicted to reduce the wheat yield by 7 to 16% ([Kokic et al., 2005](#)). However, some of the negative effects of climate stress variables such as water and temperature on plants can be offset by elevated [CO<sub>2</sub>]. This is favorable for the global food production. Gaining a better understanding of the genetic and molecular nature of crop responses to e[CO<sub>2</sub>] will improve breeding programs that can ultimately increase future crop productivity ([Ainsworth et al., 2008](#), [Semenov & Halford, 2009](#), [Tausz et al., 2013](#)).

The majority of plant species, including wheat, fix CO<sub>2</sub> via the C<sub>3</sub> photosynthetic pathway. When [CO<sub>2</sub>] increases in the atmosphere, photosynthesis increases until [CO<sub>2</sub>] reaches the saturation limit ([Sharkey, 1985](#), [Seneweera et al., 2011a](#)). The relationship between photosynthesis to the changing [CO<sub>2</sub>] concentration is well described by the biochemical model of photosynthetic CO<sub>2</sub> assimilation of [Farquhar et al. \(1980\)](#). The model indicates that conserved properties of ribulose 1-5 biphosphate carboxylase/oxygenase (Rubisco), the primary carboxylating enzyme of C<sub>3</sub> plants, is the key to such unique photosynthetic responses to rising [CO<sub>2</sub>]. Current ambient [CO<sub>2</sub>] is very low at the site of fixation and any increase in [CO<sub>2</sub>] will increase the net photosynthesis of C<sub>3</sub> plants ([Drake et al., 1997](#), [Bloom, 2015](#)). Laboratory and field studies have shown that the rate of photosynthesis of C<sub>3</sub> plants is approximately doubled when plants were grown at about 700 μmol mol<sup>-1</sup> in comparison to 400 μmol mol<sup>-1</sup> ([Drake et al., 1997](#), [Ainsworth & Long, 2005](#), [Kant et al., 2012](#)). However, the long-term photosynthesis response to elevated [CO<sub>2</sub>] is highly unpredictable ([Drake et al., 1997](#), [Seneweera et al., 2005](#), [Seneweera et al., 2011a](#)) and depends on nutrient availability, ontogenic stage and genetic background.

### **1.3 Plant responses to rising atmospheric [CO<sub>2</sub>]**

The increase of atmospheric [CO<sub>2</sub>] directly and indirectly affects both the net rate of photosynthesis and stomatal conductance and thereby regulates the growth and development of plants ([Seneweera & Conroy, 2005](#)). As a result of these fundamental processes, changes in other post-photosynthetic metabolic processes that may lead to changes in plant growth responses are observed and are significant; however, the underlying mechanism is not well understood ([Taylor \*et al.\*, 1994](#), [Seneweera \*et al.\*, 2003](#), [Gamage \*et al.\*, 2018](#))

#### **1.3.1 Plant photosynthetic responses to elevated [CO<sub>2</sub>]**

Photosynthetic rate of most C<sub>3</sub> plants increases when plants are grown under elevated [CO<sub>2</sub>] ([Makino & Mae, 1999](#)). In a high [CO<sub>2</sub>] environment, the rate of photosynthesis increases as a result of an improvement in the carboxylation efficiency of Rubisco. The carboxylation efficiency of Rubisco rises due to an increase in the CO<sub>2</sub>/O<sub>2</sub> ratio at the site of CO<sub>2</sub> fixation ([Bowes, 1993](#)). Further, changes in the CO<sub>2</sub>/O<sub>2</sub> ratio leads to a reduction in photorespiration of C<sub>3</sub> plants, i.e., at the present atmospheric oxygen concentration of 21 kPa and [CO<sub>2</sub>] of 400 μmol mol<sup>-1</sup>, a considerable amount of light energy is used up for photorespiration, which reduces photosynthetic rates by 20 to 50% depending on temperature ([Sharkey, 1985](#)). These physiological responses vary between species and within species. Therefore, growth response to elevated [CO<sub>2</sub>] is determined by the plant's capacity to adjust to the [CO<sub>2</sub>] assimilation ([Thilakarathne \*et al.\*, 2013](#), [Thilakarathne \*et al.\*, 2015](#)).

#### **1.3.2 Photosynthetic acclimation of C<sub>3</sub> plants to long-term elevated [CO<sub>2</sub>] exposure**

When plants are exposed to elevated [CO<sub>2</sub>] for an extended period, initial photosynthetic rates are increased. However, the initial stimulation of photosynthetic rates is not always maintained for a longer period ([Sharkey, 1985](#), [Sage \*et al.\*, 1989](#), [Seneweera \*et al.\*, 2011c](#)). This phenomenon is known as “photosynthetic acclimation” and has been widely reported in the literature ([Bowes, 1991](#), [Makino & Mae, 1999](#), [Seneweera \*et al.\*, 2002](#), [Nowak \*et al.\*, 2004](#)). A number of mechanisms have been proposed to explain photosynthetic acclimation. Among them, change in the nitrogen supply to growing leaf blades ([Drake \*et al.\*, 1997](#), [Nakano \*et al.\*, 1997](#), [Seneweera \*et al.\*, 2011b](#)); accumulation of non-structural carbohydrates, leading to the suppression of the photosynthesis-related gene expression through the hexokinase signalling pathway ([Nakano \*et al.\*, 1997](#), [Stitt & Krapp, 1999](#), [Thompson \*et al.\*, 2017](#)); lower nitrogen

demand in leaves due to changes in nitrogen influx/efflux balance in growing tissues ([Seneweera \*et al.\*, 2011b](#)) and lower nitrogen in shoots due to suppression of  $\text{NO}_3^-$  photo-assimilation under e[CO<sub>2</sub>] ([Bloom \*et al.\*, 2012](#)) are considered the main possible causes for accentuated photosynthesis acclimation. However, there is a very limited understanding of how these processes relate to plant nitrogen metabolism, and whether these processes are directly, or indirectly, associated with the impact of [CO<sub>2</sub>] on photosynthesis. This understanding is essential to establish proper breeding approaches to breed crops to adapt to high atmospheric [CO<sub>2</sub>].

### **1.3.3 Post-photosynthetic responses of plants to elevated [CO<sub>2</sub>]**

Increased photosynthetic capacity directly influences several post-photosynthetic key metabolic processes which play key roles in promoting plant growth and development under elevated [CO<sub>2</sub>]. It is suggested that additional carbon supply at elevated [CO<sub>2</sub>] primarily contributes to increased plant growth; however, how this additional carbon supply influences growth and what mechanisms are affected in the leaf or root tissues are still not clearly understood.

Plant growth and development is largely influenced by changes in plant carbon and nitrogen metabolism ([Seneweera & Conroy, 2005](#)). This argument is fully supported by [Leakey \*et al.\* \(2009\)](#). Changes in carbon metabolism are inevitable at elevated [CO<sub>2</sub>], as the additional carbon supply influences carbohydrate synthesis, respiration, storage and remobilization. A proper balance among these mechanisms determines the carbon partitioning to different plant organs and maintains plant growth at the whole plant level. On the other hand, many aspects of plant growth and metabolism are regulated by nitrate, and signals derived from nitrogen metabolism ([Moore \*et al.\*, 1999](#), [Ainsworth \*et al.\*, 2012](#)). Nitrate acts as a resource that accelerates nitrate assimilation, which results in higher levels of amino acids, proteins and decreased levels of starch ([Scheible \*et al.\*, 1997a](#), [Scheible \*et al.\*, 1997b](#)) thus promoting the growth rate of plants. With additional nitrogen supply, plants tend to increase their growth response to elevated [CO<sub>2</sub>], which is mainly regulated through increased plant sink capacity ([Rogers \*et al.\*, 1996](#), [Ainsworth \*et al.\*, 2004](#), [Leakey \*et al.\*, 2009](#)). These findings suggest that the capacity for photosynthesis needs to be matched with other indirect processes that control plant growth, such as plant carbon, nitrogen and hormonal metabolism at elevated [CO<sub>2</sub>].

Research also suggests that elevated [CO<sub>2</sub>] stimulates primary growth of shoots by influencing cell cycle properties, such as increasing the proportion of rapidly dividing cells, shortening the duration of the cell cycle ([Kinsman et al., 1997](#)) and promoting cell production and expansion through cell wall loosening as a result of increased xyloglucan endotransglycosylase (XET) activity under elevated [CO<sub>2</sub>] ([Ranasinghe & Taylor, 1996](#)). [Masle \(2000\)](#) indicated that cell division, cell expansion and cell patterning of plants under elevated [CO<sub>2</sub>] may be influenced by increased substrate availability, which could potentially influence the expression of genes involved in the cell cycle and cell expansion.

Plant growth regulators, including auxins, gibberellins, cytokinins, ethylene and abscisic acid mainly regulate these cellular processes within a cell cycle. Hence, changes in hormonal levels may play a significant role in determining plant growth responses at elevated [CO<sub>2</sub>] ([Yong et al., 2000](#)). Results of several studies suggest that elevated [CO<sub>2</sub>] promotes the synthesis of auxins, gibberellin, cytokines and ethylene by stimulating cell cycle processes and protein synthesis, and thereby plant growth ([Yong et al., 2000](#), [Seneweera et al., 2003](#), [Teng et al., 2006](#)). However, the metabolism of plant growth regulators also depends on the availability of carbohydrate substrate ([Farrar, 1996](#), [Jitla et al., 1997](#), [Taiz & Zeiger, 1998](#), [Kalve et al., 2014](#)). Under elevated [CO<sub>2</sub>], the carbon substrate availability is higher as a result of increased photosynthesis, which is likely to increase hormonal metabolism leading to increased plant growth and development.

Genetic factors can also play a major role in regulating plant growth response to elevated [CO<sub>2</sub>] by influencing both photosynthetic and post-photosynthetic processes. The photosynthetic response is driven through adjustments in the light reaction of photosynthesis and the carbon reduction process. The photosynthetic rate, potential acclimation propensity, carbohydrate synthesis and nitrogen use efficiency of plants varies remarkably between species and within species ([Tausz et al., 2013](#), [Thilakarathne et al., 2013](#), [Thilakarathne et al., 2015](#)). These processes are interlinked and their genetic and physiological plasticity determines the final growth responses observed under elevated [CO<sub>2</sub>] ([Rae et al., 2006](#), [Leakey et al., 2009](#)). Therefore, understanding the underlying genetic mechanisms that determine the growth response to elevated [CO<sub>2</sub>] is essential in order to increase crop growth under rising atmospheric [CO<sub>2</sub>]. However, development of improved crop varieties suitable for future climates will require intensive models that combine phenotypic characteristics with their

underlying genetic architecture; which is lacking in the current scientific literature ([Sadras & Calderini, 2015](#)).

#### **1.4 CO<sub>2</sub> responsiveness and plant growth stages**

CO<sub>2</sub> responsiveness of plants is largely determined by the ontogenetic stage of exposure ([Centritto \*et al.\*, 1999](#), [Stitt & Krapp, 1999](#)). The majority of C<sub>3</sub> species show very high growth response to elevated [CO<sub>2</sub>], especially during the early stages of vegetative development ([Poorter, 1993](#)). Early growth responses to elevated [CO<sub>2</sub>] are usually characterized by accelerated leaf growth and expansion resulting in increased leaf area ratios and relative growth rates ([Poorter, 1993](#), [Makino \*et al.\*, 1997](#)) which positively correlate with biomass accumulation and the final yield ([Thilakarathne \*et al.\*, 2015](#)). It is suggested that increased growth at elevated [CO<sub>2</sub>] results from the initial stimulation of photosynthesis and may decline or disappear over time ([Masle \*et al.\*, 1993](#), [Centritto \*et al.\*, 1999](#), [Trevisan \*et al.\*, 2014](#)). For example, relative growth rates tend to decline, as plants grow older at elevated [CO<sub>2</sub>]. Hence, the effect of elevated [CO<sub>2</sub>] on relative growth rate (RGR) is often time-dependent and occurs only during the early stages of plant growth ([Poorter & Navas, 2003](#)). Studies conducted in wheat ([Neales & Nicholls, 1978](#), [Hikosaka \*et al.\*, 2005](#)), *Arabidopsis* ([Van Der Kooij & De Kok, 1996](#)) and tobacco ([Geiger \*et al.\*, 1998](#)) showed that exposure to elevated [CO<sub>2</sub>] leads to a stimulation of RGR in young plants whereas RGR in older plants remains unaffected. Also, it is suggested that even a 10% increase in RGR at the exponential growth phase of the plant can be converted up to a 50% growth enhancement at elevated [CO<sub>2</sub>] ([Kirschbaum, 2010](#)). Therefore, it is necessary to understand the genetic variation in early growth responses to elevated [CO<sub>2</sub>] in order to improve crop productivity.

#### **1.5 Knowledge gaps in the understanding of plant growth responses to elevated [CO<sub>2</sub>]**

Despite the greater understanding of plant growth and morphological response to elevated [CO<sub>2</sub>], there is a significant knowledge gap in understanding the underlying molecular and physiological mechanisms that drive plant growth. Furthermore, the degree of contribution from photosynthetic and post-photosynthetic processes towards plant growth at elevated [CO<sub>2</sub>] is not clearly understood ([Gordillo \*et al.\*, 2001](#)). Most of the studies on dissecting plant growth mechanisms at elevated [CO<sub>2</sub>] have been focused on the photosynthetic responses, but there has been limited focus on the post-photosynthetic events that lead to subsequent growth and

development of plant tissues, organs and the whole plant ([Taylor et al., 1994](#), [Nunes-Nesi et al., 2010](#), [Gamage et al., 2018](#)).

Several studies have been conducted to investigate plant metabolism ([Leakey et al., 2009](#)), biomass accumulation ([Wang et al., 2012](#)), morphological and structural changes ([Pritchard et al., 1999](#), [Teng et al., 2006](#), [Benlloch-Gonzalez et al., 2014](#)), stress tolerance ([Vanaja et al., 2011](#), [van der Kooi et al., 2016](#)) and changes to different agronomic traits ([Bourgault et al., 2013](#), [O'Leary et al., 2015](#)) under high [CO<sub>2</sub>]; however, little is known about the molecular and physiological mechanisms of how plants respond to elevated [CO<sub>2</sub>] ([Taylor et al., 2001](#), [Huang & Xu, 2015](#), [Thilakarathne et al., 2015](#)).

Understanding the genetic variation of plant responses to elevated [CO<sub>2</sub>] will assist in the selection of plants for fitness and long-term adaptation to climate stress. A clear understanding of the genetic and physiological traits that contribute to an increase in crop productivity under high [CO<sub>2</sub>] environments is also required ([Ward & Kelly, 2004](#), [Tausz et al., 2013](#)). Physiological traits that are important for plant responses to environmental stimuli are mostly quantitative in nature ([Ferris et al., 2002](#)) and determined by a range of gene products. Therefore, identification of quantitative trait loci (QTL) that respond to elevated [CO<sub>2</sub>] can be used as a genetic tool to utilize carbon richness to increase crop productivity ([Rae et al., 2006](#)). This will provide information on whether the trait of interest has an associated genetic component, which can be utilized to capture high [CO<sub>2</sub>] in the atmosphere to increase the crop productivity through plant breeding. Identifying QTL for CO<sub>2</sub> responsiveness will also be a major starting point for future studies on individual genes, genomic regions and inheritance of traits of interest ([Rae et al., 2006](#)). However, only a few studies have been published in order to identify [CO<sub>2</sub>] responsive QTL. [Rae et al. \(2006\)](#) mapped QTL for leaf growth, development, and senescence of poplar trees. Results showed that there was a differential genetic control for traits under elevated [CO<sub>2</sub>]. Furthermore, they suggested that candidate genes co-located in the regions where response QTL were mapped. [Ferris et al. \(2002\)](#) mapped QTL for stomatal initiation, stomatal density, epidermal cell size, number and area in hybrid poplar under elevated [CO<sub>2</sub>]. QTL analysis for above and below ground tree growth and biomass was conducted by [Rae et al. \(2007\)](#) using F<sub>2</sub> hybrids of poplar and they identified important areas of the genome which determine above ground growth response and root growth response to elevated [CO<sub>2</sub>]. To our knowledge, no research studies have been published to date that elucidates the CO<sub>2</sub> responsive genomic regions for plant growth related traits in wheat.

When analyzing the plant growth responses to elevated [CO<sub>2</sub>], changes in the nutritional status, cell cycle regulations and hormonal metabolism cannot be excluded because a dynamic change in C/N relations occurs during plant development. Consequently, changes in carbon and nitrogen metabolism are likely to have a major impact on plant growth processes. For example, a sharp decline in nitrogen uptake occurs at elevated [CO<sub>2</sub>], particularly when plants reach the reproductive stage, as most of the photosynthate is used primarily for syntheses of storage and structural carbohydrates. However, there is a limited understanding on how changes in C/N metabolism interact with source-sink integration and thereby influence plant growth processes at elevated [CO<sub>2</sub>] ([Stitt & Krapp, 1999](#), [Luo \*et al.\*, 2004](#), [Lekshmy \*et al.\*, 2013](#)). With the provision of additional carbon at elevated [CO<sub>2</sub>], significant changes associated with other post-photosynthetic processes such as cell cycle functions and hormonal metabolism, especially at the molecular level is not clearly understood so far ([Gamage \*et al.\*, 2018](#)). Also, much less attention has been paid to investigate the interactions of all these post-photosynthetic processes and their contribution towards determining the source and sink organ integration at the whole plant level ([Gamage \*et al.\*, 2018](#)).

## **1.6 Contribution of the present study to scientific theory and knowledge**

Since there is a significant knowledge gap in understanding the molecular mechanisms of how plants respond to elevated [CO<sub>2</sub>], the experiments in this PhD thesis were designed and conducted to elucidate the underlying molecular mechanisms. This study focussed on dissecting the growth mechanisms of wheat (*Triticum aestivum* L.) in the early vegetative growth stages, as the CO<sub>2</sub> responsiveness of C<sub>3</sub> crops is comparatively high at this growth stage. Knowledge generated from this project will provide new insights into improving early vigor and growth characteristics of wheat, in a changing climate. With this purpose, three different strategies were employed to characterize the molecular growth mechanisms: (i) putative chromosomal locations regulating CO<sub>2</sub> responsiveness were determined through QTL mapping for different plant growth traits under elevated [CO<sub>2</sub>]; (ii) the impact of post-photosynthetic processes to enhanced growth responses at elevated [CO<sub>2</sub>] were determined using physiological and molecular approaches; (iii) interactions among photosynthetic and post-photosynthetic processes together with their contribution to improving plant growth at elevated [CO<sub>2</sub>] was investigated using physiological and proteomics approaches. Overall, this

project will advance our knowledge on mechanisms controlling plant growth response to elevated [CO<sub>2</sub>] and provide insights into the genetic factors that can be selected to increase crop productivity in a future CO<sub>2</sub> enriched atmosphere.

### **1.7 Objectives of the study**

Wheat is one of the most cultivated cereal crops showing a variable response to increasing levels of [CO<sub>2</sub>] in the atmosphere. Growth and yield stimulation of wheat in response to elevated [CO<sub>2</sub>] have shown a high intraspecific variation, suggesting that enhanced photosynthetic capacity may not be the only factor determining final growth and yield of a crop at elevated [CO<sub>2</sub>]. Therefore, it is necessary to establish the overall physiological and molecular mechanisms of how plant growth changes in response to rising [CO<sub>2</sub>]. Although there have been significant efforts to characterize the underlying physiological mechanisms of growth responses to elevated [CO<sub>2</sub>], not much is known about these mechanisms. Thus, this PhD project broadly aims to identify the underlying molecular mechanisms that regulate the plant growth responses to elevated [CO<sub>2</sub>]. To achieve this overall aim, this study was broken down into three specific objectives as outlined below.

1. Elucidate QTL associated with plant growth responses to elevated [CO<sub>2</sub>] in wheat using a doubled haploid (DH) population

It has been suggested that the identification of new functional traits associated with higher responses to elevated [CO<sub>2</sub>] is essential to improve crop productivity under a changing climate. Therefore, identification of QTL that respond to elevated [CO<sub>2</sub>] will be useful in identifying the genetic components associated with different growth traits and their regulation under rising atmospheric CO<sub>2</sub>. Incorporation of CO<sub>2</sub>-response QTL into marker-assisted selection will be beneficial in crop breeding strategies for future climate. To date, there has been no research conducted to elucidate genomic regions/QTL determining enhanced growth traits observed at elevated [CO<sub>2</sub>] in wheat. As CO<sub>2</sub> responsiveness is higher during the early vegetative stage, identification of QTL governing early growth will aid in improving growth habit and early vigour of wheat under CO<sub>2</sub> enriched conditions.

2. Determine the contribution of post-photosynthetic metabolic processes to enhanced plant growth responses at elevated [CO<sub>2</sub>] using selected DH lines that differ in CO<sub>2</sub> responsiveness

It is well established that growth stimulation at elevated [CO<sub>2</sub>] arises from the increased photosynthetic capacity of plants. This photosynthetic stimulation regulates other post-photosynthetic processes such as carbon and nitrogen metabolism and cell cycle functions that collectively contribute to whole plant growth. Elevated [CO<sub>2</sub>] impacts on plant growth even at the transcript level and thereby determines the protein synthesis that governs these important metabolic activities. However, there is limited understanding of how these key metabolic processes change in response to increased photosynthetic capacity, especially at the transcript level and their association with enhanced plant growth responses observed under high [CO<sub>2</sub>]. Therefore, to serve this objective, a series of experiments were conducted to develop an understanding of transcript level changes to post-photosynthetic processes, plant response to increased sugar supply and growth responses at elevated [CO<sub>2</sub>].

3. Investigate the interplay among photosynthesis and post-photosynthesis metabolic processes and their impact on improving plant growth at elevated [CO<sub>2</sub>] using physiological and proteomic approaches

A number of research studies have been conducted to understand the underlying physiological mechanisms of plant growth and development at elevated [CO<sub>2</sub>]. Plant response to environmental stimuli such as elevated [CO<sub>2</sub>] is a result of a complex interplay of different metabolic processes through various regulatory enzymes, metabolic proteins and other biomolecules. Analysis of the whole proteome of particular plant organs will provide an opportunity to identify the protein profile expressed at a given time. This will provide important information regarding the functionality of the proteome and thus, determine the protein network associated with the growth of a particular plant organ at elevated [CO<sub>2</sub>]. To our knowledge, no previous research studies have investigated leaf proteome changes in response to elevated [CO<sub>2</sub>]. The results of this study will serve as a preliminary report in this regard and will help to better understand the underlying molecular mechanisms of plant growth at elevated [CO<sub>2</sub>].

## 1.8 References

- Ainsworth E.A., Beier C., Calfapietra C., Ceulemans R., Durand-Tardif M., Farquhar G.D., Godbold D.L., Hendrey G.R., Hickler T. & Kaduk J. (2008) Next generation of elevated [CO<sub>2</sub>] experiments with crops: a critical investment for feeding the future world. *Plant, cell & environment*, **31**, 1317-1324.
- Ainsworth E.A. & Long S.P. (2005) What have we learned from 15 years of free-air CO<sub>2</sub> enrichment (FACE)? A meta-analytic review of the responses of photosynthesis, canopy properties and plant production to rising CO<sub>2</sub>. *New Phytologist*, **165**, 351-372.
- Ainsworth E.A., Rogers A., Nelson R. & Long S.P. (2004) Testing the “source–sink” hypothesis of down-regulation of photosynthesis in elevated [CO<sub>2</sub>] in the field with single gene substitutions in *Glycine max*. *Agricultural and Forest Meteorology*, **122**, 85-94.
- Ainsworth E.A., Yendrek C.R., Skoneczka J.A. & Long S.P. (2012) Accelerating yield potential in soybean: Potential targets for biotechnological improvement. *Plant, Cell and Environment*, **35**, 38-52.
- Benlloch-Gonzalez M., Berger J., Bramley H., Rebetzke G. & Palta J.A. (2014) The plasticity of the growth and proliferation of wheat root system under elevated CO<sub>2</sub>. *Plant and soil*, **374**, 963-976.
- Bloom A.J. (2015) Photorespiration and nitrate assimilation: a major intersection between plant carbon and nitrogen. *Photosynthesis research*, **123**, 117-128.
- Bloom A.J., Asensio J.S.R., Randall L., Rachmilevitch S., Cousins A.B. & Carlisle E.A. (2012) CO<sub>2</sub> enrichment inhibits shoot nitrate assimilation in C<sub>3</sub> but not C<sub>4</sub> plants and slows growth under nitrate in C<sub>3</sub> plants. *Ecology*, 355-367.
- Bourgault M., Dreccer M.F., James A.T. & Chapman S.C. (2013) Genotypic variability in the response to elevated CO<sub>2</sub> of wheat lines differing in adaptive traits. *Functional Plant Biology*, **40**, 172-184.
- Bowes G. (1991) Growth at Elevated CO<sub>2</sub> - Photosynthetic Responses Mediated Through Rubisco. *Plant Cell and Environment*, **14**, 795-806.
- Bowes G. (1993) Facing the inevitable: Plants and increasing atmospheric CO<sub>2</sub>. *Annual Review of Plant Physiology and Plant Molecular Biology*, **44**, 309-332.
- Centritto M., Lee H.S. & Jarvis P. (1999) Increased growth in elevated [CO<sub>2</sub>]: an early, short-term response? *Global Change Biology*, **5**, 623-633.
- Drake B.G., González-Meler M.A. & Long S.P. (1997) More efficient plants: a consequence of rising atmospheric CO<sub>2</sub>? *Annual review of plant biology*, **48**, 609-639.
- FAO (2003) *World agriculture: towards 2015/2030, an FAO perspective*. Earthscan publication Ltd.
- FAO (2009) *How to feed the world in 2050*. Food and Agriculture Organization, High Level Expert Forum.
- Farquhar G., von Caemmerer S.v. & Berry J. (1980) A biochemical model of photosynthetic CO<sub>2</sub> assimilation in leaves of C<sub>3</sub> species. *Planta*, **149**, 78-90.
- Farrar J. (1996) Regulation of root weight ratio is mediated by sucrose: opinion. *Plant and Soil*, **185**, 13-19.
- Ferris R., Long L., Bunn S., Robinson K., Bradshaw H., Rae A. & Taylor G. (2002) Leaf stomatal and epidermal cell development: identification of putative quantitative trait loci in relation to elevated carbon dioxide concentration in poplar. *Tree Physiology*, **22**, 633-640.
- Gamage D., Thompson M., Sutherland M., Hirotsu N., Makino A. & Seneweera S. (2018) New insights into the cellular mechanisms of plant growth at elevated atmospheric carbon dioxide. *Plant, cell & environment*, **41(6)**, 1233-1246.

- Geiger M., Walch-Liu P., Engels C., Harnecker J., Schulze E.D., Ludewig F., Sonnewald U., Scheible W.R. & Stitt M. (1998) Enhanced carbon dioxide leads to a modified diurnal rhythm of nitrate reductase activity in older plants, and a large stimulation of nitrate reductase activity and higher levels of amino acids in young tobacco plants. *Plant, Cell & Environment*, **21**, 253-268.
- Gordillo F.J., Niell F.X. & Figueroa F.L. (2001) Non-photosynthetic enhancement of growth by high CO<sub>2</sub> level in the nitrophilic seaweed *Ulva rigida* C. Agardh (Chlorophyta). *Planta*, **213**, 64-70.
- Hikosaka K., Onoda Y., Kinugasa T., Nagashima H., Anten N.P.R. & Hirose T. (2005) Plant responses to elevated CO<sub>2</sub> concentration at different scales: Leaf, whole plant, canopy, and population. *Ecological Research*, **20**, 243-253.
- Huang B. & Xu Y. (2015) Cellular and Molecular Mechanisms for Elevated CO<sub>2</sub>—Regulation of Plant Growth and Stress Adaptation. *Crop Science*, **55**, 1405-1424.
- IPCC (2007) *Climate change 2007: The physical science basis*. Cambridge University Press, Cambridge.
- IPCC (2013) Summary for Policymakers. In: *Climate Change 2013: The Physical Science Basis. Contribution of Working Group I to the Fifth Assessment Report of the Intergovernmental Panel on Climate change*. In: [Stocker, T.F., D. Qin, G.-K. Plattner, M. Tignor, S.K. Ailen, J. Boschung, A. Nauels, Y. Xia, V. Bex and P.M. Midgley (eds.)]. Cambridge University Press, Cambridge, United Kingdom and New York, NY, USA.
- Jitla D.S., Rogers G.S., Seneweera S.P., Basra A.S., Oldfield R.J. & Conroy J.P. (1997) Accelerated early growth of rice at elevated CO<sub>2</sub>. *Plant Physiology*, **115**, 15-22.
- Kalve S., De Vos D. & Beemster G.T. (2014) Leaf development: a cellular perspective. *Front Plant Sci*, **5**, 362.
- Kant S., Seneweera S., Rodin J., Materne M., Burch D., Rothstein S.J. & Spangenberg G. (2012) Improving yield potential in crops under elevated CO<sub>2</sub>: integrating the photosynthetic and nitrogen utilization efficiencies. *Frontiers in plant science*, **3**, 1-9.
- Kinsman E., Lewis C., Davies M., Young J., Francis D., Vilhar B. & Ougham H. (1997) Elevated CO<sub>2</sub> stimulates cells to divide in grass meristems: a differential effect in two natural populations of *Dactylis glomerata*. *Plant, Cell & Environment*, **20**, 1309-1316.
- Kirschbaum M.U. (2010) Does Enhanced Photosynthesis Enhance Growth? Lessons Learnt From CO<sub>2</sub> Enrichment Studies. *Plant physiology*, pp. 110.166819.
- Kocic P., Heaney A., Pechey L., Crimp S. & Fisher B.S. (2005) Climate change predicting on agriculture: a case study. *Australian Commodities: Forecasts and Issues*, **12**.
- Leakey A.D., Ainsworth E.A., Bernacchi C.J., Rogers A., Long S.P. & Ort D.R. (2009) Elevated CO<sub>2</sub> effects on plant carbon, nitrogen, and water relations: six important lessons from FACE. *Journal of experimental botany*, **60**, 2859-2876.
- Lekshmy S., Jain V., Khetarpal S. & Pandey R. (2013) Inhibition of nitrate uptake and assimilation in wheat seedlings grown under elevated CO<sub>2</sub>. *Indian Journal of Plant Physiology*, **18**, 23-29.
- Luo Y., Su B., Currie W.S., Dukes J.S., Finzi A., Hartwig U., Hungate B., McMurtrie R.E., Oren R. & Parton W.J. (2004) Progressive nitrogen limitation of ecosystem responses to rising atmospheric carbon dioxide. *Bioscience*, **54**, 731-739.
- Makino A., Harada M., Sato T., Nakano H. & Mae T. (1997) Growth and N allocation in rice plants under CO<sub>2</sub> enrichment. *Plant Physiology*, **115**, 199-203.
- Makino A. & Mae T. (1999) Photosynthesis and plant growth at elevated levels of CO<sub>2</sub>. *Plant and Cell Physiology*, **40**, 999-1006.
- Masle J. (2000) The effects of elevated CO<sub>2</sub> concentrations on cell division rates, growth patterns, and blade anatomy in young wheat plants are modulated by factors related to leaf position, vernalization, and genotype. *Plant Physiology*, **122**.

- Masle J., Hudson G.S. & Badger M.R. (1993) Effects of ambient CO<sub>2</sub> concentration on growth and nitrogen use in tobacco (*Nicotiana tabacum*) plants transformed with an antisense gene to the small subunit of ribulose-1, 5-bisphosphate carboxylase/oxygenase. *Plant Physiology*, **103**, 1075-1088.
- Moore B.D., Cheng S.H., Sims D. & Seemann J.R. (1999) The biochemical and molecular basis for photosynthetic acclimation to elevated atmospheric CO<sub>2</sub>. *Plant Cell and Environment*, **22**, 567-582.
- Nakano H., Makino A. & Mae T. (1997) The effect of elevated partial pressures of CO<sub>2</sub> on the relationship between photosynthetic capacity and N content in rice leaves. *Plant physiology*, **115**, 191-198.
- Neales T. & Nicholls A. (1978) Growth Responses on Young Wheat Plants to a Range of Ambient CO<sub>2</sub> Levels. *Functional Plant Biology*, **5**, 45-59.
- Nowak R.S., Ellsworth D.S. & Smith S.D. (2004) Functional responses of plants to elevated atmospheric CO<sub>2</sub>—do photosynthetic and productivity data from FACE experiments support early predictions? *New Phytologist*, **162**, 253-280.
- Nunes-Nesi A., Fernie A.R. & Stitt M. (2010) Metabolic and signaling aspects underpinning the regulation of plant carbon nitrogen interactions. *Molecular Plant*, **3**, 973-996.
- O'Leary G.J., Christy B., Nuttall J., Huth N., Cammarano D., Stöckle C., Basso B., Shcherbak I., Fitzgerald G. & Luo Q. (2015) Response of wheat growth, grain yield and water use to elevated CO<sub>2</sub> under a Free-Air CO<sub>2</sub> Enrichment (FACE) experiment and modelling in a semi-arid environment. *Global change biology*, **21**, 2670-2686.
- Poorter H. (1993) Interspecific variation in the growth response of plants to an elevated ambient CO<sub>2</sub> concentration. *Vegetatio*, **104**, 77-97.
- Poorter H. & Navas M.L. (2003) Plant growth and competition at elevated CO<sub>2</sub>: on winners, losers and functional groups. *New Phytologist*, **157**, 175-198.
- Pritchard S.G., Rogers H.H., Prior S.A. & Peterson C.M. (1999) Elevated CO<sub>2</sub> and Plant Structure: A Review. *Global Change Biology*, **5**, 807-837.
- Qaderi M.M. & Reid D.M. (2009) Crop responses to elevated carbon dioxide and temperature. In: *Climate Change and Crops*, pp. 1-18. Springer.
- Rae A., Ferris R., Tallis M. & Taylor G. (2006) Elucidating genomic regions determining enhanced leaf growth and delayed senescence in elevated CO<sub>2</sub>. *Plant, Cell & Environment*, **29**, 1730-1741.
- Rae A.M., Tricker P.J., Bunn S.M. & Taylor G. (2007) Adaptation of tree growth to elevated CO<sub>2</sub>: quantitative trait loci for biomass in *Populus*. *New Phytologist*, **175**, 59-69.
- Ranasinghe S. & Taylor G. (1996) Mechanism for increased leaf growth in elevated CO<sub>2</sub>. *Journal of Experimental Botany*, **47**, 349-358.
- Rogers G., Milham P., Gillings M. & Conroy J. (1996) Sink strength may be the key to growth and nitrogen responses in N-deficient wheat at elevated CO<sub>2</sub>. *Functional Plant Biology*, **23**, 253-264.
- Sadras V.O. & Calderini D. (2015) *Crop Physiology: Applications for Genetic Improvement and Agronomy*. Elsevier USA.
- Sage R.F., Sharkey T.D. & Seemann J.R. (1989) Acclimation of photosynthesis to elevated CO<sub>2</sub> in five C<sub>3</sub> species. *Plant Physiology*, **89**, 590-596.
- Scheible W.-R., Gonzalez-Fontes A., Lauerer M., Muller-Rober B., Caboche M. & Stitt M. (1997a) Nitrate acts as a signal to induce organic acid metabolism and repress starch metabolism in tobacco. *The Plant Cell*, **9**, 783-798.
- Scheible W.R., Lauerer M., Schulze E.D., Caboche M. & Stitt M. (1997b) Accumulation of nitrate in the shoot acts as a signal to regulate shoot-root allocation in tobacco. *The Plant Journal*, **11**, 671-691.

- Semenov M.A. & Halford N.G. (2009) Identifying target traits and molecular mechanisms for wheat breeding under a changing climate. *Journal of Experimental Botany*, **60**, 2791-2804.
- Seneweera S., Aben S., Basra A., Jones B. & Conroy J. (2003) Involvement of ethylene in the morphological and developmental response of rice to elevated atmospheric CO<sub>2</sub> concentrations. *Plant growth regulation*, **39**, 143-153.
- Seneweera S., Ghannoum O., Conroy J., Ishimaru K., Okada M., Lieffering M., Kim H.Y. & Kobayashi K. (2002) Changes in source–sink relations during development influence photosynthetic acclimation of rice to free air CO<sub>2</sub> enrichment (FACE). *Functional plant biology*, **29**, 947-955.
- Seneweera S., Makino A., Hirotsu N., Norton R. & Suzuki Y. (2011a) New insight into photosynthetic acclimation to elevated CO<sub>2</sub>: The role of leaf nitrogen and ribulose-1,5-bisphosphate carboxylase/oxygenase content in rice leaves. *Environmental and Experimental Botany*, **71**, 128-136.
- Seneweera S., Makino A., Hirotsu N., Norton R. & Suzuki Y. (2011b) New insight into photosynthetic acclimation to elevated CO<sub>2</sub>: The role of leaf nitrogen and ribulose-1,5-bisphosphate carboxylase/oxygenase content in rice leaves. *Environmental and Experimental Botany*, **71**, 128-136.
- Seneweera S., Makino A., Hirotsu N., Norton R. & Suzuki Y. (2011c) New insight into photosynthetic acclimation to elevated CO<sub>2</sub>: The role of leaf nitrogen and ribulose-1,5-bisphosphate carboxylase/oxygenase content in rice leaves. *Environmental and Experimental Botany*, **71**, 128-136.
- Seneweera S., Makino A., Mae T. & Basra A.S. (2005) Response of rice to p(CO<sub>2</sub>) enrichment: the relationship between photosynthesis and nitrogen metabolism. *Journal of Crop Improvement*, **13**, 31-53.
- Seneweera S.P. & Conroy J.P. (2005) Enhanced leaf elongation rates of wheat at elevated CO<sub>2</sub>: is it related to carbon and nitrogen dynamics within the growing leaf blade? *Environmental and experimental botany*, **54**, 174-181.
- Sharkey T.D. (1985) Photosynthesis in intact leaves of C<sub>3</sub> plants: physics, physiology and rate limitations. *The Botanical Review*, **51**, 53-105.
- Shewry P. (2009) Wheat. *Journal of experimental botany*, **60**, 1537-1553.
- Solomon S., Qin D. & Manning R. (2007) *Technical summary. Climate Change 2007: The Physical Science Basis*.
- Stitt M. & Krapp A. (1999) The interaction between elevated carbon dioxide and nitrogen nutrition: the physiological and molecular background. *Plant, Cell & Environment*, **22**, 583-621.
- Taiz L. & Zeiger E. (1998) *Plant Physiology*. Sinauer Associates, Sunderland, Massachusetts, USA.
- Tans P. & Keeling R. (2018) Trends in atmospheric carbon dioxide. NOAA/ESRL ([www.esrl.noaa.gov/gmd/ccgg/trends/](http://www.esrl.noaa.gov/gmd/ccgg/trends/))
- Tausz M., Tausz-Posch S., Norton R.M., Fitzgerald G.J., Nicolas M.E. & Seneweera S. (2013) Understanding crop physiology to select breeding targets and improve crop management under increasing atmospheric CO<sub>2</sub> concentrations. *Environmental and Experimental Botany*, **88**, 71-80.
- Taylor G., Ceulemans R., Ferris R., Gardner S. & Shao B. (2001) Increased leaf area expansion of hybrid poplar in elevated CO<sub>2</sub>. From controlled environments to open-top chambers and to FACE. *Environmental Pollution*, **115**, 463-472.
- Taylor G., Ranasinghe S., Bosac C., Gardner S.D.L. & Ferris R. (1994) Elevated CO<sub>2</sub> and plant growth: cellular mechanisms and responses of whole plants. *Journal of Experimental Botany*, **45**, 1761-1774.

- Teng N., Wang J., Chen T., Wu X., Wang Y. & Lin J. (2006) Elevated CO<sub>2</sub> induces physiological, biochemical and structural changes in leaves of *Arabidopsis thaliana*. *New Phytologist*, **172**, 92-103.
- Thilakarathne C.L., Tausz-Posch S., Cane K., Norton R.M., Fitzgerald G.J., Tausz M. & Seneweera S. (2015) Intraspecific variation in leaf growth of wheat (*Triticum aestivum*) under Australian Grain Free Air CO<sub>2</sub> Enrichment (AGFACE): is it regulated through carbon and/or nitrogen supply? *Functional Plant Biology*, **42**, 299-308.
- Thilakarathne C.L., Tausz-Posch S., Cane K., Norton R.M., Tausz M. & Seneweera S. (2013) Intraspecific variation in growth and yield response to elevated CO<sub>2</sub> in wheat depends on the differences of leaf mass per unit area. *Functional Plant Biology*, **40**, 185-194.
- Thompson M., Gamage D., Hirotsu N., Martin A. & Seneweera S. (2017) Effects of Elevated Carbon Dioxide on Photosynthesis and Carbon Partitioning: A Perspective on Root Sugar Sensing and Hormonal Crosstalk. *Frontiers in Physiology*, **8**, 578.
- Trevisan S., Manoli A. & Quaggiotti S. (2014) NO signaling is a key component of the root growth response to nitrate in *Zea mays* L. *Plant Signaling and Behavior*, **9**.
- van der Kooij C.J., Reich M., Löw M., De Kok L.J. & Tausz M. (2016) Growth and yield stimulation under elevated CO<sub>2</sub> and drought: A meta-analysis on crops. *Environmental and Experimental Botany*, **122**, 150-157.
- Van Der Kooij T.A. & De Kok L. (1996) Impact of elevated CO<sub>2</sub> on growth and development of *Arabidopsis thaliana* L. *Phyton\_Horn-*, **36**, 173-184.
- Vanaja M., Yadav S., Archana G., Lakshmi N.J., Reddy P.R., Vagheera P., Razak S.A., Maheswari M. & Venkateswarlu B. (2011) Response of C<sub>4</sub> (maize) and C<sub>3</sub> (sunflower) crop plants to drought stress and enhanced carbon dioxide concentration. *Plant, Soil and Environment*, **57**, 207-215.
- Wang D., Heckathorn S.A., Wang X. & Philpott S.M. (2012) A meta-analysis of plant physiological and growth responses to temperature and elevated CO<sub>2</sub>. *Oecologia*, **169**, 1-13.
- Ward J.K. & Kelly J.K. (2004) Scaling up evolutionary responses to elevated CO<sub>2</sub>: lessons from *Arabidopsis*. *Ecology Letters*, **7**, 427-440.
- Yong J.W.H., Wong S.C., Letham D.S., Hocart C.H. & Farquhar G.D. (2000) Effects of elevated CO<sub>2</sub> and nitrogen nutrition on cytokinins in the xylem sap and leaves of cotton. *Plant Physiology*, **124**, 767-779.

## Chapter 2

### Literature Review

In addition to the literature review in Chapter 1, this thesis also has a published literature review entitled “New insights into the cellular mechanisms of plant growth at elevated atmospheric carbon dioxide”. This review discusses the effect of elevated [CO<sub>2</sub>] on photosynthetic and post-photosynthetic metabolic processes and their relationship with the growth enhancement observed in a high CO<sub>2</sub> environment. This chapter focusses on the cellular and molecular level responses associated with plant growth at elevated [CO<sub>2</sub>]. The review first discusses the changes of two fundamental metabolic processes, photosynthesis and stomatal conductance, and how they are affected by elevated [CO<sub>2</sub>] at the cellular level. Then, this review focussed on the effect of elevated [CO<sub>2</sub>] on post-photosynthetic key metabolic processes that govern plant growth, such as carbon metabolism, nitrogen metabolism, cell cycle functions and hormonal regulation. Additionally, we discuss how plants integrate these mechanisms with source and sink activity and thereby alter plant anatomy and morphology. Finally, the knowledge gaps and potential future research are highlighted to provide the readers an understanding of what needs to be further investigated to further elucidate the molecular mechanisms underlying plant growth responses to elevated [CO<sub>2</sub>].

**Gamage D**, Thompson M, Sutherland M, Hirotsu N, Makino A, Seneweera S (2018) New insights into the cellular mechanisms of plant growth at elevated atmospheric carbon dioxide. *Plant, cell & environment* 41(6):1233-1246.

# New insights into the cellular mechanisms of plant growth at elevated atmospheric carbon dioxide concentrations

Dananjali Gamage<sup>1,4</sup>  | Michael Thompson<sup>1</sup>  | Mark Sutherland<sup>1</sup> | Naoki Hirotsu<sup>1,2</sup>  | Amane Makino<sup>3</sup>  | Saman Seneweera<sup>1,4†</sup> 

<sup>1</sup>Centre for Crop Health, University of Southern Queensland, Toowoomba, Queensland 4350, Australia

<sup>2</sup>Faculty of Life Sciences, Toyo University, Oura-gun, Gunma 374-0193, Japan

<sup>3</sup>Division of Life Sciences, Graduate School of Agricultural Science, Tohoku University, Tsutsumidori-Amamiyamachi, Sendai 981-8555, Japan

<sup>4</sup>Department of Agricultural Biology, Faculty of Agriculture, University of Ruhuna, Kamburupitiya 81 100, Sri Lanka

## Correspondence

S. Seneweera Centre for Crop Health, University of Southern Queensland, Toowoomba Queensland 4350 Australia.  
Email: Saman.Seneweera@usq.edu.au

## Funding information

University of Southern Queensland

## Abstract

Rising atmospheric carbon dioxide concentration ( $[CO_2]$ ) significantly influences plant growth, development, and biomass. Increased photosynthesis rate, together with lower stomatal conductance, has been identified as the key factors that stimulate plant growth at elevated  $[CO_2]$  ( $e[CO_2]$ ). However, variations in photosynthesis and stomatal conductance alone cannot fully explain the dynamic changes in plant growth. Stimulation of photosynthesis at  $e[CO_2]$  is always associated with post-photosynthetic secondary metabolic processes that include carbon and nitrogen metabolism, cell cycle functions, and hormonal regulation. Most studies have focused on photosynthesis and stomatal conductance in response to  $e[CO_2]$ , despite the emerging evidence of  $e[CO_2]$ 's role in moderating secondary metabolism in plants. In this review, we briefly discuss the effects of  $e[CO_2]$  on photosynthesis and stomatal conductance and then focus on the changes in other cellular mechanisms and growth processes at  $e[CO_2]$  in relation to plant growth and development. Finally, knowledge gaps in understanding plant growth responses to  $e[CO_2]$  have been identified with the aim of improving crop productivity under a  $CO_2$  rich atmosphere.

## KEYWORDS

carbon metabolism, cell cycle, climate change, elevated  $[CO_2]$  ( $e[CO_2]$ ), hormonal metabolism, nitrogen metabolism, photosynthesis, plant growth mechanism, source-sink interactions

## 1 | INTRODUCTION: OPPORTUNITIES AND CHALLENGES IN A CARBON DIOXIDE ENRICHED ATMOSPHERE

The world's population is expected to increase by 2.3 billion between 2009 and 2050, requiring significant increases in global food production to fulfil future food demand (Alexandratos & Bruinsma, 2012). Current and predicted changes in climate render the achievement of food production targets even more challenging. The continuing rapid increase in atmospheric  $[CO_2]$ , due to a range of anthropogenic

factors, including the burning of fossil fuels and deforestation, is a major driver for the current changes in climate (Qaderi & Reid, 2009). Since preindustrial times, atmospheric  $[CO_2]$  has increased more than 40% and a similar magnitude of increase is expected by the end of this century (IPCC, 2013). Current ambient  $[CO_2]$  now exceeds 400  $\mu\text{mol/mol}$  (Tans & Keeling, 2018) and is expected to increase even more causing significant changes in global temperature and thereby precipitation patterns. According to current projections, global temperature will increase by 1.4–3.1 °C when atmospheric  $[CO_2]$  reaches ~670  $\mu\text{mol/mol}$  (IPCC, 2013). The long-term exposure of plants to elevated  $[CO_2]$  ( $e[CO_2]$ ), high temperature, and water deficits will significantly influence the balance of ecosystem processes both at the regional and global level.

Carbon dioxide is the primary substrate for photosynthesis and thus can be considered as the main driver of global food production.

**Abbreviations:**  $[CO_2]$ , carbon dioxide concentration;  $e[CO_2]$ , elevated  $[CO_2]$ ;  $O_2$ , oxygen; Rubisco, ribulose-1,5-bisphosphate carboxylase/oxygenase

†Author contributions: D. M. G. (50%), M. T. (5%), M. W. S. (10%), N. H. (10%), A. M. (5%), and S. S. (20%). D. G. wrote the manuscript. M. T., M. S., N. H., A. M., and S. S. each contributed to the design and review of the final manuscript.

Nearly 90% of known plant species belong to the  $C_3$  biochemical type and are not photosynthetically saturated at the current  $CO_2$  partial pressure; therefore, photosynthesis and biomass of these species can be expected to increase under  $e[CO_2]$  conditions (Kimball, 2016; Makino & Mae, 1999). In  $C_3$  plants, photosynthesis is catalysed by Ribulose-1,5-bisphosphate carboxylase/oxygenase (Rubisco), an enzyme which reacts with both  $CO_2$  and oxygen ( $O_2$ ), initiating photosynthetic carbon reduction and photorespiratory carbon oxidation cycles, respectively (Drake, González-Meler, & Long, 1997; Makino & Mae, 1999). The efficiency of both processes is dependent on the relative partial pressures of  $CO_2$  and  $O_2$  at the site of fixation (Lorimer, 1981). Rubisco has a higher affinity for  $CO_2$  than  $O_2$ , and often, Rubisco carboxylation is the rate-limiting step in  $C_3$  photosynthesis. Increased carboxylation of Rubisco inhibits photorespiration, indirectly aiding photosynthetic rates (Makino & Mae, 1999). Photorespiration is the process that involves the oxygenation of Ribulose-1,5-bisphosphate by Rubisco, which significantly wastes energy produced by photosynthesis (Makino & Mae, 1999; Walker, VanLoocke, Bernacchi, & Ort, 2016). Photosynthesis, respiration, and water relations are the three primary physiological processes of plants influenced by  $e[CO_2]$ . Therefore, understanding the fine and coarse control of photosynthesis, respiration, and water use, and their impact on plant growth under a  $CO_2$  rich atmosphere provides a unique opportunity to improve crop productivity under a changing climate.

Laboratory and field experiments have demonstrated that  $C_3$  photosynthesis approximately doubles when plants grown at  $\sim 380 \mu\text{mol/mol}$ , are exposed to  $700 \mu\text{mol/mol}$  of  $CO_2$  (Drake et al., 1997). Changes in plant growth and phenology at  $e[CO_2]$  are well documented across  $C_3$  and  $C_4$  species (Ainsworth & Long, 2005; Ainsworth & Rogers, 2007; Kimball, 2016). However, these growth traits are complex; so an understanding of the different organizational level responses to  $e[CO_2]$  is necessary to develop new breeding strategies. Although plant growth and morphology tend to change with increased atmospheric  $[CO_2]$ , these responses cannot be fully explained by the direct effects

of  $e[CO_2]$  on photosynthesis, respiration, and water use alone (Geiger et al., 1998; Taylor, Ceulemans, Ferris, Gardner, & Shao, 2001; Thilakarathne et al., 2015). In this review, we have focused on the mechanisms by which increased carbon supply at  $e[CO_2]$  influences a range of plant growth processes and cellular functions and their relation to changes in plant growth, development, and phenology.

## 2 | MECHANISMS OF PLANT GROWTH RESPONSES TO ELEVATED $[CO_2]$

Elevated  $[CO_2]$  directly and/or indirectly affects plant growth and development by modifying a range of physiological processes. Plant growth at  $e[CO_2]$  changes due to the immediate effects of  $e[CO_2]$  on photosynthesis and stomatal conductance (Ainsworth et al., 2008; Drake et al., 1997; Seneweera & Conroy, 2005; Figure 1). On the other hand, plant growth at  $e[CO_2]$  also depends on the post-photosynthetic process that may lead to changes in carbon and nitrogen metabolism, changes in cell cycle properties, and hormonal metabolism as a result of increased supply of carbon to the growing shoots and roots under  $e[CO_2]$  (Figure 2). For example, increases in photosynthetic carbon assimilation could be offset by changes in investment in photosynthetic proteins as a consequence of foliar adjustments to plant carbon and nitrogen metabolism at  $e[CO_2]$ . Most of the research has tended to focus on changes in photosynthesis and stomatal conductance in response to  $e[CO_2]$  whereas very less attention has been paid to variations in other cellular mechanisms that may moderate plant growth response to  $e[CO_2]$ . Changes in carbon and nitrogen metabolism, cell cycle properties, and hormonal metabolism together with source-sink optimization at  $e[CO_2]$  are significant and largely determine the growth responses of plants to  $e[CO_2]$  (Seneweera, Aben, Basra, Jones, & Conroy, 2003; Taylor, Ranasinghe, Bosac, Gardner, & Ferris, 1994). Holistic changes of these processes are complex, closely interrelated, and determine the growth responses by differential allocation of

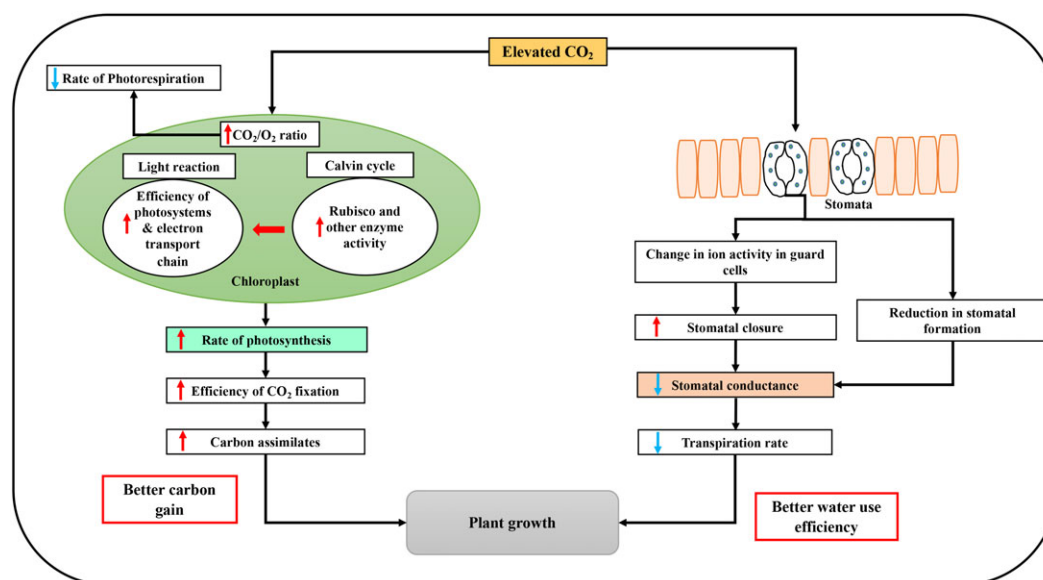


**FIGURE 1** Effects of  $CO_2$ -induced photosynthesis and stomatal conductance on plant growth responses (Green circle = chloroplast; orange squares = epidermal cells; half circles = stomata; red arrow denotes an increase; and blue arrow denotes a decrease)

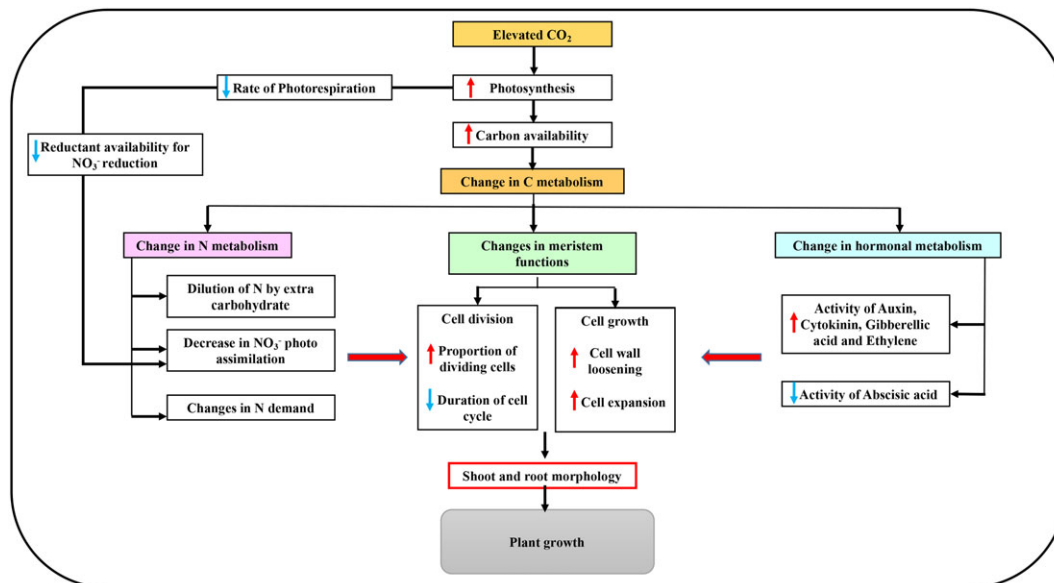


**FIGURE 2** Effect of increased carbon supply at elevated  $[\text{CO}_2]$  on other cellular processes and plant growth responses (C = Carbon; N = Nitrogen;  $\text{NO}_3^-$  = Nitrate; red arrow denotes an increase; and blue arrow denotes a decrease) [Colour figure can be viewed at [wileyonlinelibrary.com](http://wileyonlinelibrary.com)]

resources to shoot and root depending on the environmental conditions. A thorough understanding of these processes and their association with high carbon input will advance our knowledge of the mechanistic basis of differential plant phenology observed at  $e[\text{CO}_2]$ .

### 3 | PRIMARY EFFECTS OF ELEVATED $[\text{CO}_2]$ ON PLANTS—PHOTOSYNTHESIS AND STOMATAL CONDUCTANCE

#### 3.1 | Photosynthesis

Elevated  $[\text{CO}_2]$  increases photosynthetic rates and thereby crop growth and yield. The main reason for this enhanced photosynthesis is the increased carboxylation efficiency of Rubisco, which is relatively low at the current atmospheric  $[\text{CO}_2]$ . However, at  $e[\text{CO}_2]$ , the increase in  $\text{CO}_2$  concentration at the site of  $\text{CO}_2$  fixation will increase the  $\text{CO}_2/\text{O}_2$  ratio; thus, the carboxylation efficiency of Rubisco will be promoted by lowering the rate of photorespiration (Bowes, 1991; Figure 1). The efficiency of photosystems I and II (PSI and PSII) is increased at  $e[\text{CO}_2]$  and correlates well with the rate of photosynthesis, producing more adenosine triphosphate (ATP) and nicotinamide adenine dinucleotide phosphate (NADPH), the two most vital components required to activate photosynthetic enzymes at  $e[\text{CO}_2]$  (Van Heerden, Swanepoel, & Krüger, 2007; Zhang et al., 2008). It has also been demonstrated that PSII yield (number of photochemical products produced per energy quantum) is higher when plants are exposed to  $e[\text{CO}_2]$  (Habash, Paul, Parry, Keys, & Lawlor, 1995), suggesting that light utilization efficiency increased at  $e[\text{CO}_2]$ ; consequently, electron flow between PSI and PSII also increased under  $e[\text{CO}_2]$  (Sekhar, Sreeharsha, & Reddy, 2015). These findings suggest the possibility of improving photosynthesis at  $e[\text{CO}_2]$  without interfering with the photosynthetic light reaction.

When plants are exposed to  $e[\text{CO}_2]$ , a number of genes and proteins associated with photosynthesis are differentially expressed. Genes involved in the light reaction of photosynthesis, encoding for PSII core proteins such as *PSII protein K*, essential for the function and assembly of the PSII reaction centre, have been up-regulated under  $e[\text{CO}_2]$  (De Souza et al., 2008; Moore, Cheng, Rice, & Seemann, 1998). In addition, Ferredoxin-1, an electron donor to  $\text{NADP}^+$  reductase, showed increased expression under  $e[\text{CO}_2]$  (Oosten & Besford, 1995). In addition, Vicente et al. (2015) reported that genes encoding for putative *PSI P700 Chl a apoprotein A1 (PsaA)*, *apoprotein A2 (PsaB)*, *PSII protein D1* and *D2* are up-regulated in durum wheat under  $e[\text{CO}_2]$ . Increases in the expression of genes and proteins related to the light reaction of photosynthesis suggest that photochemical efficiency of photosystems is increased under  $e[\text{CO}_2]$ . However, several studies showed that transcript levels of genes and proteins involved in light dependent (i.e., chlorophyll a/b binding proteins of light harvesting complexes I and II; Nie, Hendrix, Webber, Kimball, & Long, 1995; Oosten, Wilkins, & Besford, 1994) and light independent reactions (several Calvin cycle enzymes) of photosynthesis have been down-regulated in response to prolonged exposure to  $e[\text{CO}_2]$  (S.-H. Cheng, d Moore, & Seemann, 1998; Moore et al., 1998; Nie et al., 1995). However, more detailed studies are required to establish both photosynthesis light reaction and dark reaction responses to  $e[\text{CO}_2]$ . Further, genes associated with photosynthetic carbon metabolism have been differentially expressed under  $e[\text{CO}_2]$ . For example, genes encoding fructose-1,6-bisphosphatase, transketolase, and aldolase enzymes involved in ribulose-1,5-bisphosphate regeneration were up-regulated at  $e[\text{CO}_2]$  (Wei et al., 2013). In  $\text{C}_4$  species, several enzymes associated with the light reaction of photosynthesis, for example, *NADP-malate dehydrogenase* and *pyruvate phosphate dikinase*, were up-regulated by 117% and 174% respectively at  $e[\text{CO}_2]$  14 days after leaf emergence in sugarcane followed by up-regulation of genes associated with sucrose metabolism (Vu, Allen, & Gesch, 2006). This study further

showed that key enzymes involved in photosynthesis and sucrose metabolism are up-regulated at  $e[\text{CO}_2]$ , particularly during the early stages of plant development suggesting that  $C_4$  plants behave like  $C_3$  during early leaf development. All these findings suggest the possibility to improve photosynthesis by taking advantage of the  $\text{CO}_2$  rich atmosphere.

The initial stimulation of photosynthetic rates at  $e[\text{CO}_2]$  is not always maintained over a longer period (Sage, Sharkey, & Seemann, 1989; Seneweera, 2011; Sharkey, 1985). This phenomenon is known as “photosynthetic acclimation” and has been widely reported in the literature (Alonso, Pérez, & Martínez-Carrasco, 2009; Gutiérrez et al., 2009; Martínez-Carrasco, Pérez, & Morcuende, 2005; Nakano, Makino, & Mae, 1997; Seneweera et al., 2002). A number of mechanisms have been proposed to explain plant acclimation to  $e[\text{CO}_2]$ . These include decline in nitrogen supply to the growing leaf blades (Drake et al., 1997; Nakano et al., 1997; Seneweera, Makino, Hirotsu, Norton, & Suzuki, 2011), accumulation of non-structural carbohydrates that suppress photosynthesis-related gene expression (Nakano et al., 1997; Stitt & Krapp, 1999), lower nitrogen demand in leaves due to changes in nitrogen influx/efflux balance in growing tissues (Seneweera et al., 2011), and lower shoot nitrogen due to suppression of nitrate ( $\text{NO}_3^-$ ) photo-assimilation (Bloom et al., 2012). Overall, it has been suggested that the most reasonable explanation of photosynthetic acclimation to  $e[\text{CO}_2]$  is the suppression of nitrogen assimilation at  $e[\text{CO}_2]$  (Bloom et al., 2012). In addition, photosynthetic acclimation will become even more pronounced when there is insufficient sink strength in the plant to accommodate increasing photo-assimilates at  $e[\text{CO}_2]$  (P. Li, Ainsworth et al., 2008). For example, this phenomenon was evaluated by Ainsworth, Rogers, Nelson, and Long (2004) using soybean (*Glycine max*) lines showing both determinate and indeterminate growth habit and found acclimation was more prominent in lines with determinate growth habit. This suggests that plants that are able to expand their sink capacity to utilize photo-assimilates efficiently may be more likely to sustain increased photosynthetic rates at  $e[\text{CO}_2]$ .

Leaf photosynthesis is closely correlated with both the Rubisco and nitrogen content of the leaf blade (Makino & Mae, 1999; Vicente et al., 2015). The amount of Rubisco in leaves is determined by both synthesis and degradation, and it is regulated by internal and external factors. The decline in Rubisco content at  $e[\text{CO}_2]$  is known to be often associated with the accumulation of non-structural carbohydrates (Seneweera et al., 2011). However, a negative relationship between photosynthesis and soluble sugar content has not always been reported (Makino, Nakano, Mae, Shimada, & Yamamoto, 2000). Functional Rubisco has a small and large subunit, and down-regulation of genes encoding for both sub-units (*rbcS* and *rbcL*) has been observed for many species under  $e[\text{CO}_2]$  (Takatani et al., 2014; Vicente et al., 2015). The widely accepted hypothesis for the reduced Rubisco content at  $e[\text{CO}_2]$  is the repression of the *rbcS* and *rbcL* gene expression (S.-H. Cheng et al., 1998; Moore, Cheng, Sims, & Seemann, 1999; Rolland, Moore, & Sheen, 2002; Sheen, 1994). Rubisco activase, the protein required to activate the Rubisco complex, has been reported to decrease under  $e[\text{CO}_2]$  (Bokhari et al., 2007), which could compromise the activation state of the enzyme. Further, there have been reports of a decline in transcript abundance of Rubisco activase and

two Calvin Cycle enzymes, ribulose-phosphate-3-epimerase and ribose-phosphate isomerase, which may influence the turnover of Rubisco and thus the continuance of the photosynthesis mechanism (Kontunen-Soppela et al., 2010; Leakey et al., 2009). Finally, photosynthesis is largely controlled by its related protein turnover; however, there is a limited understanding of how photosynthesis-related protein turnover is influenced by  $e[\text{CO}_2]$  (Seneweera, Makino, Mae, & Basra, 2005).

### 3.2 | Stomatal conductance

Stomatal conductance is mainly controlled by the size of the stomatal aperture (Ainsworth & Rogers, 2007); number of stomata per unit of leaf area (Casson & Gray, 2008; Casson & Hetherington, 2010); and water transport capacity of the guard cell (Leakey et al., 2009). Stomatal conductance is decreased in crops exposed to  $e[\text{CO}_2]$  (Ainsworth & Long, 2005; Leakey et al., 2009; Figure 1). The size of the stomatal aperture is mainly determined by the turgor pressure of guard cells, which is mediated through ion concentration (Araújo, Fernie, & Nunes-Nesi, 2011). It is reported that  $e[\text{CO}_2]$  increases the activity of outward rectifying  $\text{K}^+$  channels relative to that of inward rectifying  $\text{K}^+$  channels, causing stomatal closure (Brearley, Venis, & Blatt, 1997). Elevated  $[\text{CO}_2]$  also stimulates  $\text{Cl}^-$  release from guard cells and increases  $\text{Ca}^{2+}$  concentration within them (Brearley et al., 1997; Webb, McAinsh, Mansfield, & Hetherington, 1996). These changes help to depolarize the membrane potential of guard cells causing stomatal closure (Hanstein & Felle, 2002), which is very common under  $e[\text{CO}_2]$ . It has also been demonstrated that  $e[\text{CO}_2]$  increases the concentration of malate, the effector mediating flux flow between  $\text{CO}_2$  and these anion channels (Hedrich et al., 1994). Modified malate concentrations under  $e[\text{CO}_2]$  enhance the activation potential of anion channels, thus indirectly influencing stomatal closure. Because  $e[\text{CO}_2]$  is known to promote anion channels, attempts have been made to identify genes encoding guard cell anion channels.

Stomatal guard cell responses to  $e[\text{CO}_2]$  are also driven by multiple signalling components associated with guard cell activity. Because  $e[\text{CO}_2]$  is known to promote anion channels, attempts have been made to identify genes encoding guard cell anion channels. As a result, *SLAC1* (Slow Anion Channel Associated 1) was identified in *Arabidopsis thaliana* that encodes a protein mediating  $\text{CO}_2$  induced stomatal closure through regulating S-type anion channels (Laanemets et al., 2013; Negi et al., 2008; Vahisalu et al., 2008). *SLAC1* is activated by the gene *OST1* (open stomata 1) that is a SNF-1 related protein kinase 2, a positive regulator of  $\text{CO}_2$ -induced stomatal closure (Lind et al., 2015; Merilo et al., 2013). Activation of *OST1* is triggered by abscisic acid (ABA) signalling at  $e[\text{CO}_2]$  involving *PYR/RCAR* family of ABA receptors (Chater et al., 2015; Merilo et al., 2013; Merilo, Jalakas, Kollist, & Brosché, 2015). In another study, Yamamoto et al. (2016) showed that *SLAC1* channel perceives  $\text{CO}_2$  signals by an ABA-independent pathway in a transmembrane region of the guard cells. In addition, it has been reported that other phytohormones such as jasmonic acids are altered at  $e[\text{CO}_2]$ . Jasmonic acid is known to play a significant role in mediating stomatal closure at  $e[\text{CO}_2]$  (Geng et al., 2016). A very recent study by He et al. (2018) revealed that a novel allele of the *Arabidopsis* *BIG* locus named *cis1* is involved as a signalling component responsible

for controlling stomatal aperture at  $e[\text{CO}_2]$ . Further, they indicated that loss of *BIG* function compromises activation of guard cell S-type anion channels by bicarbonate at  $e[\text{CO}_2]$ .

Recent studies indicate that redox signalling, which includes reactive oxygen species produced by NADPH oxidases encoded by respiratory burst oxidase homologs, has a key role in determining stomatal conductance and density at  $e[\text{CO}_2]$  (Chater et al., 2015). Carbonic anhydrases also appear to have a role in the regulation of stomatal movement. These enzymes catalyse the conversion of  $\text{CO}_2$  to bicarbonate ( $\text{HCO}_3^-$ ), which functions as a molecular activator of *SLAC1* anion channels in the guard cells (Xue et al., 2011). Consistent with this proposition is the finding that expression of *CA1* and *CA4* ( $\beta$ -carbonic anhydrase 1 and 4) was significantly higher in guard cells at  $e[\text{CO}_2]$  (Hu et al., 2010; Xue et al., 2011). Mutants that lack these genes showed reduced  $\text{CO}_2$ -induced stomatal movements and increased stomatal density indicating that these genes play a key role in determining both stomatal movement and development (Hu et al., 2010). Additionally, studies in *Arabidopsis thaliana* revealed that protein kinase HT1 (High Leaf Temperature 1; Hashimoto et al., 2006; Hashimoto-Sugimoto et al., 2016), RHC1 (resistant to high  $\text{CO}_2$ , a MATE type transporter that link  $e[\text{CO}_2]$  with repression of HT1; Tian et al., 2015), and mitogen activated protein kinase (MPK4 and MPK12; Hörak et al., 2016; Jakobson et al., 2016) are strongly related to  $\text{CO}_2$ -induced stomatal closure. Another hypothesis for guard cell activity is based on the high levels of sucrose produced at  $e[\text{CO}_2]$  (Kang, Outlaw, Andersen, & Fiore, 2007; Kelly et al., 2013). When sucrose production rate exceeds the sucrose loading rate to the phloem at  $e[\text{CO}_2]$ , excess sucrose will be transported to the stomata via transpiration flow stimulating stomatal closure through hexokinase mediated expression of ABA-related genes (Kelly et al., 2013). Further, these authors showed that increased expression of hexokinase in guard cells is associated with the  $\text{CO}_2$  induced stomatal closure; however, the role of sugars in regulating stomatal regulation deserves further exploration.

Stomatal density is also vital for determining the efficiency of photosynthesis and water use in plants. Decreased stomatal numbers have been observed in a wide range of species at  $e[\text{CO}_2]$  (Casson & Gray, 2008; Casson & Hetherington, 2010; Woodward & Kelly, 1995). Further, molecular evidence indicates that  $e[\text{CO}_2]$  impedes stomatal development in plants. Gray et al. (2000) identified the *HIC* (High Carbon Dioxide) gene from *Arabidopsis thaliana* that encodes for an enzyme called putative 3-keto acyl coenzyme A synthase that negates stomatal development in response to  $e[\text{CO}_2]$ . In another study, Kim et al. (2006) demonstrated that the *SDD1* gene, which encodes for putative subtilisin serine protease, was down-regulated under  $e[\text{CO}_2]$ . This protein is involved in signal processing that contributes to guard cell formation and development. These changes at the molecular level are likely to contribute towards the reduction of stomatal formation under  $e[\text{CO}_2]$ . In addition, the expression of genes encoding water transport proteins, such as aquaporins, is suppressed in the guard cells of some plants under  $e[\text{CO}_2]$  (Gupta et al., 2005; Wei et al., 2013). Such adjustments of guard cell chemistry may have a major impact on the reduced stomatal conductance and thus an improvement in water use efficiency of the plant under  $e[\text{CO}_2]$ . At the same time, several other aquaporins, such as tonoplast intrinsic

protein 1 (*TIP1*), are up-regulated in stems and leaves (Ainsworth, Rogers, Vodkin, Walter, & Schurr, 2006; Wei et al., 2013). These findings suggest that  $e[\text{CO}_2]$  can facilitate intercellular and vascular water transport that may eventually contribute to improved water use efficiency of plants.

## 4 | IMPACT OF ELEVATED $[\text{CO}_2]$ ON OTHER CELLULAR MECHANISMS AND ITS INFLUENCE ON PLANT GROWTH

### 4.1 | Effects of elevated $[\text{CO}_2]$ on plant carbon metabolism

Carbon metabolism at  $e[\text{CO}_2]$  is collectively determined by photosynthesis, respiration, sugar storage, and remobilization capacity (Aranjuelo et al., 2015). In general,  $\text{C}_3$  photosynthesis increases at  $e[\text{CO}_2]$  but the magnitude of the response can change with plant developmental stages and prevailing environmental conditions (Leakey et al., 2009). Also, increased photosynthesis rates at  $e[\text{CO}_2]$  results in higher sugar production, including glucose, fructose, and raffinose, across a range of plant species (Aranjuelo et al., 2015; Watanabe et al., 2013). These additional sugars are available for development of new sink organs such as leaves, stems, tillers, and seeds. The developmental plasticity of these organs determines the final growth response to  $e[\text{CO}_2]$ . However, plant responses to  $e[\text{CO}_2]$  are much greater at early vegetative stages compared with later stages (Makino, Harada, Sato, Nakano, & Mae, 1997; Seneweera et al., 2002). This ontological variation is largely determined by sink activity and varies with both species and environmental conditions (J. Y. Li, Liu et al., 2008).

Enzymes associated with plant carbon metabolism play a key role in determining sink activity. For example, sucrose phosphate synthase (SPS) and sucrose synthase (SUS) are the key enzymes regulating sucrose biosynthesis and transport in most terrestrial plants (Koch, 2004; Rogers, Millham, Gillings, & Conroy, 1996; Seneweera, Basra, Barlow, & Conroy, 1995). It has been reported that starch to sucrose ratio in leaves correlates well with SPS activity (Chávez-Bárceñas et al., 2000), and up-regulation of both SUS and SPS proteins occurs especially in young fully expanded leaves under  $e[\text{CO}_2]$  (Aoki et al., 2003; W.-H. Cheng, Im, & Chourey, 1996; Gesch, Vu, Boote, Hartwell Allen, & Bowes, 2002; Seneweera et al., 1995). In addition, specific genes related to SUS (*RSus1*) and SPS (*sps1*) were found to be highly expressed under  $e[\text{CO}_2]$  in rice (J. Y. Li, Liu, et al., 2008). These findings suggest that  $e[\text{CO}_2]$  increases sucrose biosynthesis in many species. However, the rate of sucrose biosynthesis depends on a range of physiological and environmental factors. Plants have evolved strategies to translocate soluble sugars away from leaves, which reduces starch accumulation in the leaf blade. Starch accumulation in the leaves leads to feedback inhibition of photosynthesis at  $e[\text{CO}_2]$ . It has also been identified that the ratio of starch to sucrose is a good indicator of plant acclimation to  $e[\text{CO}_2]$  (Sharkey, Laporte, Lu, Weise, & Weber, 2004) and suggests that lower starch to sucrose ratios could be used as a breeding target to increase crop productivity under  $e[\text{CO}_2]$ .

## 4.2 | Change of nitrogen metabolism at elevated [CO<sub>2</sub>]

Long-term growth responses to e[CO<sub>2</sub>] are largely determined by nitrogen supply (Seneweera et al., 2011; Seneweera & Conroy, 2005; Stitt & Krapp, 1999; Takatani et al., 2014). However, the nitrogen concentration of plants decreases at e[CO<sub>2</sub>] (Stitt & Krapp, 1999; Takatani et al., 2014), especially in leaf tissues (Seneweera, 2011). The decrease in leaf nitrogen is not due to a simple dilution effect caused by a relative increase in plant carbohydrates but could be due to a decrease in allocation of nitrogen to leaves at the whole plant level. It has been observed that e[CO<sub>2</sub>] changes nitrogen allocation to different organs, reduces the partitioning to leaves, while increasing allocation to leaf sheaths and roots (Seneweera, 2011). However, the mechanism(s) by which e[CO<sub>2</sub>] decreases tissue concentrations of nitrogen and protein are not fully understood as growth at e[CO<sub>2</sub>] can affect multiple processes involved in nitrogen metabolism (Stitt & Krapp, 1999; Takatani et al., 2014). Vicente et al. (2015) showed down-regulation of transcripts for key enzymes of nitrogen uptake, deamination and assimilation [glutamate dehydrogenase (*GDH1*); aspartate synthetase (*ASN1*), ferredoxin-nitrate reductase (*nir*)], and nitrate transporters [low-affinity nitrate transporter (*NRT1.5B*)] may have contributed to a low nitrogen status at e[CO<sub>2</sub>]. A widely documented cause for this change in nitrogen is that e[CO<sub>2</sub>] increases the rate of carbohydrate production and consequently increases the carbon to nitrogen ratio of plants (Geiger, Haake, Ludewig, Sonnewald, & Stitt, 1999; Paul & Driscoll, 1997; Seneweera et al., 2002; Seneweera & Conroy, 2005). This increase in carbon to nitrogen ratio results in increased initial growth rates of plants, which is later hindered by nitrogen limitation under e[CO<sub>2</sub>].

Several mechanisms have been proposed to explain lower nitrogen concentration in plant shoots at e[CO<sub>2</sub>] (Figure 2): dilution of nitrogen by extra carbohydrates (Gifford, Barrett, & Lutze, 2000); reduction in nitrogen uptake relative to carbon gain (BassiriRad, Gutschick, & Lussenhop, 2001; Del Pozo et al., 2007; Vuuren et al., 1997); reduction of plant nitrogen demand (Stitt & Krapp, 1999); ontogenetic drift leading to changes in nitrogen balance (Bernacchi, Thompson, Coleman, & McConaughay, 2007; Coleman, McConaughay, & Bazzaz, 1993); and changes in NO<sub>3</sub><sup>-</sup> photo-assimilation (Bloom, 2015; Bloom, Smart, Nguyen, & Searles, 2002). Of these, the most reasonable explanation is the reduction in nitrogen influx to above-ground plant organs by lowered NO<sub>3</sub><sup>-</sup> photo-assimilation and down-regulation of gene expression through sugar sensing and signalling pathways. Plants exposed to e[CO<sub>2</sub>] accumulate excess soluble sugars, which are known to influence gene expression associated with plant carbon and nitrogen metabolism (Lastdrager, Hanson, & Smeekens, 2014; Smeekens, Ma, Hanson, & Rolland, 2010). Together with these responses, e[CO<sub>2</sub>] also reduces the transpiration flow through lowered stomatal conductance which then lowers the passive nutrient transport to the plant shoots (McDonald, Erickson, & Kruger, 2002). Hence, the nitrogen inflow to the plant shoots is reduced significantly at e[CO<sub>2</sub>].

Rubisco is the rate-limiting enzyme in photosynthesis, it accounts for nearly 50% of soluble nitrogen in leaves (Makino, Mae, & Ohira, 1984; Spreitzer & Salvucci, 2002). A high turnover of this enzyme is the key to maintaining the photosynthetic rates at e[CO<sub>2</sub>], which is

influenced by many environmental factors such as nitrogen availability, water availability, and temperature. Synthesis of this enzyme is controlled by transcriptional, posttranscriptional, and translational processes. The degradation is mainly controlled by various chloroplast proteolytic enzymes. It has been reported that Rubisco synthesis is reduced at e[CO<sub>2</sub>] whereas its degradation is accelerated. The major cause of decreased synthesis of Rubisco is suggested to be associated with the sugar sensing mechanism based on the hexokinase signalling pathway that can suppress transcription of *rbcS* and *rbcL* genes encoding the small and large subunit of Rubisco, respectively (S.-H. Cheng et al., 1998; Jang, León, Zhou, & Sheen, 1997; Makino et al., 1984). However, Seneweera and Conroy (2005) have suggested that among the number of other mechanisms contributing to lower shoot nitrogen, lower NO<sub>3</sub><sup>-</sup> photo-assimilation at e[CO<sub>2</sub>] may reduce the nitrogen flux into the leaf blade and thereby reduce Rubisco synthesis. These authors further proposed another possibility via an increase in the proteolytic enzyme activity in the chloroplasts (Seneweera et al., 2005), but its physiological relevance and the regulation of these proteases are still not well understood. However, a greater understanding of Rubisco turnover during leaf development is essential to improve crop productivity under CO<sub>2</sub> rich atmosphere.

## 4.3 | Influence of elevated [CO<sub>2</sub>] on cell cycle and cell wall properties

The cell cycle is the series of events that take place in a cell leading to cell division. All organisms are composed of one or more cells; cells are the fundamental units of structure and function in all living organisms. The cell cycle is influenced by various environmental factors including [CO<sub>2</sub>] (Kinsman et al., 1997; Figure 2). For example, increased cell division, shortening of the duration of the cell cycle, promotion of cell production, and expansion through cell wall loosening is reported at e[CO<sub>2</sub>] (Ranasinghe & Taylor, 1996). In another study, Masle (2000) demonstrated that cell division, cell expansion, and cell patterning are altered by e[CO<sub>2</sub>]. It has been suggested that high carbon supply at e[CO<sub>2</sub>] may contribute to accelerated cell division and expansion in meristematic tissues and enhance early growth and development of the plant (Thilakarathne et al., 2015).

Elevated [CO<sub>2</sub>] influences the expression of genes associated with cell division, growth, and cell wall properties. In particular, genes encoding for expansins, pectin esterase, and xyloglucan endotransglycosylase, which play a key role in cell wall loosening, are up-regulated at e[CO<sub>2</sub>] and thus facilitate leaf expansion (De Souza et al., 2008; Gupta et al., 2005; Taylor et al., 2005; Wei et al., 2013). On the other hand, gene expression of B-xylosidase, an enzyme responsible for hemicellulose metabolism of secondary cell walls, is down-regulated at e[CO<sub>2</sub>] (Kontunen-Soppela et al., 2010). Down-regulation of secondary wall construction enzymes is likely to contribute to cell wall extensibility and cell growth. Further, it has been found that cell cycle genes encoding cyclin, cyclin-dependent protein kinase, cyclin-dependent protein kinase regulator, and tubulin were up-regulated at e[CO<sub>2</sub>], together with ribosomal protein genes that regulate cytoplasm growth of plant cells (Ainsworth et al., 2006; Wei et al., 2013). Up-regulation of these enzymes involved in the cell cycle and in cytoplasmic growth may contribute to increase cell division,

growth, and expansion of plant cells observed under  $e[\text{CO}_2]$ . However, limited information is available on transcriptome level responses to  $e[\text{CO}_2]$ , and such information may allow us to have a better understanding of how the cell cycle changes in response to  $e[\text{CO}_2]$ . A clear understanding of whether this increased activity related to the cell cycle is just a general downstream effect of more photo-assimilates being available for growth, or occurs because of divergence in gene expression mediated by increased sugar levels, needs to be established.

#### 4.4 | Source-sink relationship and trehalose-6-phosphate signalling at elevated $[\text{CO}_2]$

Plant growth responses to  $\text{CO}_2$  enrichment are also linked to the source-sink status of the whole plant (Makino & Mae, 1999). Elevated  $[\text{CO}_2]$  increases the carbon source activity that results in a higher rate of photosynthetic  $\text{CO}_2$  assimilation providing more carbohydrates for metabolism (Paul & Foyer, 2001). As a result of this increase in substrate availability and up-regulation of genes encoding proteins involved in sucrose catabolism, sink activity of the plants is directly promoted (Pollock & Farrar, 1996). High sink activity of plants can be clearly observed at  $e[\text{CO}_2]$ , especially during early stages of growth (Ainsworth & Rogers, 2007; Leakey et al., 2009; Ranasinghe & Taylor, 1996), influencing cell expansion, patterning, and plant structure (Kinsman et al., 1997; Masle, 2000). The increased levels of carbohydrates at  $e[\text{CO}_2]$  are efficiently used by plants to develop additional sinks such as new tillers and secondary shoots to accommodate the photo-assimilates generated by photosynthesis (Jitla et al., 1997; Makino & Mae, 1999). When the sink strength is not sufficient to accommodate all the assimilates from photosynthesis, sugar accumulation in source tissues will decrease the photosynthesis rates through feedback inhibition. This will reduce the ratio of source to sink activity and adjust the photo-assimilate production towards an equilibrium. Therefore, both source and sink activities are strongly cross-regulated to sustain desirable plant growth rates at different development stages (Körner, 2015).

There is considerable evidence for this proposition that changes in growth responses to  $e[\text{CO}_2]$  depend on the relationship between the photosynthetic rate of source tissue and the sugar demand of the sink tissue of the plant. For example, canopy defoliation in  $e[\text{CO}_2]$  treatments that reduced the source to sink ratio, resulted in high photosynthetic rates being maintained in the remaining source leaves alleviating photosynthesis acclimation (Ainsworth et al., 2003; Rogers et al., 1998). Because the production from source leaves was less compared with the demand of the sink tissues, a higher rate of photosynthesis was maintained in the remaining tissues to sustain the equilibrium. On the other hand, a reverse response can be observed when the sink size of the plants is reduced through physical restrictions (Arp, 1991) or genetic manipulation (Ainsworth et al., 2004) that leads to an increase in the source to sink ratio. In this case, plants initially increase photosynthetic rates followed by down-regulation of photosynthetic activity due to the inadequate sink capacity (Ainsworth & Bush, 2011; White, Rogers, Rees, & Osborne, 2015). Hence, photosynthetic stimulation and growth at  $e[\text{CO}_2]$  directly depend on the sink strength and its ability to make use of additional sucrose supply at  $e[\text{CO}_2]$ .

The production and consumption of the photo-assimilates (predominantly sucrose) is a dynamic process and varies according to environmental conditions, and the metabolic demands of the plant. Thus, plants need to maintain a fast and precise balance between source and sink while adjusting them over the long run to sustain their growth (Lawlor & Paul, 2014). The mechanistic understanding of the integration of source/sink interaction with the processes of carbon assimilation is still a long-running debate (Lawlor & Paul, 2014; Paul & Pellny, 2003). One mechanism linking these two processes involves trehalose-6-phosphate (T6P), a signal molecule that influences the basic metabolism of plant proteins (Paul, 2007; Paul, Primavesi, Jhurrea, & Zhang, 2008). Trehalose-6-phosphate is an intermediate in glucose synthesis, generated from glucose-6-phosphate (G6P) and UDP-glucose in the presence of trehalose-6-phosphate synthase1 (TPS1; Lastdrager et al., 2014). It is essential for the vegetative growth of plants and the concentration of T6P is dependent on the sucrose concentration (Lawlor & Paul, 2014; van Dijken, Schlupepmann, & Smeekens, 2004). When sucrose concentration is high, such as in plants grown at  $e[\text{CO}_2]$ , high T6P availability will influence SnRK1, a SNF1-related protein kinase which is a key sensor regulating the balance of anabolic and catabolic processes in cells (Schlupepmann, Berke, & Sanchez-Perez, 2011; Y. Zhang et al., 2009). The rising T6P content will inhibit the activity of SnRK1 resulting in an increase in anabolic processes stimulating growth and development of the cells and thereby the plant production (Lawlor & Paul, 2014). Therefore, growth stimulation observed at  $e[\text{CO}_2]$  could be due to this strong correlation between sucrose, T6P content, and the T6P/SnRK1 signalling process. In response to high sucrose content generated at  $e[\text{CO}_2]$ , plants tend to alter their source-sink balance, and species with increased growth plasticity will thrive well in  $\text{CO}_2$  rich conditions (White et al., 2015). This could partly explain the large variation in growth responses that exists between and within species at  $e[\text{CO}_2]$ . Recently, Paul, Oszvald, Jesus, Rajulu, and Griffiths (2017) have highlighted the possibility of modifying T6P content to alter carbon allocation as an approach to improve the yield potential of cereal crops in a changing climate.

#### 4.5 | Plant hormonal metabolism is influenced by elevated $[\text{CO}_2]$

Plant hormones play a major role in modifying plant development at  $e[\text{CO}_2]$  (Gupta et al., 2005; Teng et al., 2006; De Souza et al., 2008; Wei et al., 2013; Figure 2). Few studies have investigated the effect of long-term  $e[\text{CO}_2]$  on endogenous hormone production in plants. Woodrow and Grodzinski (1993) and Seneweera et al. (2003) demonstrated that plants exposed to  $e[\text{CO}_2]$  produce higher levels of ethylene than plants grown under ambient  $[\text{CO}_2]$ . Further, the same plants had a greater capacity to convert ACC (1-aminocyclopropane-1-carboxylic acid) oxidase to ethylene (Seneweera et al., 2003). This conversion is mediated by ACC oxidase that was highly expressed when plants were exposed to  $e[\text{CO}_2]$ . Accumulation of ACC oxidase is higher under  $e[\text{CO}_2]$  as this enzyme has an absolute requirement of  $[\text{CO}_2]$  for its activation, and thus contributes to high levels of ethylene production (Finlayson & Reid, 1996). It has been demonstrated that an increase in ethylene production is a key feature of

accelerated growth and development in rice under  $e[\text{CO}_2]$  that accelerates tiller number and auxiliary bud development, potentially leading to higher grain yield (Seneweera et al., 2003). Despite the importance of ethylene in response to  $e[\text{CO}_2]$ , little in-depth investigation has been carried out exploring its role in plant growth responses to  $e[\text{CO}_2]$ .

Auxins, gibberellic acids, and cytokinins are important plant hormones that synergistically regulate cell division, cell expansion, control shoot meristem development, and stem elongation (Cato, Macedo, & Peres, 2013). Teng et al. (2006) investigated the effects of  $e[\text{CO}_2]$  on plant hormones using *Arabidopsis thaliana* and concluded that there was a significant increment in indole-3-acetic acid (one of the common plant hormones in the auxin class), gibberellic acid, zeatin riboside, dihydrozeatin riboside, and isopentenyl adenosine of the class cytokinin at  $e[\text{CO}_2]$ . Transcript abundance of genes related to synthesis and transport of auxins (auxin response factor, auxin influx carrier), cytokinins (cytokinin response factor), and gibberellic acids (gibberellin response modulation protein) have been reported to increase under  $e[\text{CO}_2]$  (De Souza et al., 2008; Gupta et al., 2005; Taylor et al., 2005; Wei et al., 2013). In addition,  $e[\text{CO}_2]$  influences the selective transport system of hormones that maintain hormone balance in plants. For example, reduction in gene transcripts related to auxin and cytokinin transport, such as auxin: hydrogen symporter 8 and cytokinin transporter 2 and 3, has been observed under  $e[\text{CO}_2]$  (Wei et al., 2013).

ABA plays a critical role in environmental stress responses, promoting senescence and eventually abscission (Finkelstein, 2013). Teng et al. (2006) reported that the concentration of ABA was significantly reduced under  $e[\text{CO}_2]$  and suggested that low levels of ABA are likely to be associated with delayed senescence. Molecular evidence has shown that several genes related to ABA synthesis (genes encoding ABA2 xanthoxin dehydrogenase, ABA-responsive protein) were suppressed, whereas expression of ABA degradation enzymes (ABA hydrolase and glycosyl hydrolase) was up-regulated at  $e[\text{CO}_2]$  (Wei et al., 2013). Together, these findings suggest that altered ABA metabolism at  $e[\text{CO}_2]$  may have a significant impact on plant growth and development (Figure 2). In addition, it is well-established that ABA plays a major role in determining stomatal conductance in plants (Chater et al., 2015). Such changes in ABA metabolism is likely to lower the stomatal conductance and thus improve the plant's water use efficiency.

#### 4.6 | Plant morphological and anatomical responses to elevated $[\text{CO}_2]$

The morphology of plants is significantly influenced by  $e[\text{CO}_2]$ , mainly as a result of changes in the activity of primary and secondary meristems of roots and shoots (Pritchard, Rogers, Prior, & Peterson, 1999). Growth characteristics of the shoot apex in the early stage of vegetative growth have provided important information on how  $e[\text{CO}_2]$  influences plant growth and development. Jitla et al. (1997) demonstrated changes in the shoot apex at  $e[\text{CO}_2]$  and they observed increased height and diameter of the apical dome, increased length of leaf primordia, and a greater number of tiller buds in the shoot apex of rice grown under  $e[\text{CO}_2]$ . These dynamic

changes of shoot and root meristem occur primarily as a result of increased carbon supply and increased growth of sink tissues stimulated by hormonal signalling. As a consequence of these changes, relative growth rate of the plants increases at  $e[\text{CO}_2]$  (Lambers, Chapin, & Pons, 2008; Makino et al., 1997) that leads to an increase in biomass and yield.

Leaf morphology and anatomy are influenced by environmental conditions including  $e[\text{CO}_2]$ . Stimulation of early leaf growth has been identified as one of the key physiological traits associated with final biomass and grain yield (Seneweera, Milham, & Conroy, 1994; Thilakarathne et al., 2015). Under  $e[\text{CO}_2]$ , plants tend to show an increased rate of leaf initiation and accelerated elongation coupled with enhanced leaf area (Seneweera et al., 1995; Taylor et al., 1994; Taylor et al., 2001). Canopy size can be increased by greater leaf number and individual leaf area that leads to greater photosynthetic area per given plant at  $e[\text{CO}_2]$ . However, leaf area is not always enhanced by  $\text{CO}_2$  enrichment. For example, in rice, although the leaf area increases during seedling and early vegetative stages at  $e[\text{CO}_2]$ , it frequently decreases during the later vegetative and reproductive stages (Makino et al., 1997; Seneweera et al., 1995). In addition, when plants are exposed to  $e[\text{CO}_2]$ , leaf thickness and leaf internal anatomy are also substantially altered. For example, in soybean (*Glycine max*) leaf,  $e[\text{CO}_2]$  induced an extra layer of palisade cells (Rogers, Thomas, & Bingham, 1983; Smith, Lewis, Ghannoum, & Tissue, 2012), and in the leaves of *Pinus radiata*,  $e[\text{CO}_2]$  increased both the mesophyll cross section and the area of vascular tissue (Araújo et al., 2011; Conroy, Barlow, & Bevege, 1986). Increases in mesophyll and vascular tissue area are considered important parameters that contribute to photosynthetic capacity and assimilate transport efficiency of the plant (Jitla et al., 1997; Pritchard et al., 1999). In addition, plants grown at  $e[\text{CO}_2]$  have shown a significant variation in leaf mass per unit area, which may partly explain the intraspecific variability of growth responses in  $\text{CO}_2$  rich conditions (Evans & Poorter, 2001; Thilakarathne et al., 2013). In wheat (*Triticum aestivum* L.), this trait is associated with increases in photosynthetic rates per unit leaf area, leaf nitrogen content on area basis, plant growth rates and yield at  $e[\text{CO}_2]$  (Thilakarathne et al., 2013). Differences in leaf mass per unit area indicate the ability of plants to deploy on resources in response to environmental signals (Hikosaka & Shigeno, 2009). It is highly likely that changes in leaf anatomy and morphology at  $e[\text{CO}_2]$  increase the photo-assimilate supply to the apical meristem, which promotes leaf primordial development (Pritchard et al., 1999). Further, it is suggested that increased availability of soluble carbohydrates from expanding leaf blades is a key factor contributing towards high leaf elongation rates, leaf area expansion, and whole plant growth observed under  $e[\text{CO}_2]$ .

Plant growth is influenced by both above-ground and below-ground processes under  $e[\text{CO}_2]$ . Below-ground processes of plants facilitate photosynthesis through nutrient and water uptake, which then influence above-ground biomass production (Madhu & Hatfield, 2013). Under  $e[\text{CO}_2]$ , plant root growth is also accelerated (Benlloch-Gonzalez, Berger, Bramley, Rebetzke, & Palta, 2014). Several studies have reported that plants tend to increase root biomass and dry weight, especially in wheat (Benlloch-Gonzalez et al., 2014; Chaudhuri, Kirkham, & Kanemasu, 1990), sorghum (Chaudhuri, Burnett, & Kirkham,

& Kanemasu, 1986), and soybean (Del Castillo, Acock, Reddy, & Acock, 1989; Libault, 2014) under CO<sub>2</sub> enriched conditions. Salsman, Jordan, Smith, and Neuman (1999) claim that the increase in root biomass at e[CO<sub>2</sub>] is associated with increased starch levels in roots and an increase in the levels of ABA that may have caused more carbon to be allocated to root growth.

#### 4.7 | Future research perspectives on plant growth responses to elevated [CO<sub>2</sub>]

There is greater body of knowledge on the changes in photosynthesis and stomatal conductance in response to [CO<sub>2</sub>] than of the other cellular processes influenced by the increased carbon supply generated at e[CO<sub>2</sub>]. A better understanding of these post-photosynthetic effects of e[CO<sub>2</sub>] on plant growth is essential for the development of strategies to improve crop productivity under a CO<sub>2</sub> rich atmosphere. Among these, an improved understanding of plant carbon and nitrogen metabolism, source/sink interactions, cell cycle properties and their crosstalk with hormones during atmospheric CO<sub>2</sub> enrichment is required to establish a holistic overview of the physiological mechanisms modulating plant growth responses under these conditions.

Breeding crops for a changing future climate requires the identification of key physiological and growth traits that help to enhance crop productivity. Further, understanding the genetic variation of plant responses to e[CO<sub>2</sub>] will also assist in selecting plants for greater fitness and long-term adaptation to climate stress (Ward & Kelly, 2004). However, very limited information is available on the genetic regulation of plant growth at e[CO<sub>2</sub>] (Rae, Ferris, Tallis, & Taylor, 2006). It has been reported that CO<sub>2</sub> responsiveness of plants is a quantitative trait that is determined by a range of gene products (Ferris et al., 2002). Therefore, identification of quantitative trait loci via the collection of phenotypic, biochemical, and physiological data on genetically characterized populations will help to develop an understanding of the cellular mechanism of plant responses to e[CO<sub>2</sub>] (Rae et al., 2006) and assist the selection of appropriate germplasm for use in breeding programs. In order to achieve this target, state of the art analytical techniques such as high throughput genomics, proteomics, metabolomics, and transcriptomics are required. Identification of the candidate genes involved in the plant's primary metabolism will also be helpful in understanding the regulatory networks of plant growth and shifts in carbon-nitrogen balance at e[CO<sub>2</sub>] (Vicente et al., 2015). Understanding plant sugar–hormonal crosstalk mainly associated with carbon and nitrogen metabolism will be important to adapt to a CO<sub>2</sub> rich atmosphere. However, in the real world, increased atmospheric [CO<sub>2</sub>] interacts with higher global temperatures and altered rainfall patterns to provide plants with a “triple whammy” of challenges. With experimentation on e[CO<sub>2</sub>] generally conducted under controlled temperatures and adequate water supply, it is difficult to predict the results to these actual situations. Therefore, understanding the interactions of these triple challenges (e[CO<sub>2</sub>], altered water availability and increased temperature) from cellular to whole plant level is crucial when addressing future food security targets under a changing climate.

## 5 | CONCLUDING REMARKS

Climate change is challenging the productivity of global agriculture and thus global food and nutrient security. As CO<sub>2</sub> is the primary substrate for photosynthesis and plant growth, a better understanding of the atmospheric [CO<sub>2</sub>] utilization strategies of plants will pave the way for increasing crop productivity. Considerable research has established the adjustments in photosynthesis and stomatal conductance in response to e[CO<sub>2</sub>], but not much attention has been paid to understanding the role of other key cellular processes in modifying physiological and plant growth process. The findings from long-term [CO<sub>2</sub>] enrichment studies suggest that understanding the cellular processes together with the source-sink interaction is essential to capture the full benefits of rising [CO<sub>2</sub>] on crops. Theoretically, a number of bottle necks in C<sub>3</sub> photosynthesis can be overcome with elevated levels of [CO<sub>2</sub>]; however, the physiological and molecular mechanisms to achieve this target are still not clearly understood. In particular, understanding is needed of the effects of e[CO<sub>2</sub>] on carbon and nitrogen metabolism, the cell cycle, and hormonal metabolism, which are more likely to play a major role in modifying plant growth processes. Comprehensive research in this area of study will open up new avenues for minimizing photosynthetic inefficiencies and thereby potentially improve crop productivity in a future CO<sub>2</sub>-enriched atmosphere. However, interactions with elevated temperatures and changes in available water will render this productivity goal very challenging.

### ACKNOWLEDGMENT

This work was supported by the University of Southern Queensland, Australia.

### CONFLICT OF INTEREST

The authors declare that the research was conducted in the absence of any commercial or financial relationships that could be construed as a potential conflict of interest.

### ORCID

Dananjali Gamage  <http://orcid.org/0000-0002-3128-4283>

Michael Thompson  <http://orcid.org/0000-0001-8150-7652>

Naoki Hirotsu  <http://orcid.org/0000-0002-9893-7111>

Amane Makino  <http://orcid.org/0000-0003-2779-6275>

Saman Seneweera  <http://orcid.org/0000-0001-5147-9988>

### REFERENCES

- Ainsworth, E., Davey, P., Hymus, G., Osborne, C., Rogers, A., Blum, H., ... Long, S. (2003). Is stimulation of leaf photosynthesis by elevated carbon dioxide concentration maintained in the long term? A test with *Lolium perenne* grown for 10 years at two nitrogen fertilization levels under Free Air CO<sub>2</sub> Enrichment (FACE). *Plant, Cell & Environment*, 26, 705–714.
- Ainsworth, E. A., Beier, C., Calfapietra, C., Ceulemans, R., Durand-Tardif, M., Farquhar, G. D., ... Kaduk, J. (2008). Next generation of elevated [CO<sub>2</sub>] experiments with crops: A critical investment for feeding the future world. *Plant, Cell & Environment*, 31, 1317–1324.
- Ainsworth, E. A., & Bush, D. R. (2011). Carbohydrate export from the leaf: A highly regulated process and target to enhance photosynthesis and productivity. *Plant Physiology*, 155, 64–69. 25

- Ainsworth, E. A., & Long, S. P. (2005). What have we learned from 15 years of free-air CO<sub>2</sub> enrichment (FACE)? A meta-analytic review of the responses of photosynthesis, canopy properties and plant production to rising CO<sub>2</sub>. *New Phytologist*, *165*, 351–372.
- Ainsworth, E. A., & Rogers, A. (2007). The response of photosynthesis and stomatal conductance to rising [CO<sub>2</sub>]: Mechanisms and environmental interactions. *Plant, Cell & Environment*, *30*, 258–270.
- Ainsworth, E. A., Rogers, A., Nelson, R., & Long, S. P. (2004). Testing the “source-sink” hypothesis of down-regulation of photosynthesis in elevated [CO<sub>2</sub>] in the field with single gene substitutions in Glycine max. *Agricultural and Forest Meteorology*, *122*, 85–94.
- Ainsworth, E. A., Rogers, A., Vodkin, L. O., Walter, A., & Schurr, U. (2006). The effects of elevated CO<sub>2</sub> concentration on soybean gene expression. An analysis of growing and mature leaves. *Plant Physiology*, *142*, 135–147.
- Alexandratos, N., & Bruinsma, J. (2012). World agriculture towards 2030/2050: The 2012 revision. In *ESA Working paper No* (pp. 12–03). Rome: FAO.
- Alonso, A., Pérez, P., & Martínez-Carrasco, R. (2009). Growth in elevated CO<sub>2</sub> enhances temperature response of photosynthesis in wheat. *Physiologia Plantarum*, *135*, 109–120.
- Aoki, N., Ono, K., Sasaki, H., Seneweera, S., Sakai, H., Kobayashi, K., & Ishimaru, K. (2003). Effects of elevated CO<sub>2</sub> concentration on photosynthetic carbon metabolism in flag-leaf blades of rice before and after heading. *Plant Production Science*, *6*, 52–58.
- Aranjuelo, I., Erice, G., Sanz-Sáez, A., Abadie, C., Gilard, F., Gil-Quintana, E., ... Araus, J. L. (2015). Differential CO<sub>2</sub> effect on primary carbon metabolism of flag leaves in durum wheat (*Triticum durum* Desf.). *Plant, Cell & Environment*, *38*, 2780–2794.
- Araújo, W. L., Fennie, A. R., & Nunes-Nesi, A. (2011). Control of stomatal aperture: A renaissance of the old guard. *Plant Signaling & Behavior*, *6*, 1305–1311.
- Arp, W. (1991). Effects of source-sink relations on photosynthetic acclimation to elevated CO<sub>2</sub>. *Plant, Cell & Environment*, *14*, 869–875.
- BassiriRad, H., Gutschick, V. P., & Lussenhop, J. (2001). Root system adjustments: Regulation of plant nutrient uptake and growth responses to elevated CO<sub>2</sub>. *Oecologia*, *126*, 305–320.
- Benlloch-Gonzalez, M., Berger, J., Bramley, H., Rebetzke, G., & Palta, J. A. (2014). The plasticity of the growth and proliferation of wheat root system under elevated CO<sub>2</sub>. *Plant and Soil*, *374*, 963–976.
- Bernacchi, C. J., Thompson, J. N., Coleman, J. S., & McConnaughay, K. D. (2007). Allometric analysis reveals relatively little variation in nitrogen versus biomass accrual in four plant species exposed to varying light, nutrients, water and CO<sub>2</sub>. *Plant, Cell & Environment*, *30*, 1216–1222.
- Bloom, A. J. (2015). Photorespiration and nitrate assimilation: A major intersection between plant carbon and nitrogen. *Photosynthesis Research*, *123*, 117–128.
- Bloom, A. J., Asensio, J. S. R., Randall, L., Rachmilevitch, S., Cousins, A. B., & Carlisle, E. A. (2012). CO enrichment inhibits shoot nitrate assimilation in C but not C plants and slows growth under nitrate in C plants. *Ecology*, *93*, 355–367.
- Bloom, A. J., Smart, D. R., Nguyen, D. T., & Searles, P. S. (2002). Nitrogen assimilation and growth of wheat under elevated carbon dioxide. *Proceedings of the National Academy of Sciences*, *99*, 1730–1735.
- Bokhari, S. A., Wan, X.-Y., Yang, Y.-W., Zhou, L., Tang, W.-L., & Liu, J.-Y. (2007). Proteomic response of rice seedling leaves to elevated CO<sub>2</sub> levels. *Journal of Proteome Research*, *6*, 4624–4633.
- Bowes, G. (1991). Growth at elevated CO<sub>2</sub> - Photosynthetic responses mediated through Rubisco. *Plant Cell and Environment*, *14*, 795–806.
- Brearley, J., Venis, M. A., & Blatt, M. R. (1997). The effect of elevated CO<sub>2</sub> concentrations on K<sup>+</sup> and anion channels of *Vicia faba* L. guard cells. *Planta*, *203*, 145–154.
- Casson, S., & Gray, J. E. (2008). Influence of environmental factors on stomatal development. *New Phytologist*, *178*, 9–23.
- Casson, S. A., & Hetherington, A. M. (2010). Environmental regulation of stomatal development. *Current Opinion in Plant Biology*, *13*, 90–95.
- Cato, S. C., Macedo, W. R., & Peres, L. E. P. (2013). Sinergism among auxins, gibberellins and cytokinins in tomato cv. Micro-Tom. *Horticultura Brasileira*, *31*, 549–553.
- Chater, C., Peng, K., Movahedi, M., Dunn, J. A., Walker, H. J., Liang, Y.-K., ... Wilson, I. (2015). Elevated CO<sub>2</sub>-induced responses in stomata require ABA and ABA signaling. *Current Biology*, *25*, 2709–2716.
- Chaudhuri, U., Burnett, R., Kirkham, M., & Kanemasu, E. (1986). Effect of carbon dioxide on sorghum yield, root growth, and water use. *Agricultural and Forest Meteorology*, *37*, 109–122.
- Chaudhuri, U., Kirkham, M., & Kanemasu, E. (1990). Root growth of winter wheat under elevated carbon dioxide and drought. *Crop Science*, *30*, 853–857.
- Chávez-Bárcenas, A. T., Valdez-Alarcón, J. J., Martínez-Trujillo, M., Chen, L., Xoconostle-Cázares, B., Lucas, W. J., & Herrera-Estrella, L. (2000). Tissue-specific and developmental pattern of expression of the rice *sp1* gene. *Plant Physiology*, *124*, 641–654.
- Cheng, S.-H., d Moore, B., & Seemann, J. R. (1998). Effects of short-and long-term elevated CO<sub>2</sub> on the expression of ribulose-1, 5-bisphosphate carboxylase/oxygenase genes and carbohydrate accumulation in leaves of *Arabidopsis thaliana* (L.) Heynh. *Plant Physiology*, *116*, 715–723.
- Cheng, W.-H., Im, K. H., & Chourey, P. S. (1996). Sucrose phosphate synthase expression at the cell and tissue level is coordinated with sucrose sink-to-source transitions in maize leaf. *Plant Physiology*, *111*, 1021–1029.
- Coleman, J., McConnaughay, K., & Bazzaz, F. (1993). Elevated CO<sub>2</sub> and plant nitrogen-use: Is reduced tissue nitrogen concentration size-dependent? *Oecologia*, *93*, 195–200.
- Conroy, J., Barlow, E., & Bevege, D. (1986). Response of *Pinus radiata* seedlings to carbon dioxide enrichment at different levels of water and phosphorus: growth, morphology and anatomy. *Annals of Botany*, *165*–177.
- De Souza, A. P., Gaspar, M., Da Silva, E. A., Ulian, E. C., Waclawovsky, A. J., Dos SaNTOS, R. V., ... Buckeridge, M. S. (2008). Elevated CO<sub>2</sub> increases photosynthesis, biomass and productivity, and modifies gene expression in sugarcane. *Plant, Cell & Environment*, *31*, 1116–1127.
- Del Castillo, D., Acock, B., Reddy, V., & Acock, M. (1989). Elongation and branching of roots on soybean plants in a carbon dioxide-enriched aerial environment. *Agronomy Journal*, *81*, 692–695.
- Del Pozo, A., Pérez, P., Gutiérrez, D., Alonso, A., Morcuende, R., & Martínez-Carrasco, R. (2007). Gas exchange acclimation to elevated CO<sub>2</sub> in upper-sunlit and lower-shaded canopy leaves in relation to nitrogen acquisition and partitioning in wheat grown in field chambers. *Environmental and Experimental Botany*, *59*, 371–380.
- Drake, B. G., González-Meler, M. A., & Long, S. P. (1997). More efficient plants: A consequence of rising atmospheric CO<sub>2</sub>? *Annual Review of Plant Biology*, *48*, 609–639.
- Evans, J., & Poorter, H. (2001). Photosynthetic acclimation of plants to growth irradiance: The relative importance of specific leaf area and nitrogen partitioning in maximizing carbon gain. *Plant, Cell & Environment*, *24*, 755–767.
- Ferris, R., Long, L., Bunn, S., Robinson, K., Bradshaw, H., Rae, A., & Taylor, G. (2002). Leaf stomatal and epidermal cell development: Identification of putative quantitative trait loci in relation to elevated carbon dioxide concentration in poplar. *Tree Physiology*, *22*, 633–640.
- Finkelstein, R. (2013). Abscisic acid synthesis and response. *The Arabidopsis Book*, *11*. e0166
- Finlayson, S. A., & Reid, D. M. (1996). The effect of CO<sub>2</sub> on ethylene evolution and elongation rate in roots of sunflower (*Helianthus annuus*) seedlings. *Physiologia Plantarum*, *98*, 875–881.
- Geiger, M., Haake, V., Ludewig, F., Sonnewald, U., & Stitt, M. (1999). The nitrate and ammonium nitrate supply have a major influence on the response of photosynthesis, carbon metabolism, nitrogen metabolism

- and growth to elevated carbon dioxide in tobacco. *Plant, Cell & Environment*, 22, 1177–1199.
- Geiger, M., Walch-Liu, P., Engels, C., Harnecker, J., Schulze, E. D., Ludewig, F., ... Stitt, M. (1998). Enhanced carbon dioxide leads to a modified diurnal rhythm of nitrate reductase activity in older plants, and a large stimulation of nitrate reductase activity and higher levels of amino acids in young tobacco plants. *Plant, Cell & Environment*, 21, 253–268.
- Geng, S., Misra, B. B., Armas, E., Huhman, D. V., Alborn, H. T., Sumner, L. W., & Chen, S. (2016). Jasmonate-mediated stomatal closure under elevated CO<sub>2</sub> revealed by time-resolved metabolomics. *The Plant Journal*, 88, 947–962.
- Gesch, R., Vu, J., Boote, K., Hartwell Allen, L., & Bowes, G. (2002). Sucrose-phosphate synthase activity in mature rice leaves following changes in growth CO<sub>2</sub> is unrelated to sucrose pool size. *New Phytologist*, 154, 77–84.
- Gifford, R. M., Barrett, D. J., & Lutze, J. L. (2000). The effects of elevated [CO<sub>2</sub>] on the C: N and C: P mass ratios of plant tissues. *Plant and Soil*, 224, 1–14.
- Gray, J. E., Holroyd, G. H., van der Lee, F. M., Bahrami, A. R., Sijmons, P. C., Woodward, F. I., ... Hetherington, A. M. (2000). The HIC signalling pathway links CO<sub>2</sub> perception to stomatal development. *Nature*, 408, 713–716.
- Gupta, P., Duplessis, S., White, H., Karnosky, D., Martin, F., & Podila, G. (2005). Gene expression patterns of trembling aspen trees following long-term exposure to interacting elevated CO<sub>2</sub> and tropospheric O<sub>3</sub>. *New Phytologist*, 167, 129–142.
- Gutiérrez, D., Gutiérrez, E., Pérez, P., Morcuende, R., Verdejo, A. L., & Martínez-Carrasco, R. (2009). Acclimation to future atmospheric CO<sub>2</sub> levels increases photochemical efficiency and mitigates photochemistry inhibition by warm temperatures in wheat under field chambers. *Physiologia Plantarum*, 137, 86–100.
- Habash, D. Z., Paul, M. J., Parry, M. A., Keys, A. J., & Lawlor, D. W. (1995). Increased capacity for photosynthesis in wheat grown at elevated CO<sub>2</sub>: The relationship between electron transport and carbon metabolism. *Planta*, 197, 482–489.
- Hanstein, S. M., & Felle, H. H. (2002). CO<sub>2</sub>-triggered chloride release from guard cells in intact fava bean leaves. Kinetics of the onset of stomatal closure. *Plant Physiology*, 130, 940–950.
- Hashimoto, M., Negi, J., Young, J., Israelsson, M., Schroeder, J. I., & Iba, K. (2006). Arabidopsis HT1 kinase controls stomatal movements in response to CO<sub>2</sub>. *Nature Cell Biology*, 8, 391–397.
- Hashimoto-Sugimoto, M., Negi, J., Monda, K., Higaki, T., Isogai, Y., Nakano, T., ... Iba, K. (2016). Dominant and recessive mutations in the Raf-like kinase HT1 gene completely disrupt stomatal responses to CO<sub>2</sub> in Arabidopsis. *Journal of Experimental Botany*, 67, 3251–3261.
- He, J., Zhang, R. X., Peng, K., Tagliavia, C., Li, S., Xue, S., ... Hubbard, K. E. (2018). The BIG protein distinguishes the process of CO<sub>2</sub>-induced stomatal closure from the inhibition of stomatal opening by CO<sub>2</sub>. *New Phytologist*, 218, 232–241.
- Hedrich, R., Marten, I., Lohse, G., Dietrich, P., Winter, H., Lohaus, G., & Heldt, H. W. (1994). Malate-sensitive anion channels enable guard cells to sense changes in the ambient CO<sub>2</sub> concentration. *The Plant Journal*, 6, 741–748.
- Hikosaka, K., & Shigeno, A. (2009). The role of Rubisco and cell walls in the interspecific variation in photosynthetic capacity. *Oecologia*, 160, 443–451.
- Hörak, H., Sierla, M., Töldsepp, K., Wang, C., Wang, Y.-S., Nuhkat, M., ... Salojärvi, J. (2016). A dominant mutation in the HT1 kinase uncovers roles of MAP kinases and GHR1 in CO<sub>2</sub>-induced stomatal closure. *The Plant Cell*, 28, 2493–2509. <https://doi.org/10.1105/tpc.16.00131>
- Hu, H., Boisson-Dernier, A., Israelsson-Nordström, M., Böhmer, M., Xue, S., Ries, A., ... Schroeder, J. I. (2010). Carbonic anhydrases are upstream regulators of CO<sub>2</sub>-controlled stomatal movements in guard cells. *Nature cell biology*, 12, 87.
- IPCC (2013) Summary for policymakers. In: Climate Change 2013: The Physical Science Basis. Contribution of Working Group I to the Fifth Assessment Report of the Intergovernmental Panel on Climate change. In T. F. Stocker, D. Qin, G.-K. Plattner, M. Tignor, S. K. Ailen, J. Boschung, A. Nauels, Y. Xia, V. Bex & P. M. Midgley (eds.). Cambridge, United Kingdom and New York, NY, USA: Cambridge University Press.
- Jakobson, L., Vaahtera, L., Töldsepp, K., Nuhkat, M., Wang, C., Wang, Y.-S., ... Sindarowska, Y. (2016). Natural variation in Arabidopsis Cvi-0 accession reveals an important role of MPK12 in guard cell CO<sub>2</sub> signaling. *PLoS Biology*, 14, e2000322
- Jang, J.-C., León, P., Zhou, L., & Sheen, J. (1997). Hexokinase as a sugar sensor in higher plants. *The Plant Cell*, 9, 5–19.
- Jitla, D. S., Rogers, G. S., Seneweera, S. P., Basra, A. S., Oldfield, R. J., & Conroy, J. P. (1997). Accelerated early growth of rice at elevated CO<sub>2</sub>. *Plant Physiology*, 115, 15–22.
- Kang, Y., Outlaw, W. H., Andersen, P. C., & Fiore, G. B. (2007). Guard-cell apoplastic sucrose concentration—A link between leaf photosynthesis and stomatal aperture size in the apoplastic phloem loader *Vicia faba* L. *Plant, Cell & Environment*, 30, 551–558.
- Kelly, G., Moshelion, M., David-Schwartz, R., Halperin, O., Wallach, R., Attia, Z., ... Granot, D. (2013). Hexokinase mediates stomatal closure. *The Plant Journal*, 75, 977–988.
- Kim, S. H., Sicher, R. C., Bae, H., Gitz, D. C., Baker, J. T., Timlin, D. J., & Reddy, V. R. (2006). Canopy photosynthesis, evapotranspiration, leaf nitrogen, and transcription profiles of maize in response to CO<sub>2</sub> enrichment. *Global Change Biology*, 12, 588–600.
- Kimball, B. A. (2016). Crop responses to elevated CO<sub>2</sub> and interactions with H<sub>2</sub>O, N, and temperature. *Current Opinion in Plant Biology*, 31, 36–43.
- Kinsman, E., Lewis, C., Davies, M., Young, J., Francis, D., Vilhar, B., & Ougham, H. (1997). Elevated CO<sub>2</sub> stimulates cells to divide in grass meristems: A differential effect in two natural populations of *Dactylis glomerata*. *Plant, Cell & Environment*, 20, 1309–1316.
- Koch, K. (2004). Sucrose metabolism: Regulatory mechanisms and pivotal roles in sugar sensing and plant development. *Current Opinion in Plant Biology*, 7, 235–246.
- Kontunen-Soppela, S., Parviainen, J., Ruhanen, H., Brosche, M., Keinänen, M., Thakur, R. C., ... Karnosky, D. F. (2010). Gene expression responses of paper birch (*Betula papyrifera*) to elevated CO<sub>2</sub> and O<sub>3</sub> during leaf maturation and senescence. *Environmental Pollution*, 158, 959–968.
- Körner, C. (2015). Paradigm shift in plant growth control. *Current Opinion in Plant Biology*, 25, 107–114.
- Laanemets, K., Wang, Y. F., Lindgren, O., Wu, J., Nishimura, N., Lee, S., ... Kilk, K. (2013). Mutations in the SLAC1 anion channel slow stomatal opening and severely reduce K<sup>+</sup> uptake channel activity via enhanced cytosolic [Ca<sup>2+</sup>] and increased Ca<sup>2+</sup> sensitivity of K<sup>+</sup> uptake channels. *New Phytologist*, 197, 88–98.
- Lambers, H., Chapin, F. I., & Pons, T. (2008). *Plant physiological ecology*. New York, NY, USA: Springer-Verlag.
- Lastdrager, J., Hanson, J., & Smeekens, S. (2014). Sugar signals and the control of plant growth and development. *Journal of Experimental Botany*, 65, 799–807.
- Lawlor, D. W., & Paul, M. J. (2014). Source/sink interactions underpin crop yield: The case for trehalose 6-phosphate/SnRK1 in improvement of wheat. *Frontiers in Plant Science*, 5, 418.
- Leakey, A. D., Ainsworth, E. A., Bernacchi, C. J., Rogers, A., Long, S. P., & Ort, D. R. (2009). Elevated CO<sub>2</sub> effects on plant carbon, nitrogen, and water relations: Six important lessons from FACE. *Journal of Experimental Botany*, 60, 2859–2876.
- Li, J. Y., Liu, X. H., Cai, Q. S., Gu, H., Zhang, S. S., Wu, Y. Y., & Wang, C. J. (2008). Effects of elevated CO<sub>2</sub> on growth, carbon assimilation, photosynthate accumulation and related enzymes in rice leaves during sink-source transition. *Journal of Integrative Plant Biology*, 50, 723–732.
- Li, P., Ainsworth, E. A., Leakey, A. D., Ulanov, A., Lozovaya, V., Ort, D. R., & Bohnert, H. J. (2008). Arabidopsis transcript and metabolite profiles: Ecotype-specific responses to open-air elevated [CO<sub>2</sub>]. *Plant, Cell & Environment*, 31, 1673–1687.

- Libault, M. (2014). The carbon-nitrogen balance of the nodule and its regulation under elevated carbon dioxide concentration. *BioMed Research International*, 2014, 1–7.
- Lind, C., Dreyer, I., López-Sanjurjo, E. J., von Meyer, K., Ishizaki, K., Kohchi, T., ... Al-Rasheid, K. A. (2015). Stomatal guard cells co-opted an ancient ABA-dependent desiccation survival system to regulate stomatal closure. *Current Biology*, 25, 928–935.
- Lorimer, G. H. (1981). The carboxylation and oxygenation of ribulose 1, 5-bisphosphate: The primary events in photosynthesis and photorespiration. *Annual Review of Plant Physiology*, 32, 349–382.
- Madhu, M., & Hatfield, J. L. (2013). Dynamics of plant root growth under increased atmospheric carbon dioxide. *Agronomy Journal*, 105, 657.
- Makino, A., Harada, M., Sato, T., Nakano, H., & Mae, T. (1997). Growth and N allocation in rice plants under CO<sub>2</sub> enrichment. *Plant Physiology*, 115, 199–203.
- Makino, A., & Mae, T. (1999). Photosynthesis and plant growth at elevated levels of CO<sub>2</sub>. *Plant and Cell Physiology*, 40, 999–1006.
- Makino, A., Mae, T., & Ohira, K. (1984). Relation between nitrogen and ribulose-1, 5-bisphosphate carboxylase in rice leaves from emergence through senescence. *Plant and Cell Physiology*, 25, 429–437.
- Makino, A., Nakano, H., Mae, T., Shimada, T., & Yamamoto, N. (2000). Photosynthesis, plant growth and N allocation in transgenic rice plants with decreased Rubisco under CO<sub>2</sub> enrichment. *Journal of Experimental Botany*, 51, 383–389.
- Martínez-Carrasco, R., Pérez, P., & Morcuende, R. (2005). Interactive effects of elevated CO<sub>2</sub>, temperature and nitrogen on photosynthesis of wheat grown under temperature gradient tunnels. *Environmental and Experimental Botany*, 54, 49–59.
- Masle, J. (2000). The effects of elevated CO<sub>2</sub> concentrations on cell division rates, growth patterns, and blade anatomy in young wheat plants are modulated by factors related to leaf position, vernalization, and genotype. *Plant Physiology*, 122, 1399–1416.
- McDonald, E. P., Erickson, J. E., & Kruger, E. L. (2002). Research note: Can decreased transpiration limit plant nitrogen acquisition in elevated CO<sub>2</sub>? *Functional Plant Biology*, 29, 1115–1120.
- Merilo, E., Jalakas, P., Kollist, H., & Brosché, M. (2015). The role of ABA recycling and transporter proteins in rapid stomatal responses to reduced air humidity, elevated CO<sub>2</sub>, and exogenous ABA. *Molecular Plant*, 8, 657–659.
- Merilo, E., Laanemets, K., Hu, H., Xue, S., Jakobson, L., Tulva, I., ... Brosché, M. (2013). PYR/RCAR receptors contribute to ozone-, reduced air humidity-, darkness- and CO<sub>2</sub>-induced stomatal regulation. *Plant Physiology*, 113.220608
- Moore, B., Cheng, S. H., Rice, J., & Seemann, J. (1998). Sucrose cycling, Rubisco expression, and prediction of photosynthetic acclimation to elevated atmospheric CO<sub>2</sub>. *Plant, Cell & Environment*, 21, 905–915.
- Moore, B., Cheng, S. H., Sims, D., & Seemann, J. (1999). The biochemical and molecular basis for photosynthetic acclimation to elevated atmospheric CO<sub>2</sub>. *Plant, Cell & Environment*, 22, 567–582.
- Nakano, H., Makino, A., & Mae, T. (1997). The effect of elevated partial pressures of CO<sub>2</sub> on the relationship between photosynthetic capacity and N content in rice leaves. *Plant Physiology*, 115, 191–198.
- Negi, J., Matsuda, O., Nagasawa, T., Oba, Y., Takahashi, H., Kawai-Yamada, M., ... Iba, K. (2008). CO<sub>2</sub> regulator SLAC1 and its homologues are essential for anion homeostasis in plant cells. *Nature*, 452, 483–486.
- Nie, G., Hendrix, D. L., Webber, A. N., Kimball, B. A., & Long, S. P. (1995). Increased accumulation of carbohydrates and decreased photosynthetic gene transcript levels in wheat grown at an elevated CO<sub>2</sub> concentration in the field. *Plant Physiology*, 108, 975–983.
- Oosten, J., & Besford, R. (1995). Some relationships between the gas exchange, biochemistry and molecular biology of photosynthesis during leaf development of tomato plants after transfer to different carbon dioxide concentrations. *Plant, Cell & Environment*, 18, 1253–1266.
- Oosten, J. J., Wilkins, D., & Besford, R. (1994). Regulation of the expression of photosynthetic nuclear genes by CO<sub>2</sub> is mimicked by regulation by carbohydrates: A mechanism for the acclimation of photosynthesis to high CO<sub>2</sub>? *Plant, Cell & Environment*, 17, 913–923.
- Paul, M. (2007). Trehalose 6-phosphate. *Current Opinion in Plant Biology*, 10, 303–309.
- Paul, M., & Driscoll, S. (1997). Sugar repression of photosynthesis: The role of carbohydrates in signalling nitrogen deficiency through source: Sink imbalance. *Plant, Cell & Environment*, 20, 110–116.
- Paul, M. J., & Foyer, C. H. (2001). Sink regulation of photosynthesis. *Journal of Experimental Botany*, 52, 1383–1400.
- Paul, M. J., Oszvald, M., Jesus, C., Rajulu, C., & Griffiths, C. A. (2017). Increasing crop yield and resilience with trehalose 6-phosphate: Targeting a feast–famine mechanism in cereals for better source–sink optimization. *Journal of Experimental Botany*, 68, 4455–4462.
- Paul, M. J., & Pellny, T. K. (2003). Carbon metabolite feedback regulation of leaf photosynthesis and development. *Journal of Experimental Botany*, 54, 539–547.
- Paul, M. J., Primavesi, L. F., Jhurrea, D., & Zhang, Y. (2008). Trehalose metabolism and signaling. *Annual Review of Plant Biology*, 59, 417–441.
- Pollock, C., & Farrar, J. (1996). Source-sink relations: The role of sucrose. In *Photosynthesis and the environment* (pp. 261–279). Springer.
- Pritchard, S., Rogers, H., Prior, S. A., & Peterson, C. (1999). Elevated CO<sub>2</sub> and plant structure: A review. *Global Change Biology*, 5, 807–837.
- Qaderi, M. M., & Reid, D. M. (2009). Crop responses to elevated carbon dioxide and temperature. In *Climate change and crops* (pp. 1–18). Springer.
- Rae, A., Ferris, R., Tallis, M., & Taylor, G. (2006). Elucidating genomic regions determining enhanced leaf growth and delayed senescence in elevated CO<sub>2</sub>. *Plant, Cell & Environment*, 29, 1730–1741.
- Ranasinghe, S., & Taylor, G. (1996). Mechanism for increased leaf growth in elevated CO<sub>2</sub>. *Journal of Experimental Botany*, 47, 349–358.
- Rogers, A., Fischer, B. U., Bryant, J., Frehner, M., Blum, H., Raines, C. A., & Long, S. P. (1998). Acclimation of photosynthesis to elevated CO<sub>2</sub> under low-nitrogen nutrition is affected by the capacity for assimilate utilization. Perennial ryegrass under free-air CO<sub>2</sub> enrichment. *Plant Physiology*, 118, 683–689.
- Rogers, G., Milham, P., Gillings, M., & Conroy, J. (1996). Sink strength may be the key to growth and nitrogen responses in N-deficient wheat at elevated CO<sub>2</sub>. *Functional Plant Biology*, 23, 253–264.
- Rogers, H. H., Thomas, J. F., & Bingham, G. E. (1983). Response of agronomic and forest species to elevated atmospheric carbon dioxide. *Science(Washington)*, 220, 428–429.
- Rolland, F., Moore, B., & Sheen, J. (2002). Sugar sensing and signaling in plants. *The Plant Cell*, 14, S185–S205.
- Sage, R. F., Sharkey, T. D., & Seemann, J. R. (1989). Acclimation of photosynthesis to elevated CO<sub>2</sub> in five C<sub>3</sub> species. *Plant Physiology*, 89, 590–596.
- Salsman, K. J., Jordan, D. N., Smith, S. D., & Neuman, D. S. (1999). Effect of atmospheric CO<sub>2</sub> enrichment on root growth and carbohydrate allocation of Phaseolus spp. *International Journal of Plant Sciences*, 160, 1075–1081.
- Schluempmann, H., Berke, L., & Sanchez-Perez, G. F. (2011). Metabolism control over growth: A case for trehalose-6-phosphate in plants. *Journal of Experimental Botany*, 63, 3379–3390.
- Sekhar, K. M., Sreeharsha, R. V., & Reddy, A. R. (2015). Differential responses in photosynthesis, growth and biomass yields in two mulberry genotypes grown under elevated CO<sub>2</sub> atmosphere. *Journal of Photochemistry and Photobiology B: Biology*, 151, 172–179.
- Seneweera, S. (2011). Effects of elevated CO<sub>2</sub> on plant growth and nutrient partitioning of rice (*Oryza sativa* L.) at rapid tillering and physiological maturity. *Journal of Plant Interactions*, 6, 35–42.
- Seneweera, S., Aben, S., Basra, A., Jones, B., & Conroy, J. (2003). Involvement of ethylene in the morphological and developmental response

- of rice to elevated atmospheric CO<sub>2</sub> concentrations. *Plant Growth Regulation*, 39, 143–153.
- Seneweera, S., Ghannoum, O., Conroy, J., Ishimaru, K., Okada, M., Liefvering, M., ... Kobayashi, K. (2002). Changes in source–sink relations during development influence photosynthetic acclimation of rice to free air CO<sub>2</sub> enrichment (FACE). *Functional Plant Biology*, 29, 947–955.
- Seneweera, S., Makino, A., Hirotsu, N., Norton, R., & Suzuki, Y. (2011). New insight into photosynthetic acclimation to elevated CO<sub>2</sub>: The role of leaf nitrogen and ribulose-1, 5-bisphosphate carboxylase/oxygenase content in rice leaves. *Environmental and Experimental Botany*, 71, 128–136.
- Seneweera, S., Makino, A., Mae, T., & Basra, A. (2005). Response of rice to p (CO<sub>2</sub>) enrichment: The relationship between photosynthesis and nitrogen metabolism. *Journal of Crop Improvement*, 13, 31–53.
- Seneweera, S., Milham, P., & Conroy, J. (1994). Influence of elevated CO<sub>2</sub> and phosphorus nutrition on the growth and yield of a short-duration rice (*Oryza sativa* L. cv. Jarrah). *Functional Plant Biology*, 21, 281–292.
- Seneweera, S. P., Basra, A. S., Barlow, E. W., & Conroy, J. P. (1995). Diurnal regulation of leaf blade elongation in rice by CO<sub>2</sub> (is it related to sucrose-phosphate synthase activity?). *Plant Physiology*, 108, 1471–1477.
- Seneweera, S. P., & Conroy, J. P. (2005). Enhanced leaf elongation rates of wheat at elevated CO<sub>2</sub>: Is it related to carbon and nitrogen dynamics within the growing leaf blade? *Environmental and Experimental Botany*, 54, 174–181.
- Sharkey, T., Laporte, M., Lu, Y., Weise, S., & Weber, A. (2004). Engineering plants for elevated CO<sub>2</sub>: A relationship between starch degradation and sugar sensing. *Plant Biology*, 6, 280–288.
- Sharkey, T. D. (1985). Photosynthesis in intact leaves of C3 plants: Physics, physiology and rate limitations. *The Botanical Review*, 51, 53–105.
- Sheen, J. (1994). Feedback control of gene expression. *Photosynthesis Research*, 39, 427–438.
- Smeekens, S., Ma, J., Hanson, J., & Rolland, F. (2010). Sugar signals and molecular networks controlling plant growth. *Current Opinion in Plant Biology*, 13, 273–278.
- Smith, R. A., Lewis, J. D., Ghannoum, O., & Tissue, D. T. (2012). Leaf structural responses to pre-industrial, current and elevated atmospheric CO<sub>2</sub> and temperature affect leaf function in *Eucalyptus sideroxylon*. *Functional Plant Biology*, 39, 285–296.
- Spreitzer, R. J., & Salvucci, M. E. (2002). Rubisco: Structure, regulatory interactions, and possibilities for a better enzyme. *Annual Review of Plant Biology*, 53, 449–475.
- Stitt, M., & Krapp, A. (1999). The interaction between elevated carbon dioxide and nitrogen nutrition: The physiological and molecular background. *Plant, Cell & Environment*, 22, 583–621.
- Takatani, N., Ito, T., Kiba, T., Mori, M., Miyamoto, T., Maeda, S.-i., & Omata, T. (2014). Effects of high CO<sub>2</sub> on growth and metabolism of *Arabidopsis* seedlings during growth with a constantly limited supply of nitrogen. *Plant and Cell Physiology*, 55, 281–292.
- Tans P. & Keeling R. (2018) *Trends in atmospheric carbon dioxide*. NOAA/ESRL ([www.esrl.noaa.gov/gmd/ccgg/trends/](http://www.esrl.noaa.gov/gmd/ccgg/trends/))
- Taylor, G., Ceulemans, R., Ferris, R., Gardner, S., & Shao, B. (2001). Increased leaf area expansion of hybrid poplar in elevated CO<sub>2</sub>. From controlled environments to open-top chambers and to FACE. *Environmental Pollution*, 115, 463–472.
- Taylor, G., Ranasinghe, S., Bosac, C., Gardner, S. D. L., & Ferris, R. (1994). Elevated CO<sub>2</sub> and plant growth: Cellular mechanisms and responses of whole plants. *Journal of Experimental Botany*, 45, 1761–1774.
- Taylor, G., Street, N. R., Tricker, P. J., Sjödin, A., Graham, L., Skogström, O., ... Jansson, S. (2005). The transcriptome of *Populus* in elevated CO<sub>2</sub>. *New Phytologist*, 167, 143–154.
- Teng, N., Wang, J., Chen, T., Wu, X., Wang, Y., & Lin, J. (2006). Elevated CO<sub>2</sub> induces physiological, biochemical and structural changes in leaves of *Arabidopsis thaliana*. *New Phytologist*, 172, 92–103.
- Thilakarathne, C. L., Tausz-Posch, S., Cane, K., Norton, R. M., Fitzgerald, G. J., Tausz, M., & Seneweera, S. (2015). Intraspecific variation in leaf growth of wheat (*Triticum aestivum*) under Australian Grain Free Air CO<sub>2</sub> Enrichment (AGFACE): Is it regulated through carbon and/or nitrogen supply? *Functional Plant Biology*, 42, 299–308.
- Thilakarathne, C. L., Tausz-Posch, S., Cane, K., Norton, R. M., Tausz, M., & Seneweera, S. (2013). Intraspecific variation in growth and yield response to elevated CO<sub>2</sub> in wheat depends on the differences of leaf mass per unit area. *Functional Plant Biology*, 40, 185–194.
- Tian, W., Hou, C., Ren, Z., Pan, Y., Jia, J., Zhang, H., ... He, Y. (2015). A molecular pathway for CO<sub>2</sub> response in *Arabidopsis* guard cells. *Nature Communications*, 6, 6057.
- Vahisalu, T., Kollist, H., Wang, Y.-F., Nishimura, N., Chan, W.-Y., Valerio, G., ... Desikan, R. (2008). SLAC1 is required for plant guard cell S-type anion channel function in stomatal signalling. *Nature*, 452, 487–491.
- van Dijken, A. J., Schluepmann, H., & Smeekens, S. C. (2004). *Arabidopsis* trehalose-6-phosphate synthase 1 is essential for normal vegetative growth and transition to flowering. *Plant Physiology*, 135, 969–977.
- Van Heerden, P., Swanepoel, J., & Krüger, G. (2007). Modulation of photosynthesis by drought in two desert scrub species exhibiting C<sub>3</sub>-mode CO<sub>2</sub> assimilation. *Environmental and Experimental Botany*, 61, 124–136.
- Vicente, R., Pérez, P., Martínez-Carrasco, R., Usadel, B., Kostadinova, S., & Morcuende, R. (2015). Quantitative RT-PCR platform to measure transcript levels of C and N metabolism-related genes in durum wheat: Transcript profiles in elevated [CO<sub>2</sub>] and high temperature at different levels of N supply. *Plant and Cell Physiology*, 56, 1556–1573.
- Vu, J. C., Allen, L. H., & Gesch, R. W. (2006). Up-regulation of photosynthesis and sucrose metabolism enzymes in young expanding leaves of sugarcane under elevated growth CO<sub>2</sub>. *Plant Science*, 171, 123–131.
- Vuuren, M. M., Robinson, D., Fitter, A. H., Chasalow, S. D., Williamson, L., & Raven, J. A. (1997). Effects of elevated atmospheric CO<sub>2</sub> and soil water availability on root biomass, root length, and N, P and K uptake by wheat. *New Phytologist*, 135, 455–465.
- Walker, B. J., VanLoocke, A., Bernacchi, C. J., & Ort, D. R. (2016). The costs of photorespiration to food production now and in the future. *Annual Review of Plant Biology*, 67, 107–129.
- Ward, J. K., & Kelly, J. K. (2004). Scaling up evolutionary responses to elevated CO<sub>2</sub>: Lessons from *Arabidopsis*. *Ecology Letters*, 7, 427–440.
- Watanabe, C. K., Sato, S., Yanagisawa, S., Uesono, Y., Terashima, I., & Noguchi, K. (2013). Effects of elevated CO<sub>2</sub> on levels of primary metabolites and transcripts of genes encoding respiratory enzymes and their diurnal patterns in *Arabidopsis thaliana*: Possible relationships with respiratory rates. *Plant and Cell Physiology*. p185
- Webb, A. A., McAinsh, M. R., Mansfield, T. A., & Hetherington, A. M. (1996). Carbon dioxide induces increases in guard cell cytosolic free calcium. *The Plant Journal*, 9, 297–304.
- Wei, H., Gou, J., Yordanov, Y., Zhang, H., Thakur, R., Jones, W., & Burton, A. (2013). Global transcriptomic profiling of aspen trees under elevated [CO<sub>2</sub>] to identify potential molecular mechanisms responsible for enhanced radial growth. *Journal of Plant Research*, 126, 305–320.
- White, A. C., Rogers, A., Rees, M., & Osborne, C. P. (2015). How can we make plants grow faster? A source–sink perspective on growth rate. *Journal of Experimental Botany*, 67, 31–45.
- Woodrow, L., & Grodzinski, B. (1993). Ethylene exchange in *Lycopersicon esculentum* Mill. leaves during short- and long-term exposures to CO<sub>2</sub>. *Journal of Experimental Botany*, 44, 471–480.
- Woodward, F., & Kelly, C. (1995). The influence of CO<sub>2</sub> concentration on stomatal density. *New Phytologist*, 131, 311–327.
- Xue, S., Hu, H., Ries, A., Merilo, E., Kollist, H., & Schroeder, J. I. (2011). Central functions of bicarbonate in S-type anion channel activation and OST1 protein kinase in CO<sub>2</sub> signal transduction in guard cell. *The EMBO Journal*, 30, 1645–1658.
- Yamamoto, Y., Negi, J., Wang, C., Isogai, Y., Schroeder, J. I., & Iba, K. (2016). The transmembrane region of guard cell SLAC1 channels perceives

CO<sub>2</sub> signals via an ABA-independent pathway in Arabidopsis. *The Plant Cell*, 28, 557–567.

- Zhang, D.-Y., Chen, G.-Y., Gong, Z.-Y., Chen, J., Yong, Z.-H., Zhu, J.-G., & Xu, D.-Q. (2008). Ribulose-1, 5-bisphosphate regeneration limitation in rice leaf photosynthetic acclimation to elevated CO<sub>2</sub>. *Plant Science*, 175, 348–355.
- Zhang, Y., Primavesi, L. F., Jhurrea, D., Andralojc, P. J., Mitchell, R. A., Powers, S. J., ... Paul, M. J. (2009). Inhibition of SNF1-related protein kinase1 activity and regulation of metabolic pathways by trehalose-6-phosphate. *Plant Physiology*, 149, 1860–1871.

**How to cite this article:** Gamage D, Thompson M, Sutherland M, Hirotsu N, Makino A, Seneweera S. New insights into the cellular mechanisms of plant growth at elevated atmospheric carbon dioxide concentrations. *Plant Cell Environ.* 2018;41: 1233–1246. <https://doi.org/10.1111/pce.13206>

## Chapter 3

### **Early growth mechanism of wheat (*Triticum aestivum* L.) at elevated atmospheric carbon dioxide: New physiological evidence with quantitative trait loci data**

In this study, a quantitative trait loci (QTL) analysis was carried out to identify the potential genetic components associated with plant growth responses to elevated [CO<sub>2</sub>]. A doubled haploid population of wheat was used for QTL mapping, focussing on the early vegetative growth stage. Together with QTL mapping, a detailed characterization of the parental lines of the mapping population was also conducted under ambient and elevated [CO<sub>2</sub>] conditions. QTL mapping was conducted for several important plant growth traits and the CO<sub>2</sub> responsiveness of each trait was used to determine CO<sub>2</sub>-response QTL. This chapter has been submitted as a research article to “Plant, Cell and Environment” and is currently under review.

**Damage D**, Thompson M, Okamoto M, Moriyama N, Sutherland M.W., Hirotsu N, Seneweera S, ‘Early growth mechanism of wheat (*Triticum aestivum* L.) at elevated atmospheric carbon dioxide: New physiological evidence with quantitative trait loci data’ (Under review)

1 **Article title:**

2 Early growth mechanism of wheat (*Triticum aestivum* L.) at elevated atmospheric carbon  
3 dioxide: New physiological evidence with quantitative trait loci data

4 **Authors:**

5 Dananjali Gamage<sup>1</sup>, Michael Thompson<sup>1</sup>, Mamoru Okamoto<sup>2</sup>, Nao Moriyama<sup>3</sup>, Mark W.  
6 Sutherland<sup>1</sup>, Naoki Hirotsu<sup>1&3</sup>, Saman Seneweera<sup>1&4\*1</sup>

7 **Author affiliations:**

8 <sup>1</sup> Centre for Crop Health, University of Southern Queensland, Toowoomba, QLD 4350,  
9 Australia.

10 <sup>2</sup> ARC Industrial Transformation Research Hub for Wheat in a Hot and Dry Climate, School  
11 of Agriculture, Food, and Wine, University of Adelaide, South Australia 5062, Australia.

12 <sup>3</sup> Graduate School of Life Sciences, Toyo University, 1-1-1 Izumino, Itakura, Gunma 374-  
13 0193, Japan

14 <sup>4</sup> National Institute of Fundamental Studies, Hantana Road, Kandy 20000, Sri Lanka

15 **\*Corresponding author:**

16 Saman Seneweera,

17 E-mail - [Saman.Seneweera@usq.edu.au](mailto:Saman.Seneweera@usq.edu.au), Tel: +61746315525

18 **Abbreviations:**

19 [CO<sub>2</sub>] – Carbon dioxide concentration

20 QTL – Quantitative trait loci

21 WAP – Weeks after planting

22 DH – Doubled haploid

23 Rubisco - Ribulose 1,5-bisphosphate carboxylase/oxygenase

---

<sup>1</sup> DG – Study design, acquisition, analysis and interpretation of data, drafting of manuscript, MT- Acquisition of data, NM- interpretation of data, MO & MWS – critical revision, NH – study design, analysis and interpretation of data and critical revision, SS- Study conception and design, analysis and interpretation of data, critical revision

- 24 RGR – Relative growth rate  
25 LER – Leaf elongation rate  
26  $V_{cmax}$  – Maximum carboxylation rate of Rubisco  
27  $J_{max}$  – Maximum rate of photosynthetic electron transport  
28 TPU – Rate of triose phosphate utilization  
29 DC – decimal code for wheat growth stage  
30  $C_i$  – Intra-cellular CO<sub>2</sub> concentration  
31  $G_s$  – Rate of stomatal conductance  
32 QTL – Quantitative trait loci  
33 WUE – water use efficiency  
34 NUE – nitrogen use efficiency

35

36 **Summary statement**

37 Elevated [CO<sub>2</sub>] increases biomass accumulation and growth of wheat (*Triticum aestivum* L.)  
38 during early ontogeny. Growth at elevated [CO<sub>2</sub>] was linked to 24 putative quantitative trait  
39 loci (QTL). CO<sub>2</sub> response of biomass production was associated with 3 key QTL on  
40 chromosome 2A, 1B and 4B.

41 **Abstract**

42 The underlying genetic variation of plant growth responses to elevated [CO<sub>2</sub>] is still not clearly  
43 understood. Here, a quantitative trait loci (QTL) analysis was carried out in a doubled haploid  
44 population of wheat (*Triticum aestivum* L.) grown at 700 μmol mol<sup>-1</sup> (elevated [CO<sub>2</sub>]) and 400  
45 μmol mol<sup>-1</sup> (ambient [CO<sub>2</sub>]). The mapping population including the parental lines, Kukri and  
46 RAC875 showed a significant difference in growth habit under ambient and elevated [CO<sub>2</sub>]  
47 (P<0.05), indicating a differential response to elevated [CO<sub>2</sub>]. Data for major early growth traits  
48 and their responsiveness to elevated [CO<sub>2</sub>] were used for QTL mapping. In total, 24 putative  
49 QTL were identified for CO<sub>2</sub> responsiveness. Among them, three QTL showed increased dry  
50 weight response to elevated [CO<sub>2</sub>], which were located on chromosome 2A (LOD = 4.372), 1B  
51 (LOD = 2.538) and 4B (LOD = 2.511). Of these, QTL on 2A and 4B played a role in increasing  
52 shoot dry weight (2A: LOD = 4.409, 4B: LOD = 2.506) at elevated [CO<sub>2</sub>]. These findings  
53 suggest the existence of a major mechanism that controls CO<sub>2</sub> response at the genetic level.  
54 Further in-depth analysis of these genomic regions is required to identify candidate genes  
55 responsible for enhanced plant growth under elevated [CO<sub>2</sub>].

56 **Keywords:** CO<sub>2</sub> responsiveness, Elevated [CO<sub>2</sub>]; Early growth; QTL; *Triticum aestivum* L.

## 57 1. Introduction

58 The atmospheric carbon dioxide concentration ( $[\text{CO}_2]$ ) has risen at a remarkable rate and  
59 currently exceeds  $400 \mu\text{mol mol}^{-1}$  ([Tans & Keeling, 2018](#)), which is a more than 30% increment  
60 in  $[\text{CO}_2]$  since the industrial revolution ([IPCC, 2013](#)). It is predicted that atmospheric  $[\text{CO}_2]$   
61 may reach  $550 \mu\text{mol mol}^{-1}$  in 2050 and 730 to  $1020 \mu\text{mol mol}^{-1}$  by 2100 ([Solomon \*et al.\*, 2007](#))  
62 as a consequence of anthropogenic activities such as fossil fuel combustion and deforestation.  
63 Although  $\text{CO}_2$  is considered a greenhouse gas, it is the primary substrate for plant  
64 photosynthesis and substantially stimulates photosynthesis especially in  $\text{C}_3$  plants, supporting  
65 vigorous growth and development. Plants of  $\text{C}_3$  origin are not photosynthetically saturated at  
66 the current  $\text{CO}_2$  partial pressure due to the properties of Ribulose 1,5-bisphosphate  
67 carboxylase/oxygenase (Rubisco), the primary carboxylation enzyme of  $\text{C}_3$  plants ([Makino &  
68 Mae, 1999](#)). Under current ambient conditions,  $[\text{CO}_2]$  is very low at the site of  $\text{CO}_2$  fixation  
69 and any increases in  $[\text{CO}_2]$  will increase the  $\text{CO}_2/\text{O}_2$  ratio, thereby increasing the carboxylation  
70 efficiency of Rubisco by lowering the rate of photorespiration ([Bowes, 1991](#), [Drake \*et al.\*,  
71 1997](#)). This increase in ambient  $[\text{CO}_2]$  directly and indirectly affects photosynthesis and  
72 stomatal conductance and subsequently increases the growth and development of plants  
73 ([Seneweera & Conroy, 2005](#), [Ainsworth \*et al.\*, 2008](#), [Gamage \*et al.\*, 2018](#)). To improve the  
74 crop productivity in a  $\text{CO}_2$  rich atmosphere, a thorough understanding of long-term adaptations  
75 of plants to elevated  $[\text{CO}_2]$  at the genetic level is essential ([Rae \*et al.\*, 2006](#)).

76 Growth response to elevated  $[\text{CO}_2]$  varies depending on the plant species and growth stage  
77 ([Seneweera, 2011a](#), [Fitzgerald \*et al.\*, 2016](#)). The majority of the  $\text{C}_3$  species show very high  
78 growth responses to elevated  $[\text{CO}_2]$ , especially at early stages of vegetative development  
79 ([Poorter, 1993](#)). Early growth responses to elevated  $[\text{CO}_2]$  are usually characterized by  
80 accelerated leaf growth and expansion, which will result in increased leaf area ratios and  
81 relative growth rates ([Poorter, 1993](#)). It is suggested that increased growth response to elevated  
82  $[\text{CO}_2]$  results from the initial stimulation of photosynthesis and this stimulation may disappear  
83 over time ([Masle \*et al.\*, 1993](#), [Centritto \*et al.\*, 1999](#), [Trevisan \*et al.\*, 2014](#)). Similar to  
84 photosynthesis response, relative growth rate (RGR) also tends to decline as plants grow older  
85 at elevated  $[\text{CO}_2]$  ([Makino \*et al.\*, 1997](#)). Hence, the effect of elevated  $[\text{CO}_2]$  on RGR is often  
86 time-dependent and occurs only at the early stage of plant growth ([Poorter & Navas, 2003](#)). It  
87 has also been reported with species such as wheat ([Neales & Nicholls, 1978](#), [Hikosaka \*et al.\*,  
88 2005](#)), *Arabidopsis* ([Van Der Kooij & De Kok, 1996](#)) and tobacco ([Geiger \*et al.\*, 1998](#)) that  
89 exposure to elevated  $[\text{CO}_2]$  increased the RGR in young plants whereas in old plants, RGR

90 remains unaffected. Even a slight increase in RGR in the exponential growth phase of the plants  
91 can be translated up to 50% absolute growth enhancement at elevated [CO<sub>2</sub>] ([Kirschbaum,  
92 2010](#)). In addition, increased photosynthetic capacity at elevated [CO<sub>2</sub>] leads to accelerated leaf  
93 elongation rates (LER) and contributes towards higher green leaf area production under high  
94 [CO<sub>2</sub>]. Faster rates of RGR and LER observed at elevated [CO<sub>2</sub>] strongly correlate with the  
95 total biomass production and consequently influence on grain yield production ([Jitla \*et al.\*,  
96 1997](#), [Seneweera & Conroy, 2005](#)). This early advantage of enhanced seedling growth and  
97 vigor is vital for the plant's subsequent establishment and, consequently, impacts on crop  
98 productivity ([Thilakarathne \*et al.\*, 2015](#), [Nagai \*et al.\*, 2016](#)). Therefore, an understanding of the  
99 fundamental mechanisms of how crops respond to elevated [CO<sub>2</sub>] at the early growth stages is  
100 crucial to the development of new breeding strategies for increasing crop yield potential under  
101 rising [CO<sub>2</sub>] in the atmosphere. However, plant growth, or structural development, is a complex  
102 process ([Ter Steege \*et al.\*, 2005](#)) and detailed experiments are required to identify the different  
103 organizational level responses to elevated [CO<sub>2</sub>] and uncover the holistic mechanism of plant  
104 growth at elevated [CO<sub>2</sub>].

105 A large intra-specific variation in growth response to elevated [CO<sub>2</sub>] has been widely reported  
106 ([Thilakarathne \*et al.\*, 2015](#)), however, there is limited information available for the genetic  
107 control of plant growth responses to elevated [CO<sub>2</sub>] ([Rae \*et al.\*, 2006](#)). Physiological traits that  
108 are affected by environmental factors such as elevated [CO<sub>2</sub>] are quantitatively determined  
109 ([Ferris \*et al.\*, 2002](#)). To identify the genetic response of traits changed by external  
110 environmental factors, identification of quantitative trait loci (QTL) for a particular trait is  
111 important ([Rae \*et al.\*, 2006](#)). Quantitative trait loci are the regions within a genome that  
112 correlate with the phenotypic variation of a particular quantitative trait ([Collard \*et al.\*, 2005](#))  
113 and provides information on whether the trait of interest has an associated genetic component  
114 that can be utilized in plant breeding programmes. Identification of new CO<sub>2</sub>-responsive QTL  
115 provides new tools to improve crop productivity under a CO<sub>2</sub> rich atmosphere and thus  
116 adaptation to climate stress ([Rae \*et al.\*, 2006](#)).

117

118 There had been few studies focused on identifying CO<sub>2</sub>-responsive QTLs with tree species. For  
119 example, [Rae \*et al.\* \(2006\)](#) mapped QTL for increased leaf growth and delayed senescence in  
120 hybrid poplar (*Populus spp*) and showed that candidate genes controlling the traits collocate to  
121 the regions where QTL were mapped. In another study, [Ferris \*et al.\* \(2002\)](#) determined QTL  
122 for leaf stomatal initiation, stomatal density, epidermal cell size, number and area in hybrid

123 poplar. In addition, QTL for above ground and below ground tree growth were determined in  
124 poplar by [Rae et al. \(2007\)](#), showing that there are significant genomic regions in the poplar  
125 genome that respond to shoot and root biomass at elevated [CO<sub>2</sub>]. However, only a limited  
126 number of studies have been carried out to identify QTL responsive to elevated [CO<sub>2</sub>] in  
127 cultivated crops and there have not been any studies on wheat (*Triticum aestivum* L.) ([Gamage  
128 et al., 2018](#)), which is the most widely cultivated and consumed cereal crop ([Shewry, 2009](#)).  
129 Moreover, none of the studies have been focused on the early vegetative growth despite its  
130 important role in determining final biomass and yield. Therefore, identifying key genomic  
131 regions determining plant growth traits under elevated [CO<sub>2</sub>] will provide key information to  
132 broaden our knowledge and understanding of how plants respond to high CO<sub>2</sub>.

133

134 In this study, we aimed to elucidate the genomic regions responsible for growth-related traits  
135 under elevated [CO<sub>2</sub>], focusing on the early vegetative growth stage in wheat. The main  
136 objective was to identify QTL for plant growth responses at ambient [CO<sub>2</sub>] and elevated [CO<sub>2</sub>].  
137 Further, we tested whether the variation of CO<sub>2</sub> responsiveness in wheat is associated with new  
138 QTLs and/or physiological response of the crop. The ultimate goal of this study is to identify  
139 the genetic basis of growth responses of wheat to elevated [CO<sub>2</sub>] and incorporate these traits  
140 into future breeding programs to improve the crop productivity and to maintain ecological  
141 success in a changing climate.

142

## 143 **2. Materials and methods**

144

### 145 ***2.1 Plant materials – mapping population***

146 A doubled haploid (DH) wheat mapping population (152 wheat lines including parental  
147 cultivars) derived from a cross between RAC875 and Kukri ([Fleury et al. \(2010\)](#)) was used in  
148 this study. This mapping population was obtained from the Australian Centre for Plant  
149 Functional Genomics, University of Adelaide, Australia. The parental lines of this population  
150 were physiologically characterized in detail by [Izanloo et al. \(2008\)](#). RAC875  
151 (RAC655/3/Sr21/4\*LANCE//4\*BAYONET) is a breeder's line which shows good and stable  
152 yield potential even under water-limited conditions. On the other hand, Kukri  
153 (76ECN44/76ECN36//MADDEN/6\*RAC177) is a cultivar that shows less yield potential (less  
154 than 44%) under the same conditions ([Bennett et al., 2012a](#), [Bennett et al., 2012b](#)). The harvest  
155 index (HI) and the nitrogen use efficiency (NUE) of Kukri is 41% and 100.4 kg grain yield kg<sup>-1</sup>

156 <sup>1</sup>, respectively. For RAC875, HI and NUE is 43% and 108.1 kg grain yield kg<sup>-1</sup>, respectively  
157 ([Mahjourimajd et al., 2015](#)). The differences in NUE in these cultivars is suggested to be a key  
158 determinant of variation in growth and yield response ([Gamage et al., 2018](#)). Elevated [CO<sub>2</sub>]  
159 significantly reduces the nitrate photo assimilation ([Bloom, 2015](#)), changes the nitrogen  
160 allocation to different plant organs ([Bernacchi et al., 2007](#)), reduces the nitrogen uptake relative  
161 to the carbon gain ([Del Pozo et al., 2007](#)) and thereby reduces nitrogen demand ([Stitt & Krapp,  
162 1999](#)). On the other hand, both Kukri and RAC875 have different water use efficiencies (WUE)  
163 ([Izanloo et al., 2008](#)) which was significantly changed under elevated [CO<sub>2</sub>] ([Conley et al.,  
164 2001](#), [Keenan et al., 2013](#)). It is likely that different NUE and WUE of these parental lines  
165 provided them with the ability to perform differently at elevated [CO<sub>2</sub>].

## 166 **2.2 Growth conditions**

### 167 **2.2.1. Experiment 01 – Parental lines characterization**

168 Two parental lines of the mapping population, Kukri and RAC875, were characterized for all  
169 the growth and physiological traits that were investigated in this study. Plants were grown in a  
170 temperature-controlled glasshouse under either 400 or 700 μmol mol<sup>-1</sup> [CO<sub>2</sub>] maintaining a day  
171 and night temperature of 22°C and 13°C, respectively. Plants were harvested at two different  
172 physiological stages: 4 weeks and physiological maturity. Total final biomass, thousand grain  
173 weight, tiller number at anthesis and final yield were recorded. Four weeks after planting  
174 (WAP) and at anthesis (DC 65) ([Zadoks et al., 1974](#)), gas exchange measurements were carried  
175 out in the last fully expanded leaf and flag leaf, respectively using an infrared gas analyzer  
176 (IRGA) system (Li-6400, Li-Cor, Lincoln, NE, USA) as described in [Seneweera et al. \(2002\)](#).  
177 The net photosynthesis rate, stomatal conductance, transpiration rate, and intercellular CO<sub>2</sub>  
178 concentration were measured in both growth stages. The [CO<sub>2</sub>] in the leaf chamber was  
179 maintained at 400 μmol mol<sup>-1</sup> and 700 μmol mol<sup>-1</sup> for ambient and elevated [CO<sub>2</sub>], respectively.  
180 The leaf chamber temperature was maintained at 25°C and irradiance was maintained at 1500  
181 μmol quanta m<sup>-2</sup> s<sup>-1</sup> which was supplied by a red and blue light source (6400-02B LED source).  
182 Photosynthesis gas exchange measurements were conducted during the day, between 0900  
183 hours and 1430 hours to produce *A-Ci* response curves (photosynthesis (*A*) versus intracellular  
184 [CO<sub>2</sub>] (*Ci*) curves). Prior to taking the readings for *A-Ci* response curves, each leaf was allowed  
185 10-15 mins to reach a steady state of photosynthesis at 400 μmol mol<sup>-1</sup> or 700 μmol mol<sup>-1</sup>. The  
186 initial slopes of the *A-Ci* response curves were used to calculate maximum carboxylation rate

187 of Rubisco ( $V_{c,max}$ ) and maximum rate of photosynthetic electron transport ( $J_{max}$ ) as suggested  
188 by [Farquhar \*et al.\* \(1980\)](#) and [Von Caemmerer and Farquhar \(1981\)](#), respectively.

189

### 190 **2.2.2. Experiment 02 – Glasshouse experiment**

191 One hundred and fifty-two lines of the mapping population, including the two parental lines,  
192 were germinated on moistened filter papers in Petri plates. When germinated seedlings reached  
193 2 cm in height, they were planted in pots (140 mm in diameter) filled with 1.5 kg of brown  
194 topsoil. The experiment was laid as a completely randomized design with each line of the  
195 mapping population replicated three times in three individual pots. The pots were placed in  
196 glass houses maintained at either ambient CO<sub>2</sub> (400  $\mu\text{mol mol}^{-1}$ ) or elevated CO<sub>2</sub> (700  $\mu\text{mol}$   
197  $\text{mol}^{-1}$ ). The conditions in the glasshouses were identical except for the varied [CO<sub>2</sub>]  
198 concentration. Day and night temperature was maintained at 22°C and 13°C, respectively. All  
199 pots were randomized at weekly intervals to minimize the glasshouse effect. Standard crop  
200 management practices were carried out to ensure optimum crop health and growth throughout  
201 the study period. The experiment was maintained in both glasshouses for four weeks during  
202 winter 2015 in the University of Southern Queensland, Australia (Latitude: 27° 33' 38.02" S  
203 and Longitude: 151° 55' 55.20" E).

### 204 **2.2.3. Experiment 03 – Growth chamber experiment**

205 The same 152 lines of the mapping population were again grown in two identical growth  
206 chambers (Reach in growth chambers, PGC-105, Percival, USA) under controlled  
207 environmental conditions for four weeks in 400 mm pots using the same soil type. Both  
208 chambers were maintained at a 14-hour photoperiod with day and night temperatures of 23°C  
209 and 13°C, respectively. Relative humidity in the chambers was maintained at 70% throughout  
210 the growth period. The light intensity was diurnally varied and was 1000  $\mu\text{mol m}^{-2} \text{s}^{-1}$  during  
211 midday throughout the growing period. Plants were supplied with optimum nutrients and water  
212 throughout the growth period. Elevated [CO<sub>2</sub>] conditions were maintained at ~700  $\mu\text{mol mol}^{-1}$   
213 and ambient [CO<sub>2</sub>] condition was maintained at ~400  $\mu\text{mol mol}^{-1}$  throughout the growing  
214 season.

215

### 216 **2.3. Growth trait measurements**

217 In this study, shoot dry mass, root dry mass, total dry mass, RGR, seedling height, LER and  
218 leaf width were measured as growth traits focusing on the early vegetative stage of wheat  
219 seedlings of the mapping population. All the physiological trait measurements were carried out  
220 as described by ([Pérez-Harguindeguy et al., 2013](#)). In experiment 02, measurements were taken  
221 at 2 WAP and 4 WAP in the glasshouse experiment. In both data collection rounds, one plant  
222 from each replicate was measured for seedling height, leaf width and LER. Another plant was  
223 carefully sampled to determine aboveground biomass accumulation. Plants were oven dried at  
224 70°C for 72 hours and dry weights were measured. Plant growth analysis and RGR calculations  
225 were carried out as described by [Hunt \(2003\)](#).

226 In experiment 03, seedlings were carefully harvested, including roots, at the end of the growth  
227 period (4WAP) and washed with water to remove all soil residues attached to the roots. Then,  
228 the shoot and root were separated, and oven dried at 70°C for 72 hours to determine the dry  
229 weight of shoots and roots separately. Then, the root to shoot ratio of each line of the mapping  
230 population was calculated.

#### 231 ***2.4. Calculation of CO<sub>2</sub> responsiveness of each growth trait***

232 Percentage responsiveness of each measured trait to elevated [CO<sub>2</sub>] was calculated as described  
233 in [Rae et al. \(2006\)](#). These results were then considered as the responsiveness of each trait and  
234 used for QTL mapping.

235

$$236 \text{ CO}_2 \text{ responsiveness} = \frac{(\text{Trait value at elevated [CO}_2\text{]} - \text{Trait value at ambient [CO}_2\text{]})}{\text{Trait value at ambient [CO}_2\text{]}} \times 100 (\%)$$

237

#### 238 ***2.5. QTL mapping***

239 The genetic map of this mapping population was published by [Bennett et al. \(2012b\)](#) employing  
240 456 DArT and SSR markers forming linkage groups representing all 21 chromosomes ([Bennett  
241 et al., 2012b](#), [Bennett et al., 2012c](#)). This genetic map was used in this study to identify the  
242 potential QTL associated with early growth traits of wheat. In this study, traits used for QTL  
243 mapping included seedling height, LER, leaf width, shoot dry weight, root dry weight, RGR  
244 and root to shoot dry weight ratio. Measurements for these traits were separately taken from  
245 ambient [CO<sub>2</sub>] and elevated [CO<sub>2</sub>] grown wheat seedlings. Then these data were used to map  
246 putative QTL under both ambient [CO<sub>2</sub>] and elevated [CO<sub>2</sub>]. The CO<sub>2</sub> responsiveness of each

247 trait was calculated separately as mentioned in section 2.4 and these data were used to identify  
248 response QTL under elevated [CO<sub>2</sub>]. The trait data were tested for normality before they were  
249 used in the analysis. The physiological data for each 152 wheat lines together with their relevant  
250 genotypic data were fed in to the QGene software for QTL mapping. QTL mapping was  
251 conducted using QGene software version 4.3.10 employing single trait multiple interval  
252 mapping to obtain LOD scores, additive effects and QTL effect (R<sup>2</sup>) values. For each trait, a  
253 minimum LOD value of 2.0 was used for the identification of putative QTL.

## 254 **2.6. Data analyses**

255 The trait differences in plants grown at ambient [CO<sub>2</sub>] and elevated [CO<sub>2</sub>] were analyzed using  
256 the paired t-test to confirm the suitability of data for QTL mapping. Treatment effects and  
257 interactions were determined through Analysis of Variance. Differences were considered  
258 significant at P<0.05. All the data were analyzed using SPSS statistical software version 23  
259 (IBM, Armonk, NY, USA). All the graphical representations were carried out using GraphPad  
260 Prism scientific software version 5.01 (GraphPad Software, San Diego, CA).

261

## 262 **3. Results**

### 263 **3.1. The response of Kukri and RAC875 to elevated [CO<sub>2</sub>]**

264 Elevated [CO<sub>2</sub>] increased total dry mass and total grain yield per plant, respectively, by 30%  
265 and 82.8% for Kukri compared with 23% and 64.2% for RAC875 (Table 1, P<0.01 and  
266 Supplementary Figure 1). A significant [CO<sub>2</sub>] effect was observed for the rate of  
267 photosynthesis at elevated [CO<sub>2</sub>] and for the number of tillers at anthesis (Table 1, P<0.01 and  
268 Supplementary Figure 1). Photosynthetic rates were significantly increased in both parental  
269 lines when grown at elevated [CO<sub>2</sub>] (Figure 1(a) and Supplementary Table S1, P<0.01),  
270 however, Kukri showed a slightly higher increase in photosynthetic rate (46.2%) than that of  
271 RAC875 (38.13%). The cultivar effect was significant on net photosynthesis at elevated [CO<sub>2</sub>]  
272 (P<0.01) and  $J_{max}$  (P<0.01). At anthesis, both parental lines showed a decrease in  $V_{cmax}$ , in  
273 which Kukri showed a comparatively higher decline (Figure 1(c)). However, Kukri showed a  
274 higher  $J_{max}$  under elevated [CO<sub>2</sub>] than the RAC875 and the effect of cultivars on  $J_{max}$  was  
275 statistically significant (Figure 1(d)). In addition, there was a significant interaction between  
276 [CO<sub>2</sub>] and cultivar on  $J_{max}$  (P<0.01). Further, the rate of triose phosphate utilization ( $TPU$ ) of

277 the two varieties was significantly different when grown at elevated [CO<sub>2</sub>] with Kukri showing  
278 a slightly lower *TPU* than that of RAC875 (Figure 1 (e)).

279 In the early growth stages, both parental lines showed a significantly higher photosynthetic rate  
280 at elevated [CO<sub>2</sub>] (Figure 1(b) and Supplementary Table S1, P<0.01) and the magnitude of  
281 increase in photosynthetic rates were similar for Kukri and RAC875. Despite the similar  
282 photosynthetic rates of these two varieties in the early growth stages, Kukri showed a  
283 significantly higher biomass accumulation in shoots (44%) and roots (42%) than RAC875  
284 when plants were grown at elevated [CO<sub>2</sub>] (Table 1). Shoot and root biomass accumulation,  
285 seedling height, LER and RGR of Kukri were significantly higher than those traits of RAC875  
286 at elevated [CO<sub>2</sub>] (Table 2, P<0.05)

### 287 **3.2. Mapping population response to elevated [CO<sub>2</sub>]**

288 There was a marked difference between the traits measured in ambient [CO<sub>2</sub>] and elevated  
289 [CO<sub>2</sub>] (Table 2, P<0.05), indicating that QTL mapped from these data will be relevant and of  
290 value for further detailed analysis. The frequency distributions for all the measured growth  
291 traits of the mapping populations grown in both glasshouse and growth chambers (controlled  
292 environment chambers) are shown in Figure 2 and 3, respectively, and the trait values of  
293 parental lines of the mapping population are marked under both ambient [CO<sub>2</sub>] and elevated  
294 [CO<sub>2</sub>]. All the measured parameters obtained from different CO<sub>2</sub> treatments showed continuous  
295 variation and near-normal distribution except for root dry weights, which were positively  
296 skewed (Figure 2 & Figure 3). In general, plant growth was stimulated under elevated [CO<sub>2</sub>]  
297 as assessed from biomass accumulation, seedling height, RGR and LER of different lines either  
298 grown at elevated or ambient [CO<sub>2</sub>] in glasshouse conditions. For example, the average  
299 biomass accumulation of the population was prominent at elevated [CO<sub>2</sub>] with an increase of  
300 73 mg per plant when compared with ambient [CO<sub>2</sub>] grown plants. However, growth responses  
301 of the population to elevated [CO<sub>2</sub>] greatly differed under growth chamber conditions. The  
302 average biomass accumulation in shoots and roots of the DH lines showed an increase of 175  
303 mg and 62 mg per plant, respectively, when compared with the average trait values of plants  
304 grown at ambient [CO<sub>2</sub>].

### 305 **3.3. Detection of QTL for growth traits**

306 A total of 13 QTL were identified for the population in ambient [CO<sub>2</sub>] (Table 3), 31 QTL in  
307 elevated [CO<sub>2</sub>] (Table 4) and 24 CO<sub>2</sub>-response QTL (Table 5) for the nine traits investigated

308 in this study. There was evidence of QTL for all the growth traits measured under ambient and  
309 elevated [CO<sub>2</sub>]. However, significant CO<sub>2</sub>-response QTL were identified in all traits except  
310 for LER and RGR. The QTL identified at elevated [CO<sub>2</sub>] were distributed across 15  
311 chromosomes, with the chromosomes of the A and B genomes having the most number of QTL  
312 (12 each).

313 Totally, 12 QTL were identified in this study which explained a significant phenotypic  
314 variation for biomass accumulation at elevated [CO<sub>2</sub>] (Table 4). Of them, four QTL were  
315 identified on chromosomes 2A, 3B, 7D and 3D for shoot dry weight, which explained 7.6 –  
316 9.9% variation in this trait. In experiment 03, QTL for shoot dry weight were found on 1A, 3A,  
317 6B and 6D, which explained a total of 42.6% of the phenotypic variation in the population. Of  
318 these, the QTL on chromosome 6B could explain 14.4% of shoot dry weight variation in the  
319 DH population. In addition, two QTL on chromosome 2A, two QTL on chromosomes 3B and  
320 2D, and two QTL on chromosomes 3B and 6B were identified as putative QTL for controlling  
321 root dry weight, root to shoot ratio and total dry weight, respectively (Table 4). Interestingly,  
322 the QTL for shoot dry weight on chromosome 6B is collocated with the QTL for total dry  
323 weight on the same chromosome. Three CO<sub>2</sub>-response QTL associated with increased dry  
324 weight were identified on chromosomes 2A, 1B and 4B (Table 5). Of these QTL, two  
325 (identified on 2A and 4B) played a role in determining shoot dry weight response to elevated  
326 [CO<sub>2</sub>].

327 Six QTL located on 2A, 1B, 3B, 6B and 7D were found to control seedling height (2 WAP) at  
328 elevated [CO<sub>2</sub>] and the most significant QTL was located on chromosome 3B (Table 4). This  
329 was further confirmed by the presence of a QTL on chromosome 3B for the trait of seedling  
330 height at 4WAP (Table 4). The location of the QTL for these traits at ambient [CO<sub>2</sub>] was  
331 different (chromosome 3B and 6D, Table 3). Further, different CO<sub>2</sub> response-QTL for seedling  
332 height were identified during plant development. For example, CO<sub>2</sub>-response QTL for seedling  
333 height at 2WAP were mapped on chromosomes 6A, 7A and 2D while a response QTL for  
334 seedling height at 4WAP was mapped on chromosome 1B (Table 5).

335 For LER, three QTL were identified on chromosomes 4A, 6A and 1B at elevated [CO<sub>2</sub>] which  
336 accounted for 24% phenotypic variation of this trait (Table 4). For the same trait, only one QTL  
337 was identified (chromosome 3B) under ambient [CO<sub>2</sub>] (Table 3), however, no CO<sub>2</sub>-response  
338 QTL was identified. Leaf width of plants also showed differential control under the two CO<sub>2</sub>  
339 treatments. At elevated [CO<sub>2</sub>], four QTL for leaf width were identified on chromosomes 6A,

340 1B, 6B and 2D, of which the QTL located on 6B and 2D were found to explain 38.6%  
341 phenotypic variation of the trait at elevated [CO<sub>2</sub>]. For the same trait, only two QTL were  
342 identified at ambient [CO<sub>2</sub>] and they were located on chromosomes 6B and 2D (Table 3).  
343 Further, the CO<sub>2</sub>-response QTL for leaf width was identified on chromosome 6B (Table 4).

344

## 345 **Discussion**

### 346 ***4.1. Variation of photosynthesis capacity and plant growth responses at elevated [CO<sub>2</sub>]***

347 Genetic variation in growth response to elevated [CO<sub>2</sub>] has been documented for many crop  
348 and pasture species ([Shimono et al., 2009](#), [Thilakarathne et al., 2013](#), [Thilakarathne et al.,](#)  
349 [2015](#)), however, the molecular and genetic mechanism of this response is not fully understood.  
350 To the best of our knowledge, this study is the first to report new QTL for key plant growth  
351 traits of wheat grown under elevated [CO<sub>2</sub>]. We have also established that the parental lines of  
352 the mapping population showed contrasting growth responses for elevated [CO<sub>2</sub>]. In this study,  
353 we identified contrasting growth behavior for two parents, Kukri and RAC875, and among  
354 their progenies for different growth traits, particularly at early vegetative growth. The parent  
355 line Kukri, showed a higher responsiveness to elevated [CO<sub>2</sub>], showing higher trait values for  
356 most of the traits tested in this study, especially in biomass accumulation. Significant  
357 interactions were found for [CO<sub>2</sub>] effect and genotypic effect of the mapping population for  
358 main growth traits such as dry mass accumulation and LER suggesting that even the mapping  
359 population responded to elevated and ambient [CO<sub>2</sub>] in two distinct patterns (Supplementary  
360 Table S2). It is likely that such distinct variation in response to elevated [CO<sub>2</sub>] could be linked  
361 to different water use efficiencies (WUE) of the genotypes, that mapping population was  
362 originally generated ([Bennett et al., 2012a](#), [Bennett et al., 2012c](#)). On the other hand, the  
363 parental cultivars of this mapping population also differ in their NUE which correlates with the  
364 final grain yield production ([Mahjourimajd et al., 2015](#)). Therefore, the differences in plant  
365 growth responses at elevated [CO<sub>2</sub>] could be due to the differences in plant nitrogen and water  
366 status. In addition to the genetic capacity of these genotypes for differential WUE, the increased  
367 levels of [CO<sub>2</sub>] generally enhances the rates of photosynthesis and reduces transpiration,  
368 resulting in higher WUE ([Figure 1\(f\)](#), [Hsiao & Jackson, 1999](#)) and thereby facilitate higher  
369 plant growth and productivity. Further, it is worthy to highlight that the physiological  
370 parameters of progeny lines perform slightly different manner when plants are grown under  
371 glasshouse and controlled environmental conditions. Perhaps, this could relate to the light

372 condition of the growth chambers. In both experiments, the CO<sub>2</sub> levels were strictly maintained  
373 at 400 and 700 μmol mol<sup>-1</sup> at all the time. However, the temperatures were maintained  
374 according to a schedule throughout the day, light intensity and relative humidity were  
375 maintained at a constant level throughout the growth period in the controlled growth chambers  
376 (Supplementary Table S3). In glasshouse, the temperature and [CO<sub>2</sub>] was finely controlled but  
377 plant was exposed to sunlight. However, consistently under both environmental conditions,  
378 there was a clear increase in plant growth and changes in physiological parameters at elevated  
379 [CO<sub>2</sub>].

380 Increased photosynthesis rate largely determines the biomass response to elevated [CO<sub>2</sub>] across  
381 a range of crops, including wheat ([Makino & Mae, 1999](#), [Seneweera, 2011b](#)). In this study,  
382 photosynthesis rates of the parental lines were significantly increased at elevated [CO<sub>2</sub>], but  
383 these rates depended on the plant's developmental stage. The photosynthesis rates at early  
384 growth stages were higher than the photosynthesis rates at anthesis across both cultivars.  
385 However, there was a marked difference between the biomass accumulations in the two  
386 parental lines, suggesting the presence of other regulatory mechanisms that control plant  
387 growth at elevated [CO<sub>2</sub>]. Generally, the best indicators of the whole photosynthesis process  
388 are  $V_{cmax}$  and  $J_{max}$  which represent Rubisco activity and the electron transport contributing to  
389 RuBP regeneration that are crucial for proper functioning of the photosynthesis machinery in  
390 plants ([Sharkey, 2016](#)). The  $V_{cmax}$  and  $J_{max}$  parameters of these two parents also showed a  
391 considerable difference, with Kukri displaying a comparatively higher reduction of these two  
392 important photosynthesis parameters. However, the  $J_{max}$  of Kukri was higher than RAC875  
393 suggesting that Rubisco-regeneration limitation of Kukri was less than RAC875 at elevated  
394 [CO<sub>2</sub>] ([Sun et al., 2011](#)). The effect of [CO<sub>2</sub>] on  $TPU$  was significantly reduced suggesting that  
395 net photosynthesis is no longer sensitive to increased [CO<sub>2</sub>] ([Yang et al., 2016](#)). At this stage,  
396 both Rubisco and RuBP regeneration activity may have been regulated at a rate that matches  
397 with  $TPU$  ([Yang et al., 2016](#)), which was apparent with decreased  $V_{cmax}$  values at elevated  
398 [CO<sub>2</sub>].

399 Acclimation of photosynthesis to elevated [CO<sub>2</sub>] is usually associated with significant  
400 decreases in Rubisco activity, which will lead to changes in the photosynthetic efficiency of  
401 leaves in response to the biochemical adjustments in the carbon and nitrogen metabolism of  
402 plants ([Ghildiyal & Sharma-Natu, 2000](#)). In the case of elevated [CO<sub>2</sub>], although plants become  
403 acclimated to high [CO<sub>2</sub>] levels, the acclimated photosynthesis rates of plants are higher than  
404 the photosynthesis rate of plants grown at ambient [CO<sub>2</sub>]. This may have led to improvements

405 in the overall performance of the plants in the high CO<sub>2</sub> environment. Despite the large  
406 reduction of  $V_{cmax}$  in Kukri compared to RAC875, Kukri showed the highest shoots and roots  
407 biomass response to elevated [CO<sub>2</sub>], suggesting that increased photosynthesis capacity may not  
408 be the only factor that drives increased plant growth and development in the high CO<sub>2</sub>  
409 environment. This hypothesis was further supported by recent findings that genetic variation  
410 in wheat responses to elevated [CO<sub>2</sub>] is determined by specific leaf nitrogen status rather than  
411 photosynthetic gas exchange characteristics ([Thilakarathne et al., 2015](#)). It has also been  
412 demonstrated that cultivars with a high tillering capacity/secondary shoots development  
413 capacity have a greater ability to thrive well in elevated [CO<sub>2</sub>] ([Shimono et al., 2009](#), [Tausz et](#)  
414 [al., 2013](#)), as even a slight stimulation in net assimilation rates and RGR will produce more  
415 photosynthetic tissues and leaf area during earlier stages, accelerating their growth at elevated  
416 [CO<sub>2</sub>]. This could offset the negative impacts of the downward acclimation of photosynthesis  
417 in the later stage of plant development at elevated [CO<sub>2</sub>] ([Van Der Kooij & De Kok, 1996](#)).  
418 However, if CO<sub>2</sub> responsiveness is to be capitalized on to improve crop productivity, it is  
419 important to instigate both photosynthetic and other important post-photosynthetic related CO<sub>2</sub>  
420 responsive traits such as plant nitrogen and water status together. Further, it is also required to  
421 develop a greater understanding on the coordination of light capture ([Zhu et al., 2008](#)) and  
422 energy conversion ([Murchie et al., 2009](#)) of plants to cope with the atmospheric CO<sub>2</sub> increase.

423 Increased photosynthesis at elevated [CO<sub>2</sub>] leads to increased biomass accumulation,  
424 consequently changing plant growth, development and morphology, which was mainly  
425 determined by traits such as shoot to root dry weight ratio, LER and RGR ([Masle, 2000](#),  
426 [Seneweera & Conroy, 2005](#)). Increased biomass accumulation during early growth is the key  
427 determinant of the final grain yield in cereals. The positive relationship between these two traits  
428 is widely used across the globe to increase crop yield potential ([Villegas et al., 2001](#)). Although  
429 increases in photosynthesis rates at elevated [CO<sub>2</sub>] have a positive influence on biomass  
430 accumulation, our study's results showed that there was a high variation in biomass  
431 accumulation in the parents and the progenies of the DH population despite their rate of  
432 photosynthesis being similar. However, the variation of this response, whether mediated  
433 through improved WUE and/or NUE is not known. If so, these physiological mechanisms  
434 independently operate to respond to elevated [CO<sub>2</sub>]. In a study conducted by [Izanloo et al.](#)  
435 [\(2008\)](#), Kukri and RAC875 showed a great difference in WUE, in which Kukri performed well  
436 only in well-watered conditions and RAC875 produced stable yield even under moderate  
437 drought stress conditions, suggesting that Kukri has a lower WUE compared to RAC875. Our

438 experiments were conducted under proper watering schedules and thus, WUE did not  
439 measured, except instantaneous WUE from gas exchange data. However, when plants exposed  
440 to elevated [CO<sub>2</sub>], Kukri showed a large reduction of stomatal conductance and transpiration  
441 rate compared to RAC875 which may have led to higher WUE in Kukri than the RAC875  
442 (Figure 1(f)). This increased WUE, together with the high NUE of Kukri ([Mahjourimajd et al.,](#)  
443 [2015](#), [Mahjourimajd et al., 2016](#)), may have partly contributed to the higher accumulation of  
444 biomass in shoots and roots and, consequently, all the growth traits showed a significant  
445 response to elevated [CO<sub>2</sub>]. These findings suggest that growth at elevated [CO<sub>2</sub>] is controlled  
446 by multiple physiological processes, mainly improved photosynthesis, WUE, and NUE, and  
447 these processes likely play a significant role in determining the final growth and yield response  
448 under rising [CO<sub>2</sub>].

449

#### 450 ***4.2. Genetic basis of plant growth responses to elevated [CO<sub>2</sub>] – identification of promising*** 451 ***putative QTL***

452 The progenies of the mapping population differed greatly in all growth traits related to final  
453 biomass accumulation. Presence of significant positive correlation coefficients between shoot  
454 and root biomass at ambient and elevated [CO<sub>2</sub>] suggest that these traits are under genetic  
455 control and are susceptible to environmental influence (Supplementary Table S3 and S4).  
456 These findings were further confirmed by QTL mapping in which we found a large number of  
457 QTL for different growth traits of wheat in ambient and elevated [CO<sub>2</sub>]. In this study, totally  
458 68 QTL were determined for plant growth traits, of which 31 were detected at elevated [CO<sub>2</sub>],  
459 13 QTL at ambient [CO<sub>2</sub>] and 24 QTL for CO<sub>2</sub> responsiveness (Figure 4). Although some QTL  
460 from the ambient and elevated [CO<sub>2</sub>] treatment collocated on the genetic map, there were many  
461 QTL that were solely identified in the different growing conditions. A similar pattern of results  
462 was observed in a study by ([Rae et al., 2006](#)) in which they identified QTL for enhanced leaf  
463 growth of hybrid poplar at elevated [CO<sub>2</sub>]. Out of all QTL identified at elevated [CO<sub>2</sub>], 13 QTL  
464 were related to biomass accumulation suggesting that elevated [CO<sub>2</sub>] induced biomass gain is  
465 highly genetically controlled. This was further supported by summed percentage phenotypic  
466 variance. For example, the variance of QTL related to shoot biomass accumulation was 43%  
467 while QTL mapped for root biomass explained 22% of its phenotypic variation. The genetic  
468 and environmental interaction for these two traits, shoot and root biomass, was statistically  
469 significant and suggest that DH progenies act differently under the two CO<sub>2</sub> conditions. These

470 findings further indicate that some of the regulatory mechanisms only turn on under elevated  
471 [CO<sub>2</sub>].

472 A number of QTL regions identified in this study are worthy of future research. Among the  
473 QTL mapped under elevated [CO<sub>2</sub>], 11 QTL showed a positive additive effect from Kukri for  
474 shoot dry weight (1A: wPt-6568 – wmc0215a, 2A: wPt-2052 – wPt-1139, 6B: wPt-2768 –  
475 barc0117, 3D: barc0247 – barc0134, 6D: wPt-9887 – wPt-0745), total dry weight (6B: wPt-  
476 2768 – barc0117), root to shoot dry weight ratio (7D: barc0184 – wPt-0934), seedling height  
477 (2A: wPt-9809 – wPt-0944, 6A: wPt-6003 – barc0095, 3B: stm0092tctg – wPt-7001) and leaf  
478 elongation rate (4A: wPt-7306 – wPt-9277) (Figure 4). Of these, a significant QTL was  
479 observed for shoot weight on chromosome 6B (between wPt-2768 – barc0117), which  
480 explained 14.4% of the phenotypic variation of shoot biomass accumulation. A major QTL for  
481 total plant biomass was also identified in the same locus of chromosome 6B suggesting that  
482 there might be some candidate genes that located within this region, which may be largely  
483 responsible for biomass gain at elevated [CO<sub>2</sub>].

484 Many traits tested in this study showed a differential control over the two CO<sub>2</sub> treatments,  
485 which was evident from the presence of CO<sub>2</sub>-response QTL ([Rae et al., 2006](#)). Carbon dioxide  
486 response effect was mapped using the percentage difference between plants grown at elevated  
487 and ambient [CO<sub>2</sub>], considering the possibility of using this as a potential trait score that could  
488 be used in plant breeding to capitalize on the high CO<sub>2</sub> atmosphere. Out of the CO<sub>2</sub>-response  
489 QTL detected, 10 showed a positive additive effect (Figure 4) from the parent Kukri, especially  
490 for shoot dry weight (2A: wPt-5801 – wPt-3753, 4B: barc0340a – gwm0495, 3D: barc0223 –  
491 barc0247), root dry weight (2A: wPt- 2052 – wPt-1139, 3D: barc0223 – barc0247), total dry  
492 (2A: wPt-5801 – wPt-3753, 1B: wPt-8093 – wPt-5769, 4B: barc0340a – gwm0495 weight) and  
493 seedling height (6A: wPt-6003 – wmc0111, 2D: wPt-2636 – wPt-7027). Interestingly, the CO<sub>2</sub>-  
494 response QTL for shoot dry weight and total dry weight on chromosome 2A and 4B had  
495 collocated each other, which further confirms that this region might harbor important genes  
496 that control plant adaptation to elevated CO<sub>2</sub> levels. For example, chromosome 2AS contains  
497 phenology genes such as *Ppd-A1* ([Laurie, 1997](#)) that play a key role in photoperiod sensitivity  
498 which may have an influence and thereby regulate the vegetative growth of wheat ([Kamran et](#)  
499 [al., 2014](#)). These phenology genes highly modulate by environmental stimulations and thus  
500 involve in improving plants' adaptability to a certain environment ([Miralles & Richards, 2000](#),  
501 [Royo et al., 2018](#)). In addition, CO<sub>2</sub>-response QTL identified for LER on chromosome 6A and

502 for RGR on chromosome 3D, also showed a positive additive effect, however, these two QTL  
503 were not significant at 95% confidence level.

504 In a recent study by [Mahjourimajd et al. \(2016\)](#), the same DH mapping population has been  
505 employed to map the QTL related to grain yield in response to different nitrogen applications,  
506 some of which are overlapping with regions identified in our study. For example, some QTL  
507 identified on 2A, 6B, 7A and 7D for biomass accumulation and CO<sub>2</sub>-response QTL in our study  
508 were closer to the QTL regions identified in their study. In addition, QTL for other traits such  
509 as seedling height, LER and leaf width identified on 1B, 3B and 6A were in line with their  
510 study's results ([Mahjourimajd et al., 2016](#)). It is always desirable to compare and contrast the  
511 genomic regions that have been previously identified in a similar environment to determine the  
512 validity of these genomic regions before further detailed analysis. This was a major challenge  
513 for our study as only a very limited number of studies have been conducted to identify the  
514 genomic regions responsible for plant growth and development at elevated [CO<sub>2</sub>], especially  
515 in commercially cultivated crops such as wheat.

516 Greater early vigor is considered as one of the important traits for improving wheat yield  
517 potential under different environmental conditions ([Ludwig & Asseng, 2010](#)). This trait is also  
518 known to influence biomass accumulation and nitrogen uptake throughout crop development  
519 ([Reinke et al., 2002](#), [Liao et al., 2004](#)). In our study, we identified a large number of QTL for  
520 different plant growth traits at ambient and elevated [CO<sub>2</sub>] conditions, mostly on dry matter  
521 accumulation at the early vegetative stage. Three CO<sub>2</sub>-response QTL identified on  
522 chromosomes 2A, 1B and 4B for biomass accumulation can be considered as regions worthy  
523 for future research. These QTL are assumed to be involved in sensitivity to [CO<sub>2</sub>] responses of  
524 biomass production and are likely to be associated with different post-photosynthetic  
525 processes. This natural variation provides important information about the adaptation of plants  
526 to elevated [CO<sub>2</sub>] in the long term. Thus, this information provides new insights for future  
527 research on understanding the molecular mechanisms of plant growth responses to elevated  
528 [CO<sub>2</sub>] and facilitates wheat breeding for the future changing climate. However, before utilizing  
529 these QTL into the marker-assisted breeding programs it is required to validate them to confirm  
530 their reproducibility. Then, further in-depth research is required to carry out the fine-mapping  
531 of the potential QTL to identify the candidate genes responsible for increased growth  
532 stimulation at elevated [CO<sub>2</sub>]. However, before utilizing these QTL into the marker-assisted  
533 breeding programmes it is required to validate them to confirm their reproducibility. Further

534 in-depth research is required to carry out the fine-mapping of the potential QTL to identify the  
535 candidate genes responsible for increased growth at elevated [CO<sub>2</sub>].

536

#### 537 **4. Conclusion**

538 Limited information is available on the genetic basis of plant growth responses to elevated  
539 atmospheric [CO<sub>2</sub>]. However, this information is essential in determining the ability of plants  
540 to adapt to the rapidly changing atmospheric [CO<sub>2</sub>]. High biomass accumulation of plants at  
541 the early vegetative stage is an important trait that influences their subsequent establishment  
542 and productivity in the later stages of development. Therefore, improving this trait will be  
543 highly beneficial for plants to enhance CO<sub>2</sub> utilization and thereby stimulate the early vigorous  
544 growth of the plants. In this study, we developed an understanding of the physiological and  
545 genetic variability of plant growth responses to elevated [CO<sub>2</sub>]. Further, we made an effort to  
546 identify major QTL that is associated with plant growth at elevated [CO<sub>2</sub>] using a DH  
547 population of wheat. Here, we identified some unique QTL worthy of future research. Several  
548 CO<sub>2</sub>-responsive QTL identified in this study were associated with growth traits, mainly  
549 biomass accumulation. These QTLs were collocated into the same location, suggesting that  
550 these regions might play a significant role in determining growth responses at elevated [CO<sub>2</sub>].  
551 However, these genomic regions should be further fine mapped to identify the possible genes  
552 responsible for growth at elevated [CO<sub>2</sub>]. Also, it is noteworthy to mention that increased  
553 atmospheric [CO<sub>2</sub>] interacts with higher global temperatures and altered rainfall patterns,  
554 which will continuously challenge plant communities. Therefore, understanding the  
555 interactions of these environmental conditions on plant growth is crucial in improving crop  
556 productivity under a future CO<sub>2</sub> rich atmosphere.

557 **Conflict of interest**

558 The authors declare no conflict of interest.

559 **Acknowledgment**

560 The doubled haploid mapping population was obtained from the Australian Centre for Plant  
561 Functional Genomics, University of Adelaide, Australia to carry out the research. This study  
562 was funded by the Strategic Research Fund of the University of Southern Queensland,  
563 Australia.

564 **List of Figures**

565 **Figure 1** (a) Rate of photosynthesis at anthesis; (b) Rate of photosynthesis at 4WAP (c)  $V_{cmax}$ :  
566 Maximum rate of Rubisco carboxylation at anthesis; (d)  $J_{max}$ : Maximum rate of electron  
567 transport at anthesis (e) *TPU*: Triosephosphate use limitation (f) Rate of transpiration at  
568 anthesis in Kukri and RAC875 grown at ambient [ $CO_2$ ] ( $400 \mu mol mol^{-1}$ ) and elevated [ $CO_2$ ]  
569 ( $700 \mu mol mol^{-1}$ ), respectively. All measurements were carried out at the 4 replication level.  
570 Vertical error bars represent standard errors of mean values. P values indicate the significance:  
571 \*,  $P < 0.05$ ; \*\*,  $P < 0.01$ ; ns, not significant.

572

573 **Figure 2** Frequency distribution of early growth traits in the RAC875/Kukri DH population:  
574 (a) shoot dry weight (2WAP); (c) shoot dry weight (4WAP); (e) Seedling height (2WAP); (g)  
575 seedling height (4WAP); (i) relative growth rate; (k) leaf elongation rate; (m) leaf width at  
576 ambient [ $CO_2$ ] ( $400 \mu mol mol^{-1}$ ); and (b) shoot dry weight (2WAP); (d) shoot dry weight  
577 (4WAP); (f) Seedling height (2WAP); (h) seedling height (4WAP); (j) relative growth rate; (l)  
578 leaf elongation rate; (n) leaf width at elevated [ $CO_2$ ] ( $700 \mu mol mol^{-1}$ ) under glasshouse  
579 conditions. Open circle denotes the trait value of parent Kukri and closed circle denotes the  
580 trait value for parent RAC875.

581

582 **Figure 3** Frequency distribution of (a) shoot dry weight (4WAP); (c) root dry weight (4WAP);  
583 (e) total dry weight (4WAP); (g) root to shoot ratio (4WAP) of DH population at ambient [ $CO_2$ ]  
584 ( $400 \mu mol mol^{-1}$ ) and (b) shoot dry weight (4WAP); (d) root dry weight (4WAP); (f) total dry  
585 weight (4WAP); (h) root to shoot ratio (4WAP) of DH population at elevated [ $CO_2$ ] ( $700$   
586  $\mu mol mol^{-1}$ ) under controlled growth conditions. Open circle denotes the trait value of parent  
587 Kukri and closed circle denotes the trait value for parent RAC875.

588

589 **Figure 4** Distribution of quantitative trait loci (QTL) for different early growth traits in  
590 response to ambient [ $CO_2$ ] ( $400 \mu mol mol^{-1}$ ), elevated [ $CO_2$ ] ( $700 \mu mol mol^{-1}$ ) and response  
591 QTL to elevated [ $CO_2$ ] in wheat. Numbers on the bars represent traits: **1**, Shoot Dry Weight  
592 (2WAP); **2**, Shoot Dry Weight (4WAP); **3**, Seedling Height (2WAP); **4**, Seedling Height  
593 (4WAP); **5**, Leaf Elongation Rate; **6**, Leaf Width; **7**, Relative Growth Rate; **8**, Shoot Dry  
594 Weight (4WAP, Controlled Environment); **9**, Root Dry Weight (4WAP, Controlled  
595 Environment), **10**, Total Dry Weight (4WAP, Controlled Environment), **11**, Root to Shoot Dry  
596 Weight Ratio (4WAP, Controlled Environment). Red and blue bars represent positive additive

597 effect and negative additive effect, respectively. Bars with continuous and dotted borders  
598 represents QTL at ambient [CO<sub>2</sub>] and at elevated [CO<sub>2</sub>], respectively. Bars with yellow colour  
599 borders represents response QTL to elevated [CO<sub>2</sub>].

600

601 **Supplementary Figure 1** Growth parameters of Kukri and RAC875 grown at ambient [CO<sub>2</sub>]  
602 (400 μmol mol<sup>-1</sup>) and elevated [CO<sub>2</sub>] (700 μmol mol<sup>-1</sup>); (a) Shoot dry weight, (b) Root dry  
603 weight, (c) Total dry weight and (d) root to shoot ration at 4 weeks after planting (WAP) and  
604 (e) Total dry mass per plant, (f) 1000 grain weight per plant, (g) Number of tillers per plant and  
605 (f) Total grain yield per plant at maturity.

606 **List of Tables**

607

608 **Table 1.** Growth parameters of Kukri and RAC875 grown at ambient [CO<sub>2</sub>] (a[CO<sub>2</sub>], 400 μmol  
609 mol<sup>-1</sup>) and elevated [CO<sub>2</sub>] (e[CO<sub>2</sub>], 700 μmol mol<sup>-1</sup>) at 4 weeks after planting (WAP) and at  
610 maturity. ns, not significant; \*, P<0.05; \*\*, P<0.01.

611

612 **Table 2.** Mean values of different physiological traits of parental lines and progenies of the  
613 DH population grown at ambient and elevated [CO<sub>2</sub>] conditions. a[CO<sub>2</sub>], ambient [CO<sub>2</sub>];  
614 e[CO<sub>2</sub>], elevated [CO<sub>2</sub>]; WAP, weeks after planting; Min, minimum value; Max, maximum  
615 value; \*, P <0.05.

616

617 **Table 3.** QTL for growth traits of DH population detected in ambient [CO<sub>2</sub>] conditions (400  
618 μmol mol<sup>-1</sup>). WAP, weeks after planting.

619

620 **Table 4.** QTL for growth traits of the DH population detected in elevated [CO<sub>2</sub>] conditions  
621 (700 μmol mol<sup>-1</sup>). WAP, weeks after planting.

622

623 **Table 5.** QTL for CO<sub>2</sub> responsiveness of growth traits of the DH population to elevated [CO<sub>2</sub>]  
624 conditions (700 μmol mol<sup>-1</sup>). WAP, weeks after planting.

625

626 **Supplementary Table S1.** Analysis of variance (ANOVA) results of gas exchange  
627 measurements of Kukri and RAC875 grown at ambient [CO<sub>2</sub>] (400 μmol mol<sup>-1</sup>) and elevated  
628 [CO<sub>2</sub>] (700 μmol mol<sup>-1</sup>) at 4 weeks after planting (WAP) and at anthesis (DC65). a[CO<sub>2</sub>],  
629 ambient [CO<sub>2</sub>]; e[CO<sub>2</sub>], elevated [CO<sub>2</sub>]; *G<sub>s</sub>*, rate of stomatal conductance; *C<sub>i</sub>*, intracellular  
630 [CO<sub>2</sub>]; *V<sub>max</sub>*, Maximum carboxylation rate of Rubisco; *J<sub>max</sub>*, Maximum rate of photosynthetic  
631 electron transport; *TPU*, rate of triose phosphate utilization; ns, not significant; \*, P<0.05; \*\*,  
632 P<0.01.

633 **Supplementary Table S2.** Analysis of variance (ANOVA) for different growth traits  
634 investigated in experiment 02 (glasshouse trial) and experiment 03 (growth chamber trial).  
635 WAP, weeks after planting; ns, not significant; \*, P<0.05; \*\*, P<0.01.

636

637 **Supplementary Table S3.** Controlled environmental conditions provided to the Reach-in  
638 plant growth chambers throughout the experimental period.

639 **Supplementary Table S4.** Correlation matrix of physiological traits of the DH population  
640 grown under different CO<sub>2</sub> concentrations in experiment 02 (glasshouse experiment). a[CO<sub>2</sub>],  
641 ambient [CO<sub>2</sub>]; e[CO<sub>2</sub>], elevated [CO<sub>2</sub>]; WAP, weeks after planting; \*, P<0.05; \*\* P<0.01.

642

643 **Supplementary Table S5.** Correlation matrix of physiological traits of the DH population  
644 grown under different CO<sub>2</sub> concentrations in experiment 03 (growth chamber experiment).  
645 a[CO<sub>2</sub>]; ambient [CO<sub>2</sub>]; e[CO<sub>2</sub>], elevated [CO<sub>2</sub>]; WAP, weeks after planting; \*, P<0.05; \*\*, P<0.01.  
646

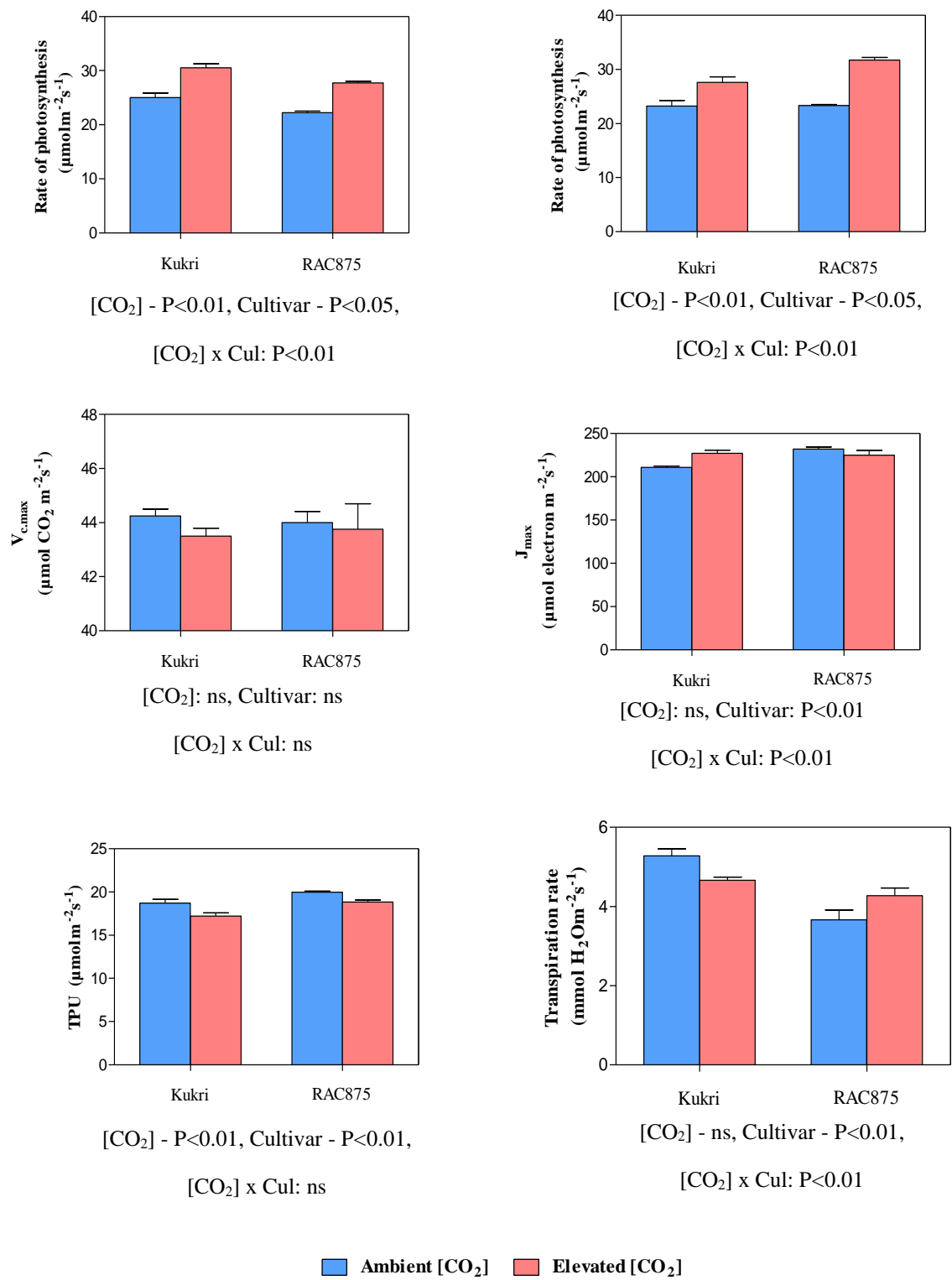
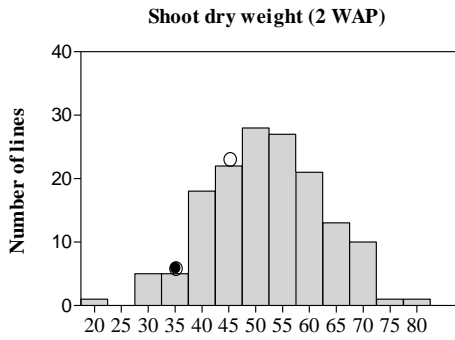


**Figure 1**

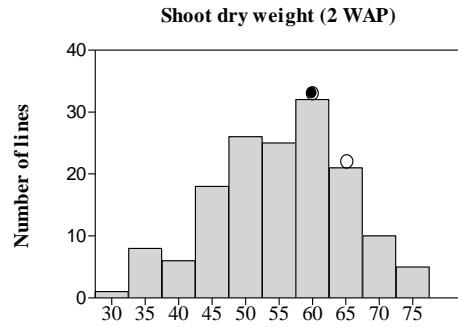
**Ambient [CO<sub>2</sub>]**

**(a)**

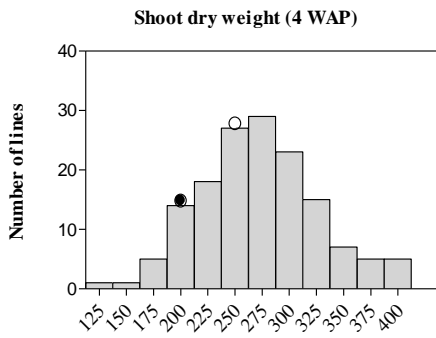


**Elevated [CO<sub>2</sub>]**

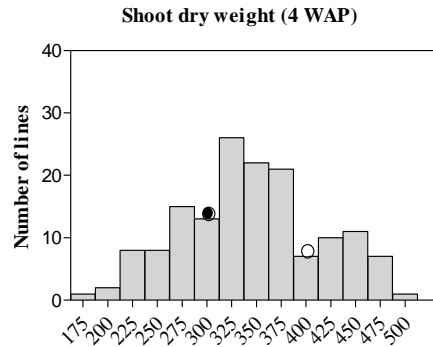
**(b)**



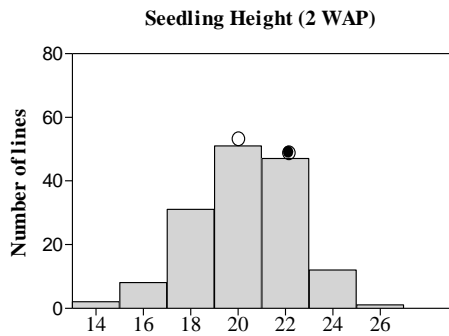
**(c)**



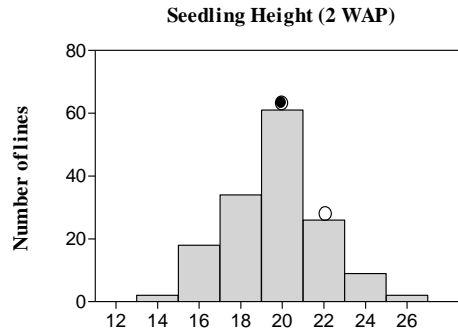
**(d)**



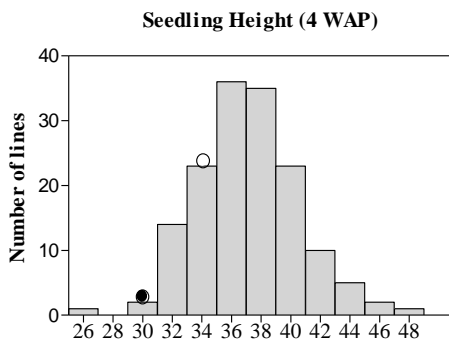
**(e)**



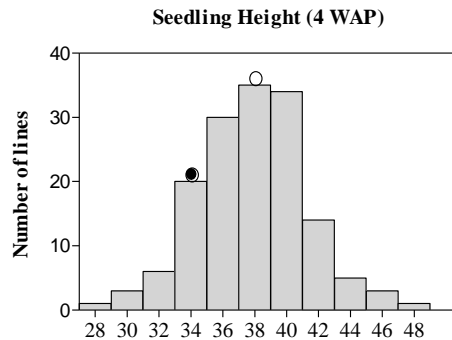
**(f)**



**(g)**



**(h)**



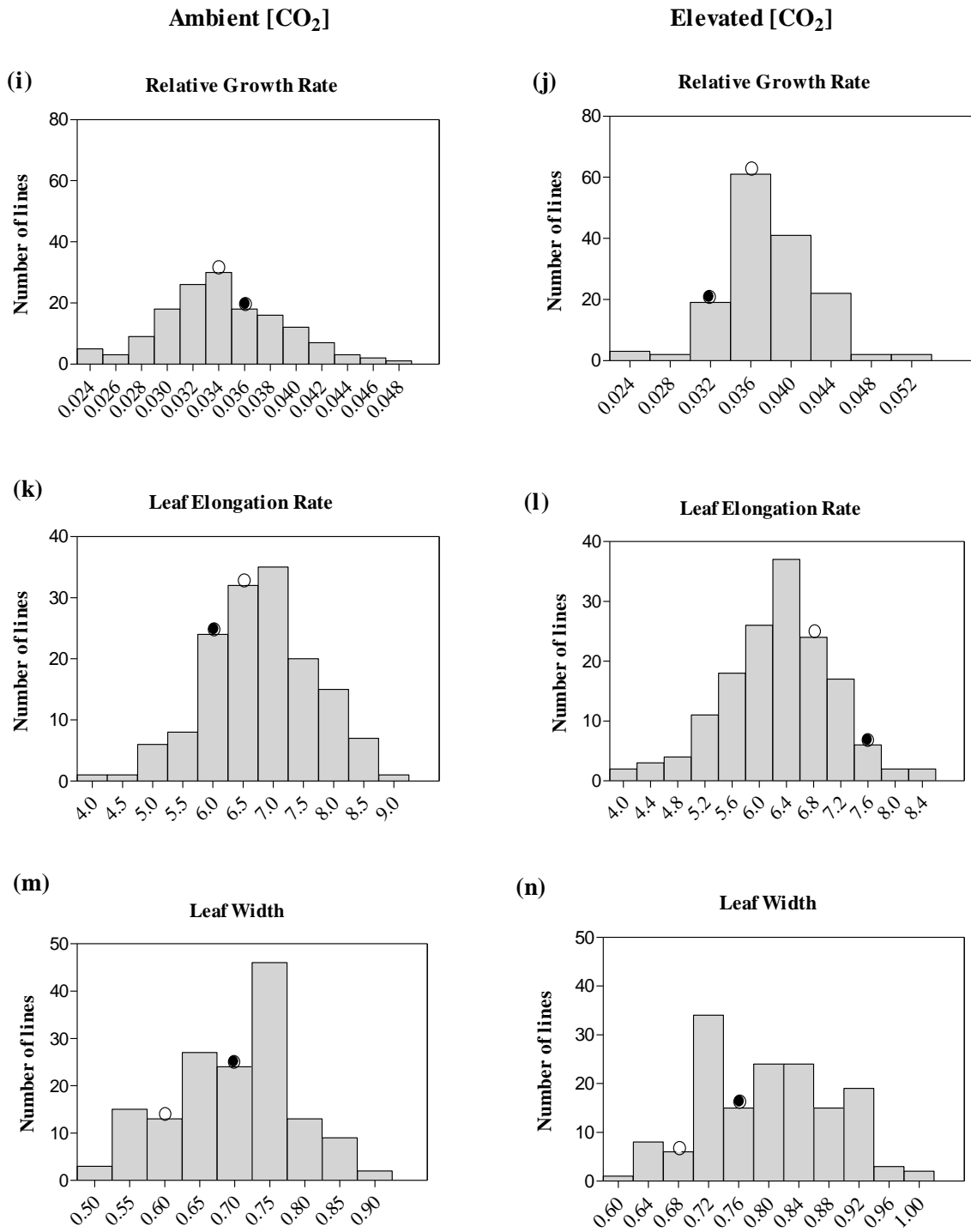


Figure 2

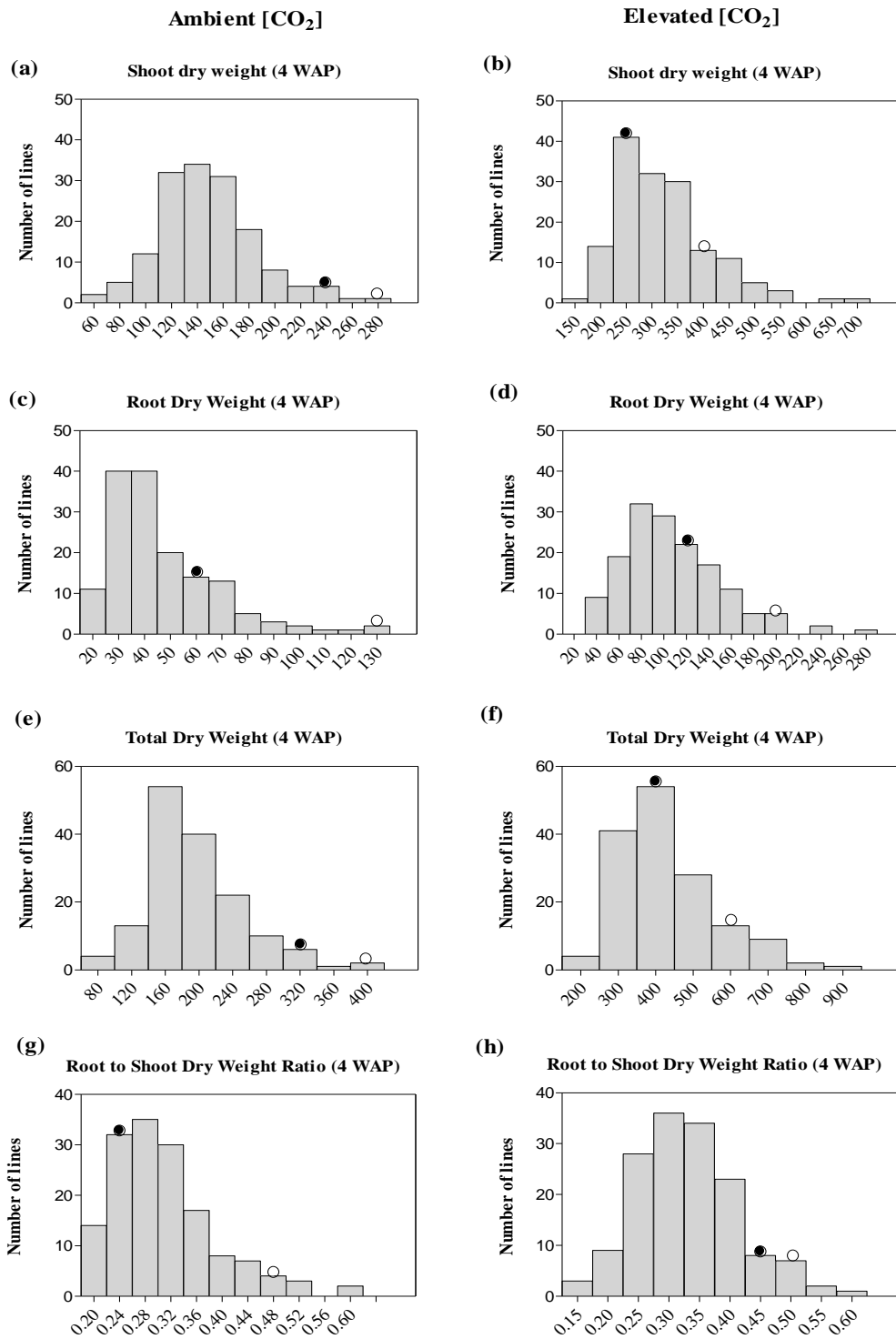


Figure 3

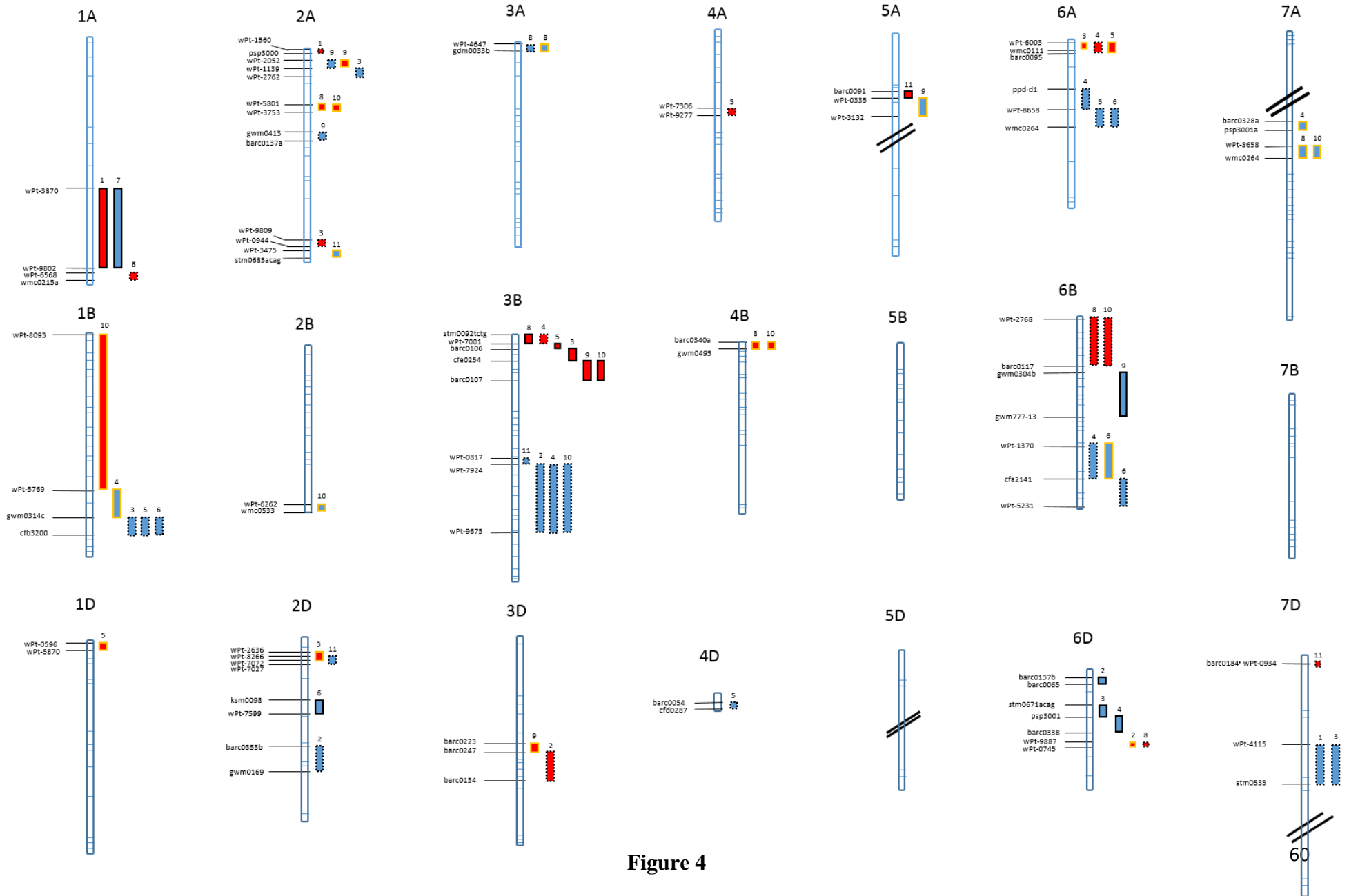


Figure 4

**Table 1.** Growth parameters of Kukri and RAC875 grown at ambient [CO<sub>2</sub>] (a[CO<sub>2</sub>], 400 μmol mol<sup>-1</sup>) and elevated [CO<sub>2</sub>] (e[CO<sub>2</sub>], 700 μmol mol<sup>-1</sup>) at 4 weeks after planting (WAP) and at maturity. ns, not significant; \*, P<0.05; \*\*, P<0.01.

Trait	Mean CO <sub>2</sub> effect		Mean cultivar effect			Interaction effect (ANOVA results)	
	a[CO <sub>2</sub> ]	e[CO <sub>2</sub> ]	ANOVA result	Kukri	RAC875	ANOVA result	[CO <sub>2</sub> ]x Cultivar
<b>Growth-related traits at 4 WAP</b>							
Shoot dry weight (mg/plant)	258.2	339.4	**	336	261.6	**	**
Root dry weight (mg/plant)	99.2	156.7	**	162.3	93.6	**	ns
Total dry weight (mg/plant)	357.4	496.1	**	498.3	355.2	**	**
Root to shoot ratio	0.38	0.46	**	0.484	0.352	**	**
<b>Growth-related traits at maturity</b>							
Total dry mass (g/plant)	11.7	14.9	**	13.3	13.3	ns	ns
Thousand grain weight (g/plant)	35.2	37.6	ns	37.6	35.1	ns	ns
Tiller number	7	9	**	8	8	ns	ns
Total grain yield (g/plant)	8.1	14	**	10.6	11.6	ns	ns

**Table 2.** Mean values of different physiological traits of parental lines and progenies of the DH population grown at ambient and elevated [CO<sub>2</sub>] conditions. a[CO<sub>2</sub>], ambient [CO<sub>2</sub>]; e[CO<sub>2</sub>], elevated [CO<sub>2</sub>]; WAP, weeks after planting; Min, minimum value; Max, maximum value; \*, P <0.05.

Traits	CO <sub>2</sub> level	Parents		DH population			Mean Squares	Broad-sense heritability
		Kukri	RAC875	Min	Max	Mean		
<b>Experiment 02 – Glasshouse experiment</b>								
Shoot dry weight (2WAP) (mg)	a[CO <sub>2</sub> ]	47.2	36.5	20.7	78.1	51.7 ± 0.9	784.7*	0.79
	e[CO <sub>2</sub> ]	65.7	61.6	31	76.9	55.3 ± 0.8		
Shoot dry weight (4WAP) (mg)	a[CO <sub>2</sub> ]	263.7	222.3	122.6	414	272.2 ± 4.5	380467.6*	0.98
	e[CO <sub>2</sub> ]	413.5	294	166.3	495	345.4 ± 5.6		
Seedling height (2WAP) (cm)	a[CO <sub>2</sub> ]	20.1	20.8	14.3	26.6	20.3 ± 0.2	31.1*	0.77
	e[CO <sub>2</sub> ]	22.6	22.6	13.8	25.6	19.6 ± 0.2		
Seedling height (4WAP) (cm)	a[CO <sub>2</sub> ]	35	30.4	26.5	47.6	37.1 ± 0.3	36.7*	0.61
	e[CO <sub>2</sub> ]	37.6	34.9	28.8	48.1	37.9 ± 0.3		
Relative growth rate (mg/day)	a[CO <sub>2</sub> ]	0.037	0.034	0.01	0.05	0.03 ± 0.0004	0.001*	0.96
	e[CO <sub>2</sub> ]	0.038	0.032	0.02	0.05	0.04 ± 0.0004		
Leaf elongation rate (mm/h)	a[CO <sub>2</sub> ]	6.3	6.1	4.1	8.4	6.3 ± 0.1	15.6*	0.89
	e[CO <sub>2</sub> ]	6.8	7.6	1.4	8.8	6.7 ± 0.1		
Leaf width (mm)	a[CO <sub>2</sub> ]	6.7	7.3	5	9	0.7 ± 0.01	0.7*	0.98
	e[CO <sub>2</sub> ]	6.7	8	6	10	0.80 ± 0.01		
<b>Experiment 03 – Growth chamber experiment</b>								
Shoot dry weight (4WAP) (mg)	a[CO <sub>2</sub> ]	271.6	247.2	61.6	251.2	146.1 ± 2.9	2293036*	0.99

	e[CO <sub>2</sub> ]	403.2	277.8	165.9	681.6	321 ± 7.5	
Root dry weight (4WAP) (mg)	a[CO <sub>2</sub> ]	133.6	63.6	16.5	131	46.3 ± 1.7	288182.2*
	e[CO <sub>2</sub> ]	192.9	121.6	32	273.1	107.9 ± 3.6	0.99
Total dry weight (4WAP) (mg)	a[CO <sub>2</sub> ]	405.2	310.9	80.1	382.1	192.3 ± 4.4	4207025.2*
	e[CO <sub>2</sub> ]	596	399.3	235.7	937.1	428.9 ± 10.5	0.99
Root to shoot ratio (4WAP)	a[CO <sub>2</sub> ]	0.49	0.26	0.15	0.85	0.33±0.008	0.048*
	e[CO <sub>2</sub> ]	0.48	0.44	0.19	0.61	0.31±0.007	0.02

**Table 3.** QTL for growth traits of DH population detected in ambient [CO<sub>2</sub>] conditions (400 μmol mol<sup>-1</sup>). WAP, weeks after planting.

Trait	Chromosome	Position	Peak LOD	Explained variance (%)	Additive effect	Nearest marker interval
<b>Experiment 02 - Glasshouse experiment</b>						
Shoot dry weight (2WAP)	1A	174	2.407	7	8.06	wPt-3870 – wPt-9802
Shoot dry weight (4WAP)	6D	0	1.311	3.9	-11.34	barc0137b-barc0065
Seedling height (2WAP)	6D	22	3.087	8.9	-0.655	Stm0671acaq-psp3001
Seedling height (4WAP)	3B	20	3.404	9.8	1.15	Barc0106-cfe0254
	6D	26	2.949	8.5	-1.109	Psp3001-barc0338
Leaf elongation rate	3B	14	4.113	11.7	0.724	wPt-7001 – barc0106
Leaf width	2D	60	2.933	8.5	-0.028	Ksm0098 - wPt-7599
	6B	58	2.511	7.3	-0.024	Gwm0304b – wmm777-13
Relative growth rate	1A	166	3.673	10.5	-0.006	wPt-3870 – wPt-9802
<b>Experiment 03 – Growth chamber experiment</b>						
Shoot dry weight (4WAP)	3B	6	2.352	6.9	0.011	Stm0092tctg – wPt-7001
Root dry weight (4WAP)	3B	30	2.119	6.2	0.006	Cfe0254 – barc0170
Total dry weight (4WAP)	3B	30	2.479	7.2	0.016	Cfe0254 – barc0170

---

Root: Shoot dry weight ratio (4WAP)	5A	56	2.191	6.4	0.023	Barc0091 – wPt-0335
--	----	----	-------	-----	-------	---------------------

---

**Table 4.** QTL for growth traits of the DH population detected in elevated [CO<sub>2</sub>] conditions (700 μmol mol<sup>-1</sup>). WAP, weeks after planting.

Trait	Chromosome	Position	Peak LOD	Explained variance (%)	Additive effect	Nearest marker interval
<b>Experiment 02 - Glasshouse experiment</b>						
Shoot dry weight (2WAP)	3B	180	3.444	9.9	-3.238	wPt-7924 – wPt-9675
	2A	16	2.958	8.6	-2.884	wPt-2052 – wPt-1139
	7D	90	2.616	7.6	4.017	wPt-4115 – stm0535
Shoot dry weight (4WAP)	3D	108	2.622	7.6	21.269	Barc0247 – barc0134
Seedling height (2WAP)	3B	176	3.605	10.3	-0.896	wPt-7924 – wPt-9675
	6B	142	3.65	10.5	-0.739	wPt-1370 – cfa2141
	2A	168	2.545	7.4	0.618	wPt-9809 – wPt-0944
	7D	100	3.107	9	0.573	wPt-4115 – stm0535
	1B	170	2.588	7.5	-0.543	Gwm0314c – cfb3200
	2A	18	2.475	7.2	-0.531	wPt-1139 – wPt-2762
Seedling height (4WAP)	3B	8	4.512	12.8	1.138	Stm0092tctg – wPt-7001
	6A	2	2.853	8.3	1.026	wPt-6003 – barc0095
	6A	40	5.869	16.3	-1.937	Ppd-d1 – wPt-0330
	4A	88	2.582	7.5	0.201	wPt-7306 – wPt-9277

Leaf elongation rate	6A	62	3.18	9.2	-0.247	wPt-0330 – barc0328b
	1B	168	2.529	7.4	-0.209	Gwm0314c – cfb3200
Leaf width	6B	146	6.418	17.7	-0.033	Cfa2141 – wPt-5231
	2D	92	7.756	20.9	-0.042	Wmc0256a – barc0353b
	6A	78	4.974	14	-0.031	wPt-0330 – barc0328b
	1B	168	3.9	11.1	-0.026	Gwm0314c – cfb3200
Relative growth rate	4D	62	1.942	3.7	-0.001	Barc0054 – cfd0287
<b>Experiment 03 – Growth chamber experiment</b>						
Shoot dry weight (4WAP)	1A	212	3.322	9.6	0.029	wPt-6568 – wmc0215a
	6B	40	5.129	14.4	0.044	wPt-2768 – barc0117
	6D	52	3.23	9.3	0.025	wPt-9887 – wPt-0745
	3A	4	3.229	9.3	-0.024	wPt-4647 – gdm0033b
Root dry weight (4WAP)	2A	0	3.232	9.3	0.013	wPt-1560 – psp3000
	2A	76	4.469	12.7	-0.035	Gwm0413 – barc0137a
Total dry weight (4WAP)	3B	142	2.611	7.6	-0.106	wPt-7924 – wPt-9675
	6B	32	4.21	12	0.077	wPt - 2768 – barc0117
Root: Shoot dry weight ratio (4WAP)	3B	116	2.636	7.7	-0.024	wPt - 0817 – wPt - 7924
	2D	26	4.36	12.4	-0.057	wPt - 8266 – wPt - 6904
	7D	24	2.915	8.5	0.048	Barc0184 – wPt - 0934

**Table 5.** QTL for CO<sub>2</sub> responsiveness of growth traits of the DH population to elevated [CO<sub>2</sub>] conditions (700 μmol mol<sup>-1</sup>). WAP, weeks after planting.

Trait	Chromosome	Position	Peak LOD	Explained variance (%)	Additive effect	Nearest marker interval
<b>Experiment 02 - Glasshouse experiment</b>						
Shoot dry weight (2WAP)	6D	52	1.811	5.3	7	wPt-9887 – wPt-0745
Shoot dry weight (4WAP)	2D	96	2.585	7.5	-9.536	Barc0353b – gwm0169
	3D	98	3.508	10.1	13.613	Barc0223 – barc0247
Seedling height (2WAP)	2D	22	3.404	9.8	3.587	wPt-2636 – wPt-7027
	6A	0	2.515	7.3	3.408	wPt-6003 – wmc0111
	7A	72	2.494	7.3	-2.861	Barc0328a – psp3001a
Seedling height (4WAP)	1B	140	2.115	6.2	-2.917	wPt-5769 – gwm0314c
Leaf elongation rate	6A	2	1.632	4.8	10.516	wPt-6003 – barc0095
Leaf width	6B	144	2.018	5.9	-4.749	wPt-1370 – cfa2141
Relative growth rate	1D	4	1.888	5.6	5.563	wPt-0596 – wPt-5870
<b>Experiment 02 - Growth chamber experiment</b>						
	4B	0	2.506	7.3	16.69	Barc0340a – gwm0495

	2A	36	4.409	12.5	22.112	wPt-5801 – wPt-3753
Shoot dry weight	3A	0	2.941	8.5	-18.782	wPt-4647 – gdm0033b
(4WAP)	7A	98	4.761	13.4	-25.25	wPt-8658 – wmc0264
	5A	60	2.62	7.6	-28.261	wPt-0335 – wPt-3132
Root dry weight	2A	8	2.34	6.8	28.42	wPt-2052 – wPt-1139
(4WAP)	3D	104	2.442	7.1	27.287	Barc0223 – barc0247
Total dry weight	4B	0	2.511	7.3	17.968	Barc0340a – gwm0495
(4WAP)	2A	36	4.372	12.4	23.778	wPt-5801 – wPt-3753
	7A	98	4.957	13.9	-27.538	wPt-8658 – wmc0264
	1B	44	2.538	7.4	17.757	wPt-8093 – wPt-5769
	2B	184	3.042	8.8	-24.901	wPt-6262 – wmc0533
Root: Shoot dry weight						
ratio (4WAP)	2A	198	2.534	7.4	-9.068	wPt-3475 – stm0658acag

573 **References**

574

- 575 Ainsworth E.A., Beier C., Calfapietra C., Ceulemans R., Durand-Tardif M., Farquhar G.D.,  
576 Godbold D.L., Hendrey G.R., Hickler T. & Kaduk J. (2008) Next generation of elevated  
577 [CO<sub>2</sub>] experiments with crops: a critical investment for feeding the future world. *Plant,*  
578 *cell & environment*, **31**, 1317-1324.
- 579 Bennett D., Izanloo A., Edwards J., Kuchel H., Chalmers K., Tester M., Reynolds M.,  
580 Schnurbusch T. & Langridge P. (2012a) Identification of novel quantitative trait loci  
581 for days to ear emergence and flag leaf glaucousness in a bread wheat (*Triticum*  
582 *aestivum* L.) population adapted to southern Australian conditions. *Theoretical and*  
583 *Applied Genetics*, **124**, 697-711.
- 584 Bennett D., Izanloo A., Reynolds M., Kuchel H., Langridge P. & Schnurbusch T. (2012b)  
585 Genetic dissection of grain yield and physical grain quality in bread wheat (*Triticum*  
586 *aestivum* L.) under water-limited environments. *Theoretical and Applied Genetics*, **125**,  
587 255-271.
- 588 Bennett D., Reynolds M., Mullan D., Izanloo A., Kuchel H., Langridge P. & Schnurbusch T.  
589 (2012c) Detection of two major grain yield QTL in bread wheat (*Triticum aestivum* L.)  
590 under heat, drought and high yield potential environments. *Theoretical and Applied*  
591 *Genetics*, **125**, 1473-1485.
- 592 Bernacchi C.J., Thompson J.N., Coleman J.S. & McConnaughay K.D. (2007) Allometric  
593 analysis reveals relatively little variation in nitrogen versus biomass accrual in four  
594 plant species exposed to varying light, nutrients, water and CO<sub>2</sub>. *Plant, cell &*  
595 *environment*, **30**, 1216-1222.
- 596 Bloom A.J. (2015) Photorespiration and nitrate assimilation: a major intersection between plant  
597 carbon and nitrogen. *Photosynthesis research*, **123**, 117-128.
- 598 Bowes G. (1991) Growth at Elevated CO<sub>2</sub> - Photosynthetic Responses Mediated Through  
599 Rubisco. *Plant Cell and Environment*, **14**, 795-806.
- 600 Centritto M., Lee H.S. & Jarvis P. (1999) Increased growth in elevated [CO<sub>2</sub>]: an early, short-  
601 term response? *Global Change Biology*, **5**, 623-633.
- 602 Collard B., Jahufer M., Brouwer J. & Pang E. (2005) An introduction to markers, quantitative  
603 trait loci (QTL) mapping and marker-assisted selection for crop improvement: the basic  
604 concepts. *Euphytica*, **142**, 169-196.
- 605 Conley M.M., Kimball B., Brooks T., Pinter Jr P., Hunsaker D., Wall G., Adam N., LaMorte  
606 R., Matthias A. & Thompson T. (2001) CO<sub>2</sub> enrichment increases water-use efficiency  
607 in sorghum. *New Phytologist*, **151**, 407-412.
- 608 Del Pozo A., Pérez P., Gutiérrez D., Alonso A., Morcuende R. & Martínez-Carrasco R. (2007)  
609 Gas exchange acclimation to elevated CO<sub>2</sub> in upper-sunlit and lower-shaded canopy  
610 leaves in relation to nitrogen acquisition and partitioning in wheat grown in field  
611 chambers. *Environmental and experimental botany*, **59**, 371-380.
- 612 Drake B.G., González-Meler M.A. & Long S.P. (1997) More efficient plants: a consequence  
613 of rising atmospheric CO<sub>2</sub>? *Annual review of plant biology*, **48**, 609-639.
- 614 Farquhar G., von Caemmerer S.v. & Berry J. (1980) A biochemical model of photosynthetic  
615 CO<sub>2</sub> assimilation in leaves of C<sub>3</sub> species. *Planta*, **149**, 78-90.
- 616 Ferris R., Long L., Bunn S., Robinson K., Bradshaw H., Rae A. & Taylor G. (2002) Leaf  
617 stomatal and epidermal cell development: identification of putative quantitative trait  
618 loci in relation to elevated carbon dioxide concentration in poplar. *Tree Physiology*, **22**,  
619 633-640.
- 620 Fitzgerald G.J., Tausz M., O'Leary G., Mollah M.R., Tausz-Posch S., Seneweera S., Mock I.,  
621 Löw M., Partington D.L. & McNeil D. (2016) Elevated atmospheric [CO<sub>2</sub>] can

622 dramatically increase wheat yields in semi-arid environments and buffer against heat  
623 waves. *Global change biology*, **22(6)**, 2269-2284.

624 Fleury D., Jefferies S., Kuchel H. & Langridge P. (2010) Genetic and genomic tools to improve  
625 drought tolerance in wheat. *Journal of experimental botany*, **61(12)**, 3211-3222.

626 Gamage D., Thompson M., Sutherland M., Hirotsu N., Makino A. & Seneweera S. (2018) New  
627 insights into the cellular mechanisms of plant growth at elevated atmospheric carbon  
628 dioxide. *Plant, cell & environment*, **41(6)**, 1233-1246.

629 Geiger M., Walch-Liu P., Engels C., Harnecker J., Schulze E.D., Ludewig F., Sonnewald U.,  
630 Scheible W.R. & Stitt M. (1998) Enhanced carbon dioxide leads to a modified diurnal  
631 rhythm of nitrate reductase activity in older plants, and a large stimulation of nitrate  
632 reductase activity and higher levels of amino acids in young tobacco plants. *Plant, Cell  
633 & Environment*, **21**, 253-268.

634 Ghildiyal M. & Sharma-Natu P. (2000) Photosynthetic acclimation to rising atmospheric  
635 carbon dioxide concentration. 961-966.

636 Hikosaka K., Onoda Y., Kinugasa T., Nagashima H., Anten N.P.R. & Hirose T. (2005) Plant  
637 responses to elevated CO<sub>2</sub> concentration at different scales: Leaf, whole plant, canopy,  
638 and population. *Ecological Research*, **20**, 243-253.

639 Hsiao T.C. & Jackson R.B. (1999) Interactive effects of water stress and elevated CO<sub>2</sub> on  
640 growth, photosynthesis, and water use efficiency. In: *Carbon dioxide and  
641 environmental stress*, pp. 3-31. Elsevier.

642 Hunt R. (2003) Growth analysis, individual plants. *Encyclopaedia of applied plant sciences*.  
643 *Academic Press, Londres*, 579-588.

644 IPCC (2013) Summary for Policymakers. In: *Climate Change 2013: The Physical Science  
645 Basis. Contribution of Working Group I to the Fifth Assessment Report of the  
646 Intergovernmental Panel on Climate change*. In: [Stocker, T.F., D. Qin, G.-K. Plattner,  
647 M. Tignor, s.K. Ailen, J. Boschung, A. Nauels, Y. Xia, V. Bex and P.M. Midgley (eds.).  
648 Cambridge University Press, Cambridge, United Kingdom and New York, NY, USA.

649 Izanloo A., Condon A.G., Langridge P., Tester M. & Schnurbusch T. (2008) Different  
650 mechanisms of adaptation to cyclic water stress in two South Australian bread wheat  
651 cultivars. *Journal of Experimental Botany*, **59**, 3327-3346.

652 Jitla D.S., Rogers G.S., Seneweera S.P., Basra A.S., Oldfield R.J. & Conroy J.P. (1997)  
653 Accelerated early growth of rice at elevated CO<sub>2</sub>. *Plant Physiology*, **115**, 15-22.

654 Kamran A., Iqbal M. & Spaner D. (2014) Flowering time in wheat (*Triticum aestivum* L.): a  
655 key factor for global adaptability. *Euphytica*, **197**, 1-26.

656 Keenan T.F., Hollinger D.Y., Bohrer G., Dragoni D., Munger J.W., Schmid H.P. & Richardson  
657 A.D. (2013) Increase in forest water-use efficiency as atmospheric carbon dioxide  
658 concentrations rise. *Nature*, **499**, 324.

659 Kirschbaum M.U. (2010) Does Enhanced Photosynthesis Enhance Growth? Lessons Learnt  
660 From CO<sub>2</sub> Enrichment Studies. *Plant physiology*, pp. 110.166819.

661 Laurie D.A. (1997) Comparative genetics of flowering time. In: *Oryza: From Molecule to  
662 Plant*, pp. 167-177. Springer.

663 Liao M., Fillery I.R. & Palta J.A. (2004) Early vigorous growth is a major factor influencing  
664 nitrogen uptake in wheat. *Functional Plant Biology*, **31**, 121-129.

665 Ludwig F. & Asseng S. (2010) Potential benefits of early vigor and changes in phenology in  
666 wheat to adapt to warmer and drier climates. *Agricultural Systems*, **103**, 127-136.

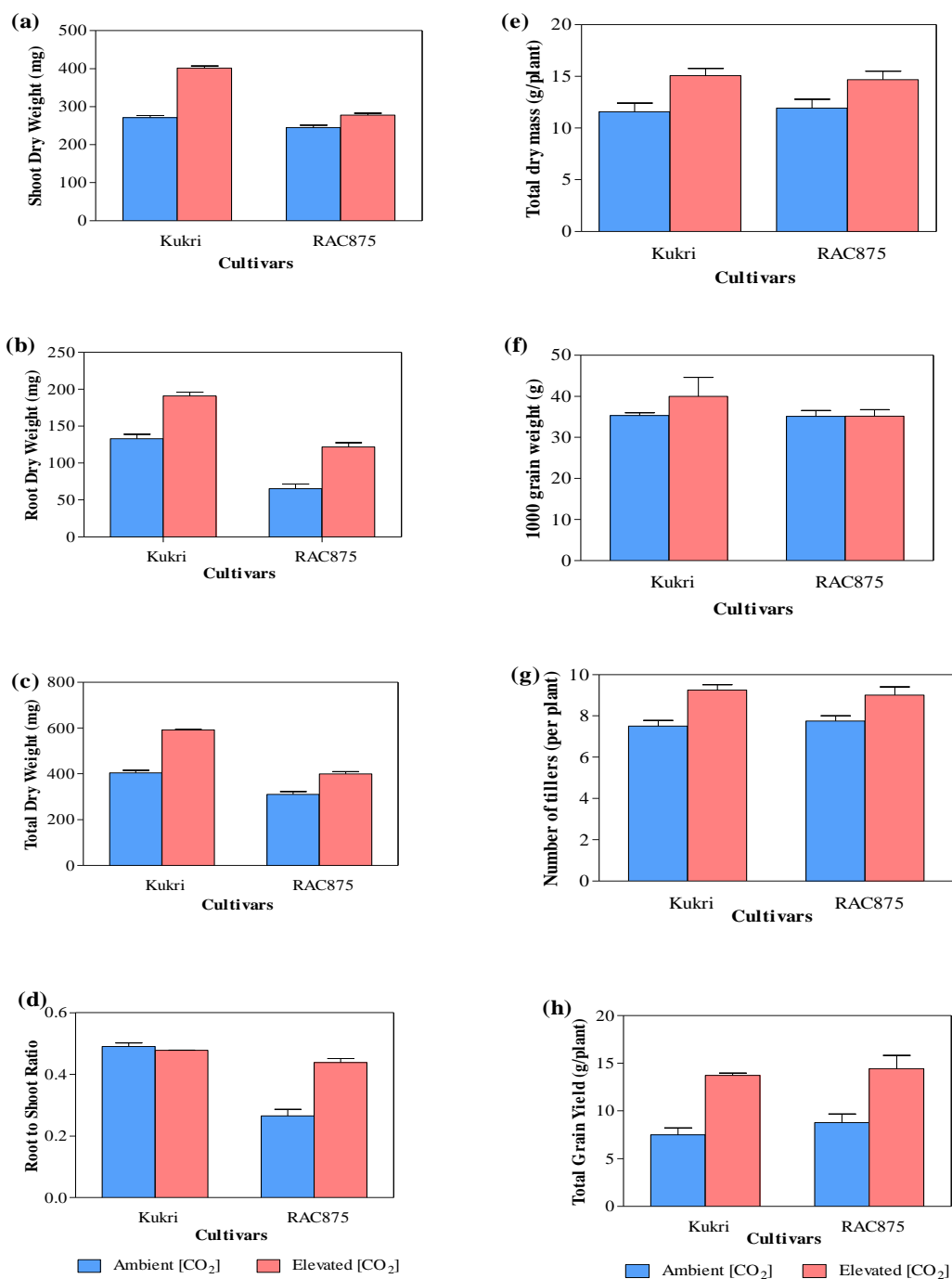
667 Mahjourimajd S., Kuchel H., Langridge P. & Okamoto M. (2015) Evaluation of Australian  
668 wheat genotypes for response to variable nitrogen application. *Plant and Soil*, 1-9.

- 669 Mahjourimajd S., Taylor J., Sznajder B., Timmins A., Shahinnia F., Rengel Z., Khabaz-Saberi  
670 H., Kuchel H., Okamoto M. & Langridge P. (2016) Genetic basis for variation in wheat  
671 grain yield in response to varying nitrogen application. *PLoS one*, **11**, e0159374.
- 672 Makino A., Harada M., Sato T., Nakano H. & Mae T. (1997) Growth and N allocation in rice  
673 plants under CO<sub>2</sub> enrichment. *Plant Physiology*, **115**, 199-203.
- 674 Makino A. & Mae T. (1999) Photosynthesis and plant growth at elevated levels of CO<sub>2</sub>. *Plant  
675 and Cell Physiology*, **40**, 999-1006.
- 676 Masle J. (2000) The effects of elevated CO<sub>2</sub> concentrations on cell division rates, growth  
677 patterns, and blade anatomy in young wheat plants are modulated by factors related to  
678 leaf position, vernalization, and genotype. *Plant Physiology*, **122**.
- 679 Masle J., Hudson G.S. & Badger M.R. (1993) Effects of ambient CO<sub>2</sub> concentration on growth  
680 and nitrogen use in tobacco (*Nicotiana tabacum*) plants transformed with an antisense  
681 gene to the small subunit of ribulose-1, 5-bisphosphate carboxylase/oxygenase. *Plant  
682 Physiology*, **103**, 1075-1088.
- 683 Miralles D. & Richards R. (2000) Responses of leaf and tiller emergence and primordium  
684 initiation in wheat and barley to interchanged photoperiod. *Annals of Botany*, **85**, 655-  
685 663.
- 686 Murchie E., Pinto M. & Horton P. (2009) Agriculture and the new challenges for  
687 photosynthesis research. *New Phytologist*, **181**, 532-552.
- 688 Nagai Y., Matsumoto K., Kakinuma Y., Ujiie K., Ishimaru K., Gamage D.M., Thompson M.,  
689 Milham P.J., Seneweera S. & Hirotsu N. (2016) The chromosome regions for increasing  
690 early growth in rice: role of sucrose biosynthesis and NH<sub>4</sub><sup>+</sup> uptake. *Euphytica*, **211**,  
691 343-352.
- 692 Neales T. & Nicholls A. (1978) Growth Responses on Young Wheat Plants to a Range of  
693 Ambient CO<sub>2</sub> Levels. *Functional Plant Biology*, **5**, 45-59.
- 694 Pérez-Harguindeguy N., Díaz S., Garnier E., Lavorel S., Poorter H., Jaureguiberry P., Bret-  
695 Harte M., Cornwell W., Craine J. & Gurvich D. (2013) New handbook for standardised  
696 measurement of plant functional traits worldwide. *Australian Journal of Botany*, **61**,  
697 167-234.
- 698 Poorter H. (1993) Interspecific variation in the growth response of plants to an elevated ambient  
699 CO<sub>2</sub> concentration. *Vegetatio*, **104**, 77-97.
- 700 Poorter H. & Navas M.L. (2003) Plant growth and competition at elevated CO<sub>2</sub>: on winners,  
701 losers and functional groups. *New Phytologist*, **157**, 175-198.
- 702 Rae A., Ferris R., Tallis M. & Taylor G. (2006) Elucidating genomic regions determining  
703 enhanced leaf growth and delayed senescence in elevated CO<sub>2</sub>. *Plant, Cell &  
704 Environment*, **29**, 1730-1741.
- 705 Rae A.M., Tricker P.J., Bunn S.M. & Taylor G. (2007) Adaptation of tree growth to elevated  
706 CO<sub>2</sub>: quantitative trait loci for biomass in *Populus*. *New Phytologist*, **175**, 59-69.
- 707 Reinke R., Richards R., Angus J. & Lewin L. (2002) Early vigor: an important foundation for  
708 rapid biomass accumulation. In: *Proceedings 2nd Temperate Rice Conference* (eds  
709 J.E.Hill & B.Hardy), pp. 429-438, Sacramento, USA, 13-17 June 1999).
- 710 Royo C., Ammar K., Alfaro C., Dreisigacker S., del Moral L.F.G. & Villegas D. (2018) Effect  
711 of Ppd-1 photoperiod sensitivity genes on dry matter production and allocation in  
712 durum wheat. *Field Crops Research*, **221**, 358-367.
- 713 Seneweera S. (2011a) Effects of elevated CO<sub>2</sub> on plant growth and nutrient partitioning of rice  
714 (*Oryza sativa* L.) at rapid tillering and physiological maturity. *Journal of Plant  
715 Interactions*, **6**, 35-42.
- 716 Seneweera S. (2011b) Reduced nitrogen allocation to expanding leaf blades suppresses  
717 ribulose-1, 5-bisphosphate carboxylase/oxygenase synthesis and leads to  
718 photosynthetic acclimation to elevated CO<sub>2</sub> in rice. *Photosynthetica*, **49**, 145-148.

- 719 Seneweera S., Ghannoum O., Conroy J., Ishimaru K., Okada M., Lieffering M., Kim H.Y. &  
720 Kobayashi K. (2002) Changes in source–sink relations during development influence  
721 photosynthetic acclimation of rice to free air CO<sub>2</sub> enrichment (FACE). *Functional plant*  
722 *biology*, **29**, 947-955.
- 723 Seneweera S.P. & Conroy J.P. (2005) Enhanced leaf elongation rates of wheat at elevated CO<sub>2</sub>:  
724 is it related to carbon and nitrogen dynamics within the growing leaf blade?  
725 *Environmental and experimental botany*, **54**, 174-181.
- 726 Sharkey T.D. (2016) What gas exchange data can tell us about photosynthesis. *Plant, Cell &*  
727 *Environment*, **39**, 1161-1163.
- 728 Shewry P. (2009) Wheat. *Journal of experimental botany*, **60**, 1537-1553.
- 729 Shimono H., Okada M., Yamakawa Y., Nakamura H., Kobayashi K. & Hasegawa T. (2009)  
730 Genotypic variation in rice yield enhancement by elevated CO<sub>2</sub> relates to growth before  
731 heading, and not to maturity group. *Journal of Experimental Botany*, **60**, 523-532.
- 732 Solomon S., Qin D. & Manning R. (2007) *Technical summary. Climate Change 2007: The*  
733 *Physical Science Basis*.
- 734 Stitt M. & Krapp A. (1999) The interaction between elevated carbon dioxide and nitrogen  
735 nutrition: the physiological and molecular background. *Plant, Cell & Environment*, **22**,  
736 583-621.
- 737 Sun J., Zhang J., Larue C.T. & Huber S.C. (2011) Decrease in leaf sucrose synthesis leads to  
738 increased leaf starch turnover and decreased RuBP regeneration-limited photosynthesis  
739 but not Rubisco-limited photosynthesis in Arabidopsis null mutants of SPSA1. *Plant,*  
740 *cell & environment*, **34**, 592-604.
- 741 Tans P. & Keeling R. (2018) Trends in atmospheric carbon dioxide. NOAA/ESRL  
742 ([www.esrl.noaa.gov/gmd/ccgg/trends/](http://www.esrl.noaa.gov/gmd/ccgg/trends/)).
- 743 Tausz M., Tausz-Posch S., Norton R.M., Fitzgerald G.J., Nicolas M.E. & Seneweera S. (2013)  
744 Understanding crop physiology to select breeding targets and improve crop  
745 management under increasing atmospheric CO<sub>2</sub> concentrations. *Environmental and*  
746 *Experimental Botany*, **88**, 71-80.
- 747 Ter Steege M.W., den Ouden F.M., Lambers H., Stam P. & Peeters A.J. (2005) Genetic and  
748 physiological architecture of early vigor in *Aegilops tauschii*, the D-genome donor of  
749 hexaploid wheat. A quantitative trait loci analysis. *Plant Physiol*, **139**, 1078-1094.
- 750 Thilakarathne C.L., Tausz-Posch S., Cane K., Norton R.M., Fitzgerald G.J., Tausz M. &  
751 Seneweera S. (2015) Intraspecific variation in leaf growth of wheat (*Triticum aestivum*)  
752 under Australian Grain Free Air CO<sub>2</sub> Enrichment (AGFACE): is it regulated through  
753 carbon and/or nitrogen supply? *Functional Plant Biology*, **42**, 299-308.
- 754 Thilakarathne C.L., Tausz-Posch S., Cane K., Norton R.M., Tausz M. & Seneweera S. (2013)  
755 Intraspecific variation in growth and yield response to elevated CO<sub>2</sub> in wheat depends  
756 on the differences of leaf mass per unit area. *Functional Plant Biology*, **40**, 185-194.
- 757 Trevisan S., Manoli A. & Quaggiotti S. (2014) NO signaling is a key component of the root  
758 growth response to nitrate in *Zea mays* L. *Plant Signaling and Behavior*, **9**.
- 759 Van Der Kooij T.A. & De Kok L. (1996) Impact of elevated CO<sub>2</sub> on growth and development  
760 of *Arabidopsis thaliana* L. *PHYTON-HORN-*, **36**, 173-184.
- 761 Villegas D., Aparicio N., Blanco R. & Royo C. (2001) Biomass accumulation and main stem  
762 elongation of durum wheat grown under Mediterranean conditions. *Annals of Botany*,  
763 **88**, 617-627.
- 764 Von Caemmerer S.v. & Farquhar G. (1981) Some relationships between the biochemistry of  
765 photosynthesis and the gas exchange of leaves. *Planta*, **153**, 376-387.
- 766 Yang J.T., Preiser A.L., Li Z., Weise S.E. & Sharkey T.D. (2016) Triose phosphate use  
767 limitation of photosynthesis: short-term and long-term effects. *Planta*, **243**, 687-698.

- 768 Zadoks J.C., Chang T.T. & Konzak C.F. (1974) A decimal code for the growth stages of  
769 cereals. *Weed research*, **14**, 415-421.
- 770 Zhu X.-G., Long S.P. & Ort D.R. (2008) What is the maximum efficiency with which  
771 photosynthesis can convert solar energy into biomass? *Current opinion in*  
772 *biotechnology*, **19**, 153-159.

773



**Supplementary Figure 1** Growth parameters of Kukri and RAC875 grown at ambient [CO<sub>2</sub>] (400  $\mu\text{mol mol}^{-1}$ ) and elevated [CO<sub>2</sub>] (700  $\mu\text{mol mol}^{-1}$ ); (a) Shoot dry weight, (b) Root dry weight, (c) Total dry weight and (d) root to shoot ration at 4 weeks after planting (WAP) and (e) Total dry mass per plant, (f) 1000 grain weight per plant, (g) Number of tillers per plant and (f) Total grain yield per plant at maturity

**Supplementary Table S1.** Analysis of variance (ANOVA) results of gas exchange measurements of Kukri and RAC875 grown at ambient [CO<sub>2</sub>] (400 μmol mol<sup>-1</sup>) and elevated [CO<sub>2</sub>] (700 μmol mol<sup>-1</sup>) at 4 weeks after planting (WAP) and at anthesis (DC65). a[CO<sub>2</sub>], ambient [CO<sub>2</sub>]; e[CO<sub>2</sub>], elevated [CO<sub>2</sub>]; *G<sub>s</sub>*, rate of stomatal conductance; *C<sub>i</sub>*, intracellular [CO<sub>2</sub>]; *V<sub>cm</sub>*, Maximum carboxylation rate of Rubisco; *J<sub>max</sub>*, Maximum rate of photosynthetic electron transport; *TPU*, rate of triose phosphate utilization; ns, not significant; \*, P<0.05; \*\*, P<0.01.

Trait	Mean CO <sub>2</sub> effect			Mean cultivar effect			Interaction effect (ANOVA results) [CO <sub>2</sub> ]x Cultivar
	a[CO <sub>2</sub> ]	e[CO <sub>2</sub> ]	ANOVA result	Kukri	RAC875	ANOVA result	
<b>Photosynthesis parameters at 4 WAP</b>							
Photosynthesis rate (μmol CO <sub>2</sub> m <sup>-2</sup> s <sup>-1</sup> )	23.6	29.1	**	27.8	24.9	**	ns
<i>G<sub>s</sub></i> (mol H <sub>2</sub> O m <sup>-2</sup> s <sup>-1</sup> )	0.35	0.311	ns	0.364	0.306	ns	ns
<i>C<sub>i</sub></i> (μmol CO <sub>2</sub> mol <sup>-1</sup> )	277.4	524.9	**	404.9	397.4	ns	ns
Transpiration	4.1	3.5	ns	3.9	3.7	*	ns
<b>Photosynthesis parameters at anthesis (DC65)</b>							
Photosynthesis rate (μmol CO <sub>2</sub> m <sup>-2</sup> s <sup>-1</sup> )	23.3	29.7	**	25.4	27.5	*	**
<i>V<sub>cm</sub></i> (mol H <sub>2</sub> O m <sup>-2</sup> s <sup>-1</sup> )	44.1	43.6	ns	43.5	43.8	ns	ns
<i>J<sub>max</sub></i> (μmol CO <sub>2</sub> mol <sup>-1</sup> )	221.3	225.9	ns	218.3	228.3	**	**
<i>TPU</i> (μmol CO <sub>2</sub> m <sup>-2</sup> s <sup>-1</sup> )	19.4	18.0	**	17.9	19.4	**	ns

Gs (mol H <sub>2</sub> O m <sup>-2</sup> s <sup>-1</sup> )	0.52	0.34	**	0.30	0.52	**	*
Ci (μmol CO <sub>2</sub> mol <sup>-1</sup> )	266.6	536.8	**	416.4	397.4	**	ns
Transpiration	4.47	4.46	ns	3.9	4.9	**	**

312

**Supplementary Table S2.** Analysis of variance (ANOVA) for different growth traits investigated in experiment 02 (glasshouse trial) and experiment 03 (growth chamber trial). WAP, weeks after planting; ns, not significant; \*, P<0.05; \*\*, P<0.01.

Variance component	Experiment 02 – glasshouse trial						Experiment 03 – growth chamber trial				
	Shoot dry weight (2WAP)	Shoot dry weight (4WAP)	Seedling height (2WAP)	Seedling height (4WAP)	Relative growth rate	Leaf elongation rate	Leaf width	Shoot dry weight (4WAP)	Root dry weight (4WAP)	Total dry weight (4WAP)	Root to shoot ratio (4WAP)
Genotype	**	**	**	**	*	**	**	**	**	**	**
[CO <sub>2</sub> ]	**	**	**	*	**	**	**	**	**	**	**
Genotype x [CO <sub>2</sub> ] interaction	**	ns	ns	ns	ns	**	**	**	**	**	**

**Supplementary Table S3.** Controlled environmental conditions provided to the Reach-in plant growth chambers throughout the experimental period.

Time Period	Temperature	Relative humidity	[CO <sub>2</sub> ] concentration		Light intensity
			Ambient [CO <sub>2</sub> ]	Elevated [CO <sub>2</sub> ]	
06:00 hrs	15°C	70%	400 μmolmol <sup>-1</sup>	700 μmolmol <sup>-1</sup>	Partial (40%)
08:00 hrs	20°C	70%	400 μmolmol <sup>-1</sup>	700 μmolmol <sup>-1</sup>	Partial (40%)
11:00 hrs	23°C	70%	400 μmolmol <sup>-1</sup>	700 μmolmol <sup>-1</sup>	Partial (40%)
15:00 hrs	20°C	70%	400 μmolmol <sup>-1</sup>	700 μmolmol <sup>-1</sup>	Partial (40%)
18:00 hrs	15°C	70%	400 μmolmol <sup>-1</sup>	700 μmolmol <sup>-1</sup>	Partial (40%)
20:00 hrs	13°C	70%	400 μmolmol <sup>-1</sup>	700 μmolmol <sup>-1</sup>	Partial (40%)

**Supplementary Table S4.** Correlation matrix of physiological traits of the DH population grown under different CO<sub>2</sub> concentrations in experiment 02 (glasshouse experiment). a[CO<sub>2</sub>], ambient [CO<sub>2</sub>]; e[CO<sub>2</sub>], elevated [CO<sub>2</sub>]; WAP, weeks after planting; \*, P<0.05; \*\* P<0.01.

Traits	CO <sub>2</sub> level	Shoot dry weight (2WAP)	Shoot dry weight (4WAP)	Seedling height (2WAP)	Seedling height (4WAP)	Relative growth rate	Leaf elongation rate	Leaf width
Shoot dry weight (2WAP)	e[CO <sub>2</sub> ]	1	0.430**	0.515**	0.147	-0.455**	0.368**	.334**
	a[CO <sub>2</sub> ]	1	0.337**	0.479**	0.088	-0.579**	0.295**	0.255**
Shoot dry weight (4WAP)	e[CO <sub>2</sub> ]		1	0.409**	0.151	0.597**	0.405**	0.36**
	a[CO <sub>2</sub> ]		1	.303**	0.174**	0.550**	0.272**	0.247**
Seedling height (2WAP)	e[CO <sub>2</sub> ]			1	0.338**	-0.051	0.701**	0.392
	a[CO <sub>2</sub> ]			1	0.207*	-0.165*	0.741**	0.412**
Seedling height (4WAP)	e[CO <sub>2</sub> ]				1	0.028	0.354**	0.090
	a[CO <sub>2</sub> ]				1	0.088	0.231**	0.356**
Relative growth rate	e[CO <sub>2</sub> ]					1	0.082	0.061
	a[CO <sub>2</sub> ]					1	-0.051	-0.005
Leaf elongation rate	e[CO <sub>2</sub> ]						1	0.277**
	a[CO <sub>2</sub> ]						1	0.375**
Leaf width	e[CO <sub>2</sub> ]							1
	a[CO <sub>2</sub> ]							1

**Supplementary Table S5.** Correlation matrix of physiological traits of the DH population grown under different CO<sub>2</sub> concentrations in experiment 03 (growth chamber experiment). a[CO<sub>2</sub>]; ambient [CO<sub>2</sub>]; e[CO<sub>2</sub>], elevated [CO<sub>2</sub>]; WAP, weeks after planting; \*, P<0.05; \*\*, P<0.01.

<b>Traits</b>	<b>CO<sub>2</sub> level</b>	<b>Shoot dry weight (4WAP)</b>	<b>Root dry weight (4WAP)</b>	<b>Total dry weight (4WAP)</b>	<b>Root to shoot ratio (4WAP)</b>
Shoot dry weight (4WAP)	e[CO <sub>2</sub> ]	1	.789**	.978**	.115
	a[CO <sub>2</sub> ]	1	.803**	.973**	.400**
Root dry weight (4 WAP)	e[CO <sub>2</sub> ]		1	.899**	.665**
	a[CO <sub>2</sub> ]		1	.919**	.851**
Total dry weight (4WAP)	e[CO <sub>2</sub> ]			1	.307**
	a[CO <sub>2</sub> ]			1	.594**
Root to shoot ratio (4WAP)	e[CO <sub>2</sub> ]				1
	a[CO <sub>2</sub> ]				1

## Chapter 4

### **Elevated carbon dioxide mediated early growth responses of wheat (*Triticum aestivum* L.): an analysis of source and sink interactions**

This study was conducted to understand the role of key photosynthetic and post-photosynthetic metabolic processes in determining plant growth responses at elevated [CO<sub>2</sub>]. A multidisciplinary approach was used to characterize photosynthesis, carbon metabolism, nitrogen metabolism and cell cycle functions using physiological and molecular tools. Experiments were conducted using selected wheat lines from the doubled haploid population based on their CO<sub>2</sub> responsiveness. Physiological characterization was carried out at the whole plant level whereas biochemical and molecular analyses were carried out at different organ levels. The last fully expanded leaf, expanding leaf, cell elongation region and shoot apex region were used in gene expression and sugar analyses to understand the source and sink interactions at elevated [CO<sub>2</sub>]. This chapter has been prepared as a research article to be submitted to “Plant, Cell and Environment”.

**Gamage D**, Thompson M, Dehigaspitiya P, Fukushima A, Sutherland M.W., Hirotsu N, Seneweera S, ‘Elevated carbon dioxide mediated early growth responses of wheat (*Triticum aestivum* L.): an analysis of source and sink interactions’ (Prepared for publication)

1 **Article title:**

2 Elevated carbon dioxide mediated early growth responses of wheat (*Triticum aestivum* L.): an  
3 analysis of source and sink interactions

4  
5 **Authors:**

6 Dananjali Gamage<sup>1&3</sup>, Michael Thompson<sup>1</sup>, Prabuddha Dehigaspitiya<sup>1</sup>, Ayaka Fukushima<sup>2</sup>,  
7 Mark W. Sutherland<sup>1</sup>, Naoki Hirotsu<sup>1&2</sup>, Saman Seneweera<sup>1,3&4\*1</sup>

8  
9 **Author affiliations:**

10 <sup>1</sup> Centre for Crop Health, University of Southern Queensland, Toowoomba QLD 4350  
11 Australia.

12 <sup>2</sup> Graduate School of Life Sciences, Toyo University, Oura-gun, Gunma, 374-0193 Japan.

13 <sup>3</sup> Department of Agricultural Biology, Faculty of Agriculture, University of Ruhuna,  
14 Kamburupitiya 81 100, Sri Lanka.

15 <sup>4</sup> National Institute of Fundamental Studies, Hantana Road, Kandy 20000, Sri Lanka

16  
17 **\*Corresponding author:**

18 A/Prof. Saman Seneweera

19 Centre for Crop Health,

20 University of Southern Queensland,

21 Toowoomba Queensland 4350 Australia.

22 Email: [Saman.Seneweera@usq.edu.au](mailto:Saman.Seneweera@usq.edu.au)

23  
24 **Abbreviations:**

25 [CO<sub>2</sub>] – Carbon dioxide concentration; Rubisco - Ribulose 1,5-bisphosphate  
26 carboxylase/oxygenase; LFELB - Last fully expanded leaf blade; ELB - Expanding leaf blade;  
27 CER – cell elongation region; LCEZ – leaf cell elongation zone; SAR – shoot apex region;  
28 *rbcL* - Ribulose 1,5 –bisphosphate carboxylase/oxygenase (large sub unit); *rbcS* - Ribulose 1,5  
29 –bisphosphate carboxylase/oxygenase (small sub unit); *SPP1* - Sucrose Phosphate Phosphatase  
30 1; *SPS1* - Sucrose Phosphate Synthase 1; *SUS1* - Sucrose Synthase type 1; *NiR* - Ferredoxin

---

<sup>1</sup> DG – Study design, acquisition, analysis and interpretation of data, drafting of manuscript, MT, PD, AF- Acquisition of data and revision of the manuscript, MWS – critical revision, NH analysis and interpretation of data and critical revision, SS- Study conception and design, analysis and interpretation of data, critical revision

31 Nitrite Reductase; *Fd-GOGAT* - Putative ferredoxin-dependent glutamate synthase; *GS2a* -  
32 Glutamine Synthetase (Plastidial) – GS2; *GS2b* - Glutamine Synthetase (Plastidial) – GS2;  
33 *NADH-GOGAT* - Putative NADH-dependent glutamate synthase; *GS1a* - Glutamine  
34 synthetase (cytosolic) – GS1; *GSr1* - Glutamine synthetase (cytosolic) – GS1; *TaEXPA1* -  $\alpha$  –  
35 expansin A1; *TaEXPA3* -  $\alpha$  – expansin A3; *TaEXPB1* -  $\beta$  – expansin B1; *TaEXPB2* -  $\beta$  –  
36 expansin B2; *TaEXPB3* -  $\beta$  – expansin B3; *TaEXPB6* -  $\beta$  – expansin B6; *TaEXPB23* -  $\beta$  –  
37 expansin B23; *TaXTH1* - Xyloglucan endotransglucosylase/hydrolase 1; *TaXTH2* - Xyloglucan  
38 endotransglucosylase/hydrolase 2; *TaXTH3* - Xyloglucan endotransglucosylase/hydrolase 3;  
39 *TaXTH4* - Xyloglucan endotransglucosylase/hydrolase 4; *TaXTH5* - Xyloglucan  
40 endotransglucosylase/hydrolase 5.

41

#### 42 **Summary statement**

43 Soluble sugar accumulation at elevated [CO<sub>2</sub>] varies between cultivar, CO<sub>2</sub> levels and the organ  
44 type. In response to the availability of different sugars, expression of key genes related to  
45 photosynthesis, carbon and nitrogen metabolism and cell wall metabolism have been  
46 upregulated.

47 **Abstract**

48 The physiological and molecular mechanisms of plant growth responses at elevated [CO<sub>2</sub>] were  
49 investigated through developing an understanding of the source and sink interaction using  
50 wheat. Wheat plants were grown under ambient [CO<sub>2</sub>] (400 μmol mol<sup>-1</sup>) and elevated [CO<sub>2</sub>]  
51 (700 μmol mol<sup>-1</sup>) for 6 weeks. Above ground and below ground biomass accumulation, total  
52 leaf area and rate of photosynthesis were measured at 42 days after planting. Total soluble  
53 carbohydrate concentration in different plant organs (last fully expanded leaf blade, expanding  
54 leaf blade and cell elongation region) was measured. Expression analysis of genes involved in  
55 photosynthesis (*rbcL*, *rbcS*), carbon metabolism (*SPPI*, *SPSI* and *SUS1*), nitrogen metabolism  
56 (*Fd-GOGAT*, *NADH-GOGAT*, *GS2a*, *GS2b*, *GSr1*, *GS1a*), cell wall metabolism ( $\alpha$  and  $\beta$  –  
57 expansins, Xyloglucan endotransglucosylase/hydrolases) was performed using real-time  
58 quantitative-PCR. There were significant interactions between [CO<sub>2</sub>] and cultivar for above  
59 (P<0.01) and below ground biomass (P<0.01), total leaf area (P<0.01), total soluble  
60 carbohydrate content (P<0.01) and leaf photosynthesis (P<0.05). Transcript abundance of key  
61 genes showed a marked difference at elevated [CO<sub>2</sub>] showing a significant [CO<sub>2</sub>] effect across  
62 all organ types and the cultivars (P<0.05). Genes involved in cell wall metabolism and sucrose  
63 synthesis were highly expressed in growing sink tissues. Significant correlations exist between  
64 sugar concentration and *SPPI* and some of the Xyloglucan endotransglucosylase/hydrolases  
65 encoding genes (*TaXTH3*, *TaXTH5*), implying that these metabolic activities may play a  
66 leading role in determining the growth response to elevated [CO<sub>2</sub>].

67

68 **Keywords:** Carbon and nitrogen metabolism, Cell wall metabolism, Elevated [CO<sub>2</sub>], Organ-  
69 specific, Post-photosynthetic processes, Transcript abundance

70

## 71 **1. Introduction**

72 By 2100, the carbon dioxide concentration ( $[\text{CO}_2]$ ) in the atmosphere is predicted to reach ~730  
73 to ~1020  $\mu\text{mol mol}^{-1}$ , which is approximately double the  $[\text{CO}_2]$  of the atmosphere today ([IPCC](#)  
74 [2014](#)). According to [Tans and Keeling \(2018\)](#), the current  $[\text{CO}_2]$  has already reached up to 400  
75  $\mu\text{molmol}^{-1}$  and has significantly impacted precipitation and temperature patterns. Despite these  
76 negative effects of elevated  $[\text{CO}_2]$ , it also has a positive impact on plant growth and  
77 development through improvements in photosynthesis capacities of crops, especially of  $\text{C}_3$   
78 origin ([Ainsworth et al. 2008](#); [Gamage et al. 2018](#)). Overarching research studies have shown  
79 that stimulation of photosynthesis and growth of  $\text{C}_3$  plants at elevated  $[\text{CO}_2]$  is primarily due  
80 to the  $\text{CO}_2$  to  $\text{O}_2$  ratio at the site of  $\text{CO}_2$  fixation. The current atmospheric  $[\text{CO}_2]$  is insufficient  
81 to saturate primary carboxylation, the rate-limiting step of photosynthesis by Ribulose-1,5-  
82 bisphosphate carboxylase/oxygenase (Rubisco), and thus, the majority of  $\text{C}_3$  plants are not  
83 photosynthetically saturated at current  $[\text{CO}_2]$  (Bowes 1993; Aranjuelo et al. 2015; Bloom  
84 2015). Therefore, high  $[\text{CO}_2]$  at the site of fixation leads to increased carboxylation efficiency  
85 of Rubisco and thereby increases the photosynthesis capacity of the plant. This process,  
86 substantially reduces a competing  $\text{O}_2$  fixing reaction commonly known as photorespiration and  
87 indirectly facilitates the primary  $\text{CO}_2$  fixation at elevated  $[\text{CO}_2]$  ([Bloom 2015](#)). However, the  
88 initial stimulation of photosynthesis at elevated  $[\text{CO}_2]$  gradually decreases and settles in the  
89 latter part of the plant development. This process is known as photosynthetic acclimation and  
90 depend on species, nutritional status and other environmental conditions ([Gutiérrez et al. 2009](#);  
91 [Alonso, Pérez, and Martínez-Carrasco 2009](#)). Consistent with this proposition, it has been  
92 demonstrated that the highest plant growth response occurs at early growth stages, which will  
93 eventually lead to structural changes, greater biomass accumulation and yield of crops ([Makino](#)  
94 [et al. 1997](#); [Seneweera et al. 2002](#); [Thilakarathne et al. 2015](#); [Kimball 2016](#); [Jitla et al. 1997](#)).  
95 Therefore, understanding the underlying physiological and molecular mechanism of plant  
96 growth responses to elevated  $[\text{CO}_2]$  at early growth stages is highly beneficial for incorporating  
97  $\text{CO}_2$  responsive traits into current breeding programs in order to improve crop productivity.  
98 ([Gamage et al. 2018](#)).

99

100 Photosynthesis and its subsequent events associated with plant growth and morphogenesis, are  
101 closely linked with the carbohydrate metabolism of the plant ([Masle 2000](#); [Paul and Pellny](#)  
102 [2003](#)). Photosynthesis is a two-way process, including carbohydrate synthesis and utilization;  
103 however, these processes are subjected to a feedback regulation process, which highly controls

104 the source and sink interaction ([Paul and Foyer 2001](#); [Paul and Pellny 2003](#); [Körner 2015](#)). It  
105 has been identified that one of the key factors that determine plant growth is the conversion of  
106 Triose Phosphate (the first stable photosynthesis intermediate) to other types of sugars. In  
107 addition, efficient loading/unloading of these sugars into phloem and transport into growing  
108 sink tissues also play a role in determining the growth response to elevated [CO<sub>2</sub>] ([Masle](#)  
109 [2000](#); [Yang et al. 2016](#)). High carbohydrate availability at elevated [CO<sub>2</sub>] will therefore be used  
110 by the plants to develop additional sinks through tiller and secondary shoot production which  
111 will significantly influence plant growth habits and thereby the final yield ([Jitla et al. 1997](#);  
112 [Makino and Mae 1999](#); [Seneweera et al. 2002](#)). This growth stimulation is then involved with  
113 meristem initiation, cell division, expansion and differentiation and integrates these processes  
114 to develop new sink tissues in order to utilize Triose Phosphate in an efficient manner ([Masle](#)  
115 [2000](#); [Gamage et al. 2018](#)).

116

117 The increased carbon supply at elevated [CO<sub>2</sub>] not only influences the source-sink integration  
118 of plants, but also has a profound effect on the plant transcriptome, which determines the  
119 mechanism for adjusting to a particular environmental change ([Vicente et al. 2015](#); [Ainsworth](#)  
120 [et al. 2006](#)). The transcript level changes in key genes associated with different metabolic  
121 pathways have been previously reported in wheat grown at elevated [CO<sub>2</sub>]. It has been well  
122 established that a number of genes, including carbon and nitrogen metabolism-related genes,  
123 function partly through a sugar sensing mechanism. These genes differentially expressed  
124 between the organs and highly cross-regulate with resource allocation and utilization among  
125 plant tissues ([Koch 1996](#); [Koch 2004](#)). For example, plants grown at elevated [CO<sub>2</sub>] showed  
126 no repression of photosynthetic genes and photosynthetic capacity with enhanced carbon  
127 supply, provided that nitrogen and sink capacity of the plants are not limited ([Geiger et al.](#)  
128 [1999](#); [Martin, Oswald, and Graham 2002](#); [Ainsworth et al. 2004](#)). This efficient carbohydrate  
129 generation and utilization can be observed especially in the early stages of plant growth at  
130 elevated [CO<sub>2</sub>] when the sink strength of the plant is generally high ([Ainsworth and Bush](#)  
131 [2011](#)).

132

133 At elevated [CO<sub>2</sub>], plants produce excess sugars, which includes different metabolically active  
134 sugars such as sucrose, glucose and fructose. Sugar concentrations in different plant tissues  
135 vary in a significant manner, facilitating a broader range of signals which may ultimately  
136 contribute to adaptive changes to different environmental conditions ([Koch 1996](#); [Gibson](#)  
137 [2005](#); [Smeekens et al. 2010](#)). For example, photosynthesis genes in carbon exporting cells or

138 in source tissues are typically upregulated, as the generated sugars are constantly translocated  
139 to sink tissues in which genes related to sucrose formation and amino acids synthesis are  
140 upregulated ([Paul and Pellny 2003](#); [Stitt, Lunn, and Usadel 2010](#)). This suggests that the roles  
141 performed by each gene and their related proteins can be tissue/organ-specific and their roles  
142 may be cross-linked with the sugar availability of a particular tissue or an organ. Despite the  
143 importance of this phenomena, tissue/organ-specific gene expression and its role in  
144 determining plant growth and development at elevated [CO<sub>2</sub>] have not been studied in detail  
145 ([Gamage et al. 2018](#); [Vicente et al. 2015](#)). The high sugar supply will result in changes in  
146 metabolism, enzyme activity and development activity, but this information has not been  
147 evaluated in an extensive manner with relation to CO<sub>2</sub> enriched conditions ([Gamage et al. 2018](#);  
148 [Koch 1996](#); [Aranjuelo et al. 2015](#); [Thompson et al. 2017](#)). Therefore, the role of sugar-  
149 responsive genes in specific tissues, crosstalk with carbon and nitrogen metabolism, together  
150 with plant growth responses, deserves further exploration.

151

152 In this study, we investigated various aspects related to the underlying physiological and  
153 molecular mechanisms of plant growth responses at elevated [CO<sub>2</sub>]. Here we tested the  
154 following hypotheses: (i) plant early growth response to elevated [CO<sub>2</sub>] varies between  
155 cultivars; (ii) plant growth responses are primarily mediated through a variation in net  
156 photosynthesis capacity; (iii) response to elevated [CO<sub>2</sub>] is partially controlled by post-  
157 photosynthetic processes, such as carbon and nitrogen metabolism, and cell cycle functions,  
158 such as cell elongation and expansion, and; (iv) both photosynthetic and post-photosynthetic  
159 processes are mediated through sugar supply and source-sink integration under elevated [CO<sub>2</sub>].  
160 This is the first step towards dissecting the mechanism of early growth of wheat in response to  
161 elevated [CO<sub>2</sub>], focusing on post-photosynthesis metabolism.

162

## 163 **2. Materials and methods**

164

### 165 ***2.1 Plant materials***

166 This study used plant material from a mapping population of wheat derived from the two  
167 parental genotypes Kukri and RAC875, which have shown contrasting growth habits, nitrogen  
168 use efficiencies and has shown a large variation of growth response to elevated [CO<sub>2</sub>] ([Izanloo  
169 et al. 2008](#), our unpublished data; [Bennett, Izanloo, et al. 2012](#); [Bennett, Reynolds, et al. 2012](#)).  
170 The two parental lines have been previously screened for their growth parameters and CO<sub>2</sub>

171 responsiveness at elevated [CO<sub>2</sub>] (unpublished data). Seeds of the mapping population were  
172 sourced from Australian Centre for Plant Functional Genomics, University of Adelaide,  
173 Australia. Based on the results of this screening trial, four high responsive and four less CO<sub>2</sub>-  
174 responsive wheat lines were selected and progressed for further analysis in this study  
175 (Supplementary Table S1). For the clarity in interpretation of results, high responsive lines will  
176 be named henceforth H<sub>1</sub>, H<sub>2</sub>, H<sub>3</sub> and H<sub>4</sub> while less responsive lines will be named as L<sub>1</sub>, L<sub>2</sub>, L<sub>3</sub>  
177 and L<sub>4</sub>.

178

## 179 ***2.2 Growth Conditions***

180 The ten selected wheat lines (four high responsive, four less responsive and two parental lines)  
181 were grown in two identical growth chambers (Reach in growth chambers, PGC-105, Percival,  
182 USA) at the University of Southern Queensland, Australia. Plants were grown with a 14-hour  
183 photoperiod and a day and night temperature of 23°C and 13°C, respectively (Supplementary  
184 Table S2). The relative humidity of both chambers was maintained at 70% throughout the day  
185 while light intensity varied. A light intensity of 1000  $\mu\text{molm}^{-2}\text{s}^{-1}$  was maintained during mid-  
186 day throughout the growing period. Elevated [CO<sub>2</sub>] conditions were maintained at ~700  
187  $\mu\text{molmol}^{-1}$  and ambient [CO<sub>2</sub>] conditions were maintained at ~400  $\mu\text{molmol}^{-1}$  throughout the  
188 growing season.

189

190 Seeds from all the ten lines were surface sterilized for 1 min in 2.6% NaClO and washed  
191 thoroughly using reverse osmosis water. Then, sterilized seeds were placed on moistened filter  
192 papers (Whatmann, Sigma-Aldrich, USA) in Petri dishes and allowed for germination. After  
193 one week of germination, seedlings were transplanted on 400 mm plastic pots filled with 500  
194 g of brown top soil. Then, these pots were either placed in elevated [CO<sub>2</sub>] or ambient [CO<sub>2</sub>].  
195 The experiment was comprised of a completely randomized design at the three-replication level  
196 and was maintained for six weeks after transplantation. Pots were randomized every four days  
197 within each chamber and swapped between chambers weekly to minimize the chamber effect.  
198 Throughout the growing period plants were carefully monitored and all the standard  
199 management practices were carried out to ensure crop health.

200

## 201 ***2.3 Biomass and leaf area determination***

202 At the end of the six weeks growth period (42 days after planting [DAP]), a set of seedlings  
203 from all ten lines were harvested and separated to last fully expanded leaf blades, other leaf

204 blades and roots to determine above-ground and below-ground biomass, total leaf area of the  
205 young wheat seedlings. Before determining biomass, leaf area of the last fully expanded leaves  
206 and other leaf blades were measured using a leaf area meter. Then, to determine the biomass,  
207 leaf blades and root samples of all the ten wheat lines were oven dried for 48 hours at 60°C.  
208

## 209 ***2.4 Tissue carbohydrate analysis***

210

### 211 ***2.4.1 Sample Collection***

212 After six weeks of transplanting, four seedlings of each replicate were carefully sampled for  
213 carbohydrate analysis. Seedlings were separated into last fully expanded leaf (LFELB),  
214 immediate growing leaf and roots. Then, the stem was cut from the base of the main plant, and  
215 the leaf sheaths removed to clear the expanding leaf blade (ELB). From the expanding leaf, a  
216 2 cm section was cut from the base of the seedling and this section was considered as the “shoot  
217 apex region” (SAR) of the young seedling. From the remaining expanding leaf, another section  
218 of 5 cm from the remaining leaf blade was cut and used for further analysis as the “leaf cell  
219 elongation zone” (LCEZ). These tissues were carefully sampled and separately stored in 1.5  
220 mL Eppendorf tubes for further analysis.  
221

### 222 ***2.4.2 Determination of Carbohydrates***

223 Samples collected; LFELB, ELB and pooled samples representing LCEZ and SAR (henceforth  
224 named as cell elongation region [CER]) of each line, were oven dried at 65°C for 72 hours. All  
225 tissue types were then ground to fine powder using a ball mill (Tissue Lyser II, QIAGEN,  
226 Australia) and 50 mg of each sample was used to analyze the glucose, fructose and sucrose in  
227 each tissue type at both elevated [CO<sub>2</sub>] and ambient [CO<sub>2</sub>]. Analysis of these sugars was  
228 assayed enzymatically using a Boehringer Mannheim kit (Catalogue No – 10716260035)  
229 according to the manufacturer’s instructions (R-Biopharm, Germany).  
230

## 231 ***2.5 Gas exchange and chlorophyll fluorescence measurements***

232 Six weeks after planting, gas exchange measurements of the last fully expanded leaf were  
233 carried out as described by [Seneweera et al. \(2002\)](#). Gas exchange measurements were carried  
234 out using a portable photosynthesis system (IRGA, LI-6400, LI-COR, USA) from 9.00 am to  
235 2.00 pm. Leaf chamber temperature and air flow rate of the LI-COR system was maintained at

236 25°C and 500  $\mu\text{mol s}^{-1}$ , respectively. Leaf chamber  $[\text{CO}_2]$  was controlled by the  $[\text{CO}_2]$  mixer  
237 and reference  $[\text{CO}_2]$  in the chamber was maintained at either 400  $\mu\text{mol mol}^{-1}$  or 700  $\mu\text{mol mol}^{-1}$   
238  $^1$  under ambient  $[\text{CO}_2]$  and elevated  $[\text{CO}_2]$ , respectively. Chamber irradiance was supplied by  
239 a red and blue light source and light intensity was maintained at 1500  $\mu\text{mol quanta m}^{-2} \text{s}^{-1}$ .  
240 Relative humidity of the leaf chamber was maintained between 50–70%. Prior to starting gas  
241 exchange measurements, the leaf was allowed to reach a steady state of photosynthesis. The  
242 steady state of photosynthesis was achieved between 10–15 min and then spot measurements  
243 of the rate of photosynthesis, stomatal conductance, intracellular  $[\text{CO}_2]$  and rate of transpiration  
244 were recorded in each genotype.

245

246 Chlorophyll fluorescence parameters were estimated using the leaf chamber fluorometer  
247 attached to an LI-6400XT portable photosynthesis system (LI-6400, LI-COR, USA). After  
248 plants reached a steady state photosynthesis rate, PSII operating efficiency ( $\phi\text{PSII}$ ), electron  
249 transport rate (ETR), photochemical quenching ( $q_p$ ), non-photochemical quenching (NPQ) and  
250 maximum PSII efficiency ( $F_v'/F_m'$ ) were measured for the two parental cultivars Kukri and  
251 RAC875.

252

## 253 ***2.6 Gene expression analysis***

254

### 255 ***2.6.1 Sample collection***

256 Another set of samples were used for gene expression analysis. From one wheat line, four  
257 different plant organs, as described in the earlier section, were used for gene expression  
258 analysis (LFELB, ELB, LCEZ and SAR). Four plants from each replicate were used for this  
259 analysis. Samples were harvested between 10:00 to 13:00 hours and, as soon as they were  
260 harvested, were carefully transferred into liquid nitrogen and stored at  $-80^\circ\text{C}$  until total RNA  
261 extraction was completed.

262

### 263 ***2.6.2 RNA extraction and quantification***

264 Total RNA was extracted from 300 mg (fresh weight basis) of frozen plant materials. Plant  
265 materials were ground with liquid nitrogen using a chilled mortar and pestle to obtain a fine  
266 powder. Then, 700  $\mu\text{l}$  of TPS buffer (100 mM Tris-HCl (pH 8), 10 mM EDTA and 1 M KCl)  
267 and 500  $\mu\text{l}$  (per 300 mg of plant tissues) of Trizol® Reagent (Invitrogen by Thermo Fisher  
268 Scientific, USA) were added to the ground plant materials and further ground until the sample

269 was completely homogenized. Then, RNA extraction for these homogenized samples was  
270 carried out according to the manufacturer's instructions. The quantity of extracted RNA was  
271 determined using a Qubit 3 Fluorimeter (Invitrogen by Thermo Fisher Scientific, USA) as per  
272 the manufacturer's instructions. Finally, total RNA concentration was adjusted to a constant  
273 concentration (1µg/µl) per sample for subsequent reactions.

274

### 275 **2.6.3 cDNA Synthesis**

276 All the samples of RNA were treated with DNase I, Amplification Grade (Invitrogen by  
277 Thermo Fisher Scientific, USA), according to the manufacturer's instructions, to avoid possible  
278 contaminations of genomic DNA in the samples. Then, cDNA synthesis was carried out by  
279 reverse transcription reactions performed using a SensiFAST™ cDNA synthesis kit (Catalogue  
280 No – Bio-65054, Bioline, UK) in a total volume of 20 µl according to manufacturer's  
281 instructions.

282

### 283 **2.6.4 Identification of gene-specific primers**

284 Gene-specific primers associated with photosynthesis, carbon metabolism, nitrogen  
285 metabolism and cell cycle were sourced from previously published literature and verified for  
286 their specificity with *Triticum aestivum* L. using the Primer-Blast option in National Centre for  
287 Biotechnology Information (NCBI). Details of the genes used in the study along with their  
288 primer sequences and relevant literature are listed in Table 1 and Supplementary Table S2. All  
289 the primers were sourced from Integrated DNA Technologies, Inc. USA.

290

### 291 **2.6.5 Real-time Quantitative PCR (qRT-PCR)**

292 The qRT-PCR assays were carried out in an optical 96 well plate with the QuantStudio 3 Real-  
293 Time PCR system (Applied Biosystems from Thermo Fisher Scientific, USA), using SYBR  
294 green to monitor double-stranded DNA synthesis. The assay reaction mixture of 20 µl  
295 contained 4 µl of diluted cDNA (1:10), 2 µl 10 mM gene-specific primer, 4 µl of DNase/RNase  
296 free water and 10 µl of 2X-SYBR Green Master Mix reagent (Applied Biosystems from  
297 Thermo Fisher Scientific, USA). The programme for the thermal cycler was 95°C for 10  
298 minutes, 40 cycles of 95°C for 15 sec and 60°C for 1 minute. The melt curve protocol followed  
299 with 15 seconds at 95°C and then 60 seconds each at 1.6°C increments between 60°C and 95°C.  
300 Samples from LFELB, ELB, LCEZ and SAR of two parental lines (Kukri and RAC0875) were

301 used in three biological replicates per treatment in the qRT-PCR assay. The efficiency of the  
302 qRT-PCR was determined using raw fluorescence data as input in LinRegPCR v2012.3 ([Ruijter  
303 et al. 2009](#)). Determination of relative expression was done using the comparative threshold  
304 cycle ( $C_t$ ) method  $2^{-\Delta\Delta C_t}$  ([Schmittgen and Livak 2008](#); [Pfaffl 2001](#)) and presented as the  $\log_2$   
305 fold change of elevated and ambient  $[\text{CO}_2]$ .

306

## 307 ***2.7 Statistical Analysis***

308 Treatment effects and interactions were determined by Analysis of Variance (ANOVA)  
309 through general linear modeling. Standard errors of differences and the Tukey's test were used  
310 to determine the differences between treatments. Differences were considered significant at  
311  $P < 0.05$ . Pearson product-moment correlation test was conducted to analyse the potential  
312 correlation between sugar content and the relative gene expression at elevated  $[\text{CO}_2]$ . All  
313 statistical analyses were performed using SPSS statistical software version 23 (IBM, Armonk,  
314 NY, USA). All graphical representations were carried out using GraphPad Prism scientific  
315 software version 5.01 (GraphPad Software, San Diego, CA).

316

317

## 318 **3. Results**

319

### 320 ***3.1 Genetic variation in growth response to elevated $[\text{CO}_2]$***

321 Growth characteristics of two parental lines of the mapping population showed a significant  
322 difference when they were grown at elevated  $[\text{CO}_2]$ . There were significant interactions  
323 between  $[\text{CO}_2]$  and cultivar for biomass accumulation (Figure 1(a),  $P < 0.05$ ) and total leaf area  
324 (Figure 1(b),  $P < 0.05$ , Details of the ANOVA results are listed in Supplementary Table S4).  
325 Above ground biomass accumulation and total leaf area of Kukri were increased by 11.5% and  
326 10.2% at elevated  $[\text{CO}_2]$ . Similarly, in RAC875, total plant dry mass and total leaf area were  
327 increased by 86% and 34.5%, respectively at elevated  $[\text{CO}_2]$ .

328

329 In the selected wheat lines, there were significant interactions between  $[\text{CO}_2]$  and cultivar for  
330 above ( $P < 0.01$ ) and below ground biomass ( $P < 0.01$ ) and total leaf area ( $P < 0.01$ , Table 2). The  
331 mean  $\text{CO}_2$  responsiveness for above and below ground biomass accumulation were 225.4%  
332 and 175.7%, respectively, for high responsive lines. Of them, the highest  $\text{CO}_2$ -responsiveness  
333 was recorded for the H<sub>2</sub> wheat line for both above and below ground dry mass accumulation.

334 Increase in above and below ground dry mass of less responsive wheat lines showed a less  
335 response to elevated [CO<sub>2</sub>] and showed an increase of 31.2% and 34.7%, respectively, under  
336 elevated [CO<sub>2</sub>]. The overall increase in leaf area production at elevated [CO<sub>2</sub>] was higher at  
337 elevated [CO<sub>2</sub>], however, there was a marked decrease in CO<sub>2</sub> responsiveness of total leaf area  
338 (-17.99%) of the less responsive lines (Table 2).

339

### 340 ***3.2 Net photosynthesis and chlorophyll fluorescence activity at elevated [CO<sub>2</sub>]***

341 The rate of photosynthesis of the parental cultivars, Kukri and RAC875, was significantly  
342 stimulated when grown under elevated [CO<sub>2</sub>] (P<0.05) (Figure 2(a)). However, RAC875  
343 showed comparatively higher photosynthetic stimulation when compared to Kukri. In  
344 RAC875, the net photosynthetic rate has been increased by 70.46% at elevated [CO<sub>2</sub>]. With  
345 regards to the chlorophyll fluorescence parameters, the maximum efficiency of PSII and non-  
346 photochemical quenching of these two cultivars were not significantly different at elevated  
347 [CO<sub>2</sub>]. However, the operating efficiency of PSII (Figure 2(b)), the rate of electron transport in  
348 PSII (Figure 2(c)) and photochemical quenching of PSII (Figure 2(d)) were significantly higher  
349 (P<0.05) in RAC875 under elevated [CO<sub>2</sub>].

350

351 The photosynthesis capacity of the other wheat lines was also substantially increased at  
352 elevated [CO<sub>2</sub>]. There was a significant interaction between [CO<sub>2</sub>] and cultivar for leaf  
353 photosynthesis of these wheat lines (P<0.05, Table 2). A higher response for photosynthesis at  
354 elevated [CO<sub>2</sub>] was demonstrated in high responsive wheat lines with the H<sub>2</sub> wheat line  
355 showing the highest percentage increase. The increases in photosynthesis capacity of less  
356 responsive lines were less under high [CO<sub>2</sub>] and showed a marked decrease in CO<sub>2</sub>  
357 responsiveness for rates of photosynthesis (-12.16%, Table 2).

358

### 359 ***3.3 Carbohydrate biosynthesis and organ-specific carbohydrate accumulation at elevated*** 360 ***[CO<sub>2</sub>]***

361 Large differences in sugar accumulation between two parental cultivars were observed under  
362 elevated [CO<sub>2</sub>]. The soluble sugar concentrations of two parental cultivars significantly varied  
363 between genotypes (P<0.05) and different organs (P<0.05) under high CO<sub>2</sub> conditions (Figure  
364 1(c)). The highest total sugar content was found in the CER at elevated [CO<sub>2</sub>] which showed  
365 an increase of 64.4% in Kukri and 117.3% in RAC875 (P<0.01, Figure 3). In ELB, the highest  
366 total soluble sugar content was observed in RAC875 with an increase of 67% at elevated [CO<sub>2</sub>]

367 (Figure 3). In general, the highest sucrose concentration was detected in the LFELB and the  
368 contents were increased by 177.9% and 398.6% in Kukri and RAC875, respectively, at elevated  
369 [CO<sub>2</sub>] (Supplementary Figure S1). Among all the sugars, glucose and fructose were the  
370 prominent soluble sugars in CER of the wheat seedlings. At elevated [CO<sub>2</sub>], glucose and  
371 fructose concentrations were increased by 145.6% and 33.8%, respectively, in Kukri and  
372 227.8% and 177.2%, respectively, in RAC0875 (Supplementary Figure S1). Overall, RAC875  
373 showed the highest response for carbohydrate biosynthesis and accumulation under elevated  
374 [CO<sub>2</sub>] across all the organ types.

375

376 Among the other eight selected wheat lines, the total soluble carbohydrate content of high  
377 responsive lines showed higher percentage increase at elevated [CO<sub>2</sub>], when compared with  
378 the less responsive lines (Table 2). The highest CO<sub>2</sub> responsiveness for total soluble  
379 carbohydrates accumulation was observed in wheat lines H<sub>1</sub> and H<sub>2</sub>, with a 31.5% and 25.1%  
380 increase in soluble carbohydrate concentration at elevated [CO<sub>2</sub>] respectively (Table 3). The  
381 least response for soluble carbohydrate accumulation was observed in the wheat line L<sub>1</sub>, which  
382 showed a – 5.5% responsiveness to elevated [CO<sub>2</sub>] (Table 3). There were significant  
383 interactions among [CO<sub>2</sub>], cultivar and organ for sucrose (P<0.01), glucose (P<0.01) and  
384 fructose (P<0.01) contents across the different wheat lines tested in this study (Table 3). The  
385 sucrose and fructose contents of LFELB, ELB and CER were higher in plants grown at elevated  
386 [CO<sub>2</sub>]. However, the glucose concentrations were lower at elevated [CO<sub>2</sub>] across all organs  
387 when compared to ambient [CO<sub>2</sub>] grown plants. The highest CO<sub>2</sub> responsiveness for total  
388 soluble carbohydrate accumulation was observed in wheat lines H<sub>1</sub> and H<sub>2</sub>, with a respective  
389 increase of 33.4% and 42.8% in last fully expanded leaves, 14.2% and 40.2% in ELB and  
390 62.36% and 35.18% in CER of the plants grown at elevated [CO<sub>2</sub>].

391

### 392 ***3.4 Effect of elevated [CO<sub>2</sub>] on the expression of key photosynthesis-related genes***

393 Genes encoding Rubisco, *rbcL* and *rbcS*, were tested to understand the variation in  
394 photosynthesis at the molecular level. Relative expression of *rbcL* and *rbcS* varied significantly  
395 among different organs (P<0.01) in two CO<sub>2</sub> levels (P<0.01) (Supplementary Table S5).  
396 Expression of *rbcL* did not differ between the genotypes, however, expression of *rbcS* showed  
397 a significant difference between the two genotypes (P<0.05). In general, *rbcL* expression was  
398 higher in photosynthetic tissues (LFELB and ELB) while *rbcS* expression was higher in non-  
399 photosynthetic tissues (SAR) (Table 4). Expression of both genes was upregulated in elevated

400 [CO<sub>2</sub>] across all plant organs. More importantly, expression of *rbcL* and *rbcS* in LFELB, was  
401 greater in RAC875 than Kukri at elevated [CO<sub>2</sub>]. The expression of *rbcL* and *rbcS* in the  
402 LFELB of RAC875 showed a 1.7 and 1.9-fold increase, respectively at elevated [CO<sub>2</sub>] when  
403 compared to the expression of these genes in Kukri.

404

### 405 ***3.5 Effect of elevated [CO<sub>2</sub>] on carbon metabolism***

406 Distinctive organ-specific expression patterns were observed for *SPP1*, *SPS1* and *SUS1* across  
407 the genotypes tested. These genes showed a significant increase in expression at elevated [CO<sub>2</sub>]  
408 when compared to plants grown at ambient [CO<sub>2</sub>] (P<0.01, Supplementary Table S5).  
409 However, a significant genotypic difference was only observed for *SPS1* gene expression at  
410 elevated [CO<sub>2</sub>] (Supplementary Table S5, P<0.01). Expression of all these genes significantly  
411 differed in different organs (P<0.01, Supplementary Table S5). In the last fully expanded leaf  
412 and expanding leaf, relative expression of *SPP1* was the highest, while *SUS1* showed the  
413 highest expression in cell elongation and shoot apex regions (Table 5).

414

415 The expression of *SPP1*, *SPS1* and *SUS1* in the LFELB of RAC875 grown at elevated [CO<sub>2</sub>]  
416 showed a significant increase in expression compared to ambient [CO<sub>2</sub>] grown plants, with a  
417 5.4, 4.8, 2.0-fold increase, respectively. The expression of *SPS1* was upregulated at elevated  
418 [CO<sub>2</sub>] across all organ types, where the highest fold increase was observed in the LFELB of  
419 both cultivars. In contrast, the *SPP1* gene was upregulated only in photosynthetic tissues, while  
420 it showed a lower transcript abundance in the non-photosynthetic tissues. This scenario was  
421 comparatively less at elevated [CO<sub>2</sub>] demonstrating an indirect upregulation of this gene.  
422 Expression of *SUS1* gene was higher in the cell elongation and shoot apex regions of RAC875,  
423 with a fold increase of 2.19 and 2.64 at elevated [CO<sub>2</sub>].

424

### 425 ***3.6 Effect of elevated [CO<sub>2</sub>] on genes associated with plant nitrogen metabolism***

426 Since the leaf is the predominant site for nitrogen assimilation in plants, key genes involved in  
427 nitrogen metabolism were examined in the LFELB and ELB of Kukri and RAC875. The  
428 expression of *NiR*, *GS1a*, *GSr1*, *NADH-GOGAT*, *GS2a*, *GS2b* and *Fd-GOGAT* at elevated  
429 [CO<sub>2</sub>] significantly differed from the expression levels observed at ambient [CO<sub>2</sub>] (P<0.01,  
430 Supplementary Table S5). Further, expression of all these genes was significantly varied  
431 between LFELB and ELB organs (P<0.05, Supplementary Table S5) except for *NADH-*  
432 *GOGAT* and *NiR* expression. Highest transcript abundance for *GS2a* and *Fd-GOGAT* was

433 observed in ELB than the LFELB under both ambient and elevated [CO<sub>2</sub>] (Table 6). However,  
434 the CO<sub>2</sub> effect on expression of these genes was higher in LFELB. For example, Kukri showed  
435 5.9 and 4.1 fold change increase and RAC875 showed 1.63 and 2.53 fold change increase,  
436 respectively, for *Fd-GOGAT* and *GS2a* expression at elevated [CO<sub>2</sub>]. Similarly, expression of  
437 *GS1a* was comparatively higher in LFELB, of which RAC875 showed the highest expression  
438 with a fold increase of 8.6 when compared to ambient [CO<sub>2</sub>]. In contrast, *GSr1* and *NADH-*  
439 *GOGAT* expressions were comparatively less in both LFELB and ELB. A marked upregulation  
440 of these two genes was observed in the LFELB of RAC875 at elevated [CO<sub>2</sub>] with a fold  
441 increase of 21 and 9.6, respectively.

442

### 443 ***3.7 Effect of elevated [CO<sub>2</sub>] on the expression of key genes related to cell elongation and*** 444 ***expansion***

445 A majority of genes associated with  $\alpha$  and  $\beta$ -expansins were highly expressed in meristematic  
446 tissues in LCEZ and SAR of both Kukri and RAC875. With reference to  $\alpha$ -expansins,  
447 expression of *TaEXPA3* varied significantly between organ types and genotypes at two  
448 different CO<sub>2</sub> treatments (P<0.05, Supplementary Table S5). In the SAR, there was a higher  
449 upregulation of this gene in both cultivars at elevated [CO<sub>2</sub>], of which Kukri showed the highest  
450 expression. Although the transcript abundance for *TaEXPA1* was high in the LCEZ and SAR,  
451 no significant differences were found between the two CO<sub>2</sub> treatments.

452

453 The expression of  $\beta$ -expansins also differed significantly between two CO<sub>2</sub> treatments except  
454 for *TaEXPB1* (P<0.01, Supplementary Table S5). In general, expression of *TaEXPB2*,  
455 *TaEXPB3*, *TaEXPB6* and *TaEXPB23* were highly expressed at elevated [CO<sub>2</sub>] in both varieties  
456 (Table 7). In the LCEZ of Kukri, *TaEXPB2*, *TaEXPB6* and *TaEXPB23* showed a marked  
457 upregulation, while all tested genes, except for *TaEXPB1*, were highly expressed in RAC875  
458 at elevated [CO<sub>2</sub>] (Table 7). In contrast, the expression of *TaEXPB1* was only upregulated in  
459 the SAR of both cultivars (P<0.05, Supplementary Table S5). The genotype differences in  
460 expression of *TaEXPB3* and *TaEXPB6* were significant, of which RAC875 showed a higher  
461 response to elevated [CO<sub>2</sub>].

462

463 The detection of several  $\alpha$  and  $\beta$ -expansins was very low in LFELB and ELB, and therefore,  
464 those results are not reported in this study. In leaf tissues, *TaEXPA3*, *TaEXPB6* and *TaEXPB23*  
465 were the only three genes in expansins category that showed a detectable relative expression at

466 both CO<sub>2</sub> levels and significantly varied between last fully expanded and expanding leaves  
467 (P<0.05, Supplementary Table S5). These three genes showed a down-regulation in LFELB  
468 while they showed an upregulation in ELB (Table 7). Further, *TaEXPA3* and *TaEXPB6*  
469 expression varied significantly between Kukri and RAC875 at elevated [CO<sub>2</sub>].

470 There effect of [CO<sub>2</sub>] (P<0.01) and genotype (P<0.05) on XTH gene expression were  
471 significant except for *TaXTH4* (Supplementary Table S5). However, the expression of all XTH  
472 members was varied significantly between different organs (P<0.01, Supplementary Table S5).  
473 and organ type on the expression of different XTH genes tested in this study. The expression  
474 of *TaXTH1*, *TaXTH2* and *TaXTH3* were highest in the ELB of both cultivars (Table 8). At  
475 elevated [CO<sub>2</sub>], expression of these genes together with *TaXTH5* was upregulated in both  
476 cultivars (Table 8). In RAC875, expression of *TaXTH1*, *TaXTH2*, *TaXTH3* and *TaXTH5*  
477 showed 2.88, 2.01, 8.39 and 2.59-fold increases, respectively, when compared to ambient  
478 [CO<sub>2</sub>]. Conversely, the LFELB of the two genotypes showed the least transcript abundance for  
479 XTH gene members compared with the other organ types, both at ambient and elevated [CO<sub>2</sub>]  
480 (Table 8). The expression of *TaXTH2*, *TaXTH3*, and *TaXTH4* in LFELB of Kukri was down-  
481 regulated while *XTH5* showed substantial upregulation at elevated [CO<sub>2</sub>]. In RAC875, *TaXTH1*  
482 and *TaXTH4* were down-regulated at elevated [CO<sub>2</sub>] while *TaXTH2*, *TaXTH3* and *TaXTH4*  
483 were upregulated.

484

485 In general, expression of all the XTH gene members was high in SAR and LCEZ (P<0.01,  
486 Supplementary Table S5), of which *TaXTH5* showed the highest expression (Table 8). At  
487 elevated [CO<sub>2</sub>], a significant genotypic difference was only observed for *TaXTH1*, *TaXTH2*  
488 and *TaXTH3* expression in the SAR (P<0.05, Supplementary Table S5), with 1.4, 0.7 and 0.8  
489 fold increases, respectively, in Kukri and 6.1, 3.4 and 3.7 fold increase, respectively, in  
490 RAC875. There was a significant upregulation of *TaXTH5* at elevated [CO<sub>2</sub>], although there  
491 was no genotypic difference. The expression of XTH genes in the LCEZ was also substantially  
492 higher than leaf tissues. In Kukri, *TaXTH1*, *TaXTH2* and *TaXTH5* showed the highest  
493 upregulation with fold increases of 1.6, 1.4 and 2.3, respectively, at elevated [CO<sub>2</sub>] (Table 8).  
494 The expression of, *TaXTH3* and *TaXTH5* was highest in RAC875, with a fold increase of 3.7  
495 and 2.6, respectively, at high CO<sub>2</sub> conditions (Table 8).

## 496 **4. Discussion**

497

498 Faster growth at elevated atmospheric [CO<sub>2</sub>] during early ontogeny appears to be a major  
499 contributor to accelerated growth for many crops ([Makino and Mae 1999](#); [Jitla et al. 1997](#)).  
500 Thus, this enhanced early growth and vigor is crucial in determining the final grain yield of a  
501 crop ([Thilakarathne et al. 2015](#); [Seneweera and Conroy 2005](#)). The genetic variation in plant  
502 responses to elevated [CO<sub>2</sub>] is well documented ([Thilakarathne et al. 2013](#); [Thilakarathne et al.](#)  
503 [2015](#); [Tausz et al. 2013](#)), but it has been suggested that this growth variation cannot only be  
504 explained through increases in photosynthetic capacity at elevated [CO<sub>2</sub>] ([Taylor et al. 1994](#);  
505 [Gamage et al. 2018](#)). A strong carbon and nitrogen relationship between source and sink tissues  
506 at elevated [CO<sub>2</sub>] has been established in previous studies ([Paul and Foyer 2001](#); [Paul and](#)  
507 [Pellny 2003](#); [Seneweera et al. 2002](#)), but the underpinning mechanisms that drive the genetic  
508 variation in plant response to elevated [CO<sub>2</sub>] are not yet established ([Gamage et al. 2018](#)).

509

### 510 ***4.1 Biomass accumulation and enhanced growth stimulation at elevated [CO<sub>2</sub>]***

511 The increased photosynthetic capacity and improved water use efficiency at elevated [CO<sub>2</sub>]  
512 have paved the way for improvements in biomass accumulation in many crops ([Ainsworth and](#)  
513 [Rogers 2007](#)), including wheat ([Thilakarathne et al. 2013](#); [Thilakarathne et al. 2015](#)). This has  
514 been further confirmed in this current study as both the parental lines (Kukri and RAC875)  
515 showed a higher carbon assimilation rate and a higher biomass accumulation at elevated [CO<sub>2</sub>]  
516 (Figure 1 and 2). Consistent with this, the total soluble sugar content of these two cultivars was  
517 also higher, indicating the greater availability of carbohydrate substrates for other post-  
518 photosynthetic key metabolic activities of the plant (Figure 1 and 3). Of the two parental lines,  
519 RAC875 consistently showed higher photosynthetic rates, soluble sugar accumulation and  
520 biomass accumulation at elevated [CO<sub>2</sub>] when compared to Kukri. On the other hand, the effect  
521 of [CO<sub>2</sub>] on photosynthesis of selected wheat lines was not statistically significant, while the  
522 interaction effect between [CO<sub>2</sub>] and genotype was significant in our study (Table 2). This  
523 supports our hypothesis that increases in rates of photosynthesis alone cannot explain the  
524 growth enhancement observed at elevated [CO<sub>2</sub>]. Thus it is suggested that along with  
525 photosynthesis, modifications in key post-photosynthetic metabolic processes such as sucrose  
526 metabolism, nitrogen metabolism and cell wall metabolism, are required ([Gamage et al. 2018](#))  
527 to maintain optimum growth rates at elevated [CO<sub>2</sub>], especially at the early vegetative growth  
528 stage. The selected wheat lines were different to their parental lines were selected on the based

529 on their CO<sub>2</sub> responsiveness. The lines H<sub>1</sub>, H<sub>2</sub>, H<sub>3</sub>, and H<sub>4</sub> showed a highest growth response  
530 to elevated [CO<sub>2</sub>] while L<sub>1</sub>, L<sub>2</sub>, L<sub>3</sub> and L<sub>4</sub> showed the lowest response to elevated [CO<sub>2</sub>]  
531 compared to parental lines. For example, the highest above biomass response to elevated [CO<sub>2</sub>]  
532 was observed in wheat line H<sub>3</sub> with 257.5% increase in biomass, which was higher than the  
533 both parental lines. Similarly, lowest response of above ground biomass at elevated [CO<sub>2</sub>] was  
534 observed in wheat line L<sub>3</sub> with 14.9% which was below both parental lines. Further, the high  
535 responsive lines showed a mean increase of below ground biomass accumulation by 176% in  
536 response to elevated [CO<sub>2</sub>] while less responsive lines showed an average increase of 34.8% at  
537 elevated [CO<sub>2</sub>]. The increase in leaf area at elevated [CO<sub>2</sub>] was higher in high responsive lines  
538 with an average increase of 27.6%. However, there was a substantial decrease in leaf area  
539 increment (-18.0%) in less responsive lines when exposed to elevated [CO<sub>2</sub>]. These results  
540 clearly showed that the selected progeny lines perform differently to the parental lines and to  
541 each other when exposed to high levels of [CO<sub>2</sub>].

542

#### 543 ***4.2 Soluble sugar contents vary among plant organs, genotypes and CO<sub>2</sub> concentrations***

544 Glucose, fructose and sucrose are the main soluble sugars that play a key role in maintaining  
545 overall plant growth and development ([Rosa et al. 2009](#)). The abundance of these sugars differ  
546 in different organ types and their accumulation largely varied during plant ontogeny. In  
547 particular, glucose and fructose are actively involved in cell division ([Koch 2004](#)), hence the  
548 supply of these sugars to growing tissues is critically important for accelerated growth ([Eveland  
549 and Jackson 2011](#)). Consistent with this proposition, our study demonstrated that glucose and  
550 fructose contents in the growing tissues such as young leaves, cell elongation and the shoot  
551 apex region were significantly higher in plants at elevated [CO<sub>2</sub>] (Supplementary Figure S1  
552 and Table 3). Perhaps, sucrose hydrolysis is accelerated at elevated [CO<sub>2</sub>] as a result of  
553 increased metabolic demand. On the other hand, sucrose availability at elevated [CO<sub>2</sub>] was high  
554 in mature tissues such as LFELB indicating its role in cell differentiation and maturation ([Koch  
555 2004](#)). As soon as sucrose is produced in the source tissues, they are rapidly translocated to  
556 sink tissues to be used for growth or to store as reserves. It has also been established that soluble  
557 sugars play a major role in controlling the proliferation of plant organs ([Gibson 2005](#)). This  
558 could be a possible reason for the observed higher leaf area stimulation of the wheat seedlings  
559 grown at elevated [CO<sub>2</sub>] in our study.

560

561 A significant genotypic variation for soluble carbohydrate production was observed under  
562 elevated [CO<sub>2</sub>]. High responsive wheat lines showed a higher soluble sugar content at elevated  
563 [CO<sub>2</sub>] while less responsive wheat lines did not show a notable increase despite the increases  
564 in CO<sub>2</sub> assimilation rates at elevated [CO<sub>2</sub>]. This suggests that carbohydrate production at  
565 elevated [CO<sub>2</sub>] not only depends on the increased photosynthetic capacity, but also varies based  
566 on the genotype and their genetic capacity to utilize these carbohydrates in different metabolic  
567 activities. For example, plants that can utilize these carbohydrates to generate more tillers or  
568 secondary shoots and increase their sink capacity are likely to produce more soluble sugar at  
569 elevated [CO<sub>2</sub>] ([Ainsworth et al. 2004](#)). Therefore, plants' genetic capacity to utilize photo-  
570 assimilates efficiently is a critical factor to sustain photosynthesis and thereby regulate their  
571 growth and development.

572

573

574

#### 575 ***4.3 Light-dependent and light independent reactions of photosynthesis are genetically varied*** 576 ***at elevated [CO<sub>2</sub>]***

577 The light reaction of photosynthesis plays a key role in increasing photosynthetic capacity of  
578 plants at elevated [CO<sub>2</sub>] ([Gamage et al. 2018](#)). The activity of Photosystem II (PSII) in the light  
579 reaction is quite sensitive to a wide range of biotic and abiotic factors making it a good indicator  
580 of how plants generally respond to climate change and adapt to ecological variations ([Murchie  
581 and Lawson 2013](#)). Chlorophyll fluorescence is one of the best tools to obtain detailed  
582 information on the state of PSII in response to an environmental change ([Sekhar, Sreeharsha,  
583 and Reddy 2015](#)). Both Kukri and RAC875 showed no significant difference in maximum PSII  
584 efficiency under light, when all the reaction centers are open ( $F_v'/F_m'$ ), and non-  
585 photochemical quenching (NPQ), suggesting that plants do not experience any stressful  
586 condition at elevated [CO<sub>2</sub>] (Figure 2). However, the effective quantum yield ( $\phi_{PSII}$ ) of both  
587 the parental lines was significantly higher in elevated [CO<sub>2</sub>] suggesting that the proportion of  
588 absorbed light used in PSII photochemistry increased under rising [CO<sub>2</sub>] (Figure 2,  
589 Supplementary Table S4). This may be because of the increased number of PSII reaction  
590 centers opened at PSII allowing reaction centers to accept further electrons. This was further  
591 confirmed by the increased photochemical quenching ( $q_p$ ) of parental cultivars at elevated  
592 [CO<sub>2</sub>]. The increased electron transport rate (ETR) observed at elevated [CO<sub>2</sub>] may have  
593 facilitated higher photochemical quenching ( $q_p$ ) as electrons are transported away from PSII

594 due to the enzymes involved in CO<sub>2</sub> fixation. Overall, chlorophyll fluorescence measurements  
595 suggested that the light utilization efficiency of PSII system is higher at elevated [CO<sub>2</sub>] and  
596 consequently the electron flow between the photosystems is increased. This correlates well  
597 with the increased photosynthesis rates of the two parental lines, which further indicates that  
598 the light reaction of photosynthesis tends to produce more ATP and NADPH to support  
599 increased rates of light independent reaction at elevated [CO<sub>2</sub>]. A good correlation between  
600 PSII efficiency and CO<sub>2</sub> assimilation has been reported in previous studies ([Sekhar, Sreeharsha,  
601 and Reddy 2015](#); [Rasineni, Guha, and Reddy 2011](#); [Brestic et al. 2012](#)) suggesting that  
602 chlorophyll fluorescence measurements can be used to screen photochemically efficient  
603 genotypes for better carbon assimilation in a changing climate.

604

605 The light-independent reaction of photosynthesis commences with catalysis by Ribulose-1,5-  
606 biphosphate carboxylase/oxygenase (Rubisco), which can carboxylate in the presence of CO<sub>2</sub>  
607 or oxygenate with O<sub>2</sub> ([Makino and Mae 1999](#); [Drake, González-Meler, and Long 1997](#)).  
608 Rubisco has a higher affinity for CO<sub>2</sub> than O<sub>2</sub>, and therefore, with the higher partial pressure  
609 of CO<sub>2</sub> at elevated [CO<sub>2</sub>], the rate of Rubisco carboxylation tends to increase, enhancing  
610 photosynthesis rates. This stromal protein contains eight small subunits and eight large subunits  
611 encoded by nuclear multigene family (*rbcS*) and single gene in the chloroplast genome (*rbcL*)  
612 ([Suzuki et al. 2010](#); [Suzuki et al. 2009](#)). Changes in Rubisco synthesis is primarily explained  
613 by the changes to transcript abundance of the Rubisco encoding genes ([Suzuki et al. 2010](#)). At  
614 elevated [CO<sub>2</sub>] conditions, expression of these two photosynthetic genes varies between the  
615 two genotypes. In general, expression of *rbcL* and *rbcS* were higher in plants grown at elevated  
616 [CO<sub>2</sub>] (Table 4). The highest expression for *rbcL* was observed in fully expanded leaves of  
617 RAC875 along with higher maximum net photosynthesis rates than Kukri at elevated [CO<sub>2</sub>].  
618 Moreover, expression of *rbcS* in fully expanded leaves was also higher in elevated [CO<sub>2</sub>] than  
619 in ambient [CO<sub>2</sub>]. Since the expression of these two genes correlates with the synthesis of  
620 Rubisco, these results suggest that more Rubisco synthesis has taken place in fully the  
621 expanded leaves than in other organs. This could have determined the increased photosynthesis  
622 capacity of the plants observed at high CO<sub>2</sub> conditions. In the expanding leaf, *rbcL* and *rbcS*  
623 expression were higher in Kukri than in RAC875 at elevated [CO<sub>2</sub>] suggesting further that  
624 transcript abundance is subject to genotypic variations. We could observe comparatively higher  
625 expression in *rbcL* in leaf tissues when compared with *rbcL* expression in non-photosynthetic  
626 tissues. For example, the expression of the *rbcL* gene was less while *rbcS* expression was high  
627 in cell elongation and shoot apex regions when compared to other photosynthetic tissues. This

628 could be due to lower abundance of the chloroplast genome to code for *rbcL* expression. A  
629 similar pattern of expression in *rbcL* and *rbcS* was also observed in previous studies conducted  
630 in amaranth ([Nikolau and Klessig 1987](#)), pea ([Sasaki, Nakamura, and Matsuno 1987](#)) and rice  
631 ([Suzuki, Makino, and Mae 2001](#)). Overall, expression of photosynthetic genes tends to change  
632 with the plants' genotype, growth stage, tissue type and the environmental conditions in which  
633 the plants are grown.

634

#### 635 ***4.4 Expression of key genes associated with sucrose metabolism was influenced by genotype,*** 636 ***organ type and elevated [CO<sub>2</sub>]***

637 Sucrose plays a critical role in plant growth, development, storage, signal transduction and  
638 support for plant acclimation to different environmental stresses ([Jiang et al. 2015](#)). Transfer  
639 of sucrose from its source tissues to sink tissues is the main factor contributing towards the  
640 source and sink integration of the plant which finally determines plant growth and yield  
641 ([Bihmidine et al. 2013](#)). In this study, there was a marked difference in expression of the genes,  
642 *SPPI*, *SPSI* and *SUS1* in different organs and CO<sub>2</sub> conditions (Table 5). Moreover, expression  
643 of these genes was varied with wheat genotype. The correlation analysis between the change  
644 of soluble sugar contents and the relative expression of sucrose metabolism genes showed that  
645 there was a strong positive correlation between *SPPI* and fructose concentration (r=0.783,  
646 P<0.05, Supplementary Table S6). This indicates that regulation of sucrose metabolism genes  
647 at elevated [CO<sub>2</sub>] may be regulated through a sugar sensing mechanisms.

648

649 Sucrose Phosphate Synthase (*SPSI*) catalyzes the conversion of fructose-6-phosphate and  
650 UDP-Glucose into Sucrose-6-Phosphate and is considered to be the major rate-limiting enzyme  
651 of sucrose biosynthesis in plants ([Lunn and MacRae 2003](#)). This also plays a key role in  
652 partitioning carbon between sucrose and starch in both photosynthetic and non-photosynthetic  
653 tissues ([MacRae and Lunn 2006](#); [Hashida et al. 2016](#)). In this study, it has been clearly  
654 demonstrated that transcript abundance of *SPSI* was increased at elevated [CO<sub>2</sub>] across all the  
655 organ types. Higher expression of SPS reflects the increased sucrose synthesis capacity of  
656 plants under elevated [CO<sub>2</sub>] leading to increased plant development ([Pessarakli 1996](#)). This  
657 was further confirmed by the increased biomass accumulation and photosynthetic rates  
658 observed for the RAC875 parental line and the same cultivar showed a higher expression for  
659 *SPSI* (Table 5). The higher expression of *SPSI* under elevated [CO<sub>2</sub>] may be due to the  
660 allosteric nature of this enzyme ([Yonekura et al. 2013](#)), which is activated by glucose-6-

661 phosphate and inhibited by inorganic phosphate ([Hashida et al. 2016](#)). As the rate of inorganic  
662 phosphate used by photosynthesis is higher at elevated [CO<sub>2</sub>], the availability of inorganic  
663 phosphate as an inhibitor of *SPSI* gene is less under high CO<sub>2</sub> conditions. Thus, increased  
664 availability of Glucose-6-Phosphate at elevated [CO<sub>2</sub>] allosterically increases the activity of  
665 SPS. The concentration of sucrose at elevated [CO<sub>2</sub>] was also higher in RAC875 suggesting  
666 that *SPSI* could also facilitate carbon partitioning to sucrose over starch in leaf tissues ([Huber  
667 and Israel 1982](#); [Huber 1983](#)). In addition, SPS activity was found to be high in growing sink  
668 tissues and similar results were reported in our study, particularly in growing leaves, the cell  
669 elongation region and shoot meristem tissues (Table 5). High expression of SPS in major sink  
670 tissues may be involved in re-synthesis of sucrose imported via apoplastic cleavage and may  
671 help in redistribution within the sink tissue ([Sturm and Tang 1999](#); [Geigenberger et al. 1999](#)).  
672 The enzyme SPP catalyzes the final step of sucrose biosynthesis, irreversibly hydrolyzing  
673 Sucrose-6-Phosphate, produced by SPS, to sucrose ([Jiang et al. 2015](#)) and is usually expressed  
674 in significant quantities in both vascular and non-vascular plants ([Lunn 2003](#)). In the current  
675 study, a higher expression of *SPP1* compared to *SPSI* and *SUS1* was observed across all tissue  
676 types in the two CO<sub>2</sub> treatments. It was suggested that maximum potential activity of SPS and  
677 SPP are similar to each other ([Lunn 2003](#)) in wheat, and that a multienzyme complex may form  
678 between these two enzymes ([Echeverria et al. 1997](#)), suggesting that both *SPSI* and *SPP1* may  
679 have worked together in the synthesis of sucrose under elevated [CO<sub>2</sub>].

680

681 Channeling sucrose into other metabolic activities, such as respiration, biosynthesis of cell wall  
682 polysaccharides and storage reserve formation, require its cleavage by different enzymes  
683 ([Sturm and Tang 1999](#)). The expression of *SUS1* was examined since SUS is one of the main  
684 sucrose-cleaving enzymes and activity of *SUS1* was higher in cell elongation and shoot  
685 meristem tissues when compared to the last fully expanded leaf (Table 5). The enzyme SUS  
686 cleaves sucrose into UDP-Glucose and fructose ([Jiang et al. 2015](#)), where UDP-Glucose then  
687 acts as the primary building block for cell wall synthesis ([Verbančič et al. 2017](#)). Since only  
688 low levels of cell wall synthesis are required in the LFELB, the majority of the UDP-Glucose  
689 produced will be directed to the synthesis of sucrose ([Stitt, Lunn, and Usadel 2010](#)) and then  
690 transported to sink tissues ([Sauer 2007](#)) suggesting SUS gene mainly expressed in primary sink  
691 tissues. Consistent with this proposition, results outlined in Table 5 showed that *SUS1*  
692 expression was higher in meristematic tissues under both CO<sub>2</sub> treatments. However, these  
693 expression patterns were even pronounced in plants grown at elevated [CO<sub>2</sub>]. As elevated  
694 [CO<sub>2</sub>] induces high cell division and expansion rates in meristematic tissues ([Gamage et al.](#)

695 [2018](#)), most of the sucrose produced will be translocated to these tissues to be used in different  
696 anabolic activities ([Sturm and Tang 1999](#)) and thus help to produce more tillers or secondary  
697 shoots and increase leaf area development, consequently leading to high biomass and yield  
698 production.

699

#### 700 ***4.5 Organ-specific expression of nitrogen assimilation genes varied at elevated [CO<sub>2</sub>]***

701 Plant cells require both carbon and nitrogen for growth and development. Carbon is essential  
702 to fuel metabolic processes while nitrogen availability is a key factor in maintaining protein  
703 turnover of cells ([White et al. 2015](#)). Glutamine Synthetase (GS) catalyzes the conversion of  
704 glutamate to glutamine using ammonia as the substrate during nitrogen assimilation. The two  
705 classes of GS (GS1 and GS2) have organ-specific roles ([Cren and Hirel 1999](#); [Masclaux-  
706 Daubresse et al. 2010](#)). The enzyme GS2 is predominantly found in leaves and catalyses the  
707 primary nitrogen assimilation of ammonia resulting from the reduction of nitrite in chloroplasts  
708 and reassimilation of respiratory ammonia ([Foyer and Zhang 2011](#)). Consistent with this, the  
709 expression of *GS2a*, encoding one of the isoenzymes of the GS2 class, was found to be  
710 significantly expressed in both LFELB and ELB of our study (Table 6). Further, this *GS2a* was  
711 upregulated in both LFELB and ELB at elevated [CO<sub>2</sub>] suggesting that increased nitrogen  
712 assimilation occurs at elevated [CO<sub>2</sub>], especially in the early development stages. The  
713 expression of GS1 enzyme related genes, *GS1a* and *GSr1* in leaf tissues was comparatively  
714 lower than the *GS2a* expression. However, the expression of *GS1a* was significantly higher in  
715 RAC875 at elevated [CO<sub>2</sub>]. It has been previously reported that GS1 supports the  
716 remobilization of nitrogen into the developing sink organs ([Masclaux-Daubresse et al. 2006](#);  
717 [Pageau et al. 2005](#); [Tabuchi, Abiko, and Yamaya 2007](#)). These GS enzymes function together  
718 with two distinct forms of GOGAT (glutamate synthase) to incorporate amino groups into  
719 amino acid precursors required for protein synthesis ([Masclaux-Daubresse et al. 2010](#)). In our  
720 results, the expression of *Fd-GOGAT* was significantly higher compared to *NADH-GOGAT* in  
721 the LFELB and ELB. These findings are consistent with [Yamaya et al. \(1992\)](#) as *NADH-  
722 GOGAT* is predominantly present in non-photosynthetic tissues of the plants while *Fd-GOGAT*  
723 is primarily located in the chloroplasts of photosynthetic tissues ([Suzuki and Knaff 2005](#)). The  
724 expression of *Fd-GOGAT* showed a substantial upregulation at elevated [CO<sub>2</sub>] across both  
725 parental cultivars while a notable upregulation of *NADH-GOGAT* was only observed in the  
726 LFELB of RAC875. This might indicate that transcriptional regulation of these genes is  
727 subjected to intra-specific variation, which may have contributed towards the different nitrogen

728 use efficiencies of these two cultivars. On the other hand, [Bernard et al. \(2008\)](#), also found that  
729 expression of these genes increases as the leaf ages while *GS2a*, *GS2b* and *Fd-GOGAT*  
730 expression decreases. For example, in RAC875, the expression of *GS2a* and *Fd-GOGAT*  
731 increased in the ELB, while expression of *GS1a*, *GSr1* and *NADH-GOGAT* was higher in the  
732 LFELB (Table 6). As carbon and nitrogen status is critically balanced in the plants, up-  
733 regulation of *GS2a*, *GS1a*, *Fd-GOGAT* and *NADH-GOGAT* at elevated [CO<sub>2</sub>] suggests that  
734 high sugar supply indirectly stimulates production and mobilization of glutamine and  
735 glutamate, which can donate amino groups to produce amino acids essential for cellular  
736 activities ([Zheng 2009](#)). Further, increased amino acid biosynthesis facilitates production of  
737 different structural and metabolic proteins that are critical for optimum plant growth in a high  
738 CO<sub>2</sub> environment.

#### 739 ***4.6 Cell expansion and cell wall loosening were influenced by elevated [CO<sub>2</sub>]***

740 At elevated [CO<sub>2</sub>], increased shoot elongation is more likely to depend on cell expansion rather  
741 than cell proliferation ([Taylor et al. 1994](#); [Ranasinghe and Taylor 1996](#); [Liu et al. 2007](#)).  
742 Expansins and Xyloglucan endotransglucosylase/hydrolases are extracellular proteins that play  
743 a key role in relaxing the cell walls during cell division and elongation ([Liu et al. 2007](#)). Our  
744 expression analysis revealed that the expression of *TaEXPA3* was prominent in the shoot apex  
745 region at elevated [CO<sub>2</sub>] in both cultivars (Table 7). Alpha-expansins have a distinct role in  
746 leaf primordia formation ([Reinhardt et al. 1998](#); [Shin et al. 2005](#)), and thus upregulation of  
747 *TaEXPA3* is consistent with the growth stimulation at elevated [CO<sub>2</sub>]. Several previous studies  
748 revealed that  $\beta$ -expansin expression is generally higher at early vegetative stages of grasses  
749 ([Wu, Meeley, and Cosgrove 2001](#); [Liu et al. 2007](#); [McQueen-Mason and Rochange 1999](#)).  
750 Consistent with this, our study's results demonstrated a higher transcript abundance of  $\beta$ -  
751 expansin genes across different organs when compared to  $\alpha$ -expansin expression (Table 7). In  
752 addition, most of the  $\beta$ -expansin genes tested in our study were upregulated at elevated [CO<sub>2</sub>],  
753 especially in the shoot apex and cell elongation regions of both parental cultivars. With high  
754 sugar supply to these regions at elevated [CO<sub>2</sub>], the activity of  $\beta$ -expansins may have been  
755 upregulated and may positively contribute towards determining the internode elongation and  
756 plant height ([Lee and Kende 2001](#); [Liu et al. 2007](#)). A noteworthy expression was observed for  
757 *TaEXPB23* among other  $\beta$ -expansins in both cultivars, with a higher upregulation at elevated

758 [CO<sub>2</sub>] implying a possible significant role played by this gene at elevated [CO<sub>2</sub>]. It has been  
759 previously found that higher expression of *TaEXPB23* in plants may result in accelerated leaf  
760 and internode growth at early development stages ([Xing et al. 2009](#)).

761  
762 With reference to XTH genes, the highest expressions of *TaXTH1*, *TaXTH2* and *TaXTH3* was  
763 observed in ELB indicating the significant role played by the XTH enzymes in cell wall  
764 loosening and expansion (Table 8). Similarly, [Taylor et al. \(1994\)](#) reported that XTH enzyme  
765 activity is increased at elevated [CO<sub>2</sub>], enabling cell walls to expand rapidly in response to  
766 increased carbon supply. However, the expression level of XTH genes was less in the LFELB  
767 which is consistent with the relative maturity of these tissues. Further, higher expression of  
768 XTH genes was reported in LCEZ and SAR at elevated [CO<sub>2</sub>] (Table 8) presumably due to a  
769 more rapid cell wall synthesis in these tissues which may have supported the increased cell  
770 division and growth. According to our expression analysis, XTH expression showed a distinct  
771 tissue/organ-specific expression pattern, implying that the expression of these genes is  
772 influenced by plant development stage. These results were consistent with [Liu et al. \(2007\)](#)  
773 who also demonstrated that XTH gene family perform tissue/organ-specific developmental  
774 roles that are not interchangeable in plant growth and development.

775  
776 Overall, our results clearly showed that  $\beta$ -expansin genes showed higher expression than the  
777  $\alpha$ -expansins at elevated [CO<sub>2</sub>]. A similar pattern of expression of these genes was observed by  
778 [Liu et al. \(2007\) in wheat](#). This differential expression further suggests functional differences  
779 in two groups of expansins:  $\alpha$ -expansins are involved mainly in cell-specific functions whereas  
780  $\beta$ -expansins play a role in expansion-related functions, mainly the maintenance of cell wall  
781 structure ([Li, Jones, and McQueen-Mason 2003](#); [Wu, Meeley, and Cosgrove 2001](#)). In addition,  
782 XTH genes had an even higher expression, which may be due to their nonsubstitutable specific  
783 function in cell wall loosening ([Liu et al. 2007](#); [Yokoyama and Nishitani 2000](#)). Most of the  $\beta$ -  
784 expansins and XTH genes tested in our study have been upregulated at elevated [CO<sub>2</sub>],  
785 implying the increased expression of these enzymes is required to support maximum growth at  
786 elevated [CO<sub>2</sub>]. The correlation analysis between the change of soluble sugar contents and the  
787 relative expression of genes indicates that cell wall metabolism-related genes tend to show a  
788 significant correlation with the soluble sugar concentration at elevated [CO<sub>2</sub>]. For example,  
789 *TaXTH5* and *TaEXPA1* showed a strong positive correlation with glucose content at elevated  
790 [CO<sub>2</sub>] ( $r=0.816$ ,  $P<0.05$ ;  $r=0.994$ ,  $P<0.01$ , respectively, Supplementary Table 5). Also,  
791 *TaXTH3* showed a strong positive correlation with total sugar content at elevated [CO<sub>2</sub>]

792 ( $r=0.74$ ,  $P<0.05$ ). These results further suggest that the expression of these genes is influenced  
793 by changes to the soluble sugar content of a particular tissue type and thus, is potentially  
794 regulated by sugars. However, apart from these key genes, there are many gene regulatory  
795 factors that influence on expression of genes associated with cell expansion and cell wall  
796 extension. For example, in Arabidopsis, expression of GCCR motif is necessary for the  
797 expression of cell cycle genes such as Cyclin (*CYCB1;1*) which is responsible for cell division  
798 in shoot meristem ([Li et al., 2005](#)). Therefore, it is also necessary to study gene regulatory  
799 factors for key genes tested in this study, as this will provide additional information on how  
800 gene regulatory network modifies at elevated  $[\text{CO}_2]$ .

801

#### 802 ***4.7 Impact of expression of key genes related to photosynthesis, sucrose metabolism,*** 803 ***nitrogen metabolism and cell wall expansion on source-sink interaction of wheat***

804

805 The key results of this study and their impact on plant source and sink interactions is  
806 summarized in Figure 4. Elevated  $[\text{CO}_2]$  increases the  $\text{CO}_2/\text{O}_2$  ratio at the site of  $\text{CO}_2$  fixation  
807 ([Bowes, 1991](#)). Therefore, the carboxylation efficiency of Rubisco is improved through the  
808 lowering of photorespiration. In the same time, the genes encoding for Rubisco large and small  
809 subunits, *rbcL* and *rbcS* substantially upregulated in LFELB, the main source organ. These  
810 findings support our previous results that increased assimilations rates requires optimum  
811 Rubisco to support the photosynthesis machinery. The chlorophyll fluorescence data supported  
812 the higher efficiency of PSII, electron transport rate and photochemical quenching at elevated  
813  $[\text{CO}_2]$  which may have involved in producing more ATP and NADPH, to fulfil the higher  
814 energy requirement to maintain photosynthesis at an optimum rate. This increased  
815 photosynthesis at elevated  $[\text{CO}_2]$  observed in all the wheat lines, and also likely to associated  
816 with increased levels of sucrose. A higher expression of *SPS1*, *SPP1* and *SUS1*, the key genes  
817 in sucrose metabolism were observed in those lines at elevated  $[\text{CO}_2]$ . This increased level of  
818 sucrose together with other photosynthetic products provide energy and carbon skeletons for  
819 amino acid biosynthesis. Respiratory breakdown of sucrose generates 2-oxoglutarate (2-OG)  
820 and this serves as the carbon skeleton for the synthesis of glutamate. In the process of  $\text{NO}_3^-$   
821 photo assimilation, conversion of  $\text{NO}_2^-$  to  $\text{NH}_4^+$  by *NiR* showed an upregulation at elevated  
822  $[\text{CO}_2]$ . Consequently, the expression of *GS2a*, *GS1a* and *GSr1* was significantly higher in  
823 LFELB at elevated  $[\text{CO}_2]$ . Further genes encoding enzyme Fd-GOGAT and NADH-GOGAT  
824 were substantially higher at elevated  $[\text{CO}_2]$  suggesting that nitrogen assimilation is efficient at  
825 early stages of plant development.

826 In the early vegetative phase, ELB and the SAR can be considered as the major sink organs. In  
827 SAR and ELB, sucrose translocated from LFELB is cleaved by sucrose synthase (*SUS1*), which  
828 showed a strong upregulation in growing tissues at elevated [CO<sub>2</sub>]. The resulting UDP-Glucose  
829 plays an important role as a substrate for the re-synthesis of sucrose from available glucose and  
830 fructose ([Koch, 2004](#)). Also, UDP-Glucose is an important component in cell wall biosynthesis  
831 of dividing cells ([Verbančič et al., 2017](#)). Increased activity of cell wall metabolism was  
832 evident from the higher expression of genes encoding  $\beta$ -expansins and Xyloglucan  
833 endotransglucosylase/hydrolases. This implied that cell wall loosening, and expansion has been  
834 promoted at elevated [CO<sub>2</sub>]. High availability of glucose and fructose of SAR and ELB  
835 positively correlates with cell division ([Koch, 2004](#)). Therefore, in the SAR and ELB, active  
836 utilization of carbohydrates and increased production and expansion of cells, may have  
837 facilitated increased plant growth rates at elevated [CO<sub>2</sub>].

## 838 **5. Conclusion**

839 In this study, we investigated the early growth response of wheat under elevated [CO<sub>2</sub>] with  
840 the aim of understanding the underlying physiological and molecular mechanisms of plant  
841 growth. Here we hypothesized that increased carbon assimilation at elevated [CO<sub>2</sub>] may alter  
842 the carbohydrate pools of plants and thereby influence the key metabolic processes that control  
843 the growth of source and sink tissues of plants. We conclude that elevated [CO<sub>2</sub>] stimulates the  
844 early growth of wheat in a significant manner, but the magnitude of these responses is largely  
845 varied between the two parental cultivars. The increased photosynthetic capacity was a key  
846 contributor towards this growth response, however, photosynthetic data alone could not explain  
847 the growth response to elevated [CO<sub>2</sub>]. Elevated [CO<sub>2</sub>] always promotes the soluble  
848 carbohydrate accumulation and allocation in an organ-specific manner. Consistently, a large  
849 amount of carbohydrates was allocated to the sink tissues, particularly in expanding leaf, apical  
850 meristem and the cell elongation zone of the expanding leaf. These increased carbon pools  
851 significantly influence other post-photosynthetic key metabolic processes, which include  
852 sucrose metabolism, nitrogen assimilation and cell elongation and expansion under elevated  
853 [CO<sub>2</sub>]. The expression of key genes associated with these metabolic processes showed  
854 significant variation in different genotypes in an organ-specific manner. The strong positive  
855 correlation between sucrose and *SPP1* (sucrose biosynthesis) *TaXTH5* and *TaEXPA1* (cell wall  
856 expansion) at elevated [CO<sub>2</sub>] further indicated that sugar plays a significant role in altering  
857 transcript level responses associated with sucrose metabolism and cell elongation and  
858 expansion, and thereby facilitate enhanced plant growth under a CO<sub>2</sub> rich environment.  
859 However, these relationships among soluble sugar concentrations and transcript abundance,  
860 and their influence on plant growth at elevated [CO<sub>2</sub>], are complex and varied even within the  
861 same species, making it challenging to establish a generalized holistic mechanism for plant  
862 growth responses to elevated [CO<sub>2</sub>] across all plant species.

863 **List of Figures and Supplementary Figures**

864

865 **Figure 1** The effect of [CO<sub>2</sub>] on (a) above ground biomass accumulation , (b) leaf area  
866 development and (c) total soluble carbohydrate content of Kukri and RAC875 grown at  
867 ambient (400 μmol mol<sup>-1</sup>) or elevated (700±10 μmol mol<sup>-1</sup>) [CO<sub>2</sub>]. Measurements were taken  
868 at 42 DAP. Summary of the ANOVA results is shown. Data presented are the mean from 3  
869 replicates. Abbreviations: ns, not significant; \*, P<0.05; \*\*, P<0.01.

870

871 **Figure 2** The effect of [CO<sub>2</sub>] on (a) rate of photosynthesis, (b) PSII operating efficiency  
872 (ϕPSII), (c) electron transport rate (ETR), (d) photochemical quenching (q<sub>p</sub>), (e) Non-  
873 photochemical quenching (NPQ), (f) Maximum PSII efficiency (F<sub>v</sub>'/F<sub>m</sub>' ) of Kukri and  
874 RAC875 grown at ambient (400 μmol mol<sup>-1</sup>) or elevated (700±10 μmol mol<sup>-1</sup>) [CO<sub>2</sub>].  
875 Measurements were taken at 42 DAP. Summary of the ANOVA results is shown. Data  
876 presented are the mean from 6 replicates. Abbreviations: ns, not significant; \*, P<0.05; \*\*,  
877 P<0.01.

878

879 **Figure 3** The effect of [CO<sub>2</sub>] on total soluble sugar content of (a) last fully expanded leaf blade  
880 (LFELB) , (b) expanding leaf blade (ELB) and (c) cell elongation region (CER) of Kukri and  
881 RAC875 grown at ambient (400 μmol mol<sup>-1</sup>) or elevated (700±10 μmol mol<sup>-1</sup>) [CO<sub>2</sub>].  
882 Measurements were taken at 42 DAP. Summary of the ANOVA results is shown. Data  
883 presented are the mean from 3 replicates. Abbreviations: ns, not significant; \*, P<0.05; \*\*,  
884 P<0.01.

885

886 **Figure 4** Schematic diagram of key gene expression of source (last fully expanded leaf) and  
887 sink (expanding leaf and shoot apex region) integration of wheat at elevated [CO<sub>2</sub>] in early  
888 vegetative stage of wheat. A: photosynthesis rate, PSII: photosystem II, ETR: electron transport  
889 rate, q<sub>p</sub>- photochemical quenching, Glc: glucose, Fru: fructose, Suc: sucrose, F6P- fructose 6  
890 phosphate, UDP-Glc: UDP glucose, Suc6P: sucrose 6 phosphate, G1P: glucose 1 phosphate,  
891 UTP: uridine triphosphate, AA- amino acids synthesis & metabolism, *rbcL* - ribulose 1,5 –  
892 biphosphate carboxylase/oxygenase (large sub unit); *rbcS* - ribulose 1,5 –biphosphate  
893 carboxylase/oxygenase (small sub unit); *SPP*- Sucrose Phosphate Phosphatase; *SPS*- Sucrose  
894 Phosphate Synthase; *SUS* - Sucrose Synthase type 1; *NiR* - Ferredoxin Nitrite Reductase; *Fd*-  
895 *GOGAT* - Putative ferredoxin-dependent glutamate synthase; *GS2a* - Glutamine Synthetase  
896 (Plastidial), *NADH-GOGAT* - Putative NADH-dependent glutamate synthase; *GS1a* -

897 Glutamine synthetase (cytosolic); *Gsr1* - Glutamine synthetase (cytosolic) *TaEXPB* -  $\beta$  -  
898 expansins *TaXTH* - Xyloglucan endotransglucosylase/hydrolases

899

900 **Supplementary Figure S1.** The effect of [CO<sub>2</sub>] on sucrose content of (a) last fully expanded  
901 leaf blade (LFELB), (b) expanding leaf blade (ELB) and (c) cell elongation region (CER);  
902 glucose content of (d) LFELB, (e) ELB, (f) CER; fructose content of (g) LFELB, (h) ELB, (f)  
903 CER of Kukri and RAC875 grown at ambient (400  $\mu\text{mol mol}^{-1}$ ) or elevated (700 $\pm$ 10  $\mu\text{mol mol}^{-1}$ )  
904 [CO<sub>2</sub>]. Measurements were taken at 42 DAP. Summary of the ANOVA results is shown.  
905 Data presented are the mean from 3 replicates. Abbreviations: ns, not significant; \*, P<0.05;  
906 \*\*, P<0.01.

907

908 **List of Tables and Supplementary Tables**

909

910 **Table 1.** List of selected genes and primer sequences used for the RT-qPCR based gene  
911 expression analysis (LFEL: Last fully expanded leaf; EL: expanding leaf; CE: cell elongation  
912 region; SA: shoot apex region).

913

914 **Table 2.** The effect of [CO<sub>2</sub>] on aboveground biomass accumulation, below ground biomass  
915 accumulation, total soluble sugar content, total leaf area per plant and photosynthesis rate of  
916 different wheat lines selected from doubled haploid mapping population of Kukri and RAC875  
917 grown at ambient [CO<sub>2</sub>] (a[CO<sub>2</sub>], 400 μmol mol<sup>-1</sup>) or elevated [CO<sub>2</sub>] (e[CO<sub>2</sub>], 700±10 μmol  
918 mol<sup>-1</sup>). Measurements were taken at 42 DAP. Summary of the ANOVA results is shown. Data  
919 presented are the mean from n=3 replicates. Abbreviations: ns, not significant; \*, P<0.05; \*\*,  
920 P<0.01.

921

922 **Table 3.** The effect of [CO<sub>2</sub>] on organ-specific sucrose, glucose and fructose concentrations of  
923 different wheat lines selected from a doubled haploid mapping population of Kukri and  
924 RAC875 grown at ambient [CO<sub>2</sub>] (a[CO<sub>2</sub>], 400 μmol mol<sup>-1</sup>) or elevated [CO<sub>2</sub>] (e[CO<sub>2</sub>], 700±10  
925 μmol mol<sup>-1</sup>). Summary of the ANOVA results is shown. Data presented are the mean from n=3  
926 replicates. Abbreviations: LFELB, last fully expanded leaf blade; ELB, expanding leaf blade;  
927 CER- cell elongation region; ns, not significant; \*, P<0.05; \*\*, P<0.01.

928

929 **Table 4.** Heatmap for transcript abundance of *rbcL* and *rbcS* genes related to photosynthesis  
930 regulation in last fully expanded leaf (LFELB), expanding leaf (ELB), cell elongation region  
931 (LCEZ) and shoot apex region (SAR) of Kukri and RAC875 grown at ambient (a[CO<sub>2</sub>], 400  
932 μmol mol<sup>-1</sup>) or elevated (e[CO<sub>2</sub>], 700±10 μmol mol<sup>-1</sup>) [CO<sub>2</sub>]. Data presented are the mean  
933 values of gene expression. Fold change of transcript relative abundance at elevated [CO<sub>2</sub>] are  
934 presented in Log<sub>2</sub> scale.

935

936 **Table 5.** Heatmap for transcript abundance of *SPP1*, *SPS1* and *SUS1* genes of sucrose  
937 metabolism in last fully expanded leaf (LFELB), expanding leaf (ELB), cell elongation region  
938 (LCEZ) and shoot apex region (SAR) of Kukri and RAC875 grown at ambient (a[CO<sub>2</sub>], 400  
939 μmol mol<sup>-1</sup>) or elevated (e[CO<sub>2</sub>], 700±10 μmol mol<sup>-1</sup>) [CO<sub>2</sub>]. Data presented are the mean  
940 values of gene expression. Fold change of transcript relative abundance at elevated [CO<sub>2</sub>] are  
941 presented in Log<sub>2</sub> scale.

942 **Table 6.** Heatmap for transcript abundance of *NiR*, *GS2a*, *GS2b*, *Fd-GOGAT* genes of nitrogen  
943 metabolism in last fully expanded leaf (LFELB) and expanding leaf (ELB) of Kukri and  
944 RAC875 grown at ambient (a[CO<sub>2</sub>], 400 μmol mol<sup>-1</sup>) or elevated (e[CO<sub>2</sub>], 700±10 μmol mol<sup>-1</sup>)  
945 [CO<sub>2</sub>]. Data presented are the mean values of gene expression. Fold change of transcript  
946 relative abundance at elevated [CO<sub>2</sub>] are presented in Log<sub>2</sub> scale.

947 **Table 7.** Heatmap for transcript abundance of α and β expansin genes of cell wall metabolism  
948 in last fully expanded leaf (LFELB), expanding leaf (ELB), cell elongation region (LCEZ) and  
949 shoot apex region (SAR) of Kukri and RAC875 grown at ambient (a[CO<sub>2</sub>], 400 μmol mol<sup>-1</sup>) or  
950 elevated (e[CO<sub>2</sub>], 700±10 μmol mol<sup>-1</sup>) [CO<sub>2</sub>]. Data presented are the mean values of gene  
951 expression. Fold change of transcript relative abundance at elevated [CO<sub>2</sub>] are presented in  
952 Log<sub>2</sub> scale.

953

954 **Table 8.** Heatmap for transcript abundance of Xyloglucan endotransglucosylase/hydrolase  
955 genes of cell wall metabolism in last fully expanded leaf (LFELB), expanding leaf (ELB), cell  
956 elongation region (LCEZ) and shoot apex region (SAR) of Kukri and RAC875 grown at  
957 ambient (a[CO<sub>2</sub>], 400 μmol mol<sup>-1</sup>) or elevated (e[CO<sub>2</sub>], 700±10 μmol mol<sup>-1</sup>) [CO<sub>2</sub>]. Data  
958 presented are the mean values of gene expression. Fold change of transcript relative abundance  
959 at elevated [CO<sub>2</sub>] are presented in Log<sub>2</sub> scale.

960

961 **Supplementary Table S1.** CO<sub>2</sub> responsiveness of the selected wheat lines of the double  
962 haploid mapping population in the previous experimental trials.

963

964 **Supplementary Table S2.** Controlled environmental conditions provided to the Reach-in plant  
965 growth chambers throughout the experimental period.

966

967 **Supplementary Table S3.** List of primer sequences of selected genes for the RT-PCR analysis.

968

969 **Supplementary Table S4.** The effect of [CO<sub>2</sub>] on growth-related traits, photosynthetic  
970 parameters and chlorophyll fluorescence parameters of Kukri and RAC875 grown at ambient  
971 [CO<sub>2</sub>] (a[CO<sub>2</sub>], 400 μmol mol<sup>-1</sup>) or elevated [CO<sub>2</sub>] (e[CO<sub>2</sub>], 700±10 μmol mol<sup>-1</sup>).  
972 Measurements were taken at 42 DAP. Summary of the ANOVA results is shown. Data  
973 presented are the mean from n=3 and 6 replicates. Abbreviations: ns, not significant; \*, P<0.05;  
974 \*\*, P<0.01.

975 **Supplementary Table S5.** Summary of the Analysis of Variance (ANOVA) results for the  
976 effect of [CO<sub>2</sub>] on different genes tested for two parental lines, Kukri and RAC875 grown at  
977 ambient (400 μmol mol<sup>-1</sup>) or elevated (700±10 μmol mol<sup>-1</sup>) [CO<sub>2</sub>]. Abbreviations: ns, not  
978 significant; \*, P<0.05; \*\*, P<0.01.

979

980 **Supplementary Table S6.** Coefficients of correlation (*r*) between the response of sugar  
981 content and gene expression to elevated [CO<sub>2</sub>]. Data used were the relative change of sugar  
982 content between ambient and elevated [CO<sub>2</sub>] and the relative expression for each gene under  
983 elevated [CO<sub>2</sub>]. Measurements were collected from Kukri and RAC875 42 DAP. Significant  
984 data are indicated in bold; \*, *P* <0.05; \*\*, *P* <0.01.

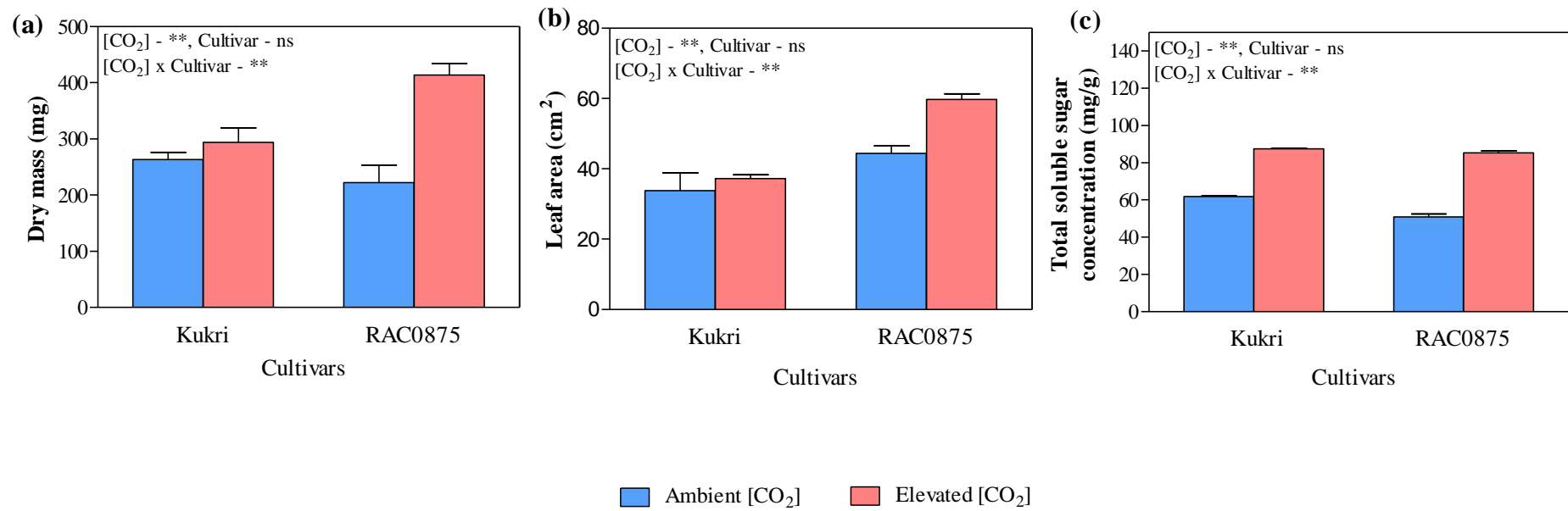


**Figure 1**

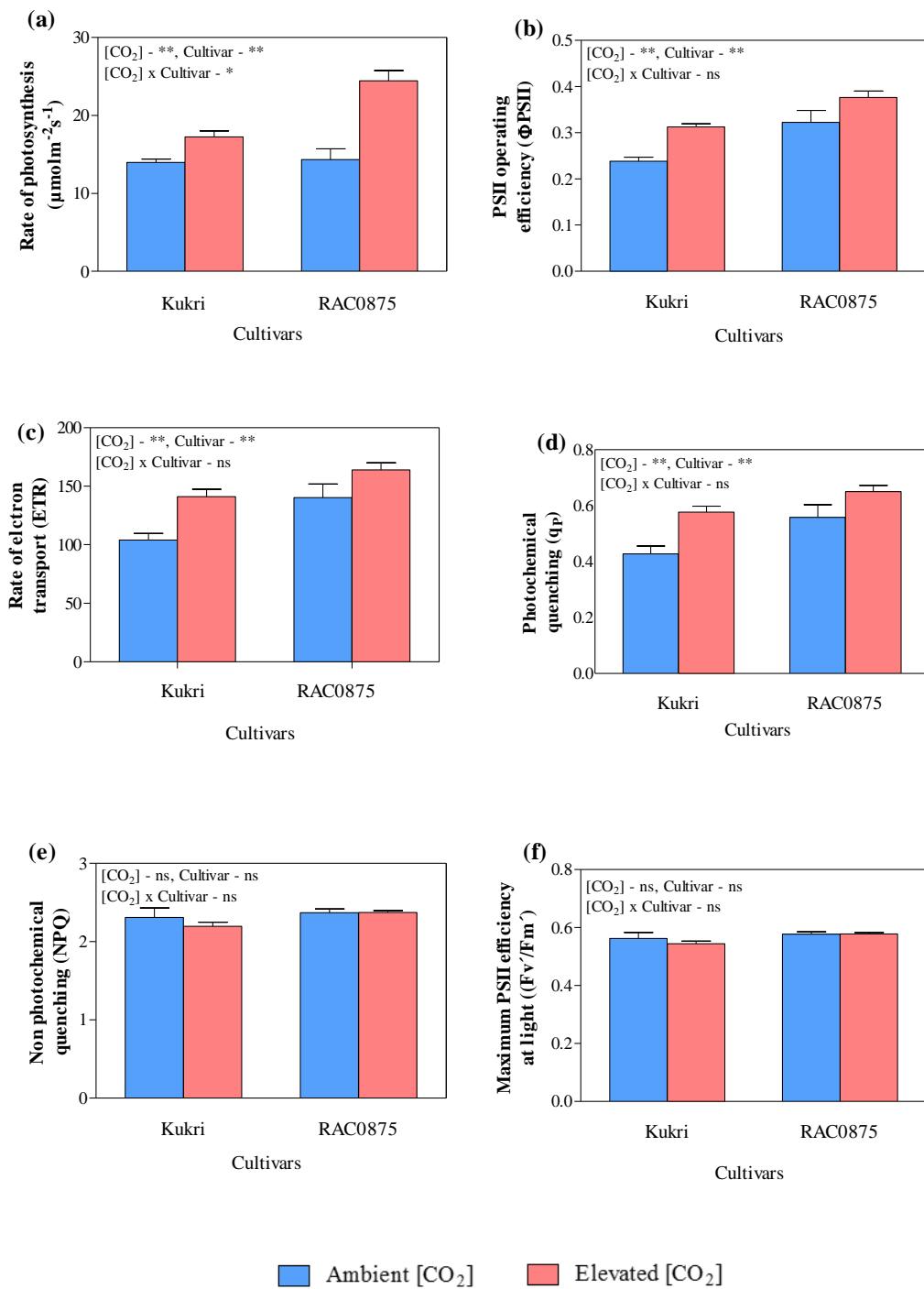
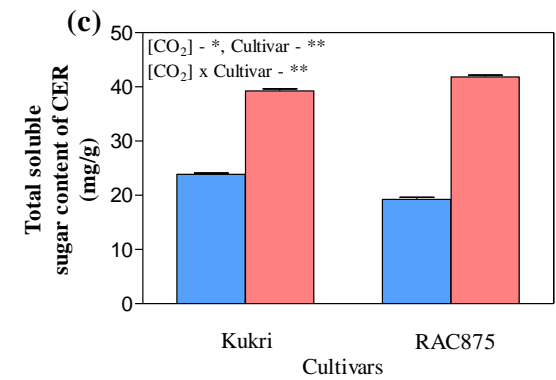
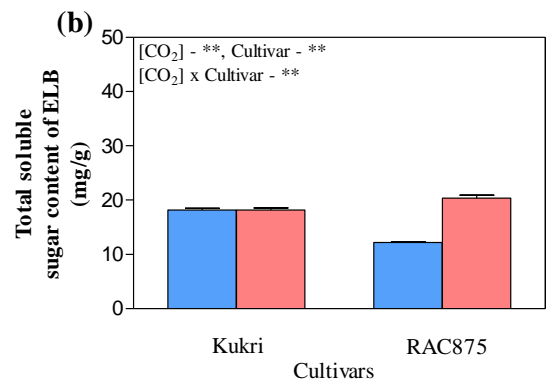
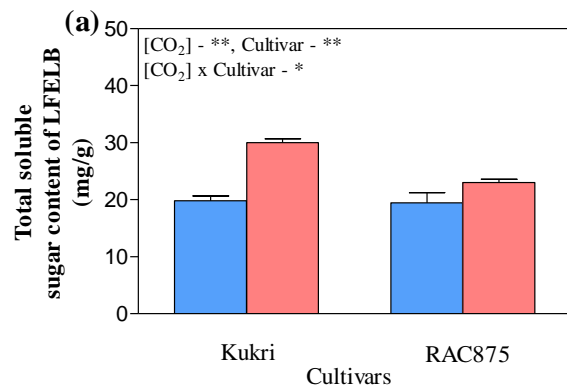


**Figure 2**



■ Ambient [CO<sub>2</sub>]    ■ Elevated [CO<sub>2</sub>]

**Figure 3**



**Table 1.** List of selected genes and primer sequences used for the RT-qPCR based gene expression analysis (LFELB: Last fully expanded leaf; ELB: expanding leaf; LCEZ: cell elongation region; SAR: shoot apex region).

<b>Metabolism</b>	<b>Accession No.</b>	<b>Name of the gene</b>	<b>Gene abbreviation</b>	<b>Tissue</b>
<b>Photosynthesis</b>	AY328025	Ribulose 1,5 –bisphosphate carboxylase/oxygenase (large sub unit)	<i>rbcL</i>	LFELB, ELB,
	AB020957	Ribulose 1,5 –bisphosphate carboxylase/oxygenase (small sub unit)	<i>rbcS</i>	LCEZ, SAR
<b>Carbon metabolism</b>	AF321556	Sucrose Phosphate Phosphatase 1	<i>SPP1</i>	LFELB, ELB,
	AF310160	Sucrose Phosphate Synthase 1	<i>SPS1</i>	LCEZ, SAR
	AF321556	Sucrose Synthase type 1	<i>SUS1</i>	
<b>Nitrogen metabolism</b>	FJ527909	Ferredoxin Nitrite Reductase	<i>NiR</i>	
	TC394038	Putative ferredoxin-dependent glutamate synthase	<i>Fd-GOGAT</i>	
	DQ124212	Glutamine Synthetase (Plastidial) – GS2	<i>GS2a</i>	
	DQ124213	Glutamine Synthetase (Plastidial) – GS2	<i>GS2b</i>	LFELB, ELB
	TC387834	Putative NADH-dependent glutamate synthase	<i>NADH-GOGAT</i>	
	DQ124209	Glutamine synthetase (cytosolic) – GS1	<i>GS1a</i>	
	AY491968	Glutamine synthetase (cytosolic) – GS1	<i>GSr1</i>	
<b>Cell wall metabolism</b>	AY589583	$\alpha$ – expansin A1	<i>TaEXPA1</i>	LCEZ, SAR
	AY692477	$\alpha$ – expansin A3	<i>TaEXPA3</i>	LFELB, ELB, LCEZ, SAR
	AY589578	$\beta$ – expansin B1	<i>TaEXPB1</i>	LCEZ, SAR
	AY589579	$\beta$ – expansin B2	<i>TaEXPB2</i>	
	AY589580	$\beta$ – expansin B3	<i>TaEXPB3</i>	
	AY692478	$\beta$ – expansin B6	<i>TaEXPB6</i>	LFELB, ELB,
	AY260547	$\beta$ – expansin B23	<i>TaEXPB23</i>	LCEZ, SAR
	AY589585	Xyloglucan endotransglucosylase/hydrolase 1	<i>TaXTH1</i>	
	AY589586	Xyloglucan endotransglucosylase/hydrolase 2	<i>TaXTH2</i>	
	AY589586	Xyloglucan endotransglucosylase/hydrolase 3	<i>TaXTH3</i>	
	AY589586	Xyloglucan endotransglucosylase/hydrolase 4	<i>TaXTH4</i>	
	AY589586	Xyloglucan endotransglucosylase/hydrolase 5	<i>TaXTH5</i>	

**Table 2.** The effect of [CO<sub>2</sub>] on aboveground biomass accumulation, below ground biomass accumulation, total soluble sugar content, total leaf area per plant and photosynthesis rate of different wheat lines selected from doubled haploid mapping population of Kukri and RAC875 grown at ambient [CO<sub>2</sub>] (a[CO<sub>2</sub>], 400 μmol mol<sup>-1</sup>) or elevated [CO<sub>2</sub>] (e[CO<sub>2</sub>], 700±10 μmol mol<sup>-1</sup>). Measurements were taken at 42 DAP. Summary of the ANOVA results is shown. Data presented are the mean from n=3 replicates. Abbreviations: ns, not significant; \*, P<0.05; \*\*, P<0.01.

Trait	Mean CO <sub>2</sub> effect			Mean genotype effect	Interaction effect [CO <sub>2</sub> ]x Cultivar	Mean Responsiveness to e[CO <sub>2</sub> ] (%)	
	a[CO <sub>2</sub> ]	e[CO <sub>2</sub> ]	ANOVA result	ANOVA result	ANOVA result	High responsive lines	Low responsive lines
Above ground biomass (mg/plant)	142.80	294.13	**	**	**	225.38	31.30
Below ground biomass (mg/plant)	44.73	81.69	**	**	**	175.67	34.74
Total soluble sugar content (mg/g)	71.88	84.56	**	**	**	19.75	14.96
Total leaf area (cm <sup>2</sup> /plant)	43.37	44.19	ns	**	**	27.58	-17.99
Photosynthesis rate (μmol CO <sub>2</sub> m <sup>-2</sup> s <sup>-1</sup> )	14.97	15.25	ns	**	*	8.82	-12.16

**Table 3.** The effect of [CO<sub>2</sub>] on organ-specific sucrose, glucose and fructose concentrations of different wheat lines selected from a doubled haploid mapping population of Kukri and RAC875 grown at ambient [CO<sub>2</sub>] (a[CO<sub>2</sub>], 400 μmol mol<sup>-1</sup>) or elevated [CO<sub>2</sub>] (e[CO<sub>2</sub>], 700±10 μmol mol<sup>-1</sup>). Summary of the ANOVA results is shown. Data presented are the mean from n=3 replicates. Abbreviations: LFELB, last fully expanded leaf blade; ELB, expanding leaf blade; CER- cell elongation region; ns, not significant; \*, P<0.05; \*\*, P<0.01.

Line	Plant organ	Mean CO <sub>2</sub> effect						ANOVA results							
		a[CO <sub>2</sub> ]			e[CO <sub>2</sub> ]			Responsiveness to e[CO <sub>2</sub> ] (%)	[CO <sub>2</sub> ] effect	Genotype effect	Organ effect	[CO <sub>2</sub> ]x Cultivar x Organ			
		Sucrose	Glucose	Fructose	Sucrose	Glucose	Fructose					Sucrose	Glucose	Fructose	
<b>H<sub>1</sub></b>	LFELB	5.88	16.26	3.94	3.57	13.53	2.45	31.50	**	**	**	**	**	**	**
	ELB	0.77	12.42	6.64	2.88	9.28	10.49								
	CER	6.59	13.17	11.32	8.54	27.22	14.72								
<b>H<sub>2</sub></b>	LFELB	5.10	16.31	3.51	15.74	10.64	9.20	25.05	**	**	**	**	**	**	**
	ELB	0.79	14.75	2.78	5.97	10.57	9.12								
	CER	9.62	19.04	5.69	4.38	33.02	9.02								
<b>H<sub>3</sub></b>	LFELB	3.11	14.99	2.50	11.62	11.59	7.10	3.74	**	**	**	**	**	**	**
	ELB	1.54	15.60	3.63	1.81	9.23	9.85								
	CER	5.55	12.97	9.65	5.01	20.88	4.78								
<b>H<sub>4</sub></b>	LFELB	6.54	13.06	3.55	6.74	9.46	4.15	1.77	**	**	**	**	**	**	**
	ELB	2.93	11.67	4.67	3.98	10.77	3.96								
	CER	5.15	18.42	6.51	6.27	18.00	7.66								
<b>L<sub>1</sub></b>	LFELB	3.08	14.52	1.74	16.75	9.35	9.07	-5.48	**	**	**	**	**	**	**
	ELB	2.33	13.87	5.02	2.57	7.21	10.85								
	CER	7.61	12.67	12.17	3.53	21.00	4.53								

<b>L<sub>2</sub></b>	LFELB	3.14	13.24	2.60	11.70	11.17	6.27	2.90	**	**	**	**	**	**
	ELB	2.09	13.55	5.24	3.02	9.40	10.40							
	CER	6.14	15.93	9.10	5.73	22.02	3.54							
<b>L<sub>3</sub></b>	LFELB	0.58	13.58	1.07	10.64	9.16	6.23	0.90	**	**	**	**	**	**
	ELE	2.30	13.18	6.28	3.24	8.76	10.04							
	CER	3.95	20.83	4.40	3.90	23.01	2.58							
<b>L<sub>4</sub></b>	LFELB	3.17	14.02	2.53	8.49	9.58	4.82	4.63	**	**	**	**	**	**
	ELB	3.16	13.03	5.62	5.88	10.67	8.61							
	CER	3.22	22.60	2.40	3.07	22.85	2.18							

**Table 4.** Heatmap for transcript abundance of *rbcL* and *rbcS* genes related to photosynthesis regulation in last fully expanded leaf (LFELB), expanding leaf (ELB), cell elongation region (LCEZ) and shoot apex region (SAR) of Kukri and RAC875 grown at ambient (a[CO<sub>2</sub>], 400 μmol mol<sup>-1</sup>) or elevated (e[CO<sub>2</sub>], 700±10 μmol mol<sup>-1</sup>) [CO<sub>2</sub>]. Data presented are the mean values of gene expression. Fold change of transcript relative abundance at elevated [CO<sub>2</sub>] are presented in Log<sub>2</sub> scale.

Organ type	Gene Name	Gene expression level				Log <sub>2</sub> fold change	
		Kukri		RAC875		Kukri	RAC875
		a[CO <sub>2</sub> ]	e[CO <sub>2</sub> ]	a[CO <sub>2</sub> ]	e[CO <sub>2</sub> ]	e[CO <sub>2</sub> ]/a[CO <sub>2</sub> ]	
LFELB	<i>rbcL</i>	1.73	3.62	4.25	6.21	1.06	0.55
	<i>rbcS</i>	0.26	2.38	1.88	4.61	3.22	1.29
ELB	<i>rbcL</i>	2.70	3.69	1.40	3.12	0.45	1.16
	<i>rbcS</i>	1.26	2.65	1.42	2.00	1.07	0.49
LCEZ	<i>rbcL</i>	3.67	2.79	1.87	2.78	-0.40	0.57
	<i>rbcS</i>	2.01	2.41	1.44	2.75	0.26	0.94
SAR	<i>rbcL</i>	0.73	1.53	0.55	1.69	1.06	1.61
	<i>rbcS</i>	3.68	3.77	4.35	9.09	0.04	1.06

**Table 5.** Heatmap for transcript abundance of *SPP1*, *SPS1* and *SUS1* genes of sucrose metabolism in last fully expanded leaf (LFELB), expanding leaf (ELB), cell elongation region (LCEZ) and shoot apex region (SAR) of Kukri and RAC875 grown at ambient (a[CO<sub>2</sub>], 400 μmol mol<sup>-1</sup>) or elevated (e[CO<sub>2</sub>], 700±10 μmol mol<sup>-1</sup>) [CO<sub>2</sub>]. Data presented are the mean values of gene expression. Fold change of transcript relative abundance at elevated [CO<sub>2</sub>] are presented in Log<sub>2</sub> scale.

Organ type	Gene Name	Gene expression level				Log <sub>2</sub> fold change	
		Kukri		RAC875		Kukri	RAC875
		a[CO <sub>2</sub> ]	e[CO <sub>2</sub> ]	a[CO <sub>2</sub> ]	e[CO <sub>2</sub> ]	e[CO <sub>2</sub> ]/a[CO <sub>2</sub> ]	
LFELB	<i>SPP1</i>	6.84	5.78	8.42	45.78	-0.24	2.44
	<i>SPS1</i>	1.51	5.57	3.70	17.76	1.88	2.26
	<i>SUS1</i>	0.32	0.82	1.09	2.18	1.36	1.01
ELB	<i>SPP1</i>	4.47	4.48	3.48	10.32	0.00	1.57
	<i>SPS1</i>	0.95	1.50	1.26	1.27	0.65	0.02
	<i>SUS1</i>	0.43	1.81	0.56	1.50	2.07	1.43
LCEZ	<i>SPP1</i>	0.34	0.27	0.12	0.62	-0.32	2.38
	<i>SPS1</i>	1.86	2.22	2.61	6.06	0.25	1.21
	<i>SUS1</i>	4.27	3.91	1.66	3.63	-0.13	1.13
SAR	<i>SPP1</i>	0.05	0.23	0.07	0.22	2.18	1.58
	<i>SPS1</i>	0.91	1.69	0.71	1.72	0.89	1.27
	<i>SUS1</i>	5.05	14.08	3.53	9.31	1.48	1.40

**Table 6.** Heatmap for transcript abundance of *NiR*, *GS2a*, *GS2b*, *Fd-GOGAT* genes of nitrogen metabolism in last fully expanded leaf (LFELB) and expanding leaf (ELB) of Kukri and RAC875 grown at ambient (a[CO<sub>2</sub>], 400 μmol mol<sup>-1</sup>) or elevated (e[CO<sub>2</sub>], 700±10 μmol mol<sup>-1</sup>) [CO<sub>2</sub>]. Data presented are the mean values of gene expression. Fold change of transcript relative abundance at elevated [CO<sub>2</sub>] are presented in Log<sub>2</sub> scale.

Organ type	Gene Name	Gene expression level				Log <sub>2</sub> fold change	
		Kukri		RAC875		Kukri	RAC875
		a[CO <sub>2</sub> ]	e[CO <sub>2</sub> ]	a[CO <sub>2</sub> ]	e[CO <sub>2</sub> ]	e[CO <sub>2</sub> ]/a[CO <sub>2</sub> ]	
LFELB	<i>NiR</i>	0.07	0.65	0.21	0.60	3.30	1.54
	<i>Fd-GOGAT</i>	2.91	11.92	8.45	21.39	2.04	1.34
	<i>GS2a</i>	0.89	5.23	1.69	2.76	2.56	0.71
	<i>GS2b</i>	0.00	0.02	0.02	0.05	2.44	1.73
	<i>GS1a</i>	3.96	3.56	4.84	41.50	-0.15	3.10
	<i>GSr1</i>	0.14	0.57	0.16	3.37	2.05	4.39
	<i>NADH-GOGAT</i>	0.10	0.15	0.19	1.79	0.56	3.26
ELB	<i>NiR</i>	0.30	0.56	0.41	1.19	0.89	1.55
	<i>Fd-GOGAT</i>	13.24	29.92	15.61	28.57	1.18	0.87
	<i>GS2a</i>	24.98	46.56	14.65	26.80	0.90	0.87
	<i>GS2b</i>	0.09	0.15	0.11	0.32	0.70	1.49
	<i>GS1a</i>	3.36	4.28	3.15	4.26	0.35	0.44
	<i>GSr1</i>	0.33	0.68	0.25	0.27	1.04	0.12
	<i>NADH-GOGAT</i>	0.29	0.71	0.26	0.26	1.31	0.04

**Table 7.** Heatmap for transcript abundance of  $\alpha$  and  $\beta$  expansin genes of cell wall metabolism in last fully expanded leaf (LFELB), expanding leaf (ELB), cell elongation region (LCEZ) and shoot apex region (SAR) of Kukri and RAC875 grown at ambient (a[CO<sub>2</sub>], 400  $\mu\text{mol mol}^{-1}$ ) or elevated (e[CO<sub>2</sub>], 700 $\pm$ 10  $\mu\text{mol mol}^{-1}$ ) [CO<sub>2</sub>]. Data presented are the mean values of gene expression. Fold change of transcript relative abundance at elevated [CO<sub>2</sub>] are presented in Log<sub>2</sub> scale.

Organ type	Gene Name	Gene expression level				Log <sub>2</sub> fold change	
		Kukri		RAC875		Kukri	RAC875
		a[CO <sub>2</sub> ]	e[CO <sub>2</sub> ]	a[CO <sub>2</sub> ]	e[CO <sub>2</sub> ]	e[CO <sub>2</sub> ]/a[CO <sub>2</sub> ]	
LFELB	<i>TaEXPA3</i>	0.01	0.03	0.46	0.95	1.31	1.05
	<i>TaEXPB6</i>	0.05	0.05	0.76	0.74	0.17	-0.03
	<i>TAEXPB23</i>	0.01	0.05	0.11	0.38	2.48	1.82
ELB	<i>TaEXPA3</i>	1.32	1.23	1.77	5.48	-0.10	1.63
	<i>TaEXPB6</i>	6.11	7.51	7.46	17.14	0.30	1.20
	<i>TAEXPB23</i>	11.55	28.49	13.23	13.55	1.30	0.03
LCEZ	<i>TaEXPA1</i>	0.03	0.02	0.04	0.06	-0.80	0.57
	<i>TaEXPA3</i>	0.06	0.39	0.38	0.44	2.71	0.20
	<i>TAEXPB1</i>	0.10	0.13	0.17	0.23	0.36	0.41
	<i>TAEXPB2</i>	0.76	2.43	0.84	1.74	1.68	1.04
	<i>TAEXPB3</i>	0.46	0.73	0.60	1.37	0.68	1.20
	<i>TAEXPB6</i>	0.64	1.82	3.15	6.19	1.51	0.98
	<i>TAEXPB23</i>	2.65	10.46	3.58	8.43	1.98	1.24
SAR	<i>TaEXPA1</i>	0.05	0.03	0.02	0.03	-0.63	0.69
	<i>TaEXPA3</i>	1.19	2.65	2.94	4.91	1.16	0.74
	<i>TAEXPB1</i>	4.99	3.32	1.19	5.58	-0.59	2.23
	<i>TAEXPB2</i>	0.52	2.94	0.88	3.94	2.50	2.16
	<i>TAEXPB3</i>	0.28	1.57	0.65	2.30	2.50	1.83

	<i>TAEXPB6</i>	4.10	5.12	6.25	9.33	0.32	0.58
	<i>TAEXPB23</i>	3.40	9.94	3.98	14.82	1.55	1.90

**Table 8.** Heatmap for transcript abundance of Xyloglucan endotransglucosylase/hydrolase genes of cell wall metabolism in last fully expanded leaf (LFELB), expanding leaf (ELB), cell elongation region (LCEZ) and shoot apex region (SAR) of Kukri and RAC875 grown at ambient (a[CO<sub>2</sub>], 400 μmol mol<sup>-1</sup>) or elevated (e[CO<sub>2</sub>], 700±10 μmol mol<sup>-1</sup>) [CO<sub>2</sub>]. Data presented are the mean values of gene expression. Fold change of transcript relative abundance at elevated [CO<sub>2</sub>] are presented in Log<sub>2</sub> scale.

Organ type	Gene Name	Gene expression level				Log <sub>2</sub> fold change	
		Kukri		RAC875		Kukri	RAC875
		a[CO <sub>2</sub> ]	e[CO <sub>2</sub> ]	a[CO <sub>2</sub> ]	e[CO <sub>2</sub> ]	e[CO <sub>2</sub> ]/a[CO <sub>2</sub> ]	
LFELB	<i>TaXTH1</i>	0.63	0.65	5.83	5.33	0.04	-0.13
	<i>TaXTH2</i>	2.26	2.10	4.32	5.90	-0.11	0.45
	<i>TaXTH3</i>	0.78	0.40	1.71	2.04	-0.96	0.25
	<i>TaXTH4</i>	0.01	0.01	0.16	0.03	-0.60	-2.64
	<i>TaXTH5</i>	0.05	2.12	0.12	0.45	5.42	1.96
ELB	<i>TaXTH1</i>	39.54	46.23	23.16	66.77	0.23	1.53
	<i>TaXTH2</i>	36.34	65.60	46.83	94.22	0.85	1.01
	<i>TaXTH3</i>	26.76	8.70	4.31	36.13	-1.62	3.07
	<i>TaXTH4</i>	0.61	0.40	0.88	1.92	-0.60	1.12
	<i>TaXTH5</i>	1.94	2.58	0.94	2.44	0.42	1.37
LCEZ	<i>TaXTH1</i>	10.53	16.27	30.98	36.44	0.63	0.23
	<i>TaXTH2</i>	4.75	6.75	9.68	17.91	0.51	0.89
	<i>TaXTH3</i>	0.91	1.30	1.82	6.77	0.52	1.90
	<i>TaXTH4</i>	0.17	1.12	3.19	2.67	2.75	-0.26
	<i>TaXTH5</i>	2.28	5.29	2.49	6.38	1.22	1.36
SAR	<i>TaXTH1</i>	5.00	6.91	3.46	21.07	0.47	2.60
	<i>TaXTH2</i>	6.60	4.49	3.90	13.09	-0.55	1.75
	<i>TaXTH3</i>	2.40	1.87	0.87	3.24	-0.36	1.89
	<i>TaXTH4</i>	2.04	1.87	9.46	17.23	-0.12	0.86
	<i>TaXTH5</i>	46.11	46.87	17.38	61.97	0.02	1.83

828 **References**

- 829 Ainsworth, Elizabeth A, Claus Beier, Carlo Calfapietra, Reinhart Ceulemans, Mylene Durand-  
830 Tardif, Graham D Farquhar, Douglas L Godbold, George R Hendrey, Thomas Hickler,  
831 and Jörg Kaduk. 2008. 'Next generation of elevated [CO<sub>2</sub>] experiments with crops: a  
832 critical investment for feeding the future world', *Plant, Cell & Environment*, 31: 1317-  
833 24.
- 834 Ainsworth, Elizabeth A, and Daniel R Bush. 2011. 'Carbohydrate export from the leaf: a highly  
835 regulated process and target to enhance photosynthesis and productivity', *Plant*  
836 *Physiology*, 155: 64-69.
- 837 Ainsworth, Elizabeth A, and Alistair Rogers. 2007. 'The response of photosynthesis and  
838 stomatal conductance to rising [CO<sub>2</sub>]: mechanisms and environmental interactions',  
839 *Plant, Cell & Environment*, 30: 258-70.
- 840 Ainsworth, Elizabeth A, Alistair Rogers, Randall Nelson, and Stephen P Long. 2004. 'Testing  
841 the "source-sink" hypothesis of down-regulation of photosynthesis in elevated [CO<sub>2</sub>]  
842 in the field with single gene substitutions in Glycine max', *Agricultural and Forest*  
843 *Meteorology*, 122: 85-94.
- 844 Ainsworth, Elizabeth A, Alistair Rogers, Lila O Vodkin, Achim Walter, and Ulrich Schurr.  
845 2006. 'The effects of elevated CO<sub>2</sub> concentration on soybean gene expression. An  
846 analysis of growing and mature leaves', *Plant Physiology*, 142: 135-47.
- 847 Alonso, Aitor, Pilar Pérez, and Rafael Martínez-Carrasco. 2009. 'Growth in elevated CO<sub>2</sub>  
848 enhances temperature response of photosynthesis in wheat', *Physiologia plantarum*,  
849 135: 109-20.
- 850 Aranjuelo, Iker, Gorka Erice, Alvaro Sanz-Sáez, Cyril Abadie, Françoise Gilard, Erena Gil-  
851 Quintana, Jean-Christophe Avice, Christiana Staudinger, Stefanie Wienkoop, and Jose  
852 L Araus. 2015. 'Differential CO<sub>2</sub> effect on primary carbon metabolism of flag leaves in  
853 durum wheat (*Triticum durum* Desf.)', *Plant, Cell & Environment*, 38: 2780-94.
- 854 Bennett, Dion, Ali Izanloo, James Edwards, Haydn Kuchel, Ken Chalmers, Mark Tester,  
855 Matthew Reynolds, Thorsten Schnurbusch, and Peter Langridge. 2012. 'Identification  
856 of novel quantitative trait loci for days to ear emergence and flag leaf glaucousness in  
857 a bread wheat (*Triticum aestivum* L.) population adapted to southern Australian  
858 conditions', *Theoretical and Applied Genetics*, 124: 697-711.
- 859 Bennett, Dion, Matthew Reynolds, Daniel Mullan, Ali Izanloo, Haydn Kuchel, Peter  
860 Langridge, and Thorsten Schnurbusch. 2012. 'Detection of two major grain yield QTL  
861 in bread wheat (*Triticum aestivum* L.) under heat, drought and high yield potential  
862 environments', *Theoretical and Applied Genetics*, 125: 1473-85.
- 863 Bernard, Stéphanie M, Anders Laurell Blom Møller, Giuseppe Dionisio, Thomas Kichey,  
864 Thomas P Jahn, Frederic Dubois, Marcela Baudo, Marta S Lopes, Thérèse Tercé-  
865 Laforgue, and Christine H Foyer. 2008. 'Gene expression, cellular localisation and  
866 function of glutamine synthetase isozymes in wheat (*Triticum aestivum* L.)', *Plant*  
867 *molecular biology*, 67: 89-105.
- 868 Bihmidine, Saadia, Charles T Hunter III, Christine E Johns, Karen E Koch, and David M  
869 Braun. 2013. 'Regulation of assimilate import into sink organs: update on molecular  
870 drivers of sink strength', *Frontiers in plant science*, 4: 177.
- 871 Bloom, Arnold J. 2015. 'Photorespiration and nitrate assimilation: a major intersection between  
872 plant carbon and nitrogen', *Photosynthesis research*, 123: 117-28.
- 873 Bowes, George. 1993. 'Facing the inevitable: plants and increasing atmospheric CO<sub>2</sub>', *Annual*  
874 *review of plant biology*, 44: 309-32.
- 875 Brestic, Marian, Marek Zivcak, Hazem M Kalaji, Robert Carpentier, and Suleyman I  
876 Allakhverdiev. 2012. 'Photosystem II thermostability in situ: environmentally induced

877 acclimation and genotype-specific reactions in *Triticum aestivum* L', *Plant Physiology*  
878 *and Biochemistry*, 57: 93-105.

879 Cren, Michèle, and Bertrand Hirel. 1999. 'Glutamine synthetase in higher plants regulation of  
880 gene and protein expression from the organ to the cell', *Plant and Cell Physiology*, 40:  
881 1187-93.

882 Drake, Bert G, Miquel A González-Meler, and Steve P Long. 1997. 'More efficient plants: a  
883 consequence of rising atmospheric CO<sub>2</sub>?', *Annual review of plant biology*, 48: 609-39.

884 Echeverria, Ed, Michael E Salvucci, Pedro Gonzalez, Gaston Paris, and Graciela Salerno. 1997.  
885 'Physical and kinetic evidence for an association between sucrose-phosphate synthase  
886 and sucrose-phosphate phosphatase', *Plant Physiology*, 115: 223-27.

887 Eveland, Andrea L, and David P Jackson. 2011. 'Sugars, signalling, and plant development',  
888 *Journal of Experimental Botany*, 63: 3367-77.

889 Foyer, Christine, and Hanma Zhang. 2011. *Annual Plant Reviews, Nitrogen Metabolism in*  
890 *Plants in the Post-genomic Era* (John Wiley & Sons).

891 Gamage, Dananjali, Michael Thompson, Mark Sutherland, Naoki Hirotsu, Amane Makino, and  
892 Saman Seneweera. 2018. 'New insights into the cellular mechanisms of plant growth at  
893 elevated atmospheric carbon dioxide', *Plant, Cell & Environment*, 41(6): 1233-46.

894 Geigenberger, Peter, Ralph Reimholz, Uta Deiting, Uwe Sonnewald, and Mark Stitt. 1999.  
895 'Decreased expression of sucrose phosphate synthase strongly inhibits the water stress-  
896 induced synthesis of sucrose in growing potato tubers', *The Plant Journal*, 19: 119-29.

897 Geiger, M, V Haake, F Ludewig, U Sonnewald, and M Stitt. 1999. 'The nitrate and ammonium  
898 nitrate supply have a major influence on the response of photosynthesis, carbon  
899 metabolism, nitrogen metabolism and growth to elevated carbon dioxide in tobacco',  
900 *Plant, Cell & Environment*, 22: 1177-99.

901 Gibson, Susan I. 2005. 'Control of plant development and gene expression by sugar signaling',  
902 *Current opinion in plant biology*, 8: 93-102.

903 Gutiérrez, Diego, Elena Gutiérrez, Pilar Pérez, Rosa Morcuende, Angel L Verdejo, and Rafael  
904 Martínez-Carrasco. 2009. 'Acclimation to future atmospheric CO<sub>2</sub> levels increases  
905 photochemical efficiency and mitigates photochemistry inhibition by warm  
906 temperatures in wheat under field chambers', *Physiologia plantarum*, 137: 86-100.

907 Hashida, Yoichi, Tatsuro Hirose, Masaki Okamura, Ken-ichiro Hibara, Ryu Ohsugi, and  
908 Naohiro Aoki. 2016. 'A reduction of sucrose phosphate synthase (SPS) activity affects  
909 sucrose/starch ratio in leaves but does not inhibit normal plant growth in rice', *Plant*  
910 *Science*, 253: 40-49.

911 Huber, Steven C. 1983. 'Role of sucrose-phosphate synthase in partitioning of carbon in leaves',  
912 *Plant Physiology*, 71: 818-21.

913 Huber, Steven C, and Daniel W Israel. 1982. 'Biochemical basis for partitioning of  
914 photosynthetically fixed carbon between starch and sucrose in soybean (*Glycine max*  
915 *Merr.*) leaves', *Plant Physiology*, 69: 691-96.

916 IPCC. 2014. 'Recent increase and projected changes in CO<sub>2</sub> concentrations', Data distribution  
917 centre, IPCC, Accessed 13th December.

918 Izanloo, Ali, Anthony G Condon, Peter Langridge, Mark Tester, and Thorsten Schnurbusch.  
919 2008. 'Different mechanisms of adaptation to cyclic water stress in two South  
920 Australian bread wheat cultivars', *Journal of Experimental Botany*, 59: 3327-46.

921 Jiang, Shu-Ye, Yun-Hua Chi, Ji-Zhou Wang, Jun-Xia Zhou, Yan-Song Cheng, Bao-Lan  
922 Zhang, Ali Ma, Jeevanandam Vanitha, and Srinivasan Ramachandran. 2015. 'Sucrose  
923 metabolism gene families and their biological functions', *Scientific reports*, 5: 17583.

924 Jitla, D.S., G.S. Rogers, S.P. Seneweera, Amarjit S. Basra, Ron J. Oldfield, and J.P. Conroy.  
925 1997. 'Accelerated early growth of rice at elevated CO<sub>2</sub>', *Plant Physiology*, 115: 15-  
926 22.

- 927 Kimball, Bruce A. 2016. 'Crop responses to elevated CO<sub>2</sub> and interactions with H<sub>2</sub>O, N, and  
928 temperature', *Current opinion in plant biology*, 31: 36-43.
- 929 Koch, Karen. 2004. 'Sucrose metabolism: regulatory mechanisms and pivotal roles in sugar  
930 sensing and plant development', *Current opinion in plant biology*, 7: 235-46.
- 931 Koch, KE. 1996. 'Carbohydrate-modulated gene expression in plants', *Annual review of plant  
932 biology*, 47: 509-40.
- 933 Körner, Christian. 2015. 'Paradigm shift in plant growth control', *Current opinion in plant  
934 biology*, 25: 107-14.
- 935 Lee, Yi, and Hans Kende. 2001. 'Expression of  $\beta$ -expansins is correlated with internodal  
936 elongation in deepwater rice', *Plant Physiology*, 127: 645-54.
- 937 Li, Yi, Louise Jones, and Simon McQueen-Mason. 2003. 'Expansins and cell growth', *Current  
938 opinion in plant biology*, 6: 603-10.
- 939 Liu, Yong, Dongcheng Liu, Haiying Zhang, Hongbo Gao, Xiaoli Guo, Daowen Wang, Xiangqi  
940 Zhang, and Aimin Zhang. 2007. 'The  $\alpha$ - and  $\beta$ -expansin and xyloglucan  
941 endotransglucosylase/hydrolase gene families of wheat: Molecular cloning, gene  
942 expression, and EST data mining', *Genomics*, 90: 516-29.
- 943 Lunn, John E. 2003. 'Sucrose-phosphatase gene families in plants', *Gene*, 303: 187-96.
- 944 Lunn, John E, and Elspeth MacRae. 2003. 'New complexities in the synthesis of sucrose',  
945 *Current opinion in plant biology*, 6: 208-14.
- 946 MacRae, E.A., and J.E. Lunn. 2006. 'Control of sucrose biosynthesis.' in W.C. Plaxton and  
947 M.T. McManus (eds.), *Advances in Plant Research* (Blackwell).
- 948 Makino, Amane, Masayo Harada, Tetsuya Sato, Hiromi Nakano, and Tadahiko Mae. 1997.  
949 'Growth and N allocation in rice plants under CO<sub>2</sub> enrichment', *Plant Physiology*, 115:  
950 199-203.
- 951 Makino, Amane, and Tadahiko Mae. 1999. 'Photosynthesis and plant growth at elevated levels  
952 of CO<sub>2</sub>', *Plant and Cell Physiology*, 40: 999-1006.
- 953 Martin, Thomas, Oliver Oswald, and Ian A Graham. 2002. 'Arabidopsis seedling growth,  
954 storage lipid mobilization, and photosynthetic gene expression are regulated by carbon:  
955 nitrogen availability', *Plant Physiology*, 128: 472-81.
- 956 Masclaux-Daubresse, Céline, Françoise Daniel-Vedele, Julie Dechorgnat, Fabien Chardon,  
957 Laure Gaufichon, and Akira Suzuki. 2010. 'Nitrogen uptake, assimilation and  
958 remobilization in plants: challenges for sustainable and productive agriculture', *Annals  
959 of Botany*, 105: 1141-57.
- 960 Masclaux-Daubresse, Céline, Michele Reisdorf-Cren, Karine Pageau, Maud Lelandais, Olivier  
961 Grandjean, Joceline Kronenberger, Marie-Hélène Valadier, Magali Feraud, Tiphaine  
962 Jouglet, and Akira Suzuki. 2006. 'Glutamine synthetase-glutamate synthase pathway  
963 and glutamate dehydrogenase play distinct roles in the sink-source nitrogen cycle in  
964 tobacco', *Plant Physiology*, 140: 444-56.
- 965 Masle, J. 2000. 'The effects of elevated CO<sub>2</sub> concentrations on cell division rates, growth  
966 patterns, and blade anatomy in young wheat plants are modulated by factors related to  
967 leaf position, vernalization, and genotype', *Plant Physiology*, 122.
- 968 McQueen-Mason, SJ, and F Rochange. 1999. 'Expansins in plant growth and development: an  
969 update on an emerging topic', *Plant biology*, 1: 19-25.
- 970 Murchie, Erik H, and Tracy Lawson. 2013. 'Chlorophyll fluorescence analysis: a guide to good  
971 practice and understanding some new applications', *Journal of Experimental Botany*,  
972 64: 3983-98.
- 973 Nikolau, Basil J, and Daniel F Klessig. 1987. 'Coordinate, organ-specific and developmental  
974 regulation of ribulose 1, 5-bisphosphate carboxylase gene expression in *Amaranthus  
975 hypochondriacus*', *Plant Physiology*, 85: 167-73.

- 976 Pageau, Karine, Michèle Reisdorf-Cren, Jean-François Morot-Gaudry, and Céline Masclaux-  
977 Daubresse. 2005. 'The two senescence-related markers, GS1 (cytosolic glutamine  
978 synthetase) and GDH (glutamate dehydrogenase), involved in nitrogen mobilization,  
979 are differentially regulated during pathogen attack and by stress hormones and reactive  
980 oxygen species in *Nicotiana tabacum* L. leaves', *Journal of Experimental Botany*, 57:  
981 547-57.
- 982 Paul, Matthew J, and Christine H Foyer. 2001. 'Sink regulation of photosynthesis', *Journal of*  
983 *Experimental Botany*, 52: 1383-400.
- 984 Paul, Matthew J, and Till K Pellny. 2003. 'Carbon metabolite feedback regulation of leaf  
985 photosynthesis and development', *Journal of Experimental Botany*, 54: 539-47.
- 986 Pessarakli, Mohammad. 1996. *Handbook of photosynthesis* (CRC Press).
- 987 Pfaffl, Michael W. 2001. 'A new mathematical model for relative quantification in real-time  
988 RT-PCR', *Nucleic acids research*, 29: e45-e45.
- 989 Ranasinghe, S., and G. Taylor. 1996. 'Mechanism for increased leaf growth in elevated CO<sub>2</sub>',  
990 *Journal of Experimental Botany*, 47: 349-58.
- 991 Rasineni, Girish Kumar, Anirban Guha, and Attipalli Ramachandra Reddy. 2011. 'Elevated  
992 atmospheric CO<sub>2</sub> mitigated photoinhibition in a tropical tree species, *Gmelina arborea*',  
993 *Journal of Photochemistry and Photobiology B: Biology*, 103: 159-65.
- 994 Reinhardt, Didier, Franz Wittwer, Therese Mandel, and Cris Kuhlemeier. 1998. 'Localized  
995 upregulation of a new expansin gene predicts the site of leaf formation in the tomato  
996 meristem', *The Plant Cell*, 10: 1427-37.
- 997 Rosa, Mariana, Carolina Prado, Griselda Podazza, Roque Interdonato, Juan A González, Mirna  
998 Hilal, and Fernando E Prado. 2009. 'Soluble sugars: Metabolism, sensing and abiotic  
999 stress: A complex network in the life of plants', *Plant signaling & behavior*, 4: 388-93.
- 1000 Ruijter, JM, C Ramakers, WMH Hoogaars, Y Karlen, O Bakker, MJB Van den Hoff, and AFM  
1001 Moorman. 2009. 'Amplification efficiency: linking baseline and bias in the analysis of  
1002 quantitative PCR data', *Nucleic acids research*, 37: e45-e45.
- 1003 Sasaki, Yukiko, Yosuke Nakamura, and Ryuichi Matsuno. 1987. 'Regulation of gene  
1004 expression of ribulose biphosphate carboxylase in greening pea leaves', *Plant*  
1005 *molecular biology*, 8: 375-82.
- 1006 Sauer, Norbert. 2007. 'Molecular physiology of higher plant sucrose transporters', *FEBS letters*,  
1007 581: 2309-17.
- 1008 Schmittgen, Thomas D, and Kenneth J Livak. 2008. 'Analyzing real-time PCR data by the  
1009 comparative C T method', *Nature protocols*, 3: 1101.
- 1010 Sekhar, Kalva Madhana, Rachapudi Venkata Sreeharsha, and Attipalli Ramachandra Reddy.  
1011 2015. 'Differential responses in photosynthesis, growth and biomass yields in two  
1012 mulberry genotypes grown under elevated CO<sub>2</sub> atmosphere', *Journal of Photochemistry*  
1013 *and Photobiology B: Biology*, 151: 172-79.
- 1014 Seneweera, Saman P, and Jann P Conroy. 2005. 'Enhanced leaf elongation rates of wheat at  
1015 elevated CO<sub>2</sub>: is it related to carbon and nitrogen dynamics within the growing leaf  
1016 blade?', *Environmental and experimental botany*, 54: 174-81.
- 1017 Seneweera, SP, Oula Ghannoum, Jann Conroy, Ken Ishimaru, Masumi Okada, Mark  
1018 Lieffering, Han Yong Kim, and Kazuhiko Kobayashi. 2002. 'Changes in source-sink  
1019 relations during development influence photosynthetic acclimation of rice to free air  
1020 CO<sub>2</sub> enrichment (FACE)', *Functional Plant Biology*, 29: 947-55.
- 1021 Shin, Jun-Hye, Dong-Hoon Jeong, Min Chul Park, and Gynheung An. 2005. 'Characterization  
1022 and Transcriptional Expression of the  $\alpha$ -Expansin Gene Family in Rice', *Molecules &*  
1023 *Cells (Springer Science & Business Media BV)*, 20.

- 1024 Smeekens, Sjef, Jingkun Ma, Johannes Hanson, and Filip Rolland. 2010. 'Sugar signals and  
1025 molecular networks controlling plant growth', *Current opinion in plant biology*, 13:  
1026 273-78.
- 1027 Stitt, Mark, John Lunn, and Björn Usadel. 2010. 'Arabidopsis and primary photosynthetic  
1028 metabolism—more than the icing on the cake', *The Plant Journal*, 61: 1067-91.
- 1029 Sturm, Arnd, and Guo-Qing Tang. 1999. 'The sucrose-cleaving enzymes of plants are crucial  
1030 for development, growth and carbon partitioning', *Trends in plant science*, 4: 401-07.
- 1031 Suzuki, Akira, and David B Knaff. 2005. 'Glutamate synthase: structural, mechanistic and  
1032 regulatory properties, and role in the amino acid metabolism', *Photosynthesis research*,  
1033 83: 191-217.
- 1034 Suzuki, Y, A Makino, and T Mae. 2001. 'Changes in the turnover of Rubisco and levels of  
1035 mRNAs of rbcL and rbcS in rice leaves from emergence to senescence', *Plant, Cell &  
1036 Environment*, 24: 1353-60.
- 1037 Suzuki, Yuji, TOMONORI KIHARA-DOI, Tetsu Kawazu, Chikahiro Miyake, and Amane  
1038 Makino. 2010. 'Differences in Rubisco content and its synthesis in leaves at different  
1039 positions in Eucalyptus globulus seedlings', *Plant, Cell & Environment*, 33: 1314-23.
- 1040 Suzuki, Yuji, Takeaki Miyamoto, Ryuichi Yoshizawa, Tadahiko Mae, and Amane Makino.  
1041 2009. 'Rubisco content and photosynthesis of leaves at different positions in transgenic  
1042 rice with an overexpression of RBCS', *Plant, Cell & Environment*, 32: 417-27.
- 1043 Tabuchi, Mayumi, Tomomi Abiko, and Tomoyuki Yamaya. 2007. 'Assimilation of ammonium  
1044 ions and reutilization of nitrogen in rice (*Oryza sativa* L.)', *Journal of Experimental  
1045 Botany*, 58: 2319-27.
- 1046 Tans, Pieter, and Ralph Keeling. 2018. 'Trends in atmospheric carbon dioxide', NOAA/ESRL  
1047 ([www.esrl.noaa.gov/gmd/ccgg/trends/](http://www.esrl.noaa.gov/gmd/ccgg/trends/)) Accessed 4th February.
- 1048 Tausz, Michael, Sabine Tausz-Posch, Robert M Norton, Glenn J Fitzgerald, Marc E Nicolas,  
1049 and Saman Seneweera. 2013. 'Understanding crop physiology to select breeding targets  
1050 and improve crop management under increasing atmospheric CO<sub>2</sub> concentrations',  
1051 *Environmental and experimental botany*, 88: 71-80.
- 1052 Taylor, Gail, Sananthanie Ranasinghe, Creana Bosac, S.D.L. Gardner, and Rachel Ferris. 1994.  
1053 'Elevated CO<sub>2</sub> and plant growth: cellular mechanisms and responses of whole plants',  
1054 *Journal of Experimental Botany*, 45: 1761-74.
- 1055 Thilakarathne, Chamindathee L, Sabine Tausz-Posch, Karen Cane, Robert M Norton, Glenn J  
1056 Fitzgerald, Michael Tausz, and Saman Seneweera. 2015. 'Intraspecific variation in leaf  
1057 growth of wheat (*Triticum aestivum*) under Australian Grain Free Air CO<sub>2</sub> Enrichment  
1058 (AGFACE): is it regulated through carbon and/or nitrogen supply?', *Functional Plant  
1059 Biology*, 42: 299-308.
- 1060 Thilakarathne, Chamindathee L, Sabine Tausz-Posch, Karen Cane, Robert M Norton, Michael  
1061 Tausz, and Saman Seneweera. 2013. 'Intraspecific variation in growth and yield  
1062 response to elevated CO<sub>2</sub> in wheat depends on the differences of leaf mass per unit  
1063 area', *Functional Plant Biology*, 40: 185-94.
- 1064 Thompson, Michael, Dananjali Gamage, Naoki Hirotsu, Anke Martin, and Saman Seneweera.  
1065 2017. 'Effects of Elevated Carbon Dioxide on Photosynthesis and Carbon Partitioning:  
1066 A Perspective on Root Sugar Sensing and Hormonal Crosstalk', *Frontiers in  
1067 Physiology*, 8: 578.
- 1068 Verbančić, Jana, John Edward Lunn, Mark Stitt, and Staffan Persson. 2017. 'Carbon supply  
1069 and the regulation of cell wall synthesis', *Molecular plant*.
- 1070 Vicente, Rubén, Pilar Pérez, Rafael Martínez-Carrasco, Björn Usadel, Svetla Kostadinova, and  
1071 Rosa Morcuende. 2015. 'Quantitative RT-PCR Platform to Measure Transcript Levels  
1072 of C and N Metabolism-Related Genes in Durum Wheat: Transcript Profiles in Elevated

1073 [CO<sub>2</sub>] and High Temperature at Different Levels of N Supply', *Plant and Cell*  
1074 *Physiology*, 56: 1556-73.

1075 White, Angela C, Alistair Rogers, Mark Rees, and Colin P Osborne. 2015. 'How can we make  
1076 plants grow faster? A source–sink perspective on growth rate', *Journal of Experimental*  
1077 *Botany*, 67: 31-45.

1078 Wu, Yajun, Robert B Meeley, and Daniel J Cosgrove. 2001. 'Analysis and expression of the  $\alpha$ -  
1079 expansin and  $\beta$ -expansin gene families in maize', *Plant Physiology*, 126: 222-32.

1080 Xing, S-C, F Li, Q-F Guo, D-R Liu, X-X Zhao, and W Wang. 2009. 'The involvement of an  
1081 expansin gene TaEXPB23 from wheat in regulating plant cell growth', *Biologia*  
1082 *plantarum*, 53: 429.

1083 Yamaya, Tomoyuki, Toshihiko Hayakawa, Keisuke Tanasawa, Kazunari Kamachi, Tadahiko  
1084 Mae, and Kunihiro Ojima. 1992. 'Tissue distribution of glutamate synthase and  
1085 glutamine synthetase in rice leaves: occurrence of NADH-dependent glutamate  
1086 synthase protein and activity in the unexpanded, nongreen leaf blades', *Plant*  
1087 *Physiology*, 100: 1427-32.

1088 Yang, Jennifer T, Alyssa L Preiser, Ziru Li, Sean E Weise, and Thomas D Sharkey. 2016.  
1089 'Triose phosphate use limitation of photosynthesis: short-term and long-term effects',  
1090 *Planta*, 243: 687-98.

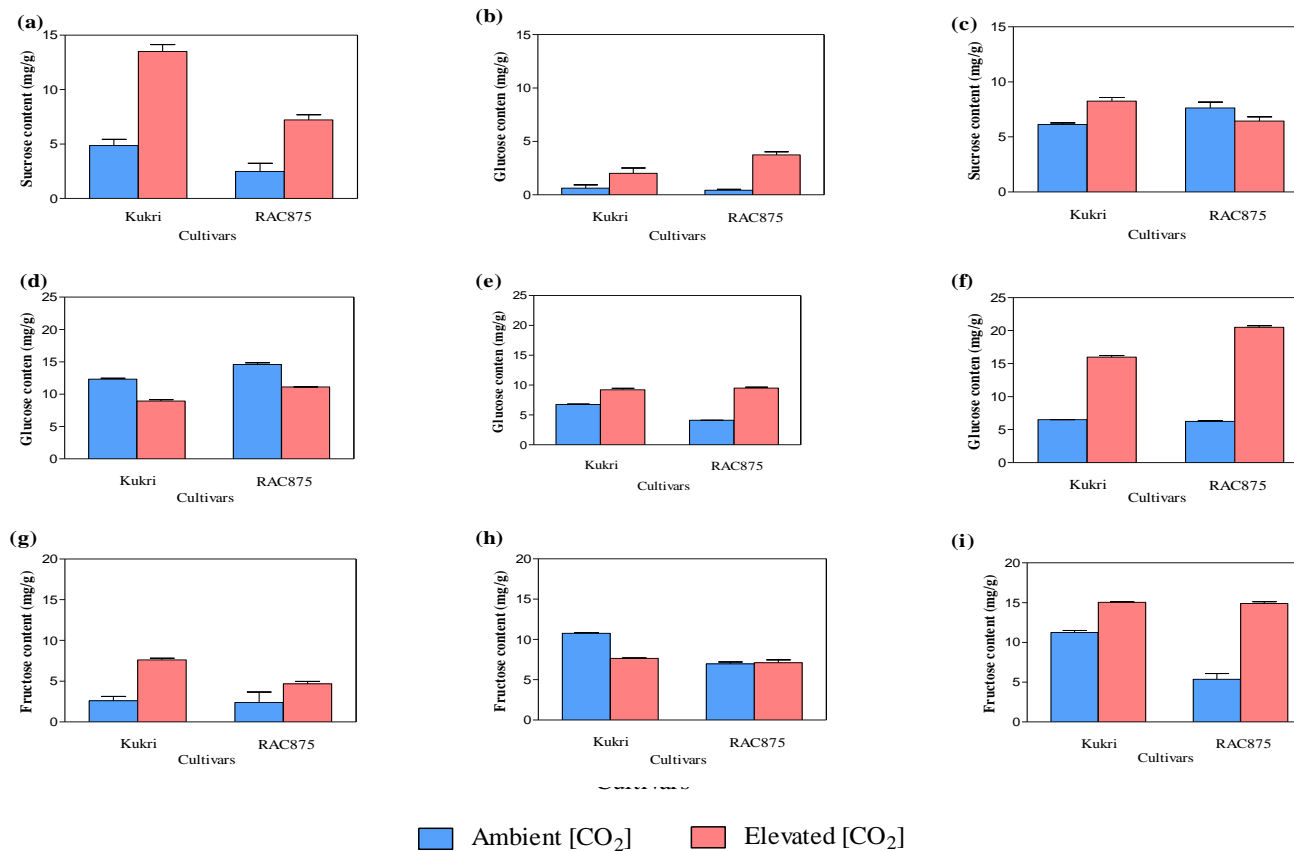
1091 Yokoyama, R, and K Nishitani. 2000. 'Functional diversity of xyloglucan-related proteins and  
1092 its implications in the cell wall dynamics in plants', *Plant biology*, 2: 598-604.

1093 Yonekura, Madoka, Naohiro Aoki, Tatsuro Hirose, Kiyoshi Onai, Masahiro Ishiura, Masaki  
1094 Okamura, Ryu Ohsugi, and Chikara Ohto. 2013. 'The promoter activities of sucrose  
1095 phosphate synthase genes in rice, OsSPS1 and OsSPS11, are controlled by light and  
1096 circadian clock, but not by sucrose', *Frontiers in plant science*, 4: 31.

1097 Zheng, Zhi-Liang. 2009. 'Carbon and nitrogen nutrient balance signaling in plants', *Plant*  
1098 *signaling & behavior*, 4: 584-91.

1099  
1100

## Supplementary Data



**Supplementary Figure S1.** The effect of [CO<sub>2</sub>] on sucrose content of (a) last fully expanded leaf blade (LFELB), (b) expanding leaf blade (ELB) and (c) cell elongation region (CER); glucose content of (d) LFELB, (e) ELB, (f) CER; fructose content of (g) LFELB, (h) ELB, (i) CER of Kukri and RAC875 grown at ambient (400 μmol mol<sup>-1</sup>) or elevated (700±10 μmol mol<sup>-1</sup>) [CO<sub>2</sub>]. Measurements were taken at 42 DAP. Summary of the ANOVA results is shown. Data presented are the mean from 3 replicates. Abbreviations: ns, not significant; \*, P<0.05; \*\*, P<0.01.

**Supplementary Table S1.** CO<sub>2</sub> responsiveness of the selected wheat lines of the double haploid mapping population in the previous experimental trials.

	<b>Reference name</b>	<b>Double haploid ID</b>	<b>CO<sub>2</sub> responsiveness of aboveground biomass accumulation</b>	<b>CO<sub>2</sub> responsiveness of below ground biomass accumulation</b>
High responsive wheat lines	H <sub>1</sub>	DH_R241	260.53%	305.94%
	H <sub>2</sub>	DH_R281	281.58%	335.77%
	H <sub>3</sub>	DH_R181	364.09%	284.60%
	H <sub>4</sub>	DH_R186	281.98%	352.34%
Less responsive wheat lines	L <sub>1</sub>	DH_R092	55.87%	55.19%
	L <sub>2</sub>	DH_R009	40.86%	41.26%
	L <sub>3</sub>	DH_R215	30.39%	-4.73%
	L <sub>4</sub>	DH_R220	52.75%	51.67%

**Supplementary Table S2.** Controlled environmental conditions provided to the Reach-in plant growth chambers throughout the experimental period.

Time Period	Temperature	Relative humidity	[CO <sub>2</sub> ] concentration		Light intensity
			Ambient [CO <sub>2</sub> ]	Elevated [CO <sub>2</sub> ]	
06:00 hrs	15°C	70%	400 $\mu\text{molmol}^{-1}$	700 $\mu\text{molmol}^{-1}$	Partial (40%)
08:00 hrs	20°C	70%	400 $\mu\text{molmol}^{-1}$	700 $\mu\text{molmol}^{-1}$	Partial (40%)
11:00 hrs	23°C	70%	400 $\mu\text{molmol}^{-1}$	700 $\mu\text{molmol}^{-1}$	Partial (40%)
15:00 hrs	20°C	70%	400 $\mu\text{molmol}^{-1}$	700 $\mu\text{molmol}^{-1}$	Partial (40%)
18:00 hrs	15°C	70%	400 $\mu\text{molmol}^{-1}$	700 $\mu\text{molmol}^{-1}$	Partial (40%)
20:00 hrs	13°C	70%	400 $\mu\text{molmol}^{-1}$	700 $\mu\text{molmol}^{-1}$	Partial (40%)

**Supplementary Table S3.** List of primer sequences of selected genes for the RT-PCR analysis.

Metabolism	Accession No.	Gene abbreviation	Forward primer sequence (5'-3' sequence)	Reverse primer sequence (5'-3' sequence)	Reference
Photosynthesis	AY328025	<i>rbcL</i>	GGCTGCAGTAGCTGCCGAATCT	TCCCCAGCAACAGGCTCGATGT	<i>Vicente et al, 2015</i>
	AB020957	<i>rbcS</i>	AGCCTCAGCAGCGTCAGCAAT	CGTGGATAGGGGTGGCAGGTAAGA	
Carbon metabolism	AF321556	<i>SPP1</i>	GCGCACGGGAAGGAGTTTTCTTCT	GACCTCCGTAGACATCATCCAGCCC	<i>Vicente et al, 2015</i>
	AF310160	<i>SPS1</i>	AGAAGGCTCTGCCTCCCATTTGGTC	AGGATCATCGGCTTGTGCGGGTT	
	AF321556	<i>SUS1</i>	GTATGTTCAACAGGGCAAGGGCA	GGCGTCAAACCTCAGCAAGCAGC	
Nitrogen metabolism	FJ527909	<i>NiR</i>	AACCTCCTCTCCTCTACATCA	CCTAGGAAGGTTGGTGATGGC	<i>Vicente et al, 2015</i>
	TC394038	<i>Fd-GOGAT</i>	CGGCAATGGAGGCTGAGCAACA	TGAGCCTGCTCGATGGTCACTGT	
	DQ124212	<i>GS2a</i>	CTCATGGTGTGTTGCGAACC	GGTCCTCCAGGTATCCTTTGC	
	DQ124213	<i>GS2b</i>	TGAAGGAAACGAGCGGAGAC	CTCGCCCCACACGAATAGAG	
	TC387834	<i>NADH-GOGAT</i>	GCCATTGAATCAGTTCAGGGCCAC	GCCAGCACCTGAGCTTTCCTGATG	
	DQ124209	<i>GS1a</i>	AGGTCATCGTGGATGCCGTGGA	TTTGCGACGCCCCAGCTGAA	
	AY491968	<i>GSr1</i>	AAGGGCTACTTCGAGGACCGCA	ATGATCTGGCGGCGGTAGGCAT	<i>Liu et al, 2007</i>
Cell wall metabolism	AY589583	<i>TaEXPA1</i>	CCACCAACAAGCAGTTCCTTAATT	CATACATCCCCACAAAAAAGGAC	<i>Yang Han et al 2012</i>
	AY692477	<i>TaEXPA3</i>	GTCTGTGTTGGTGTGTTTTTCCC	AACCATCACCTCTTACCCTAATCA	
	AY589578	<i>TaEXPB1</i>	TACAGATCCCTGGTCCAGTTTCG	CATCATAGGTAGAACAAGACGACGA	
	AY589579	<i>TaEXPB2</i>	CTCCATCGTCCAGTACAGCTGA	CATGATTCCAAATGATGAGTTTCG	
	AY589580	<i>TaEXPB3</i>	CTGCTGGCTACGATTAATTGCTC	CCCACGCAAATACAAAAGATAAA	
	AY692478	<i>TaEXPB6</i>	TGCCTTATGTAGCAGGGTGAGAC	GTACACGATGGACGACGACACTA	
	AY260547	<i>TaEXPB23</i>	CATGCGCATCACCAACGAGT	TGGACGATGGAGCGGTAGAAG	
	AY589585	<i>TaXTH1</i>	CGAGAGCAAGTACATGTCCTACGA	GAAAGGAAGAACTGATGGACGAT	
	AY589586	<i>TaXTH2</i>	ATCCAGCGTCAATTCCTTCCTT	TCGAATCGAATGGACAAACAAG	
	AY589586	<i>TaXTH3</i>	CGAGAGCAAGTACATGTCCTACGA	AAGAAAGGAAGAATTTGATGATGGA	
AY589586	<i>TaXTH4</i>	TCATTGATTAATTTCTTCCGTTGCT	AAGATGGGATGAACAAGAAGAACA		
AY589586	<i>TaXTH5</i>	CCGTCATCTGAGATGTGTTTTGTT	CATTACACCATCCGACAGAGCT		

Reference genes	<i>ADP-ribosylation factor</i>	<i>GCTCTCCAACAACATTGCCAAC</i>	<i>GCTTCTGCCTGTACATACGC</i>	<i>Vicente et al, 2015</i>
	<i>α-Tubulin</i>	<i>TTCATGTACCGTGGTGATGTTG</i>	<i>AACTGAATAGTGCGCTTGGTCTT</i>	<i>Liu et al, 2007</i>

**Supplementary Table S4.** The effect of [CO<sub>2</sub>] on growth-related traits, photosynthetic parameters and chlorophyll fluorescence parameters of Kukri and RAC875 grown at ambient [CO<sub>2</sub>] (a[CO<sub>2</sub>], 400 μmol mol<sup>-1</sup>) or elevated [CO<sub>2</sub>] (e[CO<sub>2</sub>], 700±10 μmol mol<sup>-1</sup>). Measurements were taken at 42 DAP. Summary of the ANOVA results is shown. Data presented are the mean from n=3 and 6 replicates. Abbreviations: ns, not significant; \*, P<0.05; \*\*, P<0.01.

Trait	Mean CO <sub>2</sub> effect			Mean cultivar effect			Interaction effect
	a[CO <sub>2</sub> ]	e[CO <sub>2</sub> ]	ANOVA result	Kukri	RAC875	ANOVA result	[CO <sub>2</sub> ]x Cultivar
<b>Growth-related traits</b>							
Above ground biomass (mg/plant)	242.96	353.70	**	278.8	317.86	ns	**
Total soluble sugar content (mg/g)	56.38	86.38	**	74.68	68.09	**	**
Total leaf area (cm <sup>2</sup> /plant)	39.08	48.49	**	35.48	52.09	**	ns
<b>Photosynthesis parameters</b>							
Photosynthesis rate (μmol CO <sub>2</sub> m <sup>-2</sup> s <sup>-1</sup> )	14.15	20.85	**	15.61	19.38	**	*
g <sub>s</sub> (mol H <sub>2</sub> O m <sup>-2</sup> s <sup>-1</sup> )	0.31	0.22	ns	0.26	0.27	ns	*
C <sub>i</sub> (μmol CO <sub>2</sub> mol <sup>-1</sup> )	295.50	524.33	**	411.33	408.5	ns	ns
Transpiration rate (mmol H <sub>2</sub> O m <sup>-2</sup> s <sup>-1</sup> )	4.46	3.75	ns	3.89	4.33	ns	*
<b>Chlorophyll fluorescence parameters</b>							

PSII operating efficiency ( $\phi$ PSII)	0.28	0.34	**	0.27	0.34	**	ns
Electron transport rate (ETR)	122.27	152.72	**	122.70	152.29	**	ns
Photo-chemical quenching (qP)	0.49	0.61	**	0.50	0.60	**	ns
Non-photochemical quenching (NPQ)	2.34	2.28	ns	2.25	2.37	ns	ns
Maximum PSII efficiency ( $F_v/F_m$ )	0.56	0.56	ns	0.55	0.57	ns	ns

**Supplementary Table S5.** Summary of the Analysis of Variance (ANOVA) results for the effect of [CO<sub>2</sub>] on different genes tested for two parental lines, Kukri and RAC875 grown at ambient (400 μmol mol<sup>-1</sup>) or elevated (700±10 μmol mol<sup>-1</sup>) [CO<sub>2</sub>]. Abbreviations: ns, not significant; \*, P<0.05; \*\*, P<0.01.

Metabolism	Name of the gene	Cultivar effect	[CO <sub>2</sub> ] effect	Organ effect	Cultivar x [CO <sub>2</sub> ]	Cultivar x [CO <sub>2</sub> ] x Organ
<b>Photosynthesis</b>	<i>rbcL</i>	ns	**	**	ns	ns
	<i>rbcS</i>	**	**	**	ns	**
<b>Carbon metabolism</b>	<i>SPP1</i>	ns	**	**	ns	ns
	<i>SPS1</i>	**	**	**	ns	ns
	<i>SUS1</i>	ns	**	**	ns	ns
<b>Nitrogen metabolism</b>	<i>NiR</i>	*	**	*	ns	ns
	<i>Fd-GOGAT</i>	*	**	*	ns	ns
	<i>GS2a</i>	ns	**	*	*	**
	<i>GS2b</i>	*	**	*	ns	ns
	<i>NADH-GOGAT</i>	*	**	ns	ns	ns
	<i>GS1a</i>	*	**	*	*	**
	<i>GSr1</i>	ns	**	ns	ns	ns
<b>Cell wall metabolism</b>	<i>TaEXPA1</i>	ns	ns	ns	ns	ns
	<i>TaEXPA3</i>	*	**	**	ns	ns
	<i>TaEXPB1</i>	ns	ns	**	*	*
	<i>TaEXPB2</i>	ns	**	ns	ns	ns
	<i>TaEXPB3</i>	*	**	ns	ns	ns
	<i>TaEXPB6</i>	*	**	**	ns	ns
	<i>TaEXPB23</i>	*	**	**	ns	ns
	<i>TaXTH1</i>	*	**	**	ns	ns
	<i>TaXTH2</i>	*	**	**	*	ns
	<i>TaXTH3</i>	*	**	**	*	
	<i>TaXTH4</i>	ns	ns	**	ns	*
	<i>TaXTH5</i>	*	**	**	ns	*

**Supplementary Table S6.** Coefficients of correlation ( $r$ ) between the response of sugar content and gene expression to elevated [CO<sub>2</sub>]. Data used were the relative change of sugar content between ambient and elevated [CO<sub>2</sub>] and the relative expression for each gene under elevated [CO<sub>2</sub>]. Measurements were collected from Kukri and RAC875 42 DAP. Significant data are indicated in bold; \*,  $P < 0.05$ ; \*\*,  $P < 0.01$ .

	<i>SPPI</i>							<i>TaXTH</i>				
	<i>TaEXP</i>	<i>1</i>	<i>2</i>	<i>3</i>	<i>4</i>	<i>5</i>						
	<i>A1</i>	<i>B1</i>	<i>B2</i>	<i>B3</i>	<i>B6</i>	<i>B23</i>						
<b>Sucrose</b>	-0.354	0.994*	0.701	-0.444	-0.55	0.90	-0.74*	0.72	0.142	0.156	-0.043	0.044
<b>Glucose</b>	-1.38	0.994*	0.701	-0.444	-0.55	0.625	-0.307	0.606	0.578	0.512	-0.207	0.816*
<b>Fructose</b>	0.783*	0.994*	0.701	-0.444	-0.55	-0.382	0.571	-0.45	-0.71	0.243	0.186	-0.472
<b>Total sugar</b>	0.093	0.994*	0.701	-0.444	-0.55	-0.45	0.553	0.553	0.500	0.740*	-0.109	0.420

## Chapter 5

### Leaf proteome responses of wheat (*Triticum aestivum* L.) to elevated atmospheric carbon dioxide during early vegetative growth

In this study, a comparative proteomics analysis was performed to identify differentially expressed proteins under elevated [CO<sub>2</sub>]. This chapter aims to provide information on the most active metabolic proteins, regulatory enzymes and other biomolecules involved in key metabolic processes and thus, will be beneficial in dissecting the growth mechanism of plants in a high CO<sub>2</sub> environment. The experiments in this chapter were conducted with the parental lines of the doubled haploid mapping population used in the previous chapters. Comparative proteomics analysis was conducted for the expanding leaf blades of young wheat seedlings to develop an understanding of which metabolic processes are more active in the growing tissues when exposed to elevated [CO<sub>2</sub>]. Protein expression at elevated [CO<sub>2</sub>] was compared with protein expression at ambient [CO<sub>2</sub>] to determine the effect of elevated [CO<sub>2</sub>] on the regulation of protein levels. Proteins of key metabolic processes that showed significant change at elevated [CO<sub>2</sub>] are reported in this chapter. This chapter has been prepared as a research article to be submitted to “Journal of Experimental Botany”.

**Gamage D**, Thompson M, Dehigaspitiya P, Faou P, Rajapaksha KH, Downs R, Sutherland M.W., Hirotsu N, Seneweera S, Leaf proteome responses of wheat (*Triticum aestivum* L.) to elevated atmospheric carbon dioxide during early vegetative growth (Prepared for publication)

1 **Article title:**

2 Leaf proteome responses of wheat (*Triticum aestivum* L.) to elevated atmospheric carbon  
3 dioxide during early growth

4 **Running title:** Leaf proteome responses to elevated [CO<sub>2</sub>]

5 **Authors:**

6 Dananjali Gamage<sup>1&4</sup>, Michael Thompson<sup>1</sup>, Prabuddha Dehigaspitiya<sup>1</sup>, Pierre Faou<sup>2</sup>, Kolin  
7 Harinda Rajapaksha<sup>2</sup>, Rachael Downs<sup>2</sup> Mark W. Sutherland<sup>1</sup>, Naoki Hirotsu<sup>1&3</sup>, Saman  
8 Seneweera<sup>1,4&5\*</sup>

9 **Author affiliations:**

10 <sup>1</sup>Centre for Crop Health, University of Southern Queensland, Toowoomba, QLD 4350,  
11 Australia.

12 <sup>2</sup>Department of Biochemistry and Genetics, La Trobe Institute for Molecular Life Science, La  
13 Trobe University, Bundoora, Australia

14 <sup>3</sup>Graduate School of Life Sciences, Toyo University, 1-1-1 Izumino, Itakura, Gunma 374-  
15 0193, Japan.

16 <sup>4</sup>Department of Agricultural Biology, Faculty of Agriculture, University of Ruhuna,  
17 Kamburupitiya 81 100, Sri Lanka.

18 <sup>5</sup> National Institute of Fundamental Studies, Hantana Road, Kandy 20000, Sri Lanka

19

20 **\*Corresponding author:**

21 Saman Seneweera,

22 E-mail - [Saman.Seneweera@usq.edu.au](mailto:Saman.Seneweera@usq.edu.au), Tel: +61746315525

23 **Abbreviations:**

24 [CO<sub>2</sub>] – Carbon dioxide concentration

25 Rubisco - Ribulose 1,5-bisphosphate carboxylase/oxygenase

26 LFELB - Last fully expanded leaf blade

27 ELB - Expanding leaf blade

28 CE – cell elongation region

29 **Highlight:**

30 Elevated [CO<sub>2</sub>] alters protein expression related to synthesis and respiratory breakdown of  
31 carbohydrates, protein synthesis, cell division and cell elongation and thereby influence plant  
32 growth at early vegetative stages.

33

34 **Abstract**

35 The impact of rising atmospheric carbon dioxide [CO<sub>2</sub>] on the proteome of the growing leaf  
36 blade was investigated using two winter wheat cultivars: Kukri and RAC875, focusing on the  
37 early vegetative stage. Two wheat genotypes were grown at ambient (400 μmol mol<sup>-1</sup>) and  
38 elevated (700 μmol mol<sup>-1</sup>) [CO<sub>2</sub>] in controlled environmental conditions. Elevated [CO<sub>2</sub>]  
39 increased the rate of photosynthesis and biomass production in Kukri by 16.4 and 32.6%,  
40 respectively, when compared with 20 and 48% in RAC875. The nitrogen and protein  
41 concentrations in the expanding leaf blades of both cultivars were high; however, RAC875  
42 showed the highest nitrogen percentage (56.3%). Results of the comparative proteomics  
43 analysis showed that leaf proteome responses at elevated [CO<sub>2</sub>] were genotype dependent and  
44 the proteome composition was altered at elevated [CO<sub>2</sub>]. Most of the differentially expressed  
45 proteins at elevated [CO<sub>2</sub>] belonged to carbon metabolism, energy pathways, protein synthesis  
46 and cell cycle functions. Additionally, several proteolytic enzymes involved in post-  
47 translational modifications of proteins, antioxidant enzymes and molecular chaperones showed  
48 a noteworthy upregulation at elevated [CO<sub>2</sub>] in both cultivars. These findings suggest that  
49 photosynthetic stimulation and lower stomatal conductance are not the only factors governing  
50 plant growth at elevated [CO<sub>2</sub>]. In response to increased sugar supply to developing leaves at  
51 elevated [CO<sub>2</sub>], other key regulatory processes such as cell cycle function, protein and cell  
52 redox homeostasis tend to be modified, significantly altering growth responses at the whole  
53 plant level.

54 **Keywords:** Carbon metabolism, Expanding leaf blade, Leaf proteome, Plant growth, Protein

## 55 **Introduction**

56 The rapid increase in industrialization and population growth has led to significant increases in  
57 carbon dioxide concentrations ( $[\text{CO}_2]$ ) in the atmosphere. The current atmospheric  $[\text{CO}_2]$  has  
58 already exceeded  $400 \mu\text{mol mol}^{-1}$  ([Tans and Keeling, 2018](#)) and is predicted to double by the  
59 end of this century ([IPCC, 2014](#)). As one of the prominent greenhouse gases, this increase in  
60  $[\text{CO}_2]$  leads to changes in the global climate, causing significant changes in temperature and  
61 precipitation patterns and subsequently influencing agricultural productivity ([Ainsworth et al.,](#)  
62 [2008](#); [Solomon et al., 2007](#)). On the other hand, increasing  $[\text{CO}_2]$  is beneficial for plants as it  
63 is the primary substrate for photosynthesis. Therefore, elevated  $[\text{CO}_2]$  could potentially offset  
64 losses in agricultural production caused by increased drought and high-temperature incidences  
65 ([Ainsworth et al., 2008](#)). However, it will be highly challenging to capitalize  $\text{CO}_2$  enrichment  
66 for crop improvement because of the complex relationships among elevated  $[\text{CO}_2]$ ,  
67 photosynthesis, plant growth and yield responses ([Gamage et al., 2018](#); [Thompson et al., 2017](#)).  
68 This has led researchers to investigate the underlying physiological and molecular mechanisms  
69 of plant growth responses to elevated  $[\text{CO}_2]$  as the first step in gaining a better understanding  
70 of maximizing future crop production in a changing climate.

71 The effect of elevated  $[\text{CO}_2]$  is more pronounced in  $\text{C}_3$  crops, including critical cereal crops  
72 such as rice and wheat, stimulating their growth and yield ([Seneweera, 2011](#); [Seneweera and](#)  
73 [Conroy, 2005](#); [Thilakarathne et al., 2013](#)). Generally, plants respond to elevated  $[\text{CO}_2]$  through  
74 increased photosynthesis and reduced stomatal conductance ([Ainsworth and Rogers, 2007](#)).  
75 These two primary processes are central to all the other effects observed in plant communities  
76 in response to high  $\text{CO}_2$  conditions. The increase in photosynthesis of  $\text{C}_3$  crops is mainly due  
77 to the increased carboxylation of Ribulose 1,5- biphosphate carboxylase/oxygenase  
78 (Rubisco), which is not saturated under current  $\text{CO}_2$  partial pressure ([Lorimer, 1981](#); [Makino](#)  
79 [and Mae, 1999](#)). The higher availability of  $\text{CO}_2$  at the site of fixation also suppresses  
80 photorespiration, which facilitates Rubisco carboxylation ([Makino and Mae, 1999](#)).  
81 Theoretically, photosynthesis of a mature sunlit leaf will increase by approximately 38% at  
82 elevated  $[\text{CO}_2]$  ([Long et al., 2004](#)). Conversely, stomatal conductance of both  $\text{C}_3$  and  $\text{C}_4$  crops  
83 tend to decrease at elevated  $[\text{CO}_2]$ , which significantly reduces plant evapotranspiration and  
84 leads to improvements in plant water use efficiency ([Ainsworth and Long, 2005](#); [Leakey et al.,](#)  
85 [2009](#)).

86

87 The direct effects of elevated [CO<sub>2</sub>], mainly the stimulation of photosynthesis, provides the  
88 fundamental basis for modifications to key post-photosynthetic metabolic pathways associated  
89 with plant growth and development ([Pritchard et al., 1999](#); [Taylor et al., 1994](#)).  
90 Carbon/nitrogen metabolism, cell cycle and cell wall metabolism, along with hormonal  
91 regulation, are the main metabolic networks involved in plant growth responses at elevated  
92 [CO<sub>2</sub>] ([Gamage et al., 2018](#)). For any organism to maximize its fitness in response to different  
93 environmental conditions, precise regulation and coordination of these metabolic networks to  
94 a particular environment is necessary ([Gaudinier et al., 2015](#)). Thus, in response to  
95 environmental stimuli, such as elevated [CO<sub>2</sub>], plants tend to change their transcriptional and  
96 translational regulation, which thereby affects protein synthesis that governs plant growth and  
97 development. This protein network governing plant growth at elevated [CO<sub>2</sub>] involves a  
98 complex interplay of different regulatory enzymes, components of signal transduction  
99 mechanisms and other important biomolecules, such as plant growth regulators, which  
100 collectively function in response to external environmental stimulation ([Bokhari et al., 2007](#)).

101  
102 The CO<sub>2</sub> responsiveness of C<sub>3</sub> plants is generally higher during the early growth stages and is  
103 affected by the plants' sink capacity and nutritional status ([Li et al., 2008](#); [Makino and Mae,](#)  
104 [1999](#); [Seneweera et al., 2002](#)). In the early growth stages, plants are able to generate more sink  
105 organs to utilize the increased carbon supply at elevated [CO<sub>2</sub>] ([Jitla et al., 1997](#); [Thilakarathne](#)  
106 [et al., 2015](#)). Higher relative growth rates and higher net assimilation rates have been observed  
107 for rice ([Jitla et al., 1997](#); [Makino and Mae, 1999](#)) and wheat ([Hikosaka et al., 2005](#); [Neales](#)  
108 [and Nicholls, 1978](#)) in the early growth stages at elevated [CO<sub>2</sub>]. In general, it has been reported  
109 that even a 10% increase in the RGR of plants grown at elevated [CO<sub>2</sub>] can translate into an  
110 absolute growth increment of up to 50% during the exponential growth phase of plants  
111 ([Kirschbaum, 2010](#)). Therefore, understanding how plants respond to elevated [CO<sub>2</sub>],  
112 particularly during the early growth stages, is essential for breeding crops for a future CO<sub>2</sub> rich  
113 atmosphere.

114  
115 A number of research studies have investigated the underlying physiological (For a review:  
116 [Poorter and Nagel, 2000](#); [Poorter and Navas, 2003](#)) and molecular mechanisms ([For a review:](#)  
117 [Gamage et al., 2018](#)) of plant growth responses to elevated [CO<sub>2</sub>]. The physiological responses  
118 of crops, including wheat ([Seneweera, 2011](#); [Seneweera and Conroy, 2005](#); [Thilakarathne et](#)  
119 [al., 2015](#); [Thilakarathne et al., 2013](#)), have been extensively studied to gain an understanding  
120 of how plants adapt to the high CO<sub>2</sub> environment. Despite the importance of understanding the

121 regulatory mechanisms of plant growth response to elevated CO<sub>2</sub>, the activity of different  
122 regulatory enzymes and other proteins involved in these physiological processes have not been  
123 thoroughly investigated ([Bokhari et al., 2007](#)). Without this information, it is very difficult to  
124 develop a complete understanding of the interplay of protein networks among key metabolic  
125 pathways and how they determine plant growth responses to external environmental signals  
126 such as elevated [CO<sub>2</sub>]. Therefore, a fundamental understanding of proteome-wide responses  
127 of plants to elevated [CO<sub>2</sub>] will provide a unique opportunity to unravel the mechanisms of  
128 how plants respond to elevated [CO<sub>2</sub>] ([Hashiguchi et al., 2010](#); [Hossain et al., 2011](#)).

129

130 The array of proteins within a cell or an organ, their interactions and modifications, hold the  
131 key to understanding the responses of a particular biological system under stressed or non-  
132 stressed conditions ([Salekdeh and Komatsu, 2007](#)). With recent technological advances in  
133 proteomic science, it is relatively easy to identify proteins, expression profiles, post-  
134 translational modifications and protein-protein interactions under different environmental  
135 conditions ([Hashiguchi et al., 2010](#)). Further, proteomic analysis highly beneficial in  
136 identifying the possible candidate genes that can be used as genetic markers in breeding crops  
137 for future climate ([Ahmad et al., 2016](#)).

149

150 In this study, we investigated the proteome-wide changes in young wheat leaves (*Triticum*  
151 *aestivum* L.) in order to understand the underlying molecular mechanisms of plant growth  
152 responses to elevated [CO<sub>2</sub>]. To the best of our knowledge, there has been no published report  
153 to date using a comparative proteomic approach to study the growth responses of wheat to  
154 elevated [CO<sub>2</sub>] focusing on the early vegetative stage. Our study mainly focused on  
155 understanding the functions of sink tissues of plants at elevated [CO<sub>2</sub>] during the early growth  
156 stages. Further, the expression patterns of the differentially expressed proteins identified at both  
157 elevated and ambient [CO<sub>2</sub>], and their physiological implications, are discussed with a  
158 mechanistic perspective in this paper.

159

## 160 **Materials and methods**

161

### 162 ***Plant materials and environmental conditions***

163 A solution culture experiment was carried out using two wheat (*Triticum aestivum* L.) cultivars,  
164 Kukri and RAC875, under ambient ( $400 \mu\text{mol mol}^{-1}$ ) and elevated  $[\text{CO}_2]$  ( $700 \pm 10 \mu\text{mol mol}^{-1}$ )  
165 <sup>1</sup>) in two identical controlled environment growth chambers (Reach in growth chambers, PGC-  
166 105, Percival, USA) at the University of Southern Queensland, Australia. These two cultivars  
167 are the parental lines of a doubled haploid mapping population with contrasting water use  
168 efficiencies, nitrogen use efficiencies and growth characteristics to elevated  $[\text{CO}_2]$ . Plants were  
169 provided with a 14-hour photoperiod with a day and night temperature of  $23^\circ\text{C}$  and  $13^\circ\text{C}$ ,  
170 respectively. The relative humidity of both chambers was maintained at 70% throughout the  
171 experiment and the light intensity was maintained at  $1000 \mu\text{molm}^{-2}\text{s}^{-1}$  at midday throughout  
172 the growing period.

173

### 174 ***Seedling growth***

175 Seeds from wheat (*Triticum aestivum* L.) cultivars, Kukri and RAC875, were surface sterilized  
176 using 2.6% NaClO for 1 minute and washed thoroughly using Milli-Q water. The sterilized  
177 seeds were then allowed to germinate on moistened filter papers (Whatmann, Sigma Aldrich,  
178 USA) in Petri dishes. After four days of germination, seedlings were transferred to floating  
179 nets placed on 40L opaque basins filled with an aerated nutrient solution as described in  
180 [Fernando et al. \(2017\)](#) and grown at either ambient  $[\text{CO}_2]$  ( $400 \mu\text{mol mol}^{-1}$ ) or elevated  $[\text{CO}_2]$   
181 ( $700 \pm 10 \mu\text{mol mol}^{-1}$ ) for 42 days. Macro and micronutrients included in the solution culture  
182 were adapted from ([Makino and Osmond, 1991](#)) and [Fernando et al. \(2017\)](#) (Supplementary  
183 Table S1). The nutrient solution was replenished once a week maintaining the pH at 6-6.5.  
184 Basins were re-randomized weekly within each chamber and swapped between chambers  
185 fortnightly to minimize location and chamber effect.

186

### 187 ***Physiological trait measurements and sample collection***

188 At 42 days after planting (DAP), one set of wheat seedlings was carefully harvested to  
189 determine the total dry mass of the two cultivars from both  $\text{CO}_2$  treatments. Another set of  
190 plants was harvested and separated into last fully expanded leaf blades (LFELB) and expanding

191 leaf blade (ELB), cell elongation and shoot apex region (CE) in order to determine the carbon  
192 and nitrogen concentrations of each cultivar in two different CO<sub>2</sub> conditions.

193 To determine total dry mass, harvested plants were oven dried for 48 hours at 65°C and  
194 measurements were taken when a constant weight was reached. Samples were oven dried and  
195 ground in a ball mill (Tissue Lyser II, QIAGEN, Australia) to a fine powder of ~100 µm to  
196 determine carbon and nitrogen concentration. Finely ground samples of LFELB, ELB and CE  
197 of the two cultivars were analyzed for total carbon and nitrogen content using a CN analyzer  
198 (Leco CN628, USA).

199 Gas exchange measurements for Kukri and RAC875 were carried out at 42 DAP using a  
200 portable photosynthesis system (LI-6400XT, LI-COR, USA), as described in [Seneweera et al.](#)  
201 [\(2002\)](#). The net photosynthetic rate (P<sub>n</sub>), stomatal conductance (G<sub>s</sub>), intercellular [CO<sub>2</sub>] (C<sub>i</sub>)  
202 and rate of transpiration were measured between 10:00 to 13:00 hours for each cultivar in each  
203 CO<sub>2</sub> treatment. A red and blue light source was used to supply chamber irradiance and the light  
204 intensity was maintained at 1500 µmol quanta m<sup>-2</sup>s<sup>-1</sup>. Relative humidity was maintained  
205 between 50-70%. Measurements were taken using LFELB of each cultivar and leaves were  
206 allowed to reach a steady state photosynthesis before taking spot measurements.

207 For comparative proteomics analysis, the ELB of seedlings of each cultivar grown at both  
208 ambient (control) and elevated [CO<sub>2</sub>] (treated) was collected at the same time each day. Upon  
209 collection, samples were securely packed and immediately immersed in liquid N<sub>2</sub> and stored at  
210 -80°C for subsequent protein extraction.

211

## 212 ***Leaf protein extraction***

### 213 ***(i) Total soluble protein extraction***

214 For the extraction of total leaf protein, 300mg of the sample was ground to a fine powder using  
215 liquid N<sub>2</sub>. This leaf powder was homogenated in 500 µl of modified RIPA solubilizing buffer  
216 [10mM Tris-HCl (pH 8.0, 1mM EDTA, 0.5% sodium deoxycholate, 0.1% SDS, 140mM NaCl  
217 and 1mM PMSF]. The homogenate was then alternatively vortexed and sonicated three times  
218 and allowed to incubate at 37°C with shaking for 30 minutes. The samples were then  
219 centrifuged at 18,000g for 10 minutes and the supernatant was carefully transferred to a clean  
220 Eppendorf tube. Extracted total proteins were quantified using the microplate bicinchoninic

221 acid (BCA) protein assay kit (Thermo Fisher Scientific, USA) according to the manufacturer's  
222 instructions.

223

#### 224 (ii) *Rubisco precipitation and protein purification*

225 Since Rubisco comprises a large percentage of total proteins, it tends to hinder the detection of  
226 other important low abundance signaling and regulatory proteins ([Gupta et al., 2015](#)). As the  
227 roles and fates of most of the high abundance proteins such as Rubisco are well established to  
228 date, in this study, we attempted to focus more on identifying low abundance proteins which  
229 may play a significant role in plant growth at elevated [CO<sub>2</sub>] ([Gupta et al., 2015](#)). Therefore,  
230 to the supernatant fraction of total proteins, Protamine Sulfate (PS) solution was added to a  
231 final concentration of 0.1 %, as described in [Gupta and Kim \(2015\)](#) and [Kim et al. \(2013\)](#). This  
232 was incubated in ice for 30 minutes allowing sufficient time to precipitate Rubisco. The  
233 samples were centrifuged at 12,000g for 5 min at 4°C to pellet the precipitated Rubisco.  
234 Immediately, the supernatant was transferred to a clean Eppendorf tube and the samples were  
235 further purified using Zeba spin desalting columns to desalt the protein samples.

236

#### 237 (iii) *Protein precipitation*

238 To precipitate protein, 400 µl of methanol was added to 100 µl of a soluble protein fraction and  
239 mixed thoroughly followed by centrifuging for 10 seconds at 9000 g. Then, 100 µl of  
240 chloroform was added to 100 µl of protein samples and centrifuged for 10 s at 9000 g.  
241 Afterward, 300 µl of double-distilled H<sub>2</sub>O was added to 100 µl of sample, mixed thoroughly  
242 and again centrifuged at 9000 g for 1 minute. After this step, three clear phases were obtained:  
243 an upper H<sub>2</sub>O-methanol phase, a protein interphase and a lower chloroform phase. The upper  
244 phase was carefully removed without disturbing or touching the protein interphase. Then 300  
245 µl of methanol was added to the remaining phases, mixed thoroughly and centrifuged for 2  
246 minutes at 9000 g to pellet the proteins. The resultant supernatant was removed carefully and  
247 the protein pellet was allowed to dry until no chloroform smell was detectable. Protein pellets  
248 at room temperature were sent to Comprehensive Proteomics Platform, La Trobe Institute for  
249 Molecular Science, La Trobe University, Australia for mass spectrometry analysis.

250 ***Leaf proteome analysis***

251 Leaf proteome analysis was carried out using liquid chromatography-mass spectrometry (LC-  
252 MS/MS) as described in [Lowe et al. \(2015\)](#). Comparative proteomics analysis was carried out  
253 at Comprehensive Proteomics Platform, La Trobe Institute for Molecular Science, La Trobe  
254 University, Australia. The procedure for analysis is outlined below.

255

256 **(i) *Sample preparation - Trypsin digestion***

257 Each protein sample (50 µg) was first resuspended in 100 µl of 8 M urea (pH=8.3). The protein  
258 solution was then reduced for 5 hours with 1 µl of 200 mM tris (2-carboxyethyl) phosphine  
259 (TCEP). Samples were then alkylated for 1 hour at 25°C in the dark with 4 µl of 1 M  
260 iodoacetamide (IAA). Digestions were performed overnight (37°C) by adding 1 µg of trypsin  
261 (Promega, Madison WI, USA) and 900 µL of 50 mM Tris (pH=8.3) followed by a second  
262 digestion step with 1 µg trypsin and an additional incubation of 4 hours at 37°C.

263

264 **(ii) *Solid phase extraction clean-up of tryptic peptides***

265 The digested solution was collected and dried using SpeedVac centrifugation. Digested  
266 proteins were resuspended in 100 µl of 1% (v/v) formic acid and centrifuged at 14,000 rpm for  
267 2 minutes. The solid phase extraction was performed with Empore reversed-phase extraction  
268 disks (SDB-XC reversed-phase material, 3M) according to Ishihama et al. ([Ishihama et al.,  
269 2006](#)) with the following modifications: the membrane was conditioned with 50 µl of 80%  
270 (v/v) acetonitrile (ACN), 0.1% (w/v) trifluoroacetic acid (TFA), then washed with 50 µl of  
271 0.1% TFA before the tryptic peptides were bound to the membrane. The bound peptides were  
272 eluted by 50 µL 80% (v/v) ACN, 0.1% (w/v) TFA, and dried in a SpeedVac centrifuge.

273

274 **(iii) *LC-MS/MS analysis***

275 Peptides (2 µg) were reconstituted in a final volume of 10 µl 0.1% TFA and 2% ACN (buffer  
276 A), then loaded and washed onto a trap column (C18 PepMap 100 µm i.d. × 2 cm trapping  
277 column, Thermo-Fisher Scientific) at 5 µl/min for 6 min before switching the precolumn in  
278 line with the analytical column (Easy-Spray 75 µm i.d. × 50 cm, Thermo-Fisher Scientific).  
279 The separation of peptides was performed at 250 nl/min using a linear ACN gradient of two

280 buffers: buffer A (0.1% formic acid, 2% ACN) and buffer B (0.1% formic acid, 80% ACN),  
281 starting from 5% buffer B and increasing to 60% over 300 minutes.

282 Data were collected on an Orbitrap Elite (Thermo-Fisher Scientific) in Data-Dependent  
283 Acquisition mode using m/z 300–1500 as MS scan range. *Collision-induced dissociation* (CID)  
284 MS/MS spectra were collected for the 20 most intense ions. The dynamic exclusion parameters  
285 used were: repeat count 1, duration 90 s and the exclusion list size was set at 500 with early  
286 expiration disabled. Other instrument parameters for the Orbitrap were as follows: MS scan at  
287 120 000 resolution, maximum injection time 150 ms, automatic gain control (AGC) target  $1 \times$   
288  $10^6$ , CID at 35% energy for a maximum injection time of 150 ms with AGT target of 5000.  
289 The Orbitrap Elite was operated in dual analyzer mode with the Orbitrap analyzer being used  
290 for MS and the linear trap being used for MS/MS.

291

#### 292 (iv) *Database search and quantitation*

293 Spectra analysis was performed using the MaxQuant software (version 1.6). Proteins were  
294 identified and quantified using the Andromeda peptide search engine integrated into the  
295 MaxQuant environment using the *Triticum aestivum* proteome downloaded from the UniProt  
296 database. A total of three biological replicates were used for each of the two wheat genotypes  
297 to determine the proteome response to elevated [CO<sub>2</sub>].

298

#### 299 *Statistical analysis*

300 Treatment and interaction effects of growth and photosynthesis parameters were determined  
301 through ANOVA and standard errors of differences. Differences were considered significant  
302 at  $P < 0.05$ . All the data were analyzed using SPSS statistical software version 23 (IBM,  
303 Armonk, NY, USA). Statistical analysis for proteomics data was carried out using the statistical  
304 programming language R. All the graphical representations were carried out using GraphPad  
305 Prism scientific software version 5.01 (GraphPad Software, San Diego, CA).

## 306 **Results**

### 307 **Effect of elevated [CO<sub>2</sub>] on biomass accumulation, the rate of photosynthesis and** 308 **carbon/nitrogen concentrations of two cultivars**

309 The effects of [CO<sub>2</sub>] was significant for above ground biomass accumulation ( $P \leq 0.01$ ) and rate  
310 of photosynthesis ( $P \leq 0.01$ ) of the two wheat cultivars tested (Figure 1a & 1c). Biomass  
311 accumulation ( $P < 0.05$ ) and photosynthesis ( $P < 0.01$ ) also varied significantly between the two  
312 cultivars (Figure 1). Elevated [CO<sub>2</sub>] increased photosynthesis rate and above-ground dry mass  
313 by 16.4 and 32.6% respectively for Kukri compared with 20 and 48% for RAC875. Stomatal  
314 conductance of both varieties showed a considerable reduction at elevated [CO<sub>2</sub>] (Figure 1b).

315

316 Carbon and nitrogen analysis of LFELB, ELB and CE region of the two cultivars showed  
317 significant interactions between [CO<sub>2</sub>] and cultivar for nitrogen ( $P \leq 0.01$ , Figure 2) and protein  
318 concentration ( $P \leq 0.01$ , Figure 2). Nitrogen and protein concentrations of LFELB were greatly  
319 reduced at elevated [CO<sub>2</sub>] (Figure 2a & 2b). In contrast, nitrogen concentration of ELB  
320 significantly increased at elevated [CO<sub>2</sub>], with 30.9% and 56.3% for Kukri and RAC875,  
321 respectively (Figure 2c & 2d). In addition, the nitrogen concentration of the CE region was  
322 also significantly higher at elevated [CO<sub>2</sub>], with Kukri showing the highest response (Figure  
323 3e & 3f). The effect of [CO<sub>2</sub>] on carbon concentration was significant ( $P < 0.01$ ) and  
324 significantly varied among the organ types ( $P < 0.01$ ) of the two cultivars. At elevated [CO<sub>2</sub>],  
325 there was a reduction in the carbon concentration of the different organ types and ELB showed  
326 the highest decline in both cultivars (Supplementary Figure S2).

327

### 328 **Responses of expanding leaf proteome to elevated [CO<sub>2</sub>]**

329 Overall, 1123 and 982 proteins were identified to be differentially expressed in Kukri and  
330 RAC875, respectively, at elevated [CO<sub>2</sub>]. However, significant changes in protein expression  
331 at elevated [CO<sub>2</sub>] were only observed for 61 and 76 proteins in Kukri and RAC875,  
332 respectively. Among these proteins, many (67.2% in Kukri and 67.9% in RAC875) were  
333 classified as uncharacterized proteins, as their structure and functions are not yet confirmed.  
334 The rest of the characterized proteins belonged to different key metabolic processes, that are  
335 essential for maintaining healthy growth and development of plants (Figure 3). The major  
336 proteins that showed a statistical significance from Kukri and RAC875 are listed in Table 1  
337 and Table 2, respectively.

338 In Kukri (Table 1), three main enzymes involved in carbohydrate metabolism were  
339 differentially expressed at elevated  $[\text{CO}_2]$ , with UDP-glucose 6-hydrogenase showing a fold  
340 increase of 4.68 ( $P \leq 0.01$ ). The expression of glucose-6-phosphate isomerase and Beta-amylase  
341 enzymes were significantly reduced in the ELB of Kukri at elevated  $[\text{CO}_2]$  ( $P \leq 0.05$ ). Further,  
342 it was observed that specific proteins and enzymes related to protein synthesis, processing and  
343 transport were significantly positively changed at elevated  $[\text{CO}_2]$ . Among them, 40S ribosomal  
344 protein SA, heat shock protein 90 and clathrin heavy chain proteins were prominent at elevated  
345  $[\text{CO}_2]$  with fold increases of 4.02 ( $P \leq 0.05$ ), 8.43 ( $P \leq 0.01$ ) and 5.43 ( $P \leq 0.05$ ), respectively. In  
346 addition, proteins related to cell proliferation and differentiation, such as Tubulin alpha chain  
347 (fold increase of 5.97,  $P \leq 0.05$ ) and Tubulin beta chain (fold increase of 4.48,  $P \leq 0.05$ ), were  
348 upregulated at elevated  $[\text{CO}_2]$ . Along with these proteins, it was observed that several key  
349 proteins related to the energy generation pathway, were also upregulated. For example, ATP  
350 synthase subunit D (mitochondrial) and pyruvate kinase showed the highest fold increases of  
351 6 ( $P \leq 0.01$ ) and 3.9 ( $P \leq 0.05$ ), respectively at elevated  $[\text{CO}_2]$ .

352  
353 In RAC875 (Table 2), significant upregulation of the sucrose synthase enzyme was observed  
354 with a fold increase of 2.42 at elevated  $[\text{CO}_2]$  ( $P \leq 0.01$ ). Several proteins related to protein  
355 synthesis, such as elongation factor G (mitochondrial,  $P \leq 0.05$ ), 40S ribosomal protein S15a  
356 ( $P \leq 0.01$ ) and S12 ( $P \leq 0.05$ ), were also upregulated at elevated  $[\text{CO}_2]$ . Further, significant  
357 upregulation of several proteolysis related proteins involved in post-translational modifications  
358 of proteins were identified in RAC875. For example, ATP-dependent Clp protease proteolytic  
359 subunit (fold increase of 2.02,  $P \leq 0.01$ ) and beta-type proteasome subunit (fold increase of 2.65,  
360  $P \leq 0.05$ ) were highly expressed at elevated  $[\text{CO}_2]$ . Cell proliferation and differentiation-related  
361 proteins, such as translationally controlled tumor protein homolog (fold increase of 1.01,  
362  $P \leq 0.05$ ) and alpha-type proteasome subunit (fold increase of 2.05,  $P \leq 0.05$ ), showed higher fold  
363 increases at elevated  $[\text{CO}_2]$ . Several proteins related to photosynthesis such as oxygen-evolving  
364 enhancer protein 1 (chloroplasmic,  $P \leq 0.05$ ) and uroporphyrinogen decarboxylase ( $P \leq 0.05$ ),  
365 involved in chlorophyll synthesis, were also upregulated at elevated  $[\text{CO}_2]$ .

366  
367 In both cultivars, several anti-oxidant enzymes, such as peroxidases, catalases and superoxide  
368 dismutases (Cu-Zn), were differentially expressed at elevated  $[\text{CO}_2]$  (Table 1 and 2). Among  
369 them, cell wall peroxidases; W5ANF5 in Kukri and A0A1D6BEM4 in RAC875 showed a 2.6  
370 and 1 fold increase at elevated  $[\text{CO}_2]$ . In addition, catalase was upregulated by 4.4-fold increase  
371 in Kukri (Table 1,  $P < 0.05$ ), while all the superoxide dismutases (Cu-Zn) were down-regulated

372 at elevated [CO<sub>2</sub>] in RAC875 (Table 2, P≤0.05). In addition, some of the important proteins  
373 related to signal transduction and cell homeostasis maintenance, namely calmodulin TaCaM1-  
374 1 (Ca<sup>2+</sup> signaling) and calmodulin (P≤0.05), were upregulated in RAC875 at elevated [CO<sub>2</sub>]  
375 (Table 2).

376

### 377 **Genotypic differences in the expanding leaf blade proteome responses to elevated [CO<sub>2</sub>]**

378 There was a noteworthy difference between the protein expression in the ELB of the two  
379 cultivars both at ambient and elevated [CO<sub>2</sub>] conditions. Overall, 3359 proteins were identified  
380 as differentially expressed proteins between RAC875 and Kukri at elevated [CO<sub>2</sub>]. Out of them,  
381 only 44 proteins showed a significant difference between the two cultivars. Among them, 59%  
382 were uncharacterized proteins and other significant characterized proteins are listed in Table 3.  
383 There was a significant increase in UT-glucose-1-phosphate uridylyltransferase in RAC875  
384 compared to Kukri at elevated [CO<sub>2</sub>], with a fold increase of 4.2 (P≤0.01). Along with this,  
385 proteins related to energy generation, ATP synthase subunit D (mitochondrial) and fructose bi-  
386 phosphate aldolase, increased by 6.35 (P≤0.01) and 2.17 (P≤0.05), respectively, at elevated  
387 [CO<sub>2</sub>]. Further, tubulin alpha chain (5.34, P≤0.05), TSK1 protein (1.5, P≤0.05) and  
388 phospholipase (2.07, (P≤0.05) proteins related to cell cycle functions were also more highly  
389 expressed in RAC875 than in Kukri. Protein translation and processing related proteins were  
390 highly expressed in RAC875 with elongation factor 1-alpha and heat shock protein 90 showing  
391 the highest fold increase (7.85:P≤0.01 and 7.29;P≤0.01, respectively) when compared to Kukri.  
392 In addition, expression of proteolytic enzymes such as aminopeptidase and carboxypeptidase  
393 were also higher in RAC875 at elevated [CO<sub>2</sub>] (Table 3).

394

395 In addition, the protein expression of two cultivars also differed under ambient [CO<sub>2</sub>]. Under  
396 ambient [CO<sub>2</sub>], carbohydrate metabolism of RAC875 was comparatively higher than Kukri  
397 (Supplementary Table S2). For example, RAC875 showed a substantial increase in key  
398 enzymes involved in carbohydrate metabolism such as sucrose synthase and UTP-glucose-1-  
399 phosphate uridylyltransferase by fold increases of 2.86 (P≤0.01) and 3.28 (P≤0.01), than that  
400 of Kukri. Consistent with this, Rubisco large subunit protein expression was also higher in  
401 RAC875 than in Kukri (P≤0.01). Furthermore, proteins related to cell proliferation and  
402 differentiation such as alpha type proteasome subunit and beta-glucanase in RAC875 were 2.4  
403 (P≤0.01) and 1.5 (P≤0.05) fold higher than Kukri (Supplementary Table S2).

## 404 **Discussion**

405

### 406 **Physiological mechanisms regulating growth responses at elevated [CO<sub>2</sub>]**

407 The stimulated growth response of C<sub>3</sub> species, including wheat, to elevated [CO<sub>2</sub>] during the  
408 early developmental stages is mainly characterized by the dynamics of leaf growth. Accelerated  
409 leaf area production at elevated [CO<sub>2</sub>] results from a faster leaf elongation rate (LER) and is  
410 strongly correlated with higher relative growth rates, total biomass and final grain yield  
411 production ([Jitla \*et al.\*, 1997](#); [Seneweera and Conroy, 2005](#)). Therefore, understanding the  
412 underlying mechanisms of plant growth responses to elevated [CO<sub>2</sub>] is essential to adapt to  
413 rising atmospheric CO<sub>2</sub> concentration.

414

415 Enhanced rates of photosynthesis and lower stomatal conductance are the key strategies that  
416 support plant growth at elevated [CO<sub>2</sub>] ([Ainsworth and Rogers, 2007](#)). Improving  
417 photosynthesis rate per given leaf area has been identified as one of the main targets for  
418 improving crop productivity in the 21<sup>st</sup> century ([Parry \*et al.\*, 2010](#)). Therefore, elevated  
419 atmospheric [CO<sub>2</sub>] provides a natural way to increase the photosynthesis and thereby the crop  
420 productivity. For this task, a fundamental understanding of crop responses to elevated [CO<sub>2</sub>]  
421 is essential. In our study, elevated [CO<sub>2</sub>] increased photosynthesis rates in both the cultivars  
422 studied. Of the two cultivars, RAC875 showed the highest response to elevated [CO<sub>2</sub>]. The  
423 photosynthetic response of RAC875 was 22% higher than Kukri at elevated [CO<sub>2</sub>] (Figure 1).  
424 Stomatal conductance of Kukri and RAC875 was reduced by 20 and 15% at elevated [CO<sub>2</sub>]  
425 (Figure 1), indicating that both cultivars benefitted from the improved water use efficiency at  
426 elevated [CO<sub>2</sub>]. Similar intraspecific variations in photosynthesis rates at elevated [CO<sub>2</sub>] have  
427 been observed in many studies ([Thilakarathne \*et al.\*, 2015](#); [Thilakarathne \*et al.\*, 2013](#)). Such  
428 changes in photosynthetic rates and stomatal conductance is likely to contributed towards the  
429 variability in biomass accumulation observed in the tested cultivars. The above ground biomass  
430 accumulation was significantly higher in both Kukri and RAC875, but this response was  
431 genotype dependent, suggesting that there is a fine genetic controlling mechanism for biomass  
432 accumulation in response to elevated [CO<sub>2</sub>].

433

434 Plant growth is tightly coordinated by plant carbon and nitrogen metabolism; leaf level  
435 investments of these nutrients is central to whole plant growth ([Zheng, 2009](#)). Our study clearly  
436 indicated that growth at elevated [CO<sub>2</sub>] alters the dynamics of carbon and nitrogen at the plant

437 organ level. We observed a reduction in nitrogen concentration in the LFELB of both Kukri  
438 and RAC875 at elevated [CO<sub>2</sub>], with Kukri showing the highest reduction (35%, Figure 2).  
439 Similarly, the protein concentration of Kukri was less than RAC875 at elevated [CO<sub>2</sub>]. The  
440 reduction in leaf nitrogen concentration may be due to the dilution of nitrogen by the increased  
441 biomass observed at early growth stages ([Thilakarathne et al., 2015](#)). Further, this could have  
442 been due to the changes in the concentrations of enzymes that contain high nitrogen  
443 concentrations such as Rubisco ([Seneweera et al., 2011](#)). However, the nitrogen and protein  
444 concentrations of the ELB and the CE region were significantly higher at elevated [CO<sub>2</sub>]. This  
445 may be due to the increased partitioning of nitrogen into the growing sink tissues such as  
446 expanding leaf blade and shoot apex region where more nitrogen is needed to produce proteins  
447 required for the production of new cells ([Seneweera and Conroy, 2005](#)). In a previous study by  
448 [Thilakarathne et al. \(2015\)](#), it was reported that higher nitrogen concentrations in ELB at  
449 elevated [CO<sub>2</sub>]. Perhaps, such increased nitrogen in ELB could be linked to rapid protein  
450 synthesis, due to increases in cell division, synthesis of photosynthetic proteins and regulation  
451 of cell pressure potential that govern cell expansion ([Radin and Boyer, 1982](#)).

452

453 Together with nitrogen, carbon is also required for amino acid biosynthesis. At elevated [CO<sub>2</sub>],  
454 a reduction in carbon concentration was observed across all the organ types with the highest  
455 reduction observed in the ELB of RAC875. Such reductions could be due to the breakdown of  
456 carbohydrates to provide biochemical energy for leaf expansion and growth at elevated [CO<sub>2</sub>]  
457 ([Ainsworth et al., 2006](#)). On the other hand, it has also been demonstrated that sugar  
458 accumulation at elevated [CO<sub>2</sub>] depends on the species and growth conditions ([Nakano et al.,](#)  
459 [1997](#); [Rogers et al., 1996](#)). Carbohydrate analysis of RAC875 and Kukri (unpublished data)  
460 showed that total soluble carbohydrate concentration at elevated [CO<sub>2</sub>] was higher across both  
461 the cultivars, however RAC875 showing a higher soluble sugar accumulation in expanding  
462 leaves than Kukri at elevated [CO<sub>2</sub>] (Supplementary Figure S3(a)). The sucrose content of the  
463 ELB in Kukri and RAC875 showed a fold increase of 3.2 and 8.7, respectively, at elevated  
464 [CO<sub>2</sub>] (Supplementary Figure S1(b)). Similarly, glucose content of the two cultivars was also  
465 significantly increased at elevated [CO<sub>2</sub>] with a fold increase of 1.4 for Kukri and 2.3 for  
466 RAC875 (Supplementary Figure S1(c)). Therefore, high sucrose availability, together with  
467 increased nitrogen partitioning to ELB, may have contributed positively towards accelerated  
468 LER observed under elevated [CO<sub>2</sub>]. The higher nitrogen content in ELB was observed in a  
469 study conducted by [Thilakarathne et al. \(2015\)](#) at elevated [CO<sub>2</sub>]. An increase in nitrogen may  
470 have supported rapid rates of protein synthesis required for cell division, synthesis of

471 photosynthetic proteins and regulation of cell pressure potential that govern cell expansion  
472 ([Radin and Boyer, 1982](#)). Together with the carbon skeletons provided by sucrose and glucose,  
473 and ammonium provided by nitrogen partitioning, synthesis of amino acids takes place in the  
474 expanding leaf blades. These amino acids and resultant proteins govern the growth and  
475 development of the leaf blades.

476

### 477 **Leaf proteome responses to elevated [CO<sub>2</sub>] is genotypically varied**

478 This study is the first attempt in investigating changes in the leaf proteome of wheat in response  
479 to elevated [CO<sub>2</sub>]. Protein expression of RAC875 and Kukri varied under high [CO<sub>2</sub>] with  
480 RAC875 showing a higher number of significantly affected proteins than Kukri. These findings  
481 suggest that the proteome changes observed in leaves under elevated [CO<sub>2</sub>], also depend on the  
482 genotype. Similarly, in a study conducted by [Arachchige et al. \(2017\)](#), grain proteome  
483 responses of wheat to elevated [CO<sub>2</sub>] also genotypically varied. Overall, characterized proteins  
484 could be categorized into those associated with photosynthesis, carbohydrate metabolism, cell  
485 division, cell wall metabolism, energy pathways, protein synthesis and processing, post-  
486 translational modifications (PTM), key anti-oxidant enzymes, signal transduction, nitrogen and  
487 amino acid metabolism, lipid metabolism, hormonal metabolism and other intermediate  
488 metabolic proteins that are involved in several metabolic activities (Figure 3). A similar  
489 expression of proteins was observed using rice seedlings grown at elevated [CO<sub>2</sub>] in a study  
490 conducted by [Bokhari et al. \(2007\)](#).

491

### 492 **Elevated [CO<sub>2</sub>] shuffles the carbohydrate metabolism**

493 Increased photosynthesis capacity at elevated [CO<sub>2</sub>] contributes to the greater accumulation of  
494 soluble carbohydrates and starch, which causes a major shift in plant carbon metabolism  
495 ([Makino and Mae, 1999](#)). Despite a large number of proteins being differentially expressed at  
496 elevated [CO<sub>2</sub>], oxygen-evolving enhancer protein 1 (chloroplastic) was the only protein  
497 showing a significant upregulation (Table 2). This protein is responsible for photosystem II  
498 assembly and stabilization ([Ali et al., 2018](#)), and hence, upregulation of this protein may  
499 contribute towards improving the efficiency of photosynthesis light-dependent reactions. At  
500 elevated [CO<sub>2</sub>], upregulation of Uroporphyrinogen decarboxylase, a key enzyme in chlorophyll  
501 biosynthesis was also observed (Table 2). Generally, higher chlorophyll production at elevated  
502 [CO<sub>2</sub>] contributes to improved efficiency in harvesting light and subsequent energy conversion  
503 in the light reaction of photosynthesis.

504 In RAC875, increased abundance of sucrose synthase at elevated [CO<sub>2</sub>], one of the key  
505 enzymes involved in sucrose metabolism, was observed (Table 2). Sucrose synthase is capable  
506 of cleaving sucrose into UDP-Glucose and fructose and channeling them into multiple  
507 pathways involved in metabolic, structural and storage functions ([Jiang et al., 2015](#); [Sturm and  
508 Tang, 1999](#)). Sucrose synthase did not only increase at the protein level, the transcript  
509 abundance of *SUS1* (sucrose synthase 1) gene in ELB of RAC875 also showed a fold increase  
510 of 1.43 at elevated [CO<sub>2</sub>] when compared to ambient [CO<sub>2</sub>] (unpublished data, Table 4).  
511 Similarly, in RAC875, UTP-glucose-1-phosphate uridylyltransferase enzyme was upregulated  
512 by 4 folds higher than Kukri at elevated [CO<sub>2</sub>] (Table 3). This is the key enzyme that  
513 synthesizes UDP-glucose from glucose-1-phosphate and Uridine Triphosphate (UTP)  
514 ([Kleczkowski et al., 2010](#)). UDP-glucose is one of the key substrates to produce sucrose-6-  
515 phosphate, from which sucrose is produced in plant cells ([Jiang et al., 2015](#); [Koch, 2004](#)). High  
516 sucrose availability in RAC875 at elevated [CO<sub>2</sub>] could be due to the increased expression of  
517 UTP-glucose-1-phosphate uridylyltransferase which provides more UDP-glucose as a  
518 substrate to produce sucrose. On the other hand, UDP-glucose is the primary building block  
519 for cell wall synthesis ([Wai et al., 2017](#)) and thus, more substrate would be available for  
520 biosynthesis of cell wall polysaccharides for the dividing cells in the ELB. Generally, UDP-  
521 Glucose is highly available in the growing sink tissues such as meristems and developing leaves  
522 where the majority of cell wall synthesis takes place ([Verbančič et al., 2017](#)). Higher  
523 availability of sucrose and glucose in the expanding leaves of RAC875 and Kukri could be due  
524 to increased expression of these proteins at elevated [CO<sub>2</sub>].

525

526 In Kukri, glucose-6-phosphate isomerase, which is involved in the respiratory breakdown of  
527 carbohydrates, was down-regulated at elevated [CO<sub>2</sub>] (Table 1), suggesting the facilitation of  
528 carbohydrate anabolism over catabolism in a high CO<sub>2</sub> environment. In addition, beta-amylase,  
529 the main enzyme responsible for starch granule breakdown in leaves was down-regulated in  
530 Kukri at elevated [CO<sub>2</sub>]. Therefore, less degradation of starch to sucrose could be the reason  
531 for the difference in total soluble carbohydrate concentration of Kukri observed at elevated  
532 [CO<sub>2</sub>]. However, UDP-glucose 6-dehydrogenase, a key enzyme involved in the synthesis of  
533 UDP-glucuronic acid ([Kärkönen et al., 2005](#); [Klinghammer and Tenhaken, 2007](#)), a common  
534 precursor in the formation of pectin and hemicellulose in the plant's primary cell wall, was  
535 upregulated at high [CO<sub>2</sub>] (Table 1). Upregulation of this enzyme at elevated [CO<sub>2</sub>] suggests  
536 that cell wall biosynthesis is accelerated at elevated [CO<sub>2</sub>].

537 **High energy demand at elevated [CO<sub>2</sub>] supported by the induction of proteins in the**  
538 **energy metabolism pathway**

539 Enhanced rates of photosynthesis at elevated [CO<sub>2</sub>] demands a greater energy input in the form  
540 of ATP ([Gonzalez-Meler et al., 2004](#)). Exposure to elevated [CO<sub>2</sub>] induced the expression of  
541 ATP synthesizing enzymes in our study. A similar pattern in the upregulation of ATP  
542 synthesizing enzymes was observed by [Bokhari et al. \(2007\)](#) under elevated [CO<sub>2</sub>]. In Kukri,  
543 ATP synthase subunit d (mitochondrial) and pyruvate kinase enzyme involved in ATP  
544 synthesis was highly expressed suggesting that ATP synthesis is higher at elevated [CO<sub>2</sub>]  
545 (Table 1). At elevated [CO<sub>2</sub>], expression of ATP synthase subunit d (mitochondrial) and  
546 Fructose bi-phosphate aldolase was 6 and 3 folds higher in RAC875 than in Kukri (Table 3).  
547 These findings suggest that protein expression related to energy metabolism is largely cultivar  
548 dependent. Expression of proteins related to energy generation implies that apart from  
549 carbohydrate synthesis, elevated [CO<sub>2</sub>] also stimulates the respiratory breakdown of the  
550 carbohydrates in order to obtain sufficient energy for leaf expansion and carbon skeletons  
551 required for further anabolic purposes ([Ainsworth et al., 2006](#)).

552

553 **Cell wall metabolism and cell division related proteins were upregulated by elevated**  
554 **[CO<sub>2</sub>]**

555 Cell cycle functions tend to change as a result of increased sugar supply to the growing sink  
556 tissues at elevated [CO<sub>2</sub>] ([Gamage et al., 2018](#)). It has been demonstrated that cell division, cell  
557 expansion and cell wall loosening increased at elevated [CO<sub>2</sub>] and results in increased growth  
558 ([Masle, 2000](#); [Ranasinghe and Taylor, 1996](#)). Consistent with the above findings, upregulation  
559 of proteins related to these cell cycle functions was observed at elevated [CO<sub>2</sub>]. In RAC875, a  
560 translationally controlled tumor protein homolog that stabilizes microtubules during cell  
561 division ([Toscano-Morales et al., 2015](#)) was prominently upregulated (Table 2). Essential  
562 components in cell microtubules such as  $\alpha$  and  $\beta$  chains of tubulin, that facilitate chromosome  
563 segregation during cell division ([Hashimoto, 2015](#)) were upregulated in Kukri at elevated  
564 [CO<sub>2</sub>] (Table 1). Important nucleosome proteins (GTP-binding nuclear protein and histone H4  
565 protein) involved in chromatin formation and condensation during cell cycle processes  
566 ([Bischoff et al., 1999](#); [Loginova and Silkova, 2017](#)) were differentially expressed at elevated  
567 [CO<sub>2</sub>] (Table 1 and 2). Additionally,  $\alpha$  type proteasome subunit was found to be highly  
568 expressed in highly proliferating cells ([Genschik et al., 1994](#)) and was upregulated at elevated  
569 [CO<sub>2</sub>] in RAC875 (Table 3). This protein performs an important proteolytic activity in cell

570 cycle-related proteins involved in the progression of the cell cycle and thereby facilitating  
571 growth and development of the plant.

572

573 Beta-galactosidase, identified in both Kukri and RAC875, is an important enzyme related to  
574 cell wall expansion in growing tissues, however, the expression of this protein was found to be  
575 downregulated in our study (Table 2). On the other hand, upregulation of cell wall peroxidases  
576 at elevated [CO<sub>2</sub>] was prominent in both cultivars (Table 1 and 2). Peroxidases favor cell  
577 elongation either by generating reactive oxygen species (ROS) and/or by regulating the  
578 apoplastic concentrations of H<sub>2</sub>O<sub>2</sub> ([Passardi et al., 2004](#)). Reactive oxygen species play an  
579 important role in cell wall loosening by cleaving cell wall components such as xyloglucans and  
580 pectins ([Passardi et al., 2004](#)). This allows other cell wall loosening enzymes such as  
581 xyloglucan endotransglucosylase/endohydrolases (XTHs) to act on xyloglucans to loosen the  
582 plant cell wall permitting cell elongation ([Van Sandt et al., 2007](#)). Consistent with this,  
583 expression of XTH gene members was found to be upregulated at elevated [CO<sub>2</sub>] which may  
584 have facilitated increased leaf elongation at high [CO<sub>2</sub>] (unpublished data, Table 4). However,  
585 the mechanism by which ROS mediate leaf development still remains unclear ([Schmidt et al.,](#)  
586 [2016](#)).

587

#### 588 **Protein synthesis, processing and transport respond to elevated [CO<sub>2</sub>]**

589 Several important proteins involved as structural constituents of ribosomes were upregulated  
590 at elevated [CO<sub>2</sub>] (Table 1 and 2). Increased photosynthesis rates observed at elevated [CO<sub>2</sub>]  
591 requires a corresponding increase in other cellular proteins, including structural (i.e. light  
592 harvest protein complexes, components in electron transport chain and thylakoids) and  
593 metabolic proteins (i.e. carbon assimilating enzymes such as Rubisco). Thus, a sufficient  
594 turnover of these proteins is constantly required to provide the building blocks for these  
595 structural components and maintain their related enzymatic activities ([Lawlor, 2002](#)). Further,  
596 significant ribosome biosynthesis is required to support increased cytoplasmic growth and cell  
597 proliferation occurring in the expanding leaf blade ([Ainsworth et al., 2006](#); [Sugimoto-Shirasu](#)  
598 [and Roberts, 2003](#)). Increased protein turnover in the ELB could be due to the increased  
599 nitrogen partitioning observed at elevated [CO<sub>2</sub>]. This is further confirmed by the high  
600 transcript abundance of the key nitrogen assimilation genes (*GS2b*, *Fd-GOGAT* and *NADH-*  
601 *GOGAT*) in both cultivars under high [CO<sub>2</sub>] conditions (unpublished data, Table 4).

602

603 A number of molecular chaperone proteins that facilitate proper folding of the polypeptide  
604 chains and process proteins, were identified at elevated [CO<sub>2</sub>] in this study. Of them, heat shock  
605 protein 90 was a highly expressed protein found in both cultivars (Table 1 and 3). This protein  
606 plays an important role in maintaining cellular homeostasis through protein folding, assembly  
607 and translocation ([Park and Seo, 2015](#)). Along with these, a significant upregulation of clathrin  
608 heavy chain proteins (5 fold higher than ambient [CO<sub>2</sub>]) was observed at elevated [CO<sub>2</sub>] (Table  
609 1), which facilitates intra-cellular protein transport required for proper cell division and  
610 functioning ([Popova et al., 2013](#)).

611

612 Post-translational modifications (PTM) of proteins improves the functional diversity of a  
613 proteome increasing protein responsiveness to external factors ([Friso and van Wijk, 2015](#)).  
614 Proteolysis is one of the PTMs in plants which is critical in maintaining cellular protein  
615 concentrations within a cell ([Vierstra, 1996](#)). Several proteolytic proteins such as alpha type  
616 proteasome subunits and ATP-dependent Clp protease subunit were upregulated in RAC875 at  
617 elevated [CO<sub>2</sub>]. Expression of Aminopeptidase differed in the two cultivars. Kukri showed an  
618 upregulation while RAC875 showed a down-regulation at elevated [CO<sub>2</sub>] (Table 1 and 2).  
619 These proteolytic enzymes and components are responsible for cleaving polypeptide bonds for  
620 different cellular activities, removing unassembled protein subunits or misfolded proteins from  
621 the cell and thereby controlling cell metabolism.

622

### 623 **Signal transduction proteins were upregulated at elevated [CO<sub>2</sub>]**

624 Since plants change their morphologies in response to environmental cues, different signaling  
625 pathways interact together to co-ordinate biochemical and physiological responses, such as  
626 photosynthetic regulation, with plant growth responses ([Mulligan et al., 1997](#)). Our results  
627 showed an upregulation of Calmodulin (Table 2), a ubiquitous Ca<sup>2+</sup> binding protein which  
628 mediates control of various ion channels, transcription factors, protein kinases and other  
629 metabolic enzymes ([Zeng et al., 2015](#)). The cytosolic Ca<sup>2+</sup> concentration changes in response  
630 to environmental stimuli ([Zhu et al., 2014](#)) including elevated [CO<sub>2</sub>]. For example, one of the  
631 main mechanisms driving stomatal conductance at elevated [CO<sub>2</sub>] involves the interaction of  
632 CO<sub>2</sub> with the guard cell membranes, which operate largely via Ca<sup>2+</sup> signaling pathway  
633 ([Brodribb and McAdam, 2013](#)). Up-regulation of S-formylglutathione hydrolase (Table 2), the  
634 key enzyme that catalyzes the production of glutathione, indicates its increased production at  
635 elevated [CO<sub>2</sub>]. Glutathione has been shown to participate in several signaling processes

636 including protein synthesis, amino acid transport and control of cell division ([Hossain et al.,](#)  
637 [2017](#)). In addition, phospholipases (PL), which are often regulated by external factors such as  
638  $\text{Ca}^{2+}$  concentration, have also been upregulated at elevated  $[\text{CO}_2]$  ([Table 3, Singh et al., 2015](#)).  
639 This enzyme was suggested to be involved in various metabolic and cell signaling networks  
640 and subsequent phosphatidic production by PL. It is suggested that such changes are likely to  
641 determine plant growth responses under a particular environmental condition ([Singh et al.,](#)  
642 [2015](#)).

643 Apart from these proteins, there were many uncharacterized proteins that showed a differential  
644 expression at elevated  $[\text{CO}_2]$ . Some of the uncharacterized proteins were present in both  
645 cultivars and showed a similar pattern of expression. For example, W5H8Z0 uncharacterized  
646 protein showed a significant upregulation in both the cultivars at elevated  $[\text{CO}_2]$ , suggesting  
647 that this might play a role in moderating plant metabolism in a high  $\text{CO}_2$  environment. Since,  
648 the whole proteome of wheat is not completely interpreted, developing a complete  
649 understanding of the protein network associated with growth responses to elevated  $[\text{CO}_2]$  is a  
650 great challenge, but it is essential in order to adapt to increasing  $[\text{CO}_2]$  in the atmosphere.

651

## 652 **Conclusion**

653 We investigated the physiological and proteomic-wide responses of the ELB of two winter  
654 wheat cultivars to elevated  $[\text{CO}_2]$  in order to understand the underlying molecular mechanisms  
655 of plant growth responses to elevated  $[\text{CO}_2]$ . Elevated  $[\text{CO}_2]$  increases the sugar accumulation  
656 and affects different regulatory mechanisms, which results in altered protein expression to  
657 maintain plant carbon and nitrogen metabolism and cell homeostasis.

658

659 We conclude that elevated  $[\text{CO}_2]$  increases the rate of carbon assimilation and carbohydrate  
660 metabolism in a significant manner. At the same time, the respiratory breakdown of  
661 carbohydrates is upregulated to meet the high energy demand required for maximum leaf  
662 growth and elongation at elevated  $[\text{CO}_2]$ . Consistent with the increased sugar and nitrogen  
663 supply to the ELB, proteins including cell wall loosening, expansion and cell proliferation  
664 increase at elevated  $[\text{CO}_2]$ , which contributes to the accelerated growth of plants. There was a  
665 notable increase in the molecular chaperones and PTM through proteolytic proteins, implying  
666 the plants' ability to improve the functionality of their proteome in response to environmental  
667 stimuli such as elevated  $[\text{CO}_2]$ . This evidence clearly suggests that enhanced plant growth at

668 elevated [CO<sub>2</sub>] is not only due to the direct effect of [CO<sub>2</sub>] on photosynthesis and stomatal  
669 conductance. Variations in other associated key metabolic processes such as carbon/nitrogen  
670 metabolism and cell cycle functions also contribute to plant growth responses to elevated  
671 [CO<sub>2</sub>]. However, protein expression between the two genotypes significantly varied at elevated  
672 [CO<sub>2</sub>] suggesting a significant genetic variation for CO<sub>2</sub> responsiveness. Therefore,  
673 identification of genotypes that can thrive at elevated [CO<sub>2</sub>] is essential to improve the crop  
674 productibility under a CO<sub>2</sub> enriched environment.

675

676

#### 677 **Conflict of interest**

678 The authors declare no conflict of interest.

#### 679 **Acknowledgment**

680 This study was funded by the Strategic Research Fund of the University of Southern  
681 Queensland, Australia. The parental lines of the doubled haploid mapping population were  
682 obtained from the Australian Centre for Plant Functional Genomics, University of Adelaide,  
683 Australia to carry out the research. The proteomics analysis was conducted by La Trobe  
684 Comprehensive Proteomics Platform (La Trobe University, Melbourne, Australia).

685 **List of Figures and Supplementary Figures**

686

687 **Figure 1.** (a) rate of photosynthesis, (b) stomatal conductance, (c) above ground biomass  
688 accumulation of Kukri and RAC875 grown at ambient ( $400 \mu\text{mol mol}^{-1}$ ) or elevated ( $700\pm 10$   
689  $\mu\text{mol mol}^{-1}$ ) [ $\text{CO}_2$ ]. Data presented are the mean ( $\pm\text{SE}$ ) of  $n=3$ . P values indicate the  
690 significance: \*,  $P<0.05$ ; \*\*,  $P<0.01$ ; ns, not significant.

691

692 **Figure 2.** Total nitrogen and total protein concentration of (a) & (b) Last fully expanded leaf  
693 blades (LFELB), (c) & (d) expanding leaf blades (ELB), and (e) & (f) cell elongation and shoot  
694 apex regions of Kukri and RAC875 grown at ambient ( $400 \mu\text{mol mol}^{-1}$ ) or elevated ( $700\pm 10$   
695  $\mu\text{mol mol}^{-1}$ ) [ $\text{CO}_2$ ]. Data presented are the mean ( $\pm\text{SE}$ ) of  $n=3$ . P values indicate the  
696 significance: \*,  $P<0.05$ ; \*\*,  $P<0.01$ ; ns, not significant.

697

698 **Figure 3.** Ven diagram showing percentages of the identified proteins belonging to different  
699 categories in (a) Kukri and (b) RAC875 in response to elevated ( $700\pm 10 \mu\text{mol mol}^{-1}$ ) [ $\text{CO}_2$ ].  
700 Data are presented as percentages. **A**-photosynthesis, **B**-carbohydrate metabolism, **C**-cell  
701 division and cell wall metabolism, **D**-energy pathway, **E**-protein synthesis and processing, **F**-  
702 proteins involved in Post-translational modifications (PTM), **G**-anti oxidant enzymes, **H**-  
703 Signal transduction proteins, **I**-nitrogen and amino acid metabolism, **J**-lipid metabolism, **K**-  
704 hormonal metabolism, **L**- other intermediate metabolic proteins.

705

706 **Supplementary Figure S1.** (a) Total soluble sugar content, (b) sucrose content, (c) glucose  
707 content and (d) fructose content in expanding leaf blades of Kukri and RAC875 grown at  
708 ambient ( $400 \mu\text{mol mol}^{-1}$ ) or elevated ( $700\pm 10 \mu\text{mol mol}^{-1}$ ) [ $\text{CO}_2$ ]. Data presented are the mean  
709 ( $\pm\text{SE}$ ) of  $n=3$ . P values indicate the significance: \*,  $P<0.05$ ; \*\*,  $P<0.01$ ; ns, not significant.

710

711 **Supplementary Figure S2.** Total carbon concentration of (a) Last fully expanded leaf blades  
712 (LFELB), (b) expanding leaf blades (ELB), and (c) cell elongation region of Kukri and  
713 RAC875 grown at ambient ( $400 \mu\text{mol mol}^{-1}$ ) or elevated ( $700\pm 10 \mu\text{mol mol}^{-1}$ ) [ $\text{CO}_2$ ]. Data  
714 presented are the mean ( $\pm\text{SE}$ ) of  $n=3$ . P values indicate the significance: \*,  $P<0.05$ ; \*\*,  $P<0.01$ ;  
715 ns, not significant.

716

717 **List of Tables and Supplementary Tables**

718

719 **Table 1.** Leaf proteome response of Kukri in response to elevated [CO<sub>2</sub>] (e[CO<sub>2</sub>]) (Protein  
720 expression relative to Kukri proteome at ambient [CO<sub>2</sub>], Fold change is given in Log<sub>2</sub>  
721 transformation, \*\* P<0.01, \* P<0.05).

722

723 **Table 2.** Leaf proteome response of RAC875 in response to elevated [CO<sub>2</sub>] (e[CO<sub>2</sub>]) (Protein  
724 expression relative to RAC875 proteome at ambient [CO<sub>2</sub>], fold change is given in Log<sub>2</sub>  
725 transformation, \*\*P<0.01, \* P<0.05).

726

727 **Table 3.** Comparison of leaf proteome response of RAC875 relative to Kukri at elevated [CO<sub>2</sub>]  
728 (Protein expression relative to Kukri proteome at elevated [CO<sub>2</sub>], fold change is given in Log<sub>2</sub>  
729 transformation, \*\*P<0.01, \* P<0.05).

730

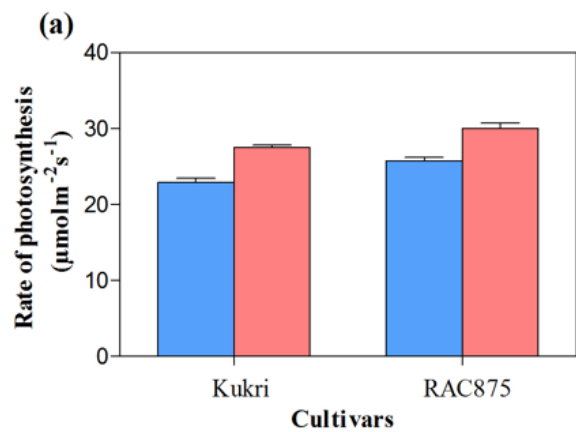
731 **Table 4.** Heatmap for transcript abundance of key genes in carbon, nitrogen and cell wall  
732 metabolism in Kukri and RAC875 grown at ambient (a[CO<sub>2</sub>], 400 μmol mol<sup>-1</sup>) or elevated  
733 (e[CO<sub>2</sub>], 700±10 μmol mol<sup>-1</sup>) [CO<sub>2</sub>]. Data presented are the mean values of gene expression.  
734 Fold change of transcript abundance at elevated [CO<sub>2</sub>] are presented in Log<sub>2</sub> scale.

735

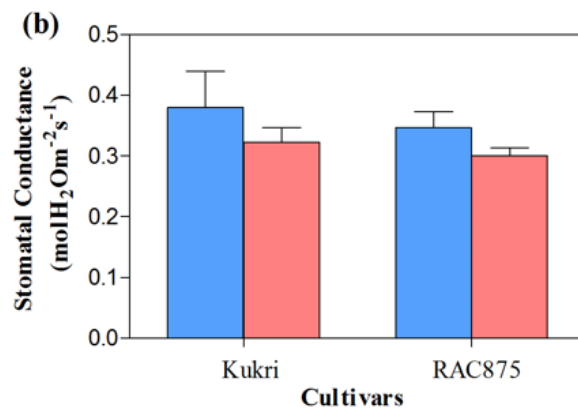
736 **Supplementary Table S1.** Concentration of macro and micronutrients in the growing solution  
737 provided during wheat growth during early vegetative stage. Half strength nutrient solution  
738 was provided. Adapted from ([Fernando et al., 2017](#); [Makino et al., 1983](#)).

739

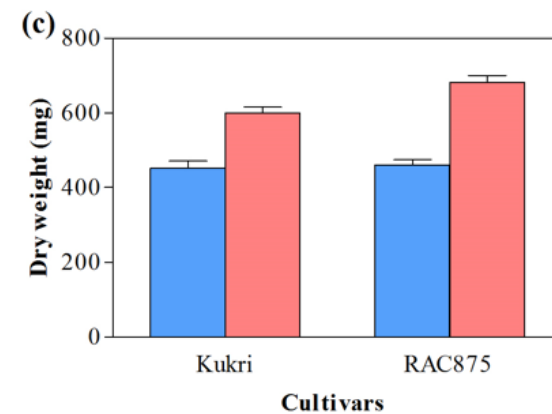
740 **Supplementary Table S2.** Comparison of leaf proteome response of RAC875 relative to Kukri  
741 at ambient [CO<sub>2</sub>] (Protein expression relative to Kukri proteome at ambient [CO<sub>2</sub>], fold change  
742 is given in Log<sub>2</sub> transformation, \*\*P<0.01, \* P<0.05).



Cultivar -  $P \leq 0.01$   
 [CO<sub>2</sub>] -  $P \leq 0.01$   
 Cultivar x [CO<sub>2</sub>] - ns



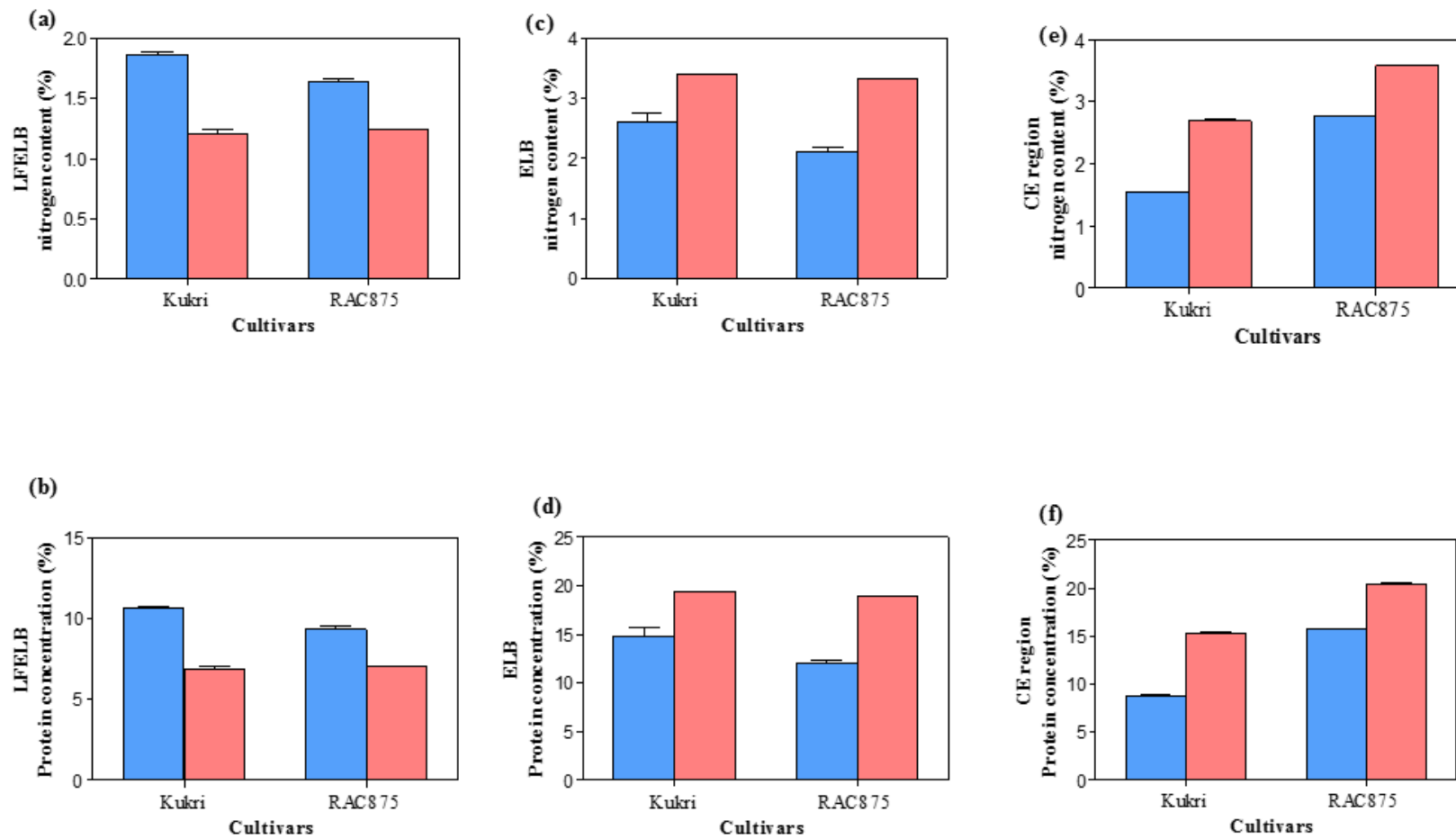
Cultivar - ns  
 [CO<sub>2</sub>] - ns  
 Cultivar x [CO<sub>2</sub>] - ns



Cultivar -  $P \leq 0.05$   
 [CO<sub>2</sub>] -  $P \leq 0.01$   
 Cultivar x [CO<sub>2</sub>] - ns

■ Ambient [CO<sub>2</sub>]    ■ Elevated [CO<sub>2</sub>]

**Figure 1**



For all the variables -  
 Cultivar -  $P \leq 0.01$ , [CO<sub>2</sub>]-  $P \leq 0.01$ , Organ -  $P \leq 0.01$   
 Cultivar x [CO<sub>2</sub>] x Organ-  $P \leq 0.01$

■ Ambient [CO<sub>2</sub>]    ■ Elevated [CO<sub>2</sub>]

**Figure 2**

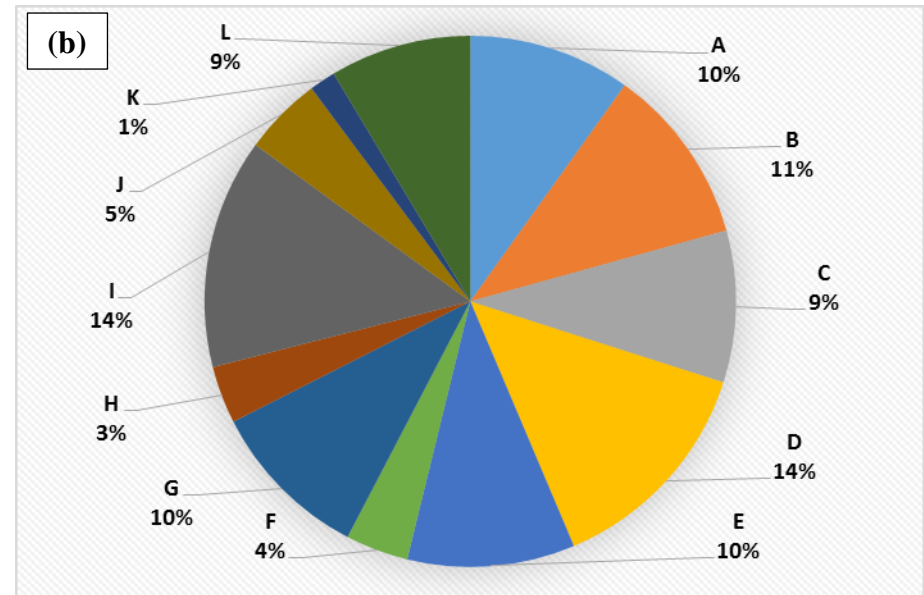
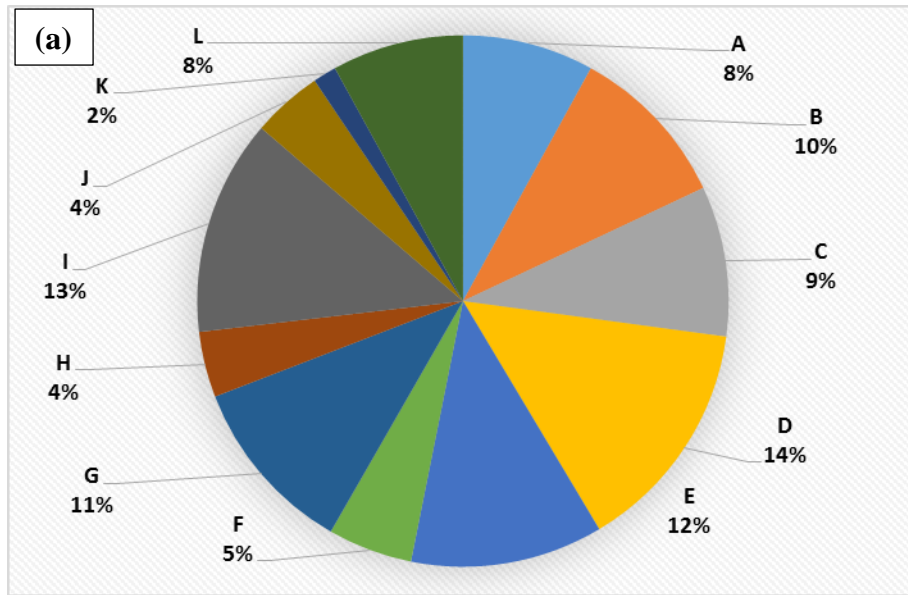


**Figure 3**

**Table 1.** Leaf proteome response of Kukri in response to elevated [CO<sub>2</sub>] (e[CO<sub>2</sub>]) (Protein expression relative to Kukri proteome at ambient [CO<sub>2</sub>], Fold change is given in Log<sub>2</sub> transformation, \*\* P<0.01, \* P<0.05).

Accession No	Protein Name	Fold change at e[CO <sub>2</sub> ]	Molecular weight (kDa)	P value
<b>Carbohydrate metabolism</b>				
A0A1D5S2P8	Glucose-6-phosphate isomerase	-1.64	62.308	*
A0A1D6DBP9	Beta-amylase	-2.20	56.102	*
A0A1D5ZJB9	UDP-glucose 6-dehydrogenase	4.68	51.527	**
<b>Energy pathway</b>				
W5BEP1	ATP synthase subunit D, mitochondrial	6.00	19.548	**
A0A1D5UPJ6	Pyruvate kinase	3.92	35.432	*
C7AE91	Blue copper protein	3.28	17.393	*
<b>Cell proliferation and differentiation</b>				
A0A1D5SQY8	Tubulin alpha chain	5.97	45.863	*
A0A1D5Z8I6	Histone H4	5.72	16.412	*
A0A1D6BQY9	Tubulin beta chain	4.48	50.211	*
<b>Protein synthesis</b>				
Q5I7K5	Ribosomal protein P1	-0.89	11.193	*
W5E2W7	40S ribosomal protein SA	4.02	33.271	*
<b>Protein processing and transport</b>				
Q0Q0I7	Heat shock protein 90	8.43	80.460	**
W5D5R6	Cold-induced protein	-1.33	16.199	*
A0A1D5ZA24	Clathrin heavy chain	5.43	189.889	*
<b>Post-translational modifications – Proteolytic enzymes</b>				
A0A1D6B0C9	Aminopeptidase	2.10	98.207	*
<b>Anti-oxidant enzymes – responds to ROS</b>				
A0A1D5SM88	Dihydrolipoyl dehydrogenase	-2.50	52.795	*
W5C5X0	Peroxidase	-1.93	33.077	*
W5ANF5	Peroxidase	2.67	37.449	*

F1DKC1	Catalase	4.47	56.883	*
<b>Signal transduction</b>				
W5CUZ3	FVE	-1.18	50.298	*
A0A1D6CA52	4-hydroxy-4-methyl-2-oxoglutarate aldolase	1.74	16.581	*
A0A1D6RJH6	Plasma membrane ATPase	8.49	102.253	*

**Table 2.** Leaf proteome response of RAC875 in response to elevated [CO<sub>2</sub>] (e[CO<sub>2</sub>]) (Protein expression relative to RAC875 proteome at ambient [CO<sub>2</sub>], fold change is given in Log<sub>2</sub> transformation, \*\*P<0.01, \* P<0.05).

Accession No	Protein Name	Fold change at e[CO <sub>2</sub> ]	Molecular weight (kDa)	P value
<b>Photosynthesis</b>				
A0A1D6BXL7	Ferredoxin--NADP reductase, chloroplastic	-2.06	39.843	*
P27665	Oxygen-evolving enhancer protein 1, chloroplastic	2.66	34.740	*
<b>Porphyrin biochemical pathway – Chlorophyll Synthesis</b>				
W5DYLO	Uroporphyrinogen decarboxylase	0.96	42.951	*
A0A1D5VZ17	Uroporphyrinogen decarboxylase	0.61	45.934	*
<b>Carbohydrate metabolism</b>				
W5I774	Sucrose synthase	2.42	92.400	**
<b>Energy pathway</b>				
P20858	ATP synthase subunit beta, chloroplastic	-1.96	53.857	*
<b>Cell proliferation and differentiation</b>				
Q8LRM8	Translationally-controlled tumor protein homolog	1.01	18.806	*
A0A1D5RY72	GTP-binding nuclear protein	0.77	19.912	*
W5C3H4	Proteasome subunit alpha type	2.05	25.828	*
<b>Cell wall metabolism</b>				
A0A1D6RX96	Beta-galactosidase	-0.87	87.227	*
A0A1D6CMU1	Beta-galactosidase	-0.93	75.744	*
<b>Protein synthesis</b>				
E2F3W4	40S ribosomal protein S15a	1.40	14.790	**
A0A1D5UFM0	40S ribosomal protein S12	1.22	15.235	*
A0A1D5T990	Elongation factor G, mitochondrial	1.18	72.841	*
<b>Post translation modifications – Proteolytic enzymes</b>				
A0A1D6B0C9	Aminopeptidase	-1.50	98.207	**
A0A1D5TF03	ATP-dependent Clp protease proteolytic subunit	1.95	27.092	**

W5F826	Proteasome subunit beta type	2.65	24.333	*
A0A1D6AKZ2	ATP-dependent Clp protease proteolytic subunit	2.02	32.197	*
<b>Amino acid metabolism</b>				
A0A1D6S822	S-adenosylmethionine synthase	-2.37	42.827	*
<b>Anti-oxidant enzymes – responds to ROS</b>				
A0A1D5XAW6	Superoxide dismutase [Cu-Zn]	-1.13	16.576	*
H9NAV6	Superoxide dismutase [Cu-Zn]	-1.26	15.092	*
A0A1D6BEM4	Peroxidase	1.06	33.623	*
A0A1D6CM42	Superoxide dismutase [Cu-Zn]	-0.95	19.325	**
W5AS89	Peroxidase	-0.73	36.521	*
W5BAV5	Peroxidase	-0.69	33.724	*
<b>Signal transduction</b>				
Q7DMG9	Calmodulin TaCaM1-1 (Ca <sup>2+</sup> signalling)	1.08	16.832	*
P04464	Calmodulin	0.91	16.847	*
W5D6S5	S-formylglutathione hydrolase	1.70	31.599	*

**Table 3.** Comparison of leaf proteome response of RAC875 relative to Kukri at elevated [CO<sub>2</sub>] (Protein expression relative to Kukri proteome at elevated [CO<sub>2</sub>], fold change is given in Log<sub>2</sub> transformation, \*\*P<0.01, \* P<0.05).

Accession No	Protein Name	Fold change at e [CO <sub>2</sub> ] relative to Kukri	Molecular weight (kDa)	P value
<b>Carbohydrate metabolism</b>				
A0A1D6S518	UTP-glucose-1-phosphate uridylyltransferase	4.20	51.664	**
<b>Energy pathway</b>				
W5BEP1	ATP synthase subunit D, mitochondrial	6.35	19.548	**
W5D5L4	Fructose bi-phosphate aldolase	2.17	38.810	*
A0A1D6AQV8	Aconitate hydratase	-0.42	106.306	*
<b>Cell proliferation and differentiation</b>				
A0A1D5SQY8	Tubulin alpha chain	5.34	45.863	**
A0A173FEH2	TSK1 protein	1.50	19.059	*
A0A1D5VHL0	Phospholipase	2.07	92.062	*
	Protein synthesis			
A0A1D5YL72	Elongation factor 1-alpha	7.85	47.806	**
W5E2W7	40S ribosomal protein SA	2.11	33.271	*
A0A1D6C4Q5	60S acidic ribosomal protein PO	3.73	33.770	*
<b>Protein processing</b>				
Q0Q0I7	Heat shock protein 90	7.29	80.460	**
<b>Post-translational modifications – Proteolytic enzymes</b>				
A0A1D6S4L2	Carboxypeptidase	1.77	51.327	*
A0A1D6B0C9	Aminopeptidase	2.15	98.207	*
D2KZ08	Aminotransferase	0.77	55.546	*
A0A1D5TM94	Carboxypeptidase	1.31	55.914	*
<b>Amino acid metabolism</b>				
A0A1D5XQ85	Alanine--tRNA ligase	1.94	109.594	*
A0A1D6B308	S-adenosylmethionine synthase	2.12	42.766	*

<b>Signal transduction</b>				
A0A1D5ZA24	Clathrin heavy chain	4.64	189.889	**
A0A1D5VHL0	Phospholipase	2.07	92.062	*
<b>Nitrogen assimilation</b>				
A0A1D6AQV8	Aconitate hydratase	-0.42	106.306	*

**Table 4.** Heatmap for transcript abundance of key genes in carbon, nitrogen and cell wall metabolism in Kukri and RAC875 grown at ambient (a[CO<sub>2</sub>], 400 μmol mol<sup>-1</sup>) or elevated (e[CO<sub>2</sub>], 700±10 μmol mol<sup>-1</sup>) [CO<sub>2</sub>]. Data presented are the mean values of gene expression. Fold change of transcript abundance at elevated [CO<sub>2</sub>] are presented in Log<sub>2</sub> scale.

Plant metabolism	Gene Name	Gene expression level				Log <sub>2</sub> fold change	
		Kukri		RAC875		Kukri	RAC875
		a[CO <sub>2</sub> ]	e[CO <sub>2</sub> ]	a[CO <sub>2</sub> ]	e[CO <sub>2</sub> ]	e[CO <sub>2</sub> ]/a[CO <sub>2</sub> ]	
Phtotosynthesis	<i>rbcL</i>	2.70	3.69	1.40	3.12	0.45	1.16
	<i>rbcS</i>	1.26	2.65	1.42	2.00	1.07	0.49
Carbon metabolism	<i>SPP1</i>	4.47	4.48	3.48	10.32	0.00	1.57
	<i>SPS1</i>	0.95	1.50	1.26	1.27	0.65	0.02
	<i>SUS1</i>	0.43	1.81	0.56	1.50	2.07	1.43
Nitrogen metabolism	<i>NiR</i>	0.30	0.56	0.41	1.19	0.89	1.55
	<i>Fd-GOGAT</i>	13.24	29.92	15.61	28.57	1.18	0.87
	<i>GS2a</i>	24.98	46.56	14.65	26.80	0.90	0.87
	<i>GS2b</i>	0.09	0.15	0.11	0.32	0.70	1.49
	<i>GS1a</i>	3.36	4.28	3.15	4.26	0.35	0.44
	<i>GSr1</i>	0.33	0.68	0.25	0.27	1.04	0.12
	<i>NADH-GOGAT</i>	0.29	0.71	0.26	0.26	1.31	0.04
Cell wall metabolism	<i>TaEXPA3</i>	1.32	1.23	1.77	5.48	-0.10	1.63
	<i>TaEXPB6</i>	6.11	7.51	7.46	17.14	0.30	1.20
	<i>TAEXPB23</i>	11.55	28.49	13.23	13.55	1.30	0.03
	<i>TaXTH1</i>	39.54	46.23	23.16	66.77	0.23	1.53
	<i>TaXTH2</i>	36.34	65.60	46.83	94.22	0.85	1.01
	<i>TaXTH3</i>	26.76	8.70	4.31	36.13	-1.62	3.07
	<i>TaXTH4</i>	0.61	0.40	0.88	1.92	-0.60	1.12
	<i>TaXTH5</i>	1.94	2.58	0.94	2.44	0.42	1.37

742 **References**

- 743
- 744 **Ahmad P, Latef A, Arafat A, Rasool S, Akram NA, Ashraf M, Gucel S.** 2016. Role of  
745 proteomics in crop stress tolerance. *Frontiers in plant science* **7**, 1336.
- 746 **Ainsworth EA, Beier C, Calfapietra C, Ceulemans R, Durand-Tardif M, Farquhar GD,**  
747 **Godbold DL, Hendrey GR, Hickler T, Kaduk J.** 2008. Next generation of elevated  
748 [CO<sub>2</sub>] experiments with crops: a critical investment for feeding the future world. *Plant,*  
749 *Cell & Environment* **31**, 1317-1324.
- 750 **Ainsworth EA, Long SP.** 2005. What have we learned from 15 years of free-air CO<sub>2</sub>  
751 enrichment (FACE)? A meta-analytic review of the responses of photosynthesis,  
752 canopy properties and plant production to rising CO<sub>2</sub>. *New Phytologist* **165**, 351-372.
- 753 **Ainsworth EA, Rogers A.** 2007. The response of photosynthesis and stomatal conductance to  
754 rising [CO<sub>2</sub>]: mechanisms and environmental interactions. *Plant, Cell & Environment*  
755 **30**, 258-270.
- 756 **Ainsworth EA, Rogers A, Vodkin LO, Walter A, Schurr U.** 2006. The effects of elevated  
757 CO<sub>2</sub> concentration on soybean gene expression. An analysis of growing and mature  
758 leaves. *Plant Physiology* **142**, 135-147.
- 759 **Ali A, Goswami S, Kumar RR, Singh K, Singh JP, Kumar A, Kumari A, Sakhrey A, Rai**  
760 **GK, Praveen S.** 2018. Wheat Oxygen Evolving Enhancer Protein: Identification and  
761 Characterization of Mn-Binding Metalloprotein of Photosynthetic Pathway Involved in  
762 Regulating Photosystem II Integrity and Network of Antioxidant Enzymes under Heat  
763 Stress. *Int. J. Curr. Microbiol. App. Sci* **7**, 177-192.
- 764 **Arachchige PMS, Ang C-S, Nicolas ME, Panozzo J, Fitzgerald G, Hirotsu N, Seneweera**  
765 **S.** 2017. Wheat (*Triticum aestivum* L.) grain proteome response to elevated [CO<sub>2</sub>]  
766 varies between genotypes. *Journal of Cereal Science* **75**, 151-157.
- 767 **Bischoff F, Molendijk A, Rajendrakumar C, Palme K.** 1999. GTP-binding proteins in  
768 plants. *Cellular and Molecular Life Sciences CMLS* **55**, 233-256.
- 769 **Bokhari SA, Wan X-Y, Yang Y-W, Zhou L, Tang W-L, Liu J-Y.** 2007. Proteomic response  
770 of rice seedling leaves to elevated CO<sub>2</sub> levels. *Journal of proteome research* **6**, 4624-  
771 4633.
- 772 **Brodribb TJ, McAdam SA.** 2013. Unique responsiveness of angiosperm stomata to elevated  
773 CO<sub>2</sub> explained by calcium signalling. *PLoS one* **8**, e82057.
- 774 **Fernando N, Hirotsu N, Panozzo J, Tausz M, Norton RM, Seneweera S.** 2017. Lower grain  
775 nitrogen content of wheat at elevated CO<sub>2</sub> can be improved through post-anthesis NH<sub>4</sub><sup>+</sup>  
776 supplement. *Journal of Cereal Science* **74**, 79-85.
- 777 **Friso G, van Wijk KJ.** 2015. Posttranslational protein modifications in plant metabolism.  
778 *Plant Physiology* **169**, 1469-1487.
- 779 **Gamage D, Thompson M, Sutherland M, Hirotsu N, Makino A, Seneweera S.** 2018. New  
780 insights into the cellular mechanisms of plant growth at elevated atmospheric carbon  
781 dioxide. *Plant, Cell & Environment* **41(6)**, 1233-1246.
- 782 **Gaudinier A, Tang M, Kliebenstein DJ.** 2015. Transcriptional networks governing plant  
783 metabolism. *Current Plant Biology* **3**, 56-64.
- 784 **Genschik P, Jamet E, Phillips G, Parmentier Y, Gigot C, Fleck J.** 1994. Molecular  
785 characterization of a β-type proteasome subunit from *Arabidopsis thaliana* co-  
786 expressed at a high level with an α-type proteasome subunit early in the cell cycle. *The*  
787 *Plant Journal* **6**, 537-546.
- 788 **Gonzalez-Meler MA, Taneva L, Trueman RJ.** 2004. Plant respiration and elevated  
789 atmospheric CO<sub>2</sub> concentration: cellular responses and global significance. *Annals of*  
790 *Botany* **94**, 647-656.

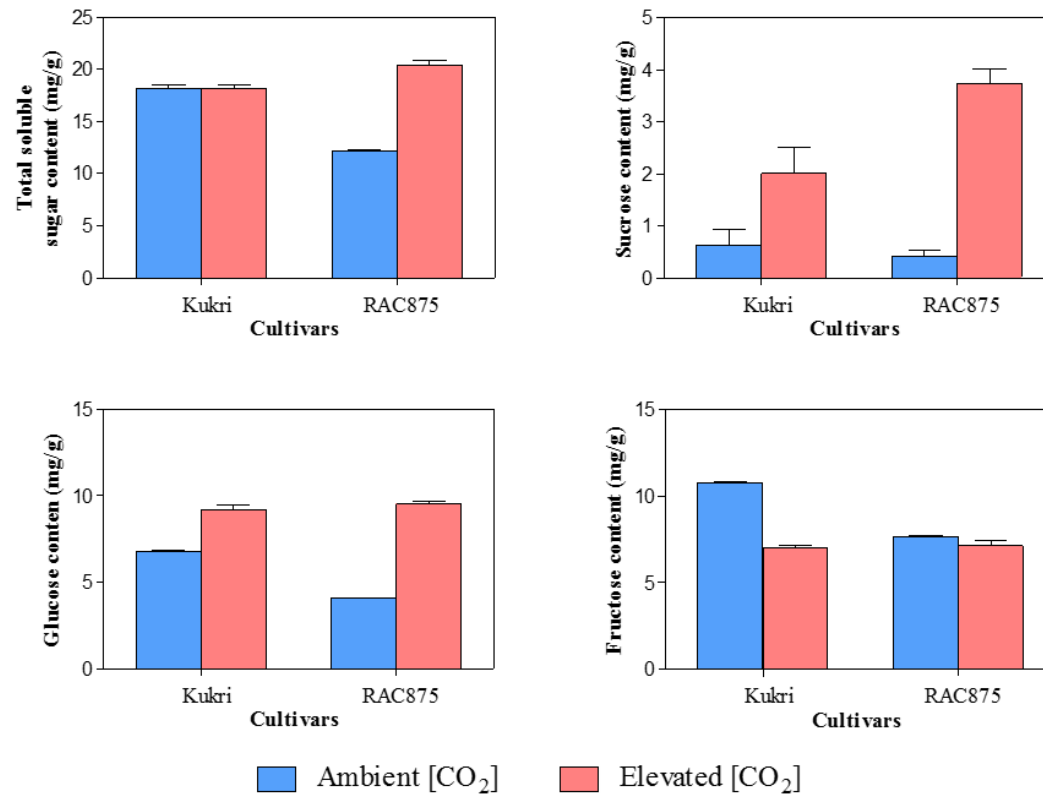
- 791 **Gupta R, Kim ST.** 2015. Depletion of RuBisCO protein using the protamine sulfate  
792 precipitation method. *Proteomic Profiling*: Springer, 225-233.
- 793 **Gupta R, Wang Y, Agrawal GK, Rakwal R, Jo IH, Bang KH, Kim ST.** 2015. Time to dig  
794 deep into the plant proteome: a hunt for low-abundance proteins. *Frontiers in plant*  
795 *science* **6**, 22.
- 796 **Hashiguchi A, Ahsan N, Komatsu S.** 2010. Proteomics application of crops in the context of  
797 climatic changes. *Food Research International* **43**, 1803-1813.
- 798 **Hashimoto T.** 2015. Microtubules in plants. *The Arabidopsis Book/American Society of Plant*  
799 *Biologists* **13**.
- 800 **Hikosaka K, Onoda Y, Kinugasa T, Nagashima H, Anten NP, Hirose T.** 2005. Plant  
801 responses to elevated CO<sub>2</sub> concentration at different scales: leaf, whole plant, canopy,  
802 and population. *Forest Ecosystems and Environments*: Springer, 3-13.
- 803 **Hossain MA, Mostofa MG, Diaz-Vivancos P, Burritt DJ, Fujita M, Tran L-SP.** 2017.  
804 *Glutathione in Plant Growth, Development, and Stress Tolerance*: Springer.
- 805 **Hossain Z, Nouri M-Z, Komatsu S.** 2011. Plant cell organelle proteomics in response to  
806 abiotic stress. *Journal of proteome research* **11**, 37-48.
- 807 **IPCC.** 2014. Recent increase and projected changes in CO<sub>2</sub> concentrations. *Carbon dioxide:*  
808 *Projected emissions and concentrations* Vol. 2015. Online Data distribution centre,  
809 IPCC.
- 810 **Ishihama Y, Rappsilber J, Mann M.** 2006. Modular stop and go extraction tips with stacked  
811 disks for parallel and multidimensional Peptide fractionation in proteomics. *J Proteome*  
812 *Res* **5**, 988-994.
- 813 **Jiang S-Y, Chi Y-H, Wang J-Z, Zhou J-X, Cheng Y-S, Zhang B-L, Ma A, Vanitha J,**  
814 **Ramachandran S.** 2015. Sucrose metabolism gene families and their biological  
815 functions. *Scientific reports* **5**, 17583.
- 816 **Jitla DS, Rogers GS, Seneweera SP, Basra AS, Oldfield RJ, Conroy JP.** 1997. Accelerated  
817 early growth of rice at elevated CO<sub>2</sub>. *Plant Physiology* **115**, 15-22.
- 818 **Kärkönen A, Murigneux A, Martinant J-P, Pepey E, Tatout C, Dudley BJ, Fry SC.** 2005.  
819 UDP-glucose dehydrogenases of maize: a role in cell wall pentose biosynthesis.  
820 *Biochemical Journal* **391**, 409-415.
- 821 **Kim YJ, Lee HM, Wang Y, Wu J, Kim SG, Kang KY, Park KH, Kim YC, Choi IS,**  
822 **Agrawal GK.** 2013. Depletion of abundant plant R u B is CO protein using the  
823 protamine sulfate precipitation method. *Proteomics* **13**, 2176-2179.
- 824 **Kirschbaum MU.** 2010. Does Enhanced Photosynthesis Enhance Growth? Lessons Learnt  
825 From CO<sub>2</sub> Enrichment Studies. *Plant Physiology*, pp. 110.166819.
- 826 **Kleczkowski LA, Kunz S, Wilczynska M.** 2010. Mechanisms of UDP-glucose synthesis in  
827 plants. *Critical Reviews in Plant Sciences* **29**, 191-203.
- 828 **Klinghammer M, Tenhaken R.** 2007. Genome-wide analysis of the UDP-glucose  
829 dehydrogenase gene family in Arabidopsis, a key enzyme for matrix polysaccharides  
830 in cell walls. *Journal of Experimental Botany* **58**, 3609-3621.
- 831 **Koch K.** 2004. Sucrose metabolism: regulatory mechanisms and pivotal roles in sugar sensing  
832 and plant development. *Current opinion in plant biology* **7**, 235-246.
- 833 **Lawlor DW.** 2002. Carbon and nitrogen assimilation in relation to yield: mechanisms are the  
834 key to understanding production systems. *Journal of Experimental Botany* **53**, 773-787.
- 835 **Leakey AD, Ainsworth EA, Bernacchi CJ, Rogers A, Long SP, Ort DR.** 2009. Elevated  
836 CO<sub>2</sub> effects on plant carbon, nitrogen, and water relations: six important lessons from  
837 FACE. *Journal of Experimental Botany* **60**, 2859-2876.
- 838 **Li JY, Liu XH, Cai QS, Gu H, Zhang SS, Wu YY, Wang CJ.** 2008. Effects of Elevated CO<sub>2</sub>  
839 on Growth, Carbon Assimilation, Photosynthate Accumulation and Related Enzymes

- 840 in Rice Leaves during Sink-Source Transition. *Journal of integrative plant biology* **50**,  
841 723-732.
- 842 **Loginova D, Silkova O.** 2017. H3Ser10 histone phosphorylation in plant cell division. *Russian*  
843 *Journal of Genetics: Applied Research* **7**, 46-56.
- 844 **Long SP, Ainsworth EA, Rogers A, Ort DR.** 2004. Rising atmospheric carbon dioxide: plants  
845 FACE the Future\*. *Annu. Rev. Plant Biol.* **55**, 591-628.
- 846 **Lorimer GH.** 1981. The carboxylation and oxygenation of ribulose 1, 5-bisphosphate: the  
847 primary events in photosynthesis and photorespiration. *Annual review of plant*  
848 *physiology* **32**, 349-382.
- 849 **Lowe RG, McCorkelle O, Bleackley M, Collins C, Faou P, Mathivanan S, Anderson M.**  
850 2015. Extracellular peptidases of the cereal pathogen *Fusarium graminearum*. *Frontiers*  
851 *in plant science* **6**, 962.
- 852 **Makino A, Mae T.** 1999. Photosynthesis and plant growth at elevated levels of CO<sub>2</sub>. *Plant*  
853 *and Cell Physiology* **40**, 999-1006.
- 854 **Makino A, Mae T, Ohira K.** 1983. Photosynthesis and ribulose 1, 5-bisphosphate carboxylase  
855 in rice leaves changes in photosynthesis and enzymes involved in carbon assimilation  
856 from leaf development through senescence. *Plant Physiology* **73**, 1002-1007.
- 857 **Makino A, Osmond B.** 1991. Effects of nitrogen nutrition on nitrogen partitioning between  
858 chloroplasts and mitochondria in pea and wheat. *Plant Physiology* **96**, 355-362.
- 859 **Masle J.** 2000. The effects of elevated CO<sub>2</sub> concentrations on cell division rates, growth  
860 patterns, and blade anatomy in young wheat plants are modulated by factors related to  
861 leaf position, vernalization, and genotype. *Plant Physiology* **122**.
- 862 **Mulligan RM, Chory J, Ecker JR.** 1997. Signaling in plants. *Proceedings of the National*  
863 *Academy of Sciences* **94**, 2793-2795.
- 864 **Nakano H, Makino A, Mae T.** 1997. The effect of elevated partial pressures of CO<sub>2</sub> on the  
865 relationship between photosynthetic capacity and N content in rice leaves. *Plant*  
866 *Physiology* **115**, 191-198.
- 867 **Neales T, Nicholls A.** 1978. Growth Responses on Young Wheat Plants to a Range of Ambient  
868 CO<sub>2</sub> Levels. *Functional Plant Biology* **5**, 45-59.
- 869 **Park C-J, Seo Y-S.** 2015. Heat shock proteins: a review of the molecular chaperones for plant  
870 immunity. *The plant pathology journal* **31**, 323.
- 871 **Parry MA, Reynolds M, Salvucci ME, Raines C, Andralojc PJ, Zhu X-G, Price GD,**  
872 **Condon AG, Furbank RT.** 2010. Raising yield potential of wheat. II. Increasing  
873 photosynthetic capacity and efficiency. *Journal of Experimental Botany* **62**, 453-467.
- 874 **Passardi F, Penel C, Dunand C.** 2004. Performing the paradoxical: how plant peroxidases  
875 modify the cell wall. *Trends in plant science* **9**, 534-540.
- 876 **Poorter H, Nagel O.** 2000. The role of biomass allocation in the growth response of plants to  
877 different levels of light, CO<sub>2</sub>, nutrients and water: a quantitative review. *Functional*  
878 *Plant Biology* **27**, 1191-1191.
- 879 **Poorter H, Navas ML.** 2003. Plant growth and competition at elevated CO<sub>2</sub>: on winners, losers  
880 and functional groups. *New Phytologist* **157**, 175-198.
- 881 **Popova N, Deyev I, Petrenko A.** 2013. Clathrin-mediated endocytosis and adaptor proteins.  
882 *Acta Naturae (англоязычная версия)* **5**.
- 883 **Pritchard S, Rogers H, Prior SA, Peterson C.** 1999. Elevated CO<sub>2</sub> and plant structure: a  
884 review. *Global Change Biology* **5**, 807-837.
- 885 **Radin JW, Boyer JS.** 1982. Control of leaf expansion by nitrogen nutrition in sunflower  
886 plants: role of hydraulic conductivity and turgor. *Plant Physiology* **69**, 771-775.
- 887 **Ranasinghe S, Taylor G.** 1996. Mechanism for increased leaf growth in elevated CO<sub>2</sub>. *Journal*  
888 *of Experimental Botany* **47**, 349-358.

- 889 **Rogers G, Milham P, Gillings M, Conroy J.** 1996. Sink strength may be the key to growth  
890 and nitrogen responses in N-deficient wheat at elevated CO<sub>2</sub>. *Functional Plant Biology*  
891 **23**, 253-264.
- 892 **Salekdeh GH, Komatsu S.** 2007. Crop proteomics: aim at sustainable agriculture of  
893 tomorrow. *Proteomics* **7**, 2976-2996.
- 894 **Schmidt R, Kunkowska AB, Schippers JH.** 2016. Role of reactive oxygen species during  
895 cell expansion in leaves. *Plant Physiology* **172**, 2098-2106.
- 896 **Seneweera S.** 2011. Effects of elevated CO<sub>2</sub> on plant growth and nutrient partitioning of rice  
897 (*Oryza sativa* L.) at rapid tillering and physiological maturity. *Journal of Plant*  
898 *Interactions* **6**, 35-42.
- 899 **Seneweera S, Ghannoum O, Conroy J, Ishimaru K, Okada M, Lieffering M, Kim HY,**  
900 **Kobayashi K.** 2002. Changes in source–sink relations during development influence  
901 photosynthetic acclimation of rice to free air CO<sub>2</sub> enrichment (FACE). *Functional*  
902 *Plant Biology* **29**, 947-955.
- 903 **Seneweera S, Makino A, Hirotsu N, Norton R, Suzuki Y.** 2011. New insight into  
904 photosynthetic acclimation to elevated CO<sub>2</sub>: The role of leaf nitrogen and ribulose-1,  
905 5-bisphosphate carboxylase/oxygenase content in rice leaves. *Environmental and*  
906 *experimental botany* **71**, 128-136.
- 907 **Seneweera SP, Conroy JP.** 2005. Enhanced leaf elongation rates of wheat at elevated CO<sub>2</sub>: is  
908 it related to carbon and nitrogen dynamics within the growing leaf blade?  
909 *Environmental and experimental botany* **54**, 174-181.
- 910 **Singh A, Bhatnagar N, Pandey A, Pandey GK.** 2015. Plant phospholipase C family:  
911 Regulation and functional role in lipid signaling. *Cell Calcium* **58**, 139-146.
- 912 **Solomon S, Qin D, Manning R.** 2007. Technical summary. Climate Change 2007: The  
913 Physical Science Basis. In: Solomon S, Qin D, Manning M, Z. Chen, Marquis M,  
914 Averyt KB, Tignor M, Miller HL, eds. *Contribution of Working Group I to the Fourth*  
915 *Annual Assessment Report of the Intergovernmental Panel on Climate Change*.  
916 Cambridge University Press, Cambridge, UK/New York, NY, USA., 996.
- 917 **Sturm A, Tang G-Q.** 1999. The sucrose-cleaving enzymes of plants are crucial for  
918 development, growth and carbon partitioning. *Trends in plant science* **4**, 401-407.
- 919 **Sugimoto-Shirasu K, Roberts K.** 2003. “Big it up”: endoreduplication and cell-size control  
920 in plants. *Current opinion in plant biology* **6**, 544-553.
- 921 **Tans P, Keeling R.** 2018. Trends in atmospheric carbon dioxide. Vol. 2018: NOAA/ESRL  
922 ([www.esrl.noaa.gov/gmd/ccgg/trends/](http://www.esrl.noaa.gov/gmd/ccgg/trends/))
- 923 **Taylor G, Ranasinghe S, Bosac C, Gardner SDL, Ferris R.** 1994. Elevated CO<sub>2</sub> and plant  
924 growth: cellular mechanisms and responses of whole plants. *Journal of Experimental*  
925 *Botany* **45**, 1761-1774.
- 926 **Thilakarathne CL, Tausz-Posch S, Cane K, Norton RM, Fitzgerald GJ, Tausz M,**  
927 **Seneweera S.** 2015. Intraspecific variation in leaf growth of wheat (*Triticum aestivum*)  
928 under Australian Grain Free Air CO<sub>2</sub> Enrichment (AGFACE): is it regulated through  
929 carbon and/or nitrogen supply? *Functional Plant Biology* **42**, 299-308.
- 930 **Thilakarathne CL, Tausz-Posch S, Cane K, Norton RM, Tausz M, Seneweera S.** 2013.  
931 Intraspecific variation in growth and yield response to elevated CO<sub>2</sub> in wheat depends  
932 on the differences of leaf mass per unit area. *Functional Plant Biology* **40**, 185-194.
- 933 **Thompson M, Gamage D, Hirotsu N, Martin A, Seneweera S.** 2017. Effects of Elevated  
934 Carbon Dioxide on Photosynthesis and Carbon Partitioning: A Perspective on Root  
935 Sugar Sensing and Hormonal Crosstalk. *Frontiers in Physiology* **8**, 578.
- 936 **Toscano-Morales R, Xoconostle-Cázares B, Cabrera-Ponce JL, Hinojosa-Moya J, Ruiz-**  
937 **Salas JL, Galván-Gordillo VS, Guevara-González RG, Ruiz-Medrano R.** 2015.

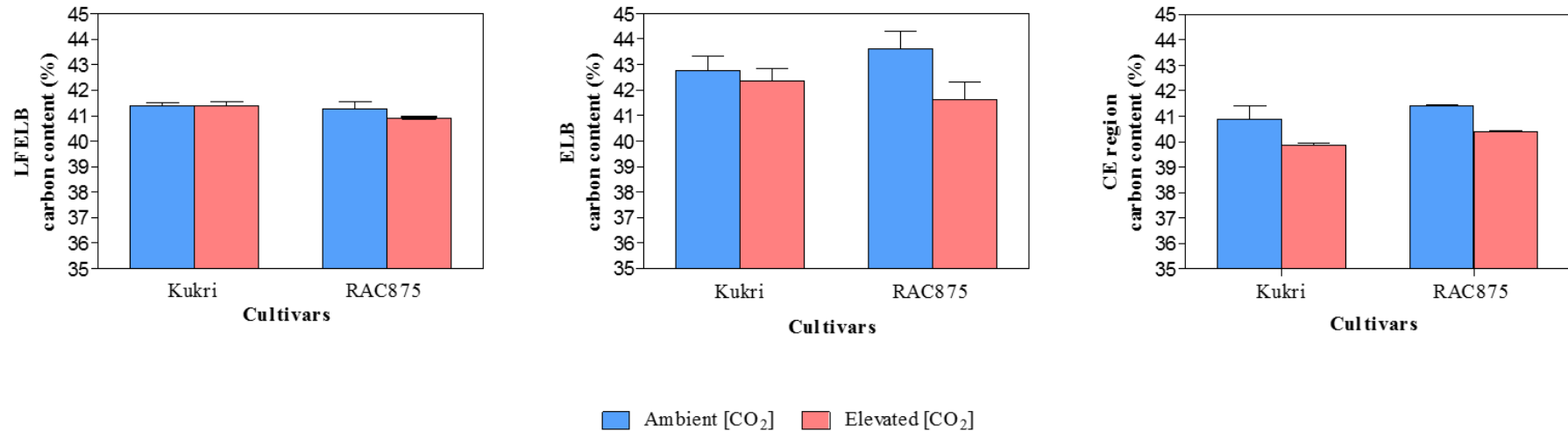
938 AtTCTP2, an Arabidopsis thaliana homolog of Translationally Controlled Tumor  
939 Protein, enhances in vitro plant regeneration. *Frontiers in plant science* **6**, 468.  
940 **Van Sandt VS, Suslov D, Verbelen J-P, Vissenberg K.** 2007. Xyloglucan  
941 endotransglucosylase activity loosens a plant cell wall. *Annals of Botany* **100**, 1467-  
942 1473.  
943 **Verbančič J, Lunn JE, Stitt M, Persson S.** 2017. Carbon supply and the regulation of cell  
944 wall synthesis. *Molecular plant*.  
945 **Vierstra RD.** 1996. Proteolysis in plants: mechanisms and functions. *Post-Transcriptional*  
946 *Control of Gene Expression in Plants*: Springer, 275-302.  
947 **Wai CM, Zhang J, Jones TC, Nagai C, Ming R.** 2017. Cell wall metabolism and hexose  
948 allocation contribute to biomass accumulation in high yielding extreme segregants of a  
949 *Saccharum* interspecific F<sub>2</sub> population. *BMC genomics* **18**, 773.  
950 **Zeng H, Xu L, Singh A, Wang H, Du L, Poovaiah B.** 2015. Involvement of calmodulin and  
951 calmodulin-like proteins in plant responses to abiotic stresses. *Frontiers in plant*  
952 *science* **6**, 600.  
953 **Zheng Z-L.** 2009. Carbon and nitrogen nutrient balance signaling in plants. *Plant signaling &*  
954 *behavior* **4**, 584-591.  
955 **Zhu X, Taylor A, Zhang S, Zhang D, Feng Y, Liang G, Zhu J-K.** 2014. Measuring spatial  
956 and temporal Ca<sup>2+</sup> signals in Arabidopsis plants. *Journal of visualized experiments:*  
957 *JoVE*.

## Supplementary Data



For all the variables - Cultivar -  $P \leq 0.01$ ,  $[\text{CO}_2]$ -  $P \leq 0.01$ , Cultivar x  $[\text{CO}_2]$ -  $P \leq 0.01$

**Supplementary Figure S1.** (a) Total soluble sugar content, (b) sucrose content, (c) glucose content and (d) fructose content in expanding leaf blades of Kukri and RAC875 grown at ambient ( $400 \mu\text{mol mol}^{-1}$ ) or elevated ( $700 \pm 10 \mu\text{mol mol}^{-1}$ )  $[\text{CO}_2]$ . Data presented are the mean ( $\pm \text{SE}$ ) of  $n=3$ . P values indicate the significance: \*,  $P < 0.05$ ; \*\*,  $P < 0.01$ ; ns, not significant.



Cultivar - ns, [CO<sub>2</sub>]- P<0.01, Organ- P<0.01, Cultivar x [CO<sub>2</sub>] x Organ- ns

**Supplementary Figure S2.** Total carbon concentration of (a) Last fully expanded leaf blades (LFELB), (b) expanding leaf blades (ELB), and (c) cell elongation region of Kukri and RAC875 grown at ambient (400  $\mu\text{mol mol}^{-1}$ ) or elevated ( $700 \pm 10 \mu\text{mol mol}^{-1}$ ) [CO<sub>2</sub>]. Data presented are the mean ( $\pm$ SE) of n=3. P values indicate the significance: \*, P<0.05; \*\*, P<0.01; ns, not significant.

733

**Supplementary Table S1.** Concentration of macro and micronutrients in the growing solution provided during wheat growth during early

734

vegetative stage. Half strength nutrient solution was provided. Adapted from ([Fernando et al., 2017](#); [Makino et al., 1983](#)).

Chemical given in the reference	Available form	Element	Full strength of final solution (mM)	Molecular weight (g/mol)	Nutrient concentration in final solution (X)	Final concentration in the solution (mM)	Stock solution concentration (mM)	Amount of chemicals to be dissolved in stock solution (g/L)	Volume of stock solution per litre of final solution (ml)	Half strength solution (ml)	Volume of stock solution per litre of final solution (mM)
<i>Macronutrients</i>											
NH <sub>4</sub> NO <sub>3</sub>	NH <sub>4</sub> NO <sub>3</sub>	N	1	80.04	1000	0.5	500	40.02	1	0.25	0.5
KH <sub>2</sub> PO <sub>4</sub>	KH <sub>2</sub> PO <sub>4</sub>	K	0.8	136.09	1000	0.8	800	108.87	1	0.4	0.5
		P	0.8								
CaCl <sub>2</sub> .2H <sub>2</sub> O	CaCl <sub>2</sub> .2H <sub>2</sub> O	Ca	0.6	147.02	1000	0.6	600	88.21	1	0.3	0.5
		Cl	1.2								
MgSO <sub>4</sub>	MgSO <sub>4</sub> .7H <sub>2</sub> O	S	0.5	246.48	1000	0.5	500	123.24	1	0.25	0.5
		Mg	0.5								
<i>Micronutrients</i>											
Fe-EDTA	C <sub>10</sub> H <sub>12</sub> FeNaO <sub>8</sub>	Fe	0.05	367.05	1000	0.05	50	18.35	1	0.025	0.5
H <sub>3</sub> BO <sub>3</sub>	H <sub>3</sub> BO <sub>3</sub>	B	0.04	61.83	10000	0.04	400	24.73	0.1	0.02	0.05
MnSO <sub>4</sub>	MnSO <sub>4</sub> .H <sub>2</sub> O	Mn	0.007	169.02	10000	0.007	70	11.83	0.1	0.0035	0.05
ZnSO <sub>4</sub>	ZnSO <sub>4</sub> .7H <sub>2</sub> O	Zn	0.0005	287.54	10000	0.0005	5	1.44	0.1	0.00025	0.05
CuSO <sub>4</sub>	CuSO <sub>4</sub> .5H <sub>2</sub> O	Cu	0.0002	249.69	10000	0.0002	2	0.49	0.1	0.0001	0.05
Na <sub>2</sub> MoO <sub>4</sub>	Na <sub>2</sub> MoO <sub>4</sub> .2H <sub>2</sub> O	Mo	0.0001	241.95	10000	0.0001	1	0.24	0.1	0.00005	0.05

735

736

737

738  
739  
740

**Supplementary Table S2.** Comparison of leaf proteome response of RAC875 relative to Kukri at ambient [CO<sub>2</sub>] (Protein expression relative to Kukri proteome at ambient [CO<sub>2</sub>], fold change is given in Log<sub>2</sub> transformation, \*\*P<0.01, \* P<0.05).

Accession No	Protein Name	Fold change at a[CO <sub>2</sub> ] relative to Kukri	Molecular weight (kDa)	P value
<b>Carbohydrate metabolism</b>				
A0A1D6S518	UTP-glucose-1-phosphate uridylyltransferase	3.28	51.664	**
A0A1D6DCS0	Ribokinase	1.63	36.971	**
Q1XIR9	4-hydroxy-7-methoxy-3-oxo-3,4-dihydro-2H-1,4-benzoxazin-2-yl glucoside beta-D-glucosidase 1a, chloroplastic	-3.24	64.508	**
W5I774	Sucrose synthase	2.86	92.400	**
A0A1D5XY50	Glyceraldehyde-3-phosphate dehydrogenase	0.32	46.858	*
<b>Post-translational modifications</b>				
A0A1D6AKZ2	ATP-dependent Clp protease proteolytic subunit	3.00	32.197	**
W5F826	Proteasome subunit beta type	2.20	24.333	**
W5D591	Small ubiquitin-related modifier	0.36	11.101	**
A9EEM6	Triticain beta 2	-0.08	50.417	*
W5ERM8	Proteasome subunit beta type	1.75	23.198	*
A0A1D6B0C9	Aminopeptidase	-1.22	98.207	*
<b>Amino acid metabolism</b>				
A0A1D5TXK5	Histidinol dehydrogenase, chloroplastic	0.29	46.697	**
A0A1D5VKI1	Cysteine synthase	1.33	40.934	**
P38076	Cysteine synthase	1.50	34.114	**
A0A1D5YM24	Cysteine synthase	0.81	40.452	**
A0A1D6RR58	Glutamate decarboxylase	1.27	53.899	*
W5GBW4	S-adenosylmethionine synthase	-0.75	43.252	*
A0A1D5SPT9	Branched-chain-amino-acid aminotransferase	-0.83	34.435	*
W5GE58	Aspartate aminotransferase	0.23	47.328	*
<b>Cell proliferation and differentiation</b>				

W5EMA7	Proteasome subunit alpha type	2.39	27.436	**
A0A173FEH2	TSK1 protein	0.42	19.059	*
W5C3H4	Proteasome subunit alpha type	1.82	25.828	*
W5H3N4	Proteasome subunit alpha type	1.53	31.311	*
A0A1D5SZ32	(1,31,4) beta glucanase	1.49	31.492	*
<b>Anti-oxidant enzymes</b>				
A0A1D6CV93	Peroxidase	2.13	38.416	**
R9W6A6	ER molecular chaperone	1.52	73.186	**
A0A1D5UU04	Peroxidase	-0.78	35.388	**
Q43206	Catalase-1	0.92	56.808	*
A0A1D6BEM4	Peroxidase	1.09	33.623	*
<b>Energy pathway</b>				
W5C3E3	Pyruvate dehydrogenase E1 component subunit alpha	0.50	45.927	**
W5D0E3	Fructose-bisphosphate aldolase	1.13	38.895	**
A0A1D5SM88	Dihydrolipoyl dehydrogenase	1.15	52.795	*
A3KLL4	Malate dehydrogenase	-0.36	35.486	*
A0A1D5WER2	Isocitrate dehydrogenase [NADP]	0.09	50.575	*
A0A1D6AQ51	Pyruvate dehydrogenase E1 component subunit alpha	0.13	42.569	*
A0A1D6BYZ7	ATP-dependent 6-phosphofructokinase	1.02	48.041	*
<b>Photosynthesis</b>				
P11383	Ribulose bisphosphate carboxylase large chain	1.89	52.851	**
<b>Cell wall metabolism</b>				
A0A1D5XZ43	Beta-galactosidase	-0.47	92.126	**
<b>Signal transduction</b>				
A0A1D5ST71	Gamma-glutamyl hydrolase	-0.04	41.489	**
I3RN54	Inorganic pyrophosphatase	1.90	24.287	**
<b>Protein synthesis</b>				
A0A1D6C4Q5	60S acidic ribosomal protein P0	2.39	33.770	*
Q5I7K5	Ribosomal protein P1	1.02	11.193	*

W5FWT6	Aldehyde dehydrogenase 7B1	1.55	54.361	*
<b>Gene expression</b>				
Q2QKB4	Splicing factor U2af large subunit B	0.32	60.586	*
<b>Hormone biosynthesis</b>				
Q69G22	Pyridoxal kinase	0.82	34.241	*
<b>Nitrogen assimilation</b>				
A0A1D5WER2	Isocitrate dehydrogenase [NADP]	0.09	24.287	*

## Chapter 6

### Discussion, Conclusions and Future Directions

Optimization of crop responses to rising atmospheric carbon dioxide concentration ( $[\text{CO}_2]$ ) is considered as one of the best strategies to achieve future food production targets in a changing climate ([Tausz \*et al.\*, 2013](#)). The atmospheric carbon dioxide concentration ( $[\text{CO}_2]$ ) now exceeds  $400 \mu\text{molmol}^{-1}$  ([Tans & Keeling, 2018](#)) and is predicted to reach up to  $1020 \mu\text{molmol}^{-1}$  by the end of this century ([IPCC, 2014](#)). As  $[\text{CO}_2]$  is the primary substrate for photosynthesis, crops are benefited by this increase resulting in greater biomass accumulation, growth and thereby the final yield ([Ainsworth \*et al.\*, 2008](#)). These improvements in biomass and growth are higher in  $\text{C}_3$  crops such as wheat and rice, as  $\text{C}_3$  biochemistry is not photosynthetically saturated at the current  $[\text{CO}_2]$  concentration ([Ainsworth & Rogers, 2007](#)). The magnitude of plant responses to elevated  $[\text{CO}_2]$ , varies even within the same species suggesting that there is a significant genetic variation in  $\text{CO}_2$  responsiveness ([Thilakarathne \*et al.\*, 2015](#)).

Increase in photosynthesis capacity and reduction in stomatal conductance are the two fundamental factors influencing the enhanced plant growth observed at elevated  $[\text{CO}_2]$  ([Ainsworth & Rogers, 2007](#)). Increases in photosynthesis rate in the exponential growth phase of plants could translate into higher absolute growth enhancements ([Kirschbaum, 2010](#)). Therefore, elevated  $[\text{CO}_2]$  provides a unique opportunity to increase crop productivity in a changing climate. Growth stimulation at elevated  $[\text{CO}_2]$  cannot be explained only by changes in photosynthesis rates alone. Modifications in other post-photosynthetic processes; carbon, nitrogen metabolism, cell cycle functions and hormonal regulation are also crucial in moderating plant growth responses to elevated  $[\text{CO}_2]$  ([Gamage \*et al.\*, 2018](#)). Many research studies to date have focused on characterizing photosynthetic responses, whilst paying little attention to the changes in post-photosynthetic processes in response to elevated  $[\text{CO}_2]$ . Characterizing this post-photosynthetic response will be beneficial in dissecting the physiological and molecular mechanisms of how plants respond to elevated  $[\text{CO}_2]$ . To that end, this study focussed on investigating the molecular basis of several key areas of post-photosynthetic processes likely to be linked with the control of growth responses at elevated  $[\text{CO}_2]$  using wheat (*Triticum aestivum* L.). As the  $\text{CO}_2$  responsiveness of plants is high during the early vegetative growth stages, this study mainly focused on characterizing the early growth responses of wheat to elevated  $[\text{CO}_2]$ .

In this research project, quantitative trait loci (QTL) associated with plant growth traits at the early vegetative stage were mapped with the purpose of identifying potential genetic components associated with plant growth responses in a CO<sub>2</sub> rich atmosphere. We then narrowed down our study to understand the transcriptome level changes of key genes associated with carbon, nitrogen metabolism and cell cycle functions in response to increased carbohydrate generation at elevated [CO<sub>2</sub>] and their relationship with plant growth responses at elevated [CO<sub>2</sub>]. Finally, we investigated the changes in leaf proteome to examine the interplay of different regulatory metabolic processes that may have contributed towards growth enhancement at elevated [CO<sub>2</sub>]. Each of these objectives contributes to the advancement of our knowledge in the underlying molecular mechanisms of plant growth responses in a high CO<sub>2</sub> world.

### **6.1 Significant findings of the study**

In the first experimental chapter (Chapter 03), QTL for shoot and root biomass accumulation, root to shoot dry weight ratio, total biomass accumulation, seedling height, leaf elongation rate and leaf width were determined in a doubled haploid (DH) population of wheat grown at elevated [CO<sub>2</sub>] (700 μmolmlol<sup>-1</sup>). Parental line characterization results indicated that the two parental cultivars, Kukri and RAC875 showed different responses at elevated [CO<sub>2</sub>]. For both cultivars, elevated [CO<sub>2</sub>] substantially increased biomass accumulation, the rate of photosynthesis and different growth parameters. Consistent with this, the DH lines of the mapping population also showed a differential response to all the growth traits tested when grown under elevated [CO<sub>2</sub>]. These results suggested that QTL mapped from this data would be of value for further detailed analysis. Overall, in this study we mapped 28 putative QTL under elevated [CO<sub>2</sub>] and 24 putative QTL CO<sub>2</sub>-response QTL for the above mentioned nine growth traits. Amongst the CO<sub>2</sub>-response QTL, three QTL identified on chromosome 2A, 1B and 4B showed an increased responsiveness for biomass accumulation at elevated [CO<sub>2</sub>]. Interestingly, the QTL on 2A and 4B also contributed to the increase in shoot dry weight under high [CO<sub>2</sub>]. This suggests that these three QTL may play a significant role in increasing biomass accumulation at elevated [CO<sub>2</sub>] and impact on the genetic component of phenotypic variation of a particular genotype. Overall, the identification of different QTL for growth traits at ambient and elevated [CO<sub>2</sub>] further implied that there might be a differential genetic control for plant growth at elevated [CO<sub>2</sub>]. To the best of our knowledge, this study is the first report

to identify genomic regions in wheat, which may influence plant growth traits at elevated [CO<sub>2</sub>], focusing on early vegetative growth stages.

Chapter 4 of this thesis focussed on examining the changes in elevated CO<sub>2</sub> mediated gene expression related to photosynthetic and several post-photosynthetic processes and their potential association with growth responses during the early vegetative stage. Physiological analysis of different DH lines selected based on the CO<sub>2</sub> responsiveness of biomass accumulation along with Kukri and RAC875 (parental lines) showed that biomass accumulation, leaf area production and carbohydrate generation are genotypically varied at elevated [CO<sub>2</sub>]. This intraspecific variation in response to elevated [CO<sub>2</sub>] is of great importance as this opens the way for the selection of higher yielding genotypes under future climate conditions ([Tausz et al., 2013](#)). Gene expression analysis of key genes related to photosynthesis, carbon/nitrogen metabolism and cell-wall metabolism further indicates that CO<sub>2</sub> responsiveness among different genotypes varied even at the transcript level. In particular, differential expression of genes in carbon (*SPSI* and *SUS1*) and cell-wall metabolism (gene members of  $\beta$ -expansins and Xyloglucan endotransglucosylase/hydrolases) was observed in response to elevated [CO<sub>2</sub>]. Of the two parental cultivars, RAC875 showed higher transcript abundance for most of the genes examined in this study. Any change related to the key metabolic processes (carbon/nitrogen, cell cycle functions) at transcript level would affect the subsequent protein synthesis and thereby influence plant growth at elevated [CO<sub>2</sub>]. Further, the differential expression of key genes related to different metabolic processes is organ-specific and expression is closely linked with the availability of soluble carbohydrate of a particular organ. This organ-specific gene expression pattern may be the key controlling force of carbon and nitrogen partitioning to different plant organs and thereby maintain carbohydrate production in source organs (e.g. last fully expanded leaf) and utilization demand in sink organs (i.e expanding leaf and shoot apex region). This source and sink integration will then contribute to the growth of an organ and thereby the whole plant.

In the final experimental chapter (Chapter 5), a comparative proteomic approach was employed to investigate the changes in leaf proteome in response to elevated [CO<sub>2</sub>]. Since, Chapter 4 results indicated that there are significant transcriptome level responses of key metabolic processes, a proteomic analysis would be able to investigate changes in protein turnover in response to elevated [CO<sub>2</sub>]. Proteome changes were investigated using the expanding leaf blades of Kukri and RAC875 (parental cultivars of the DH population) because of the high

nitrogen concentration observed at elevated [CO<sub>2</sub>]. Due to the elimination of Rubisco, the most abundant protein in C<sub>3</sub> crops, we were able to examine the changes of other less abundant proteins under high CO<sub>2</sub> conditions. Results of this study showed that most of the differentially expressed proteins at elevated [CO<sub>2</sub>] belong to carbon metabolism (sucrose synthase), energy generation, synthesis and processing of proteins (mainly ribosomal proteins), cell cycle proteins (histones) and cell wall loosening enzymes (cell wall peroxidases). This indicates that along with carbohydrate synthesis through increased photosynthetic carbon fixation, elevated [CO<sub>2</sub>] also stimulates the breakdown of carbohydrates through respiration to provide sufficient energy for leaf expansion and growth. Ribosomal protein synthesis was significantly higher at elevated [CO<sub>2</sub>], which may have facilitated increased cell proliferation and cytoplasmic content, thereby enhancing leaf expansion. Also, differential expression of anti-oxidant enzymes was observed under elevated [CO<sub>2</sub>] suggesting a change in reactive oxygen species (ROS) within the plant. It is possible that these ROS together with cell wall peroxidases perform a noteworthy role in cell wall expansion. In addition to these, several signaling proteins involved in the Ca<sup>2+</sup> signaling pathway, control of cell division/ signaling and protein synthesis were differentially expressed at elevated [CO<sub>2</sub>]. This differential expression of proteins in our study was similar to a proteomics analysis conducted by [Bokhari et al. \(2007\)](#) using ten day old rice seedlings under high [CO<sub>2</sub>]. To our knowledge, this is the first study to investigate the wheat leaf proteome changes in response to elevated [CO<sub>2</sub>] focusing on the early growth stage.

## **6.2 Proposed mechanism for early growth stimulation of wheat at elevated [CO<sub>2</sub>]**

The proposed mechanism of growth responses of wheat to elevated [CO<sub>2</sub>] during early vegetative stage is represented in Figure 1.

In the source tissues, primarily in the last fully expanded leaf blades (LFELB) at the early vegetative stage, elevated [CO<sub>2</sub>] increases the CO<sub>2</sub>/O<sub>2</sub> ratio at the site of CO<sub>2</sub> fixation. Therefore, the efficiency of the carboxylation efficiency of Rubisco is promoted through the lowering of photorespiration. The genes encoding Rubisco large and small subunits, *rbcL* and *rbcS* substantially upregulated at early vegetative stage (Chapter 4) supporting optimum Rubisco synthesis to utilize the increased [CO<sub>2</sub>]. The higher efficiency of PSII, electron transport rate and photochemical quenching correlated with the increased photosynthesis rate at elevated [CO<sub>2</sub>] (Chapter 4) and this may have been involved in producing ATP and NADPH, the vital energy components required to maintain photosynthesis at an optimum rate. This increased photosynthesis capacity at elevated [CO<sub>2</sub>], then leads to high levels of sucrose

production in the source leaves (Chapter 4). The key genes encoding primary enzymes of sucrose metabolism, sucrose phosphate synthase (*SPSI*) and sucrose phosphate phosphatase (*SPPI*) were markedly upregulated in the LFELB to facilitate sucrose production (Chapter 4). Sucrose and other photosynthetic products provide energy and carbon skeletons for amino acid biosynthesis ([Zheng, 2009](#)). Respiratory breakdown of sucrose generates 2-oxoglutarate (2-OG) and this serves as the carbon skeleton for the synthesis of glutamate ([Zheng, 2009](#)). In the process of  $\text{NO}_3^-$  photo assimilation, conversion of  $\text{NO}_2^-$  to  $\text{NH}_4^+$  by *NiR* showed an upregulation at elevated  $[\text{CO}_2]$ . However, this expression was less when compared with the expression of genes encoding the GS/GOGAT pathway (Chapter 4).  $\text{NH}_4^+$  from this primary nitrogen metabolism is then incorporated to glutamate, which is catalysed, by glutamine synthetase (GS) and results in glutamine production ([Stitt & Krapp, 1999](#)). The expression of *GS2a* that encode plastidial GS and *GS1a* and *GSr1*, which encode cytosol, GS was significantly higher in LFELB at elevated  $[\text{CO}_2]$  (Chapter 4). Further genes encoding enzyme Fd-GOGAT and NADH-GOGAT were substantially higher at elevated  $[\text{CO}_2]$  indicating efficient nitrogen assimilation in the early vegetative stage of the plants. Glutamine and glutamate serve as the  $\text{NH}_4^+$  donors to the synthesis of other amino acids required for protein synthesis ([Stitt & Krapp, 1999](#)). The sucrose and the amino acids generated in the LFELB would then be translocated to sink organs via the phloem.

In the early vegetative phase, expanding leaf blades (ELB) and the shoot apex region (SAR) can be considered as the major sink organs. In SAR, sucrose translocated from LFELB will be cleaved by sucrose synthase (*SUS1*), which showed a higher upregulation in growing tissues at elevated  $[\text{CO}_2]$  (Chapter 4). The resulting UDP-Glucose plays an important role as a substrate for the re-synthesis of sucrose from available glucose and fructose ([Yong et al., 2000](#), [Koch, 2004](#)). Also, UDP-Glucose is an important component in cell wall biosynthesis of dividing cells ([Verbančič et al., 2017](#)). Increased activity of cell wall metabolism was evident from the higher expression of genes encoding  $\beta$ -expansins and Xyloglucan endotransglucosylase/hydrolases (Chapter 4). This implied that cell wall loosening, and expansion has been promoted at elevated  $[\text{CO}_2]$ . High availability of glucose and fructose of SAR positively correlates with cell division ([Koch, 2004](#)). Therefore, in the shoot apex region, active utilization of carbohydrates and increased production and expansion of cells may have facilitated increased growth rates at elevated  $[\text{CO}_2]$ .

A similar pattern for sucrose metabolism was observed in the ELB of wheat at elevated  $[\text{CO}_2]$ . The results of proteomics analysis showed that SUS enzyme was significantly upregulated at

elevated [CO<sub>2</sub>] resulting in the production of UDP-Glucose. Other than this, UTP-glucose-1-phosphate uridylyltransferase, the enzyme that produces UDP-Glucose from Glucose 1 phosphate and UTP had been significantly upregulated (Chapter 5) indicating a higher production of UDP-Glucose in the ELB at elevated [CO<sub>2</sub>]. This may have contributed for increased UDP-Glucose production which is an essential substrate for sucrose and cell wall biosynthesis of growing tissues. The increased sucrose supply from LFELB and resynthesizes of sucrose within the tissue increases the sucrose concentration of ELB. This increased sugar supply then promotes expression of proteins related to cell division such as tubulin and protein synthesis such as ribosomal proteins required for cytoplasmic growth (Chapter 5). As a result of these metabolic changes, increased cell proliferation and expansion takes place within the ELB and thus, increases the leaf elongation rate at elevated [CO<sub>2</sub>]. The increased photosynthetic capacity at elevated [CO<sub>2</sub>] remains high until the sink utilization of carbohydrate supply remains high. In the early vegetative stages, plants' plasticity to develop sink organs is relatively high and thus, higher growth stimulation can be observed at elevated [CO<sub>2</sub>].

However, this growth stimulation observed under elevated [CO<sub>2</sub>] varied significantly between wheat cultivars indicating a noticeable intraspecific variability. The CO<sub>2</sub> responsiveness of wheat is genetically determined (Chapter 3), and this may be depending on the plants' ability to expand their sink capacity in response to increased sugar supply at elevated [CO<sub>2</sub>]. This intraspecific variability in plant responses to elevated [CO<sub>2</sub>] was observed even at transcript (Chapter 4) and proteomic level (Chapter 5). These variable responses are of great importance for selecting the best genotypes that can thrive well in a high CO<sub>2</sub> world.

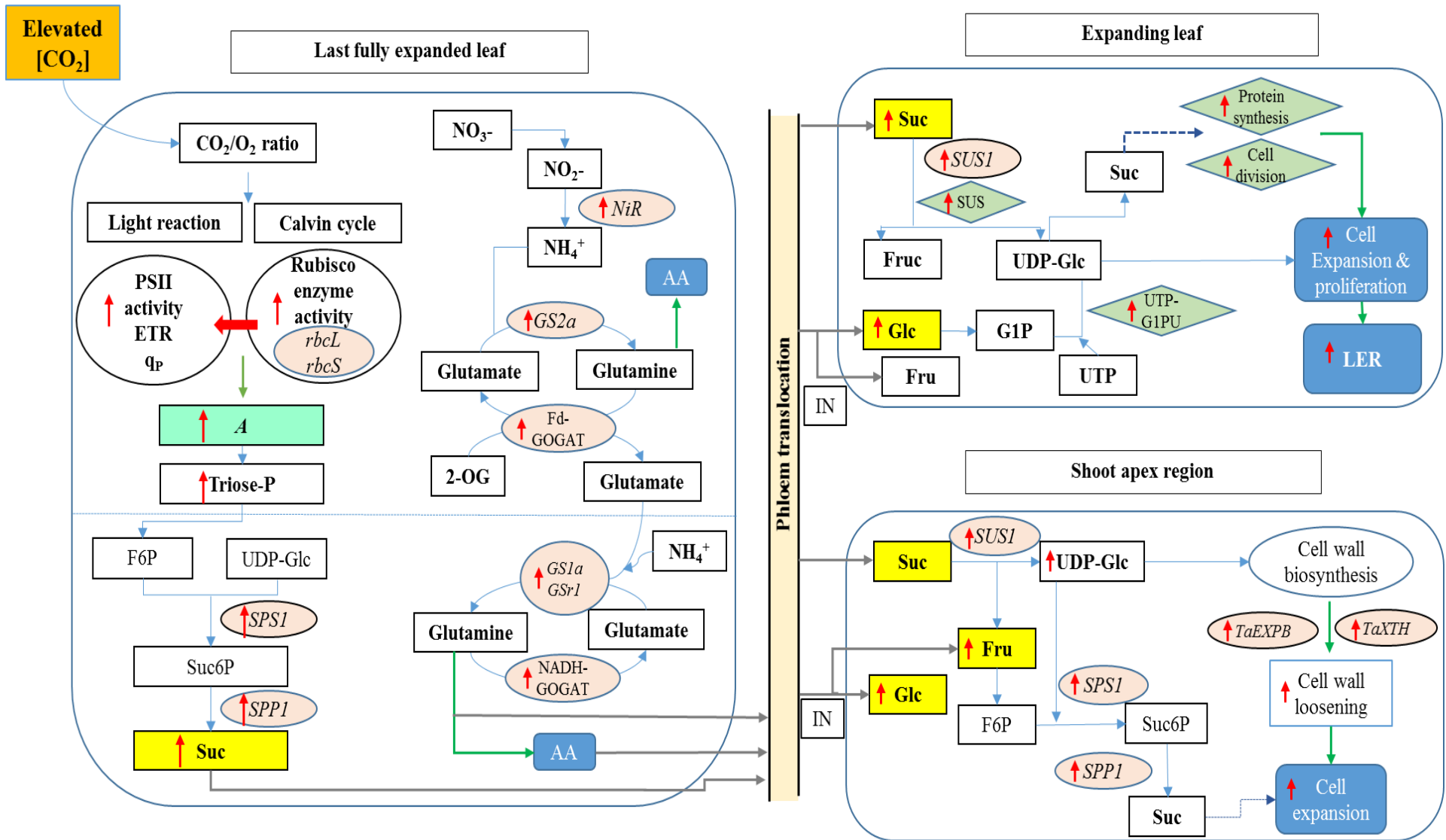


**Figure 1.** Schematic diagram of molecular changes of source (last fully expanded leaf) and sink (expanding leaf and shoot apex region) integration of wheat at elevated [CO<sub>2</sub>] in early vegetative stage of wheat. Circles with light orange colour represent the transcript level changes of relevant genes at elevated [CO<sub>2</sub>]. Green diamonds represent the differential protein expression of relevant metabolic activities at elevated [CO<sub>2</sub>]. Blue colour rectangles

A: photosynthesis rate, PSII: photosystem II, ETR: electron transport rate, q<sub>p</sub>- photochemical quenching, Glc: glucose, Fru: fructose, Suc: sucrose, F6P- fructose 6 phosphate, UDP-Glc: UDP glucose, Suc6P: sucrose 6 phosphate, G1P: glucose 1 phosphate, UTP: uridine triphosphate, AA- amino acids synthesis & metabolism, UTP-G1PU: UTP-glucose-1-phosphate uridylyltransferase *rbcL* - ribulose 1,5 -bisphosphate carboxylase/oxygenase (large sub unit); *rbcS* - ribulose 1,5 -bisphosphate carboxylase/oxygenase (small sub unit); *SPP*- Sucrose Phosphate Phosphatase; *SPS*- Sucrose Phosphate Synthase; *SUS* - Sucrose Synthase type 1; *NiR* - Ferredoxin Nitrite Reductase; *Fd-GOGAT* - Putative ferredoxin-dependent glutamate synthase; *GS2a* - Glutamine Synthetase (Plastidial), *NADH-GOGAT* - Putative NADH-dependent glutamate synthase; *GS1a* - Glutamine synthetase (cytosolic); *GSr1* - Glutamine synthetase (cytosolic) *TaEXPB* - β – expansins *TaXTH* - Xyloglucan endotransglucosylase/hydrolases

### 6.3 Future directions

The experiments discussed in this thesis employed a multidisciplinary approach to further elucidate the molecular mechanisms of plant growth responses to elevated atmospheric [CO<sub>2</sub>]. The study attempted to dissect the underlying mechanisms of plant growth at the genomic, transcriptomic and proteomic level focusing on the early vegetative growth stage. More research is required both to confirm these initial observations and to establish in much more detail the regulation of growth responses under elevated [CO<sub>2</sub>]. This will be beneficial for developing climate-smart wheat genotypes for the future high CO<sub>2</sub> world.

The results of our QTL mapping experiment indicated several putative QTL that might potentially play a significant role in determining biomass accumulation at elevated [CO<sub>2</sub>]. However, in our study we could not further validate the QTL to confirm their reproducibility. Before using them in marker-assisted breeding, these QTL regions have to be validated to rule out possible errors associated with QTL mapping. Therefore, re-running the QTL mapping using the same DH mapping population in different locations, especially under field conditions and in different years to test whether the same QTL effect can be detected even under different environmental conditions is necessary. For this purpose, Near-Isogenic lines (NIL) can be selected for a particular trait or molecular marker through a series of backcrosses to a recurrent parent, which does not express the trait of interest. Phenotypic differences between the parental lines and the NIL lines will allow investigation of phenotypic differences due to the QTL of interest. If the identified QTL are good enough to be used in the breeding programmes, these QTL can be combined into the same line through pyramiding and can be used in breeding crops for future CO<sub>2</sub> enriched atmosphere. Further, in-depth analysis of these QTL regions is necessary to identify candidate genes that may be essential for plant growth and adaptation to future CO<sub>2</sub> levels. Our study was limited to the identification of QTL regions during the early vegetative growth stage. Therefore, this study can be further extended to elucidate the CO<sub>2</sub> responsive genomic regions associated with other key developmental stages of wheat.

The results of the second study implied that elevated [CO<sub>2</sub>] significantly influences plant transcriptome level changes and organ-specific expression patterns of key genes might play a role in determining source-sink integration under high CO<sub>2</sub> levels. Our study only investigated a few selected key genes related to photosynthesis, carbon/nitrogen metabolism and cell-wall metabolism. To obtain a more complete picture, it is better to conduct an in-depth analysis of

transcript level changes of each metabolic process at elevated [CO<sub>2</sub>], which could be possibly achieved through microarray analysis. Therefore, comparative analysis of mature and growing organs using a microarray analysis might provide a more complete overview regarding changes at transcriptome level to elevated [CO<sub>2</sub>]. Further in our study, we did not investigate the change of key genes related to hormonal regulation, though this plays a major role in moderating plant growth responses. Hence, studies into the investigation of transcript level changes of genes related to hormonal metabolism would assist in improving our understanding of the underlying molecular mechanisms at elevated [CO<sub>2</sub>]. The transcript abundance during the vegetative stage and in the transition to reproductive stage will indicate the plants' transcriptome level changes to elevated [CO<sub>2</sub>] and their relation to the source-sink integration of a plant.

Results of the comparative proteomics analysis revealed that key regulatory enzymes, intermediate metabolic proteins/biomolecules and signal transducing proteins were differentially expressed under elevated [CO<sub>2</sub>]. The changes in the proteome of expanding leaves allowed us to identify more proteins related to carbohydrate utilization, protein synthesis, cell division and expansion. Similarly, a comparative proteomic analysis of the shoot apex region will give a more complete picture of how cell cycle functions change in response to elevated [CO<sub>2</sub>] as Chapter 4 results indicated that cell cycle functions are likely to be more responsive to elevated [CO<sub>2</sub>]. Of all the identified proteins, a significant proportion was uncharacterized proteins; the functionality of these proteins is not yet confirmed. There were a few uncharacterized proteins that showed significant differential expression in both cultivars. Studies into annotation and curation of these uncharacterized proteins will be beneficial in unravelling the underlying mechanisms of plant growth responses to elevated [CO<sub>2</sub>]. Overall, out of two parental cultivars of the DH mapping population used in this thesis, RAC875 showed a noteworthy CO<sub>2</sub> responsiveness both at the transcriptome and proteome level. Thus, possibilities to use RAC875 as a potential breeding line for crop breeding programmes designed for a future CO<sub>2</sub> enriched atmosphere need to be investigated.

## 6.4 Conclusion

It is crucial to understand the underlying molecular mechanisms of plant growth responses to elevated  $[\text{CO}_2]$  in order to develop effective crop breeding strategies for a future  $\text{CO}_2$  enriched world. Each of the experimental chapters of this thesis, contributed to elucidating the molecular mechanism of how plants respond to elevated  $[\text{CO}_2]$  at the genomic, transcriptomic and proteomic level using wheat, focusing on the early vegetative growth stages. In Chapter 3, three main  $\text{CO}_2$ -response QTL for biomass accumulation were identified on chromosome 2A, 1B and 4B, of which QTL on chromosome 2A and 4B also contributed to increasing shoot dry weight at elevated  $[\text{CO}_2]$ . These QTL can be validated and used for further in-depth analysis to identify the candidate genes involved in moderating plant adaptations to elevated  $[\text{CO}_2]$ . The results of Chapter 4 indicated that plants show an organ-specific expression pattern for key genes associated with photosynthesis and post-photosynthetic processes at elevated  $[\text{CO}_2]$ . Carbon metabolism, nitrogen metabolism and cell-wall metabolism are highly influenced by increased sugar supply under high  $\text{CO}_2$  conditions and of them, several genes related to cell-wall metabolism showed strong positive correlations with the soluble carbohydrate content. These changes in the transcriptome may have influenced protein synthesis that governs plant growth and development. Results of Chapter 5 showed that proteins involved in carbohydrate synthesis and respiratory breakdown, protein synthesis and processing, cell division and cell-wall metabolism significantly changed their expression at elevated  $[\text{CO}_2]$  and are likely to be involved in enhanced leaf elongation observed in the high  $\text{CO}_2$  environment. Overall, this project contributes to the lessening of the knowledge gaps in our understanding of molecular mechanisms of plant growth responses to elevated  $[\text{CO}_2]$  and yet more work is required to develop a more refined mechanism of how elevated  $[\text{CO}_2]$  regulates plant growth. However, in the real world, elevated  $[\text{CO}_2]$  closely interacts with other climatic parameters such as increased temperatures and prolonged drought conditions. Therefore, elucidation of the underlying mechanisms of plant growth responses to elevated  $[\text{CO}_2]$  is very challenging under this triple whammy of challenges (elevated  $\text{CO}_2$ , high temperature and water scarcity) anticipated in the future.

## 6.5 References

- Ainsworth E.A., Beier C., Calfapietra C., Ceulemans R., Durand-Tardif M., Farquhar G.D., Godbold D.L., Hendrey G.R., Hickler T. & Kaduk J. (2008) Next generation of elevated [CO<sub>2</sub>] experiments with crops: a critical investment for feeding the future world. *Plant, cell & environment*, **31**, 1317-1324.
- Ainsworth E.A. & Rogers A. (2007) The response of photosynthesis and stomatal conductance to rising [CO<sub>2</sub>]: mechanisms and environmental interactions. *Plant, cell & environment*, **30**, 258-270.
- Bokhari S.A., Wan X.-Y., Yang Y.-W., Zhou L., Tang W.-L. & Liu J.-Y. (2007) Proteomic response of rice seedling leaves to elevated CO<sub>2</sub> levels. *Journal of proteome research*, **6**, 4624-4633.
- Gamage D., Thompson M., Sutherland M., Hirotsu N., Makino A. & Seneweera S. (2018) New insights into the cellular mechanisms of plant growth at elevated atmospheric carbon dioxide. *Plant, cell & environment*, **41**(6), 1233-1246.
- IPCC (2014) Recent increase and projected changes in CO<sub>2</sub> concentrations. In: *Carbon dioxide: Projected emissions and concentrations*. Data distribution centre, IPCC, Online
- Kirschbaum M.U. (2010) Does Enhanced Photosynthesis Enhance Growth? Lessons Learnt From CO<sub>2</sub> Enrichment Studies. *Plant physiology*, pp. 110.166819.
- Koch K. (2004) Sucrose metabolism: regulatory mechanisms and pivotal roles in sugar sensing and plant development. *Current opinion in plant biology*, **7**, 235-246.
- Stitt M. & Krapp A. (1999) The interaction between elevated carbon dioxide and nitrogen nutrition: the physiological and molecular background. *Plant, Cell & Environment*, **22**, 583-621.
- Tans P. & Keeling R. (2018) Trends in atmospheric carbon dioxide. NOAA/ESRL ([www.esrl.noaa.gov/gmd/ccgg/trends/](http://www.esrl.noaa.gov/gmd/ccgg/trends/))
- Tausz M., Tausz-Posch S., Norton R.M., Fitzgerald G.J., Nicolas M.E. & Seneweera S. (2013) Understanding crop physiology to select breeding targets and improve crop management under increasing atmospheric CO<sub>2</sub> concentrations. *Environmental and Experimental Botany*, **88**, 71-80.
- Thilakarathne C.L., Tausz-Posch S., Cane K., Norton R.M., Fitzgerald G.J., Tausz M. & Seneweera S. (2015) Intraspecific variation in leaf growth of wheat (*Triticum aestivum*) under Australian Grain Free Air CO<sub>2</sub> Enrichment (AGFACE): is it regulated through carbon and/or nitrogen supply? *Functional Plant Biology*, **42**, 299-308.
- Verbančič J., Lunn J.E., Stitt M. & Persson S. (2017) Carbon supply and the regulation of cell wall synthesis. *Molecular plant*.
- Yong J.W.H., Wong S.C., Letham D.S., Hocart C.H. & Farquhar G.D. (2000) Effects of elevated CO<sub>2</sub> and nitrogen nutrition on cytokinins in the xylem sap and leaves of cotton. *Plant Physiology*, **124**, 767-779.
- Zheng Z.-L. (2009) Carbon and nitrogen nutrient balance signaling in plants. *Plant Signaling & Behavior*, **4**, 584-591.